

Topological String Amplitudes, Complete Intersection Calabi–Yau Spaces and Threshold Corrections

A. Klemm^{*}, M. Kreuzer[◇], E. Riegler[◇] and E. Scheidegger^{◇1}

** UW-Madison Physics Department
1150 University Avenue
Madison, WI 53706-1390, USA*

*◇ Institut für Theoretische Physik, Technische Universität Wien
Wiedner Hauptstr. 8-10/136, A-1040 Vienna, Austria*

ABSTRACT

We present the most complete list of mirror pairs of Calabi–Yau complete intersections in toric ambient varieties and develop the methods to solve the topological string and to calculate higher genus amplitudes on these compact Calabi–Yau spaces. These symplectic invariants are used to remove redundancies in examples. The construction of the B–model propagators leads to compatibility conditions, which constrain multi–parameter mirror maps. For K3 fibered Calabi–Yau spaces without reducible fibers we find closed formulas for all genus contributions in the fiber direction from the geometry of the fibration. If the heterotic dual to this geometry is known, the higher genus invariants can be identified with the degeneracies of BPS states contributing to gravitational threshold corrections and all genus checks on string duality in the perturbative regime are accomplished. We find, however, that the BPS degeneracies do not uniquely fix the non-perturbative completion of the heterotic string. For these geometries we can write the topological partition function in terms of the Donaldson–Thomas invariants and we perform a non-trivial check of S–duality in topological strings. We further investigate transitions via collapsing D_5 del Pezzo surfaces and the occurrence of free \mathbb{Z}_2 quotients that lead to a new class of heterotic duals.

¹email: aklemm@physics.wisc.edu, kreuzer, riegler & esche@hep.itp.tuwien.ac.at

1 Introduction

Mirror symmetry in Calabi–Yau compactifications makes the calculations of low derivative terms in the effective action with $N = 2$ and $N = 1$ supersymmetry feasible and leads to a wealth of insights in gauge and string theory, many of which come from concrete examples. In this paper we construct the most complete list of Calabi–Yau mirror pairs. They are realized as hypersurfaces and complete intersection in general toric varieties.

A motivation to go beyond the hypersurface case can already be seen locally. While all 2d canonical singularities are described by a singular (ADE) hypersurface, the 3d canonical singularities are generally not realizable in this way. Simple 3d examples, such as the D_5 elliptic singularity, require a realization by complete intersections, here by two polynomials in \mathbb{C}^5 . Globally the complete intersection examples naturally lead to string backgrounds with new spectra, new interactions and new symmetries.

Important terms in the exact low energy effective action are given by the same supersymmetric family indices, calculable as topological string amplitudes, that are also the natural mathematical invariants to control the redundancy in these constructions. In the A-model picture the expansion coefficients of the family indices are completely determined either by Gromov–Witten invariants, by numbers of BPS states (Gopakumar–Vafa invariants) or by Donaldson–Thomas invariants. These are symplectic invariants. Solving the topological string in the compact case is a challenge whose solution will determine these invariants and shed light on 4d black hole physics [1], [2], [3], the physics of the NS five–brane [4], non-perturbative string theory and low energy effective actions.

From the available techniques to calculate higher genus topological string amplitudes, localization and large N transitions presently fail in the compact case for reasons discussed in more detail at the beginning of Section 4. As direct computation of the cohomology of BPS moduli spaces and utilization of heterotic type II duality yields only information for certain classes in the Kähler cone, the topological B-model is still the most powerful tool for calculating higher genus amplitudes on compact Calabi–Yau spaces. We therefore first extend the methods for the calculation of the genus zero and one topological string amplitudes to the case of complete intersections in general toric varieties. This can be viewed as a completion of the work of [5], [6]. An important application is the study of the non-perturbative completion of $N = 2$ heterotic string compactifications via its duality to type II strings on K3 fibered Calabi–Yau spaces. It requires the calculation of topological string amplitudes on compact multi–parameter Calabi–Yau 3-folds at higher genus. This has not been done before, partly because the construction of the B-model propagators implies differential constraints on the mirror maps, which have not been solved. We solve those in various examples and make the first higher genus calculations for compact multi–parameter models. The solution to the constraint equations itself can shed light on the mirror maps whose integrality property is one of the most enigmatic features of mirror symmetry.

Using the Hilbert scheme for points on the K3 fiber we find closed formulas for higher genus amplitudes on K3 fibrations without reducible singular fibers in the limit of large \mathbb{P}^1

base, which corresponds to weak heterotic coupling. Unlike in the case of local limits to non-compact toric surfaces or del Pezzos, which have no complex structure deformations, we use the invariance under complex structure deformations of the geometry to find a good model for the calculation of the BPS moduli spaces. Even though restricted to the K3 classes in the Calabi–Yau X the calculated invariants do contain global information of X . For K3 fibrations with two parameters, the resulting formulas involve modular forms of subgroups of $\mathrm{SL}(2, \mathbb{Z})$, which we obtain directly from the geometry. For a fixed fiber type of the normal fibration these modular forms for different fibrations depend on the singular fibers and can be parameterized in an elegant way by the Euler number of X . In the case where the heterotic dual is known they are calculated by integrals of worldsheet indices related to the gravitational threshold corrections and we perform all genus checks by comparing to our B-model results and to calculations extending the methods of [2].

We also find that the partition function of the topological string has in general a very simple product form, which corresponds to a free field theory partition function with a $\mathrm{U}(1)$ charge. This might give some hope that one can understand the indices of the non-perturbative heterotic string or the dependence of the topological string theory for all classes of curves in a Calabi–Yau by the world sheet index of some 2d conformal field theory. However, one has to be careful with the non-perturbative completion of the heterotic string, because we find for well-known examples such as the ST model that there are several dual K3 fibered Calabi–Yau spaces, which reproduce the same holomorphic data at weak coupling except for the triple intersection of T in $\mathcal{F}^{(g=0)}$ and the leading coefficient of T in $\mathcal{F}^{(g=1)}$, which have not been fixed on the heterotic side. These series of K3 fibrations are rational homotopy equivalent. They have identical perturbative BPS spectrum in the fiber direction, but different non-perturbative BPS numbers for nonzero base degrees. Turning on base degrees includes the non-perturbative $e^{-8\pi^2 S}$ effects and one finds that the non-perturbative moduli including the heterotic dilaton are globally different for the members of the series.

S–duality in the topological string is conjectured to map the partition function of the topological A–model expressed in terms of the Gopakumar–Vafa invariants into a dual partition function of the B–model on the same Calabi–Yau manifold expressed in terms of Donaldson–Thomas invariants. Using our simple product form of the former partition function, restricting it to maps in the fiber direction, and applying S–duality, we explicitly compute in Section 6.10 a subset of the Donaldson–Thomas invariants of a compact Calabi–Yau manifold. We find that these invariants are indeed integral as expected, and hence our result can be viewed as a highly non-trivial check of the S–duality in the topological string.

In order to use mirror symmetry to go from the B–model propagators to the invariants in the A–model, the initial data is a mirror pair of families of complex 3d compact complete intersections with vanishing first Chern class. Such a pair can be given by a pair of reflexive polyhedra (Δ, ∇) of dimension ≥ 4 together with a dual pair of nef partitions of (Δ^*, ∇^*) . We have compiled a list with some 10^8 new examples of such (2,2) vacua. The deformation family is w.r.t. the complex and the symplectic structure, and it is in general not of fixed topological type. To fix the latter a choice of the Kähler cone is needed. The possible choices follow from the triangulations of Δ^* . The enormous amount of data leads immediately to the

question of identification of families. The Hodge numbers are included in the list of models. For small Picard number, many but not all of the models with equal Hodge numbers have diffeomorphic large radius phases according to the characterization of topological type by C.T.C. Wall. The mirrors of manifolds with diffeomorphic phases are usually in the same family of complex structures, but the parameterization of the complex family differs by coordinate changes and different gauge choices of the $(3, 0)$ form. We also find Calabi–Yau threefolds that are rational homotopy equivalent, but have different A–model amplitudes, hence different symplectic structures. Furthermore, we find examples of mirror pairs of diffeomorphic Calabi–Yau spaces that have different symplectic structures.

We provide methods to systematically select models with desired properties from the list. We focus mainly on two properties: K3 fibration structures and free quotients. The first are of obvious interest for reasons discussed above. Many new Calabi–Yau spaces with non-trivial fundamental group emerge from the latter search. In the toric construction the abelian \mathbb{Z}_n group actions are easily obtained by specifying a sublattice M' in the lattice M , with index $n = |M|/|M'|$. Such examples are phenomenologically important, as one can put Wilson lines to break the gauge group. They also caught attention because the distinction between the K -theory and the cohomological classification of D-branes on such spaces is particularly noticeable.

By taking the intersection of the two searches we get a class of type II compactifications, which has interesting and mostly new heterotic duals. In this class we have $\mathcal{F}^{(1),\text{het}}(S, T) = \frac{1}{2}S + \dots$ and avoid a supergravity argument [7] that the $\mathcal{F}^{(1),\text{het}}R_+^2$ coupling has to go with $\mathcal{F}^{(1),\text{het}}(S, T) = S + \dots$. The latter matches the criterion $\int_X c_2 S = 24$ of Oguiso [8] for simply connected K3 fibrations on the type II side. The heterotic cases seem to have higher level gauge groups. One special case has been studied in [9]. In this case it was argued that the $N = 2$ supergravity is of ‘no-scale’ type, which implies that there are no instantons corrections to the couplings. Necessary is also a vanishing Euler number χ , because a scale dependence is introduced by the four loop σ model contribution, which is proportional to χ . We find that all our toric examples are scale dependent, even the ones which have the same Hodge numbers as the model in [9]. This is checked by explicitly calculating the instanton contributions to the prepotential.

On the heterotic side another interesting class of compactifications with extended supersymmetry involves local products of $K3 \times T^2$. A number of these spaces, which have a fundamental group of rank 1, was obtained as Landau–Ginzburg orbifolds with $h^{1,1} \in \{3, 5, 9, 13\}$ by a \mathbb{Z}_2 or \mathbb{Z}_3 acting freely on the torus [10]. The latter two cases can be realized as toric complete intersections. The additional gravitini are built from the nonvanishing $(0, 1)$ –forms of these manifolds. As the possible automorphisms of K3 were classified by Nikulin it should be straightforward to construct many more examples with free \mathbb{Z}_n or $\mathbb{Z}_n \times \mathbb{Z}_m$ actions on the torus, which can, however, not be realized as toric complete intersections.

The organization of the paper is as follows: To set our definitions we review in Section 2 the mirror construction of Calabi–Yau complete intersections due to Batyrev and Borisov and describe the resolution of singularities. Our aim is to relate the algebraic data of the threefolds as directly as possible to the combinatorics of the polyhedra. We describe the criterion for

fibrations as well as the construction of the free quotient examples. The lists of CICYs are available on a web page [11]. We also introduce the example of the $(h^{11} = 2, h^{21} = 30)$ free \mathbb{Z}_2 quotient which is realized as a complete intersection in codimension two. This is later used to exemplify the reduction of the redundancies via the calculation of $\mathcal{F}^{(0)}$ and $\mathcal{F}^{(1)}$.

The geometry of the toric complete intersections is described in Section 3 with special emphasis on the reduction of redundancies due to different ambient spaces or to different nef partitions of the same reflexive polytope. We exemplify variants of equivalent realizations for the $(2, 30)$ model. In the course of the discussion we explain how to get from the triangulation to the Kähler cone and to the generators of the Mori cone. These will be used later for the calculation of the B-model amplitudes. Further explicit examples with small Hodge numbers are treated in Appendix B. In Appendix C we present the most complete list of Calabi–Yau spaces in toric varieties with small Picard numbers. For codimension $r \leq 2$ these are probably complete.

In Section 4 we briefly review the structure of the genus zero sector of the topological string. As an example we discuss the $(2, 30)$ model, whose details are relegated to Appendix A. The main point is the derivation of the multi parameter B-model propagators and the discussion of the integrability conditions. These are solved in Section 6 for many cases. In Section 5 we give the product form for the holomorphic partition function of the topological string in terms of the Gopakumar-Vafa invariants.

In Section 6 we give a geometrical derivation of the general formula for the topological string amplitudes in the fiber direction for K3 fibrations with no reducible fibers. We apply the formula to a series of K3 fibrations with the same fiber type and fixed self intersection of the fiber class $E^2 = k$, but different Euler number. In each case we find the modular form of $\Gamma(2k)$, which fixes the all genus prediction in the fiber direction. We solve the B-model propagators and make genus 2 predictions also for the base class. The predictions are checked against the direct calculation of the cohomology of the moduli space of the M2-brane [2]. We then discuss the more subtle differences in the cases with the same generic fiber and the same Euler number. In this case we find rational homotopy equivalent fibrations with different GV invariants. Finally, we discuss the mirror geometry of a diffeomorphic pair with $E^2 = 4$ fiber. It turns out that one large complex structure limit contains terms diverging with $\text{Li}_3(e^{t_1-t_2})$. We then turn to models whose dual heterotic string is known. After a short review of the relevant heterotic indices we make all genus checks of the heterotic type II dualities for the ST model. We summarize the $\Gamma(2k)$ modular forms for many two parameter fibrations with $E^2 = 2, 4, 6$ in Section 6.9 and discuss the subtleties with the non-perturbative completion of the heterotic string. The section is finished with a discussion of the STU model. Beside finding the propagators and making higher loop tests, we analyze the restrictions that the STU -trality symmetry imposes on the non-perturbative topological string amplitudes. We find that in this case the non-perturbative BPS numbers can also be described by quasi modular functions. In Appendix E we analyze the moduli space of this model in some detail.

Section 7 contains an application of our formalism to the counting of BPS states in the D_5 del Pezzo surface. Collapsing of this surface leads to an elliptic D_5 singularity and the geometry can only be described as complete intersection. We further discuss the models with

\mathbb{Z}_2 torsion, i.e. free \mathbb{Z}_2 quotients. Particularly interesting from the point of view of the duality between the heterotic and the type II string are free quotients which are both elliptically and K3 fibered. Some general aspects are discussed in this section while a list of examples is presented in Appendix D. Moreover, we consider a class of examples with Euler number 0. These have similar properties as the FHSV model but are nevertheless different, due to instanton corrections in genus zero. We also discuss certain aspects of self-mirrors.

2 Toric CICYs, fibrations and torsion

In this section we first recall the construction of Calabi–Yau complete intersections in toric varieties and explain how fibrations and free quotients (*i.e.* manifolds with non-trivial fundamental group) manifest themselves in the combinatorics of reflexive polytopes. We will also devote a section on the resolution of singularities.

2.1 Complete intersections in toric varieties

The toric ambient spaces V_Σ are defined in terms of a fan Σ , which is a collection of rational polyhedral cones $\sigma \in \Sigma$, such that it contains all faces and intersections of its elements [12–15]. V_Σ is compact if the support of Σ covers all of the real extension $N_{\mathbb{R}}$ of some d -dimensional lattice N . A simple example is the case where Σ consists of the cones over the faces of a rational polytope $\Delta^* \subset N_{\mathbb{R}}$ containing the origin and the 0-dimensional cone $\{0\}$. Let $\Sigma(1)$ denote the set of one-dimensional cones with primitive generators ρ_i , $i = 1, \dots, n$. The resulting variety V_Σ is smooth if all cones are simplicial and if all maximal cones are generated by a lattice basis. Singularities at codimension 4 of such an ambient space are irrelevant for a sufficiently generic choice of equation for a Calabi–Yau 3-fold. Higher-dimensional singularities have to be resolved by a subdivision of the fan, *i.e.* by adding to $\Sigma(1)$ rays that are generated by lattice points on faces of $k\Delta^*$, $k \geq 1$. We will address this issue in more detail in Section 2.3.

The simplest description of V_Σ introduces homogeneous coordinates z_i for the n generators ρ_i of the rays in $\Sigma(1)$ and weighted projective identifications

$$(z_1 : \dots : z_n) \sim (\lambda^{q_1^{(a)}} z_1 : \dots : \lambda^{q_n^{(a)}} z_n) \quad a = 1, \dots, h \quad (2.1)$$

where $\lambda \in \mathbb{C}^*$ is a nonzero complex number, and the n -vectors $q_i^{(a)}$ are generators of the linear relations $\sum q_i^{(a)} \rho_i = 0$ among the primitive lattice vectors ρ_i . To obtain a well-behaved quotient $V_\Sigma = (\mathbb{C}^n - Z)/(\mathbb{C}^*)^h$ we have to exclude an exceptional set $Z \subset \mathbb{C}^n$ that is defined in terms of the fan [15, 16]. There are $h = n - d$ independent \mathbb{C}^* identifications so that the dimension of V_Σ equals the dimension d of the lattice N .

We have to be more precise about the quotient defining V_Σ : Let N' be the sublattice of N that is generated by the lattice vectors in $\Sigma(1)$. If N' is a sublattice of N with index $I > 1$ then we need some additional identifications [16]. Let Σ' be the fan obtained from Σ by relating

everything to the lattice N' . Then $V_\Sigma = V_{\Sigma'}/G$ is a quotient of $V_{\Sigma'}$ by a finite abelian group G isomorphic to N/N' that acts by multiplication with phases ω^{α_i} on the homogeneous coordinates z_i . Here ω is a $|G|^{\text{th}}$ root of unity. We will denote such group actions by $(\alpha_1, \dots, \alpha_n)/|G|$, where $\sum_{i=1}^n \alpha_i = 0 \pmod{|G|}$. To see how this comes about we note that the ring of regular functions on an affine coordinate patch U_σ of V_Σ is spanned by the monomials $\prod z_i^{\langle m, \rho_i \rangle}$, where $m \in \sigma^\vee \cap M$ is a vector in the dual lattice $M = \text{Hom}(N, \mathbb{Z})$. If we change from the lattice N' to the finer lattice N then we have to exclude all monomials corresponding to vectors $m \in M'$ that do not belong to the sublattice $M \subset M'$. Thus there are no more functions available to distinguish points in $V_{\Sigma'}$ that live on orbits of G (in turn, this can be used to define G). The quotient $V_\Sigma = V_{\Sigma'}/G$ is never free for a toric variety [14]. If, however, a (Calabi–Yau) hypersurface or complete intersection does not intersect the set of fixed points then we get a manifold with nontrivial fundamental group as will be discussed in subsection 2.2.

Batyrev showed that a generic section of the anticanonical bundle of $\mathbb{P}_{\Delta^*} = V_{\Sigma(\Delta^*)}$ defines a Calabi–Yau hypersurface if Δ is reflexive, which means, by definition, that Δ and its dual

$$\Delta^* = \{x \in N_{\mathbb{R}} \mid (x, y) \geq -1 \ \forall y \in \Delta\} \quad (2.2)$$

are both lattice polytopes. Mirror symmetry corresponds to the exchange of Δ and Δ^* [17]. The generalization of this construction to complete intersections of codimension $r > 1$ (CICYs) was obtained by Batyrev and Borisov [18] who introduced the notion of a nef partition. If $\Delta \subset M_{\mathbb{R}}, \Delta^* \subset N_{\mathbb{R}}$ is a dual pair of d -dimensional reflexive polytopes then a partition $E = E_1 \cup \dots \cup E_r$ of the set of vertices of Δ^* into disjoint subsets E_1, \dots, E_r is called a nef-partition if there exist r integral upper convex $\Sigma(\Delta^*)$ -piecewise linear support functions $\phi_l : N_{\mathbb{R}} \rightarrow \mathbb{R}$ ($l = 1, \dots, r$) such that

$$\phi_l(\rho^*) = \begin{cases} 1 & \text{if } \rho^* \in E_l, \\ 0 & \text{otherwise.} \end{cases}$$

Each ϕ_l corresponds to a semi-ample Cartier divisor

$$D_{0,l} = \sum_{\rho^* \in E_l} D_{\rho^*} \quad (2.3)$$

on \mathbb{P}_{Δ^*} , where D_{ρ^*} is the irreducible component of $\mathbb{P}_{\Delta^*} \setminus \mathbb{T}$ corresponding to the vertex $\rho^* \in E_l$, and $X = D_{0,1} \cap \dots \cap D_{0,r}$ defines a family of Calabi–Yau complete intersections of codimension r . Moreover, each ϕ_l corresponds to a lattice polyhedron Δ_l defined as

$$\Delta_l = \{x \in M_{\mathbb{R}} : (x, y) \geq -\phi_l(y) \ \forall y \in N_{\mathbb{R}}\} \quad (2.4)$$

supporting global sections of the semi-ample invertible sheaf $\mathcal{O}(D_i)$. (The sum of the functions ϕ_l is equal to the support function of the anticanonical bundle of \mathbb{P}_{Δ^*} .) Since the knowledge of the decomposition $E = E_1 \cup \dots \cup E_r$ is equivalent to that of the set of supporting polyhedra $\Pi(\Delta) = \{\Delta_1, \dots, \Delta_r\}$, this data is often also called a nef partition. [18] further observed that, for a nef partition $\Pi(\Delta)$, the polytopes $\nabla_l = \langle \{0\} \cup E_l \rangle \subset N_{\mathbb{R}}$ also define a nef partition $\Pi^*(\nabla) = \{\nabla_1, \dots, \nabla_r\}$ such that the Minkowski sum $\nabla = \nabla_1 + \dots + \nabla_r$ is a reflexive polytope.

This leads to a combinatorial manifestation of mirror symmetry in terms of dual pairs of nef partitions of Δ^* and ∇^* ,

$$\begin{array}{ccc} M_{\mathbb{R}} & & N_{\mathbb{R}} \\ \Delta = \Delta_1 + \dots + \Delta_r & (\Delta_l, \nabla_{l'}) \geq -\delta_{ll'} & \Delta^* = \langle \nabla_1, \dots, \nabla_r \rangle \\ \nabla^* = \langle \Delta_1, \dots, \Delta_r \rangle & & \nabla = \nabla_1 + \dots + \nabla_r \end{array} \quad (2.5)$$

where the angles denote the convex hull. This yields a pair (X, X^*) of Calabi–Yau varieties, where $X \subset \mathbb{P}_{\Delta^*}$ and $X^* \subset \mathbb{P}_{\nabla^*}$ are mirror to each other.

Mirror symmetry identifies the quantum corrected Kähler moduli space of X with the uncorrected complex structure moduli space of X^* . For details see the excellent treatise in [19]. The deformations of the complex structure of X^* are encoded in the periods $\int_{\gamma} \Omega$ and the latter can be computed from the equations that cut X^* out of \mathbb{P}_{∇^*} . For this reason, we now describe these equations for X^* (instead of those of X which is the space of interest). Given the nef partition $\Delta^* = \langle \nabla_1, \dots, \nabla_r \rangle$, $\nabla_l = \langle E_l, \{0\} \rangle$, we define $a_m \in \mathbb{C}$ to be the coefficients of the Laurent polynomials f_1, \dots, f_r

$$f_l(t) = a_{0,l} - \sum_{m \in A_l} a_m t^m, \quad l = 1, \dots, r \quad (2.6)$$

where $t^m = \prod_{j=1}^d t_j^{m_j}$ and $t \in \mathbb{T} \subset \mathbb{P}_{\nabla^*}$ are the coordinates in the algebraic torus. The set A_l is the set of all points in ∇_l . The simultaneous vanishing of these polynomials f_l then defines the complete intersection Calabi–Yau manifold $X^* \subset \mathbb{P}_{\Delta^*}$, or in other words, the ∇_l are the Newton polyhedra for the f_l . Similarly, the Δ_l are the Newton polyhedra for X . In Section 2.5 we will discuss the combinatorial duality in (2.5) in detail for an example. The computation of the periods starting from (2.6) will be exhibited in the same example in Appendix A.

In [20] Batyrev and Borisov were able to obtain a formula for the generating function

$$E(t, \bar{t}) = \sum (-1)^{p+q} h^{pq} t^p \bar{t}^q = \sum_{I=[x,y]} \frac{(-)^{\rho_x t^{\rho_y}}}{(t\bar{t})^r} S(C_x, \frac{\bar{t}}{t}) S(C_y^*, t\bar{t}) B_I(t^{-1}, \bar{t}) \quad (2.7)$$

of the Hodge numbers h^{pq} of a toric CICY with dimension $d - r$ in terms of the combinatorial data of the $d + r$ dimensional Gorenstein cone $\Gamma(\Delta_l)$ spanned by vectors of the form (e_l, v) , where e_l is a unit vector in \mathbb{R}^r and $v \in \Delta_l$.² In this formula x, y label faces C_x of dimension ρ_x of $\Gamma(\nabla_l)$ and C_x^* denotes the dual face of the dual cone $\Gamma(\Delta_l)$. The interval $I = [x, y]$ labels all cones that are faces of C_y containing C_x . The polynomials $B_I(t, \bar{t})$ encode the combinatorics of the face lattice [20]. The polynomials $S(C_x, t) = (1 - t)^{\rho_x} \sum_{n \geq 0} t^n l_n(C_x)$ of degree $\rho_x - 1$ are related to the numbers $l_n(C_x)$ of lattice points at degree n in C_x and hence to the Ehrhart polynomial [23] of the Gorenstein polytope generating C_x [20]. A Gorenstein cone Γ is, by definition, generated by lattice points ρ_i with $\langle \rho_i, n_0 \rangle = 1$ for some vector n_0 in the dual lattice.

²The $d + r$ dimensional cone $\Gamma(\nabla_l)$ originates from the Cayley trick, which relates the vanishing set of the r equations $f_l = 0$ to the complement of the hypersurfaces $1 - \sum a_l f_l = 0$ [21, 22] with Δ_l being the Newton polytopes of f_l .

n_0 is unique if Γ has maximal dimension and its duality pairing defines a nonnegative grading of Γ . The points of degree 1 form the Gorenstein polytope, whose vertices generate Γ . The points of higher degree will play an important role in Section 2.3.

When we define the variety $\mathbb{P}_{\Delta^*} = V_{\Sigma(\Delta^*)}$, the fan $\Sigma(\Delta^*)$ is not only specified by the lattice N , and the polyhedron $\Delta^* \subset N$ but also by a triangulation $T = T(\Delta^*)$. For simplicity, we will suppress the choice of a triangulation in the notation. However, we want to point out that in the case of complete intersections only those triangulations are compatible with a given nef partition that can be lifted to a triangulation of the corresponding Gorenstein cone $\Gamma(\Delta^*)$ [24], i.e. the triangulation actually is $T = T(\Gamma(\Delta^*))$. Note that in the case of hypersurfaces, triangulating the Gorenstein cone is the same as triangulating the polyhedron. Hence, the distinction does not play a role. In codimension $r > 1$, however, there are in general differences due to the nef partition. An example will be discussed in Section 3.2.4.

In the case of hypersurfaces, $r = 1$, it is known [17] that the Picard number can also be computed with the formula

$$h^{11} = l(\Delta^*) - 1 - d - \sum_{\text{codim}(\Theta^*)=1} l^*(\Theta^*) + \sum_{\text{codim}(\Theta^*)=2} l^*(\Theta^*)l^*(\Theta) \quad (2.8)$$

where Θ and Θ^* are faces Δ and Δ^* , respectively. $l(\Theta)$ is the number of lattice points of a face Θ , and $l^*(\Theta)$ the number of its interior points. This formula has a simple interpretation (see also [25]): The principal contributions come from the toric divisors $D_i = \{z_i = 0\}$ that correspond to points in Δ^* different from the origin. There are d linear relations among these divisors. The first sum corresponds to the subtraction of interior points of facets. The corresponding divisors of the ambient space do not intersect a generic Calabi–Yau hypersurface. Lastly, the bilinear terms in the second sum can be understood as multiplicities of toric divisors so that their presence indicates that only a subspace of the cohomology (*i.e.* the Kähler moduli space) can be analyzed with toric methods.

Unfortunately, the general formula (2.7) does not lend itself to a similar interpretation in any known way.³ As for hypersurfaces, interior points of facets of Δ^* never contribute divisors to a toric Calabi–Yau, but explicit computations of intersection rings show that for complete intersection it may happen that even for vertices ρ_i the corresponding divisor D_i does not intersect $[X] = \bigcap_{l=1}^r D_{0,l}$, where corresponds to the l^{th} equation f_l of the mirror X^* of the Calabi–Yau variety X . A simple example is the blowup by a non-intersecting divisor of the degree (3,4) CICY in \mathbb{P}_{111112}^5 with Hodge numbers (1,79) that is discussed in [26]. It is very important to find a more explicit formula for the Picard number of a complete intersection that allows for an interpretation in terms of the multiplicities of divisors D_i after restriction to the Calabi–Yau. There is a good chance that such a formula exists: While intersection numbers depend on the triangulation of the fan we observed in many examples that these multiplicities are independent of the triangulation and thus should depend only on the combinatorics of the data of the polytope that enter (2.7).

³There are, however, more suggestive formulas for h^{11} in special cases [18].

2.2 Free quotients

We now come to the discussion of toric Calabi–Yau spaces with non-trivial fundamental groups. We mainly restrict our attention to the situation where they arise from free quotients coming from group actions that correspond to lattice quotients. We call such quotients *toric*. As we noted above, a refinement of the lattice N always entails singularities in the ambient space and no contributions to the fundamental group [14]. If, however, a CICY does not intersect the singular locus of that quotient then the group acts freely on that variety and π_1 becomes isomorphic to G . This is the case if the refinement of the lattice does not lead to additional lattice points of Δ^* . For a given pair of reflexive polytopes, the dual of the lattice M' that is spanned by the vertices of Δ is the finest lattice N' with respect to which the polytope is reflexive. If the lattice N_0 that is spanned by the vertices of Δ^* is a proper sublattice of the lattice N' then any subgroup of N'/N_0 corresponds to a different choice of the N lattice and hence to a different toric CY hypersurface. There is thus only a finite number of lattices that have to be checked to find all toric free quotients.

Some well-known examples are the free \mathbb{Z}_5 quotient of the quintic and the free \mathbb{Z}_3 quotient of the CY hypersurface in $\mathbb{P}^2 \times \mathbb{P}^2$. For both cases cyclic permutation of the coordinates of the projective spaces defines another free group action of the same order that commutes with the toric quotient, leading to Euler numbers 8 and 18, respectively. These free “double quotients” are, however, not toric in the sense that the resulting manifold is not a CICY in a toric variety. Analyzing the complete list of 473'800'776 reflexive polytopes for CY hypersurfaces [27–29] one finds 14 more examples of toric free quotients [30]: The elliptically fibered \mathbb{Z}_3 quotient of the degree 9 surface in \mathbb{P}_{11133}^4 , whose group action on the homogeneous coordinates is given by the phases $(1, 2, 1, 2, 0)/3$, and 13 elliptic K3 fibrations where the lattice quotient has index 2. Among the latter there is the \mathbb{Z}_2 quotient of $(\mathbb{P}^1)^4$ with phases $(0, \frac{1}{2})$ on each factor which admits an additional \mathbb{Z}_2 freely acting on the CY hypersurface by simultaneous exchange of the coordinates of all \mathbb{P}^1 factors. Models of a similar type are currently studied because of their promising phenomenological properties [31], [32].

The condition that $\Delta^* \cap N$ and $\Delta^* \cap N'$ coincide is sufficient for a free quotient of a CICY with dimension up to 3 because the singularities of a maximal crepant resolution are at codimension 4 and can be avoided by a generic choice of the defining equations. It is, however, not necessary: Divisors corresponding to interior points of facets of Δ^* do not intersect the CY and hence do not kill the fundamental group if they are generated by a refinement of the N lattice⁴.

An analysis of the complete lists of reflexive polytopes with up to 4 dimensions shows that the only case where the weaker condition is relevant for hypersurfaces is that of the torus. In that case a free \mathbb{Z}_3 quotient in \mathbb{P}^2 , and a free \mathbb{Z}_2 in \mathbb{P}_{112}^2 and in $\mathbb{P}^1 \times \mathbb{P}^1$ can be realized torically in the obvious way. Taking a product with a (toric) K3 this can be used to construct CICYs at codimension 2 with first Betti number $b_1 = 2$. The resulting Hodge numbers are $h^{11} = 13$ for the \mathbb{Z}_2 quotients and $h^{11} = 9$ in case of \mathbb{Z}_3 ; the simplest examples are $\mathbb{P}^2 \times \mathbb{P}_{1122}^3$ with group action $(0, 1, 2; 0, 1, 0, 2)/3$ for \mathbb{Z}_3 , and $\mathbb{P}_{112}^2 \times \mathbb{P}^3$ with phases $(0, 1, 1; 0, 1, 0, 1)/2$ or $\mathbb{P}^1 \times \mathbb{P}^1 \times \mathbb{P}^3$ with phases $(0, 1; 0, 1; 0, 1, 0, 1)/2$ for \mathbb{Z}_2 . These Hodge numbers have also been

⁴This criterion has been suggested by Victor Batyrev (private communication).

obtained for Landau–Ginzburg orbifold models [10], where the values $h^{11} = 3, 5, 9, 13$ were found for $h^{01} = 1$ [10, 29]. One might expect that the models with 3 and 5 would require a larger order of the free group action. It was shown, however, in [10] that the 1-forms in Landau–Ginzburg models can only arise if the model factors into $T^2 \times K3$. Moreover, the twist that reduces the Picard number must act with unit determinant on the T^2 and hence must agree with the free \mathbb{Z}_3 on the elliptic curve in \mathbb{P}^2 or with the free \mathbb{Z}_2 on \mathbb{P}_{112}^2 that we already know from the other examples. Only the K3s can be realized in different ways. Indeed, analyzing the lists of [10] we found several realizations of these Hodge numbers with K3s that correspond to the generalized Calabi–Yau varieties in the sense of [33, 34] like the cubic in \mathbb{P}^5 , where a \mathbb{Z}_3 -twist with phases $(1, 1, 1, 0, 0, 0)/3$ and a free action on the torus leads to $h^{11} = h^{12} = 3$ and the degree 12 hypersurface in \mathbb{P}_{334446}^5 where a \mathbb{Z}_2 with phases $(0, 0, 0, 0, 1, 1)/2$ and a free action on the torus in \mathbb{P}_{112}^2 leads to $h^{11} = h^{12} = 5$. For all of these models a mirror construction is available both in the CFT framework [35, 36] and, more geometrically, in terms of reflexive Gorenstein cones [34].

There are many more examples of toric free quotients for CICYs with codimension $r > 1$, some of which will play a role later on. In that case a group may act freely under even weaker conditions because even divisors that correspond to vertices may not intersect the CY. But with the present state of the art this requires a case by case analysis of the intersection ring. For Calabi–Yau 4-folds, on the other hand, the above criterion for a free quotient is no longer sufficient because the codimensions of the singularities in the ambient space may be too small to avoid them by an appropriate choice of the hypersurface equations. There are many examples where this happens.⁵

2.3 Resolution of terminal singularities

It is known that the points on the polyhedron Δ^* are in general not sufficient to give a smooth ambient space [5, 37]. In addition, one may have to take into account certain points in degree greater than one, *i.e.* points in $k\Delta^*$, $k > 1$, in order to resolve all singularities. In this section we give a general discussion of these points, in particular in the context of constructing smooth complete intersection Calabi–Yau spaces.

The toric ambient space is smooth if its fan is simplicial and unimodular, *i.e.* if all its cones are simplicial and generated by (a subset of) a lattice basis. Suppose we have added all the lattice points in the polyhedron Δ^* and determined one of the possible star triangulations of this set of points. A star triangulation is a triangulation T for which all maximal simplices

⁵Free quotients can be constructed easily with PALP [30]. To find all candidates among quotients of the sextic 4-fold one can use the following commands (`zbin.aux` is an auxiliary file storing polytopes on sublattices)

```
$ cws.x -w5 6 6 -r | class.x -f -sv -po zbin.aux
$ class.x -b -pi zbin.aux | class.x -sp -f
```

and obtains the N -lattice polytopes in a basis where the lattice quotient is diagonal.

```
$ class.x -b -pi zbin.aux | class.x -sp -f | cws.x -N -f | poly.x -fg
```

displays weight systems and Hodge data. This yields 6 candidates for free \mathbb{Z}_3 quotients. They are, however, all singular, as the Euler numbers are bigger than $1/3$ of those of the respective covering spaces.

contain the origin of Δ^* . In other words, each simplex $\sigma \in T$ determines a pointed cone C_σ , *i.e.* a cone over a facet of Δ^* whose apex is the origin. If there is a simplex, say σ , with $\text{Vol}(\sigma) > 1$, then the corresponding coordinate patch $U_\sigma = \text{Spec } \mathbb{C}[\sigma^\vee \cap M]$ of the toric variety will be singular. Reflexivity implies that the resulting triangulation of the fan is unimodular if and only if the induced triangulations of the facets only consist of unimodular simplices. This is always the case in 3 dimensions, but for higher-dimensional ambient spaces there can be singularities at codimension 4. Generic complete intersection Calabi–Yau 3-fold (and even more so K3 surfaces) are smooth because the singularities of the ambient space can be avoided by an appropriate choice of the parameter on dimensional grounds. For the evaluation of the Mori cone of the ambient space we will, however, need to resolve all of its singularities. Resolutions that involve points at higher degree $k > 1$ are discrepant, *i.e.* they contribute to the canonical class of the ambient space. This does not, however, spoil triviality of the canonical bundle of the Calabi–Yau complete intersection, which does not intersect the additional exceptional divisors.

We first discuss the case of 4-dimensional polytopes, which is relevant for Calabi–Yau hypersurfaces. For the 3-dimensional intersection of the cone with volume V with the relevant facet we can always choose a basis with $\nu_0^* = 0$, $\nu_1^* = e_1$, $\nu_2^* = e_2$ and $\nu_3^* = (x, y, V)^T$ with $0 \leq x \leq y < V$. Emptiness of this tetrahedron, *i.e.* absence of additional lattice points in the convex hull, further constrains the vector (x, y) and lattice automorphisms make some of the allowed combinations redundant. Clearly the number of lattice points in the semi-open parallelepiped $\Pi_\sigma = \{\sum \lambda_i \nu_i^* \mid \lambda_i \in [0, 1) \subset \mathbb{R}\}$ is equal to the volume. The $V - 1$ non-zero lattice points in Π_σ form the Hilbert basis $\text{Hilb}_\sigma = \Pi_\sigma \cap N - \{0\}$ of the semi-group of lattice points in the cone that is generated by ν_i^* . There is a duality $\lambda_i \rightarrow 1 - \lambda_i$ so that it is sufficient to determine all lattice points at degree up to half the dimension of the facet, where ν_i^* have degree 1. It is natural to try to resolve the singularities by first adding the rays that are generated by the points in Hilb_σ . This turned out to be sufficient for all our examples. There are, however, empty simplices that span Gorenstein cones whose resolution requires additional rays (see below).

The simplest case in 4 dimensions, which are relevant for CY hypersurfaces, is the simplex with $x = y = 1$. It obviously is empty for any volume. The $V - 1$ interior points of Π are $\frac{l}{V}(\nu_0^* + \nu_3^*) + (1 - \frac{l}{V})(\nu_1^* + \nu_2^*)$ for $0 < l < V$. This leads to the matrix

$$\begin{pmatrix} 1 & 1 & 1 & 1 & 2 & 2 & \dots & 2 \\ 0 & 1 & 0 & 1 & 1 & 1 & \dots & 1 \\ 0 & 0 & 1 & 1 & 1 & 1 & \dots & 1 \\ 0 & 0 & 0 & V & 1 & 2 & \dots & V-1 \end{pmatrix} \quad (2.9)$$

of column vectors, whose first coordinate is the degree of the corresponding point in the Gorenstein cone spanned by ν_i^* in an appropriate basis. It is easily checked that the unique maximal star triangulation, consisting of the $4(V - 1)$ simplicial cones spanned by the tetrahedra

- 1.: ν_1^*, ν_2^* , the first point at degree 2 and one of ν_0^* or ν_3^* ,
- 2.: $(\nu_0^*, \nu_1^*), (\nu_0^*, \nu_2^*), (\nu_1^*, \nu_3^*)$ or (ν_2^*, ν_3^*) and two adjacent points at degree 2,
- 3.: ν_0^*, ν_3^* , the last point at degree 2 and one of ν_1^* or ν_2^* ,

is unimodular for every $V > 1$. The first example that cannot be brought into this form shows

up at volumes 5. In an appropriate basis we find

$$\begin{pmatrix} 1 & 1 & 1 & 1 & 2 & 2 & 2 & 2 \\ 0 & 1 & 0 & 1 & 1 & 1 & 1 & 1 \\ 0 & 0 & 1 & 2 & 1 & 1 & 2 & 2 \\ 0 & 0 & 0 & 5 & 1 & 2 & 3 & 4 \end{pmatrix} \quad (2.10)$$

This is the simplest example where Hilb_σ is not sufficient and a point at degree 3 is required for a unimodular triangulation.

For complete intersections at codimension two we need a similar discussion for 5-dimensional polytopes. At this point it is useful to recall the notion of a circuit (see e.g. [22]). A circuit is a collection Z of points in an affine space such that any proper subset $Z' \subset Z$ is affinely independent but Z itself is not, *i.e.* the points satisfy

$$\sum_{\nu_m^* \in Z} c_m \nu_m^* = 0 \qquad \sum_{\nu_m^* \in Z} c_m = 0 \quad (2.11)$$

In other words, we can obtain a circuit by adding one point in general position to the set of vertices of a simplex. It can be shown that the convex hull of a circuit has precisely the two triangulations $T_\pm = \{\text{conv}(Z \setminus \{\nu_m^*\}) | \nu_m^* \in Z_\pm\}$, where $Z_\pm = \{\nu_m^* \in Z | c_m \lessgtr 0\}$. As an easy consequence we note that the volumes $\text{Vol}(Z \setminus \{\nu_m^*\})$ are proportional to the modulus $|c_m|$ of the coefficients in the linear relation. This gives therefore an easy way to find simplices of the triangulation of Δ^* whose volume is larger than one, and have to be subdivided.

The simplest case of a singularity in higher-dimensional simplices is the one where the volume comes from a facet, from which the remaining vertex thus has distance 1. This effectively reduced the dimension of the problem by one because we just need to triangulate the facet and joining the (unimodular) simplices of the triangulation with additional vertices. Clearly such singularities come in pairs and the simplex on the other side of the facet has to be triangulated in a consistent way. As long as the triangulation of the facet is unique (as in all our examples) this is automatic.

This leaves us with a discussion of simplices whose volume is larger than that of any of its facets. In 5 dimensions this can only occur for volume $V > 2$. We again choose a basis of the form⁶ $\nu_0^* = 0$ and $\nu_i^* = e_i$ for $i < 4$. For volume 3 there is only one case with points in the interior Π^0 of Π , namely $\nu_4^* = (2, 2, 2, 3)^T$, so that $\mu = (2\nu_0^* + \nu_1^* + \nu_2^* + \nu_3^* + \nu_4^*)/3 \in \Pi^0$ has degree 2 and $\mu' = S - \mu$ with $S = \sum \nu_i^*$ is its dual interior point at degree 3. Addition of the ray generated by μ splits the cone into 5 simplices, four of which are unimodular while $\langle \mu \nu_1^* \nu_2^* \nu_3^* \nu_4^* \rangle$ has volume 2. Since $2\mu' = \mu + \nu_1^* + \nu_2^* + \nu_3^* + \nu_4^*$ the remaining singularity is resolved by adding the unique interior point $\mu' \in \Pi^0$ at degree 3. We thus end up with the 9 unimodular cones generated by $\langle \mu 0 \widehat{1234} \rangle$ and $\langle \mu' \widehat{\mu 1234} \rangle$, where the vertices ν_i^* of the original simplex are represented by their indices i and the hat indicates to take all simplices that arise by dropping one of the respective points.

⁶This would not cover the most general case for 6-dimensional Gorenstein cones because there are empty simplices in \mathbb{R}^5 with no unimodular facets [38].

At volume 4 there must be at least one nonsimplicial facet (this is true for every even volume in 5 dimensions because interior points of Π come in pairs at degrees 2 and 3, respectively). There is, again, only one class of cones with an interior point μ , for which we can choose $\nu_4^* = (1, 1, 1, 4)^T$ and thus $\mu = (2\nu_0^* + \nu_1^* + \nu_2^* + \nu_3^* + 3\nu_4^*)/4 \in \Pi^0$. If we first resolve the singularity of the facet with volume 2, which does not contain ν_0^* , by adding its degree two point $\rho = (\nu_1^* + \nu_2^* + \nu_3^* + \nu_4^*)/2$ we are left with 4 simplices of volume 2. Since $\mu = (\rho + \nu_0^* + \nu_4^*)/2$ is located at the intersection of 3 of these simplices it resolves all but the simplex $\langle \nu_0^* \nu_1^* \nu_2^* \nu_3^* \rho \rangle$, which has volume 2. The remaining singularity is resolved by the interior point $\mu' = S - \mu = (\nu_0^* + \nu_1^* + \nu_2^* + \nu_3^* + \rho)/2 \in \Pi^0$ at degree 3. We thus obtain the 14 unimodular cones $\langle \rho \widehat{\mu 04} \widehat{123} \rangle$ and $\langle \mu' \widehat{0123} \rho \rangle$.

We finish our discussion with the case of volume 5. In addition to the two cases where the volume comes from a facet there are two inequivalent situations with interior points:

For the first class of examples with 5 unimodular facets we can choose $\nu_4^* = (1, 2, 2, 5)^T$. Adding the rays generated by the two points $\mu_1 = (\nu_0^* + \nu_1^* + 2\nu_2^* + 2\nu_3^* + 4\nu_4^*)/5$ and $\mu_2 = (3\nu_0^* + 3\nu_1^* + \nu_2^* + \nu_3^* + 2\nu_4^*)/5$ at degree 2 we find a unique maximal triangulation with 8 unimodular cones and the 3 singular cones $\langle \widehat{01\mu_1} 23\mu_2 \rangle$ with volume two, which are resolved by adding the rays through the points $\mu'_1 = \frac{1}{2}(\nu_0^* + \nu_1^* + \nu_2^* + \nu_3^* + \mu_2)$ and $\mu'_2 = \frac{1}{2}(\nu_2^* + \nu_3^* + \mu_1 + \mu_2)$. All together this yields the 21 unimodular cones $\langle \widehat{01} 234\mu_1 \rangle$, $\langle \widehat{01\mu_1} \widehat{23} 4\mu_2 \rangle$, $\langle \widehat{0123\mu_2} \mu_1 \mu'_1 \rangle$ and $\langle \widehat{01} \widehat{23\mu_1\mu_2} \mu'_2 \rangle$. The last case at volume 5 is given by $\nu_4^* = (1, 1, 3, 5)^T$. It is slightly more complicated because the interior points $\mu_1 = (\nu_0^* + \nu_1^* + \nu_2^* + 3\nu_3^* + 4\nu_4^*)/5$ and $\mu_2 = (2\nu_0^* + 2\nu_1^* + 2\nu_2^* + \nu_3^* + 3\nu_4^*)/5$ at degree 2 now admit two different maximal triangulations. Only the one where we first add μ_2 and then subdivide with $\mu_1 = \frac{1}{2}(\nu_3^* + \nu_4^* + \mu_2)$, which consists of 10 unimodular simplices and the simplex $\langle 0123\mu_2 \rangle$ with volume 3, is refined to a unimodular triangulation by $\mu'_1 = \frac{1}{3}(\mu_2 + 2\nu_0^* + 2\nu_1^* + 2\nu_2^* + \nu_3^*)$ and $\mu'_2 = \frac{1}{2}(\mu'_1 + \mu_2 + \nu_3^*)$. The resolution of the singularity thus again requires 21 simplices, namely $\langle \widehat{012} \widehat{34\mu_2} \mu_1 \rangle$, $\langle 0124\mu_2 \rangle$, $\langle 012 \widehat{3\mu_2} \mu'_1 \rangle$ and $\langle \widehat{012} \widehat{3\mu_2\mu'_1} \mu'_2 \rangle$.

Since we are ultimately interested in complete intersection Calabi–Yau spaces in toric varieties described by the polyhedron Δ^* , we also have to associate these extra points with the nef partition of Δ^* and determine their contributions to the corresponding divisors $D_{0,l}$. This follows from the properties of the integral piecewise linear functions used in the definition of the nef-partition given in section 2.1. Indeed, while the additional rays need not belong to any of the cones over ∇_l , the values of the corresponding linear functions are integral on their generators (and obviously add up to their degrees). Therefore, (2.3) becomes

$$D_{0,l} = \sum_{\nu_i^* \in E_l} D_i + \sum_q c_{r,q,l} D_{r,q}, \quad (2.12)$$

where the second sum runs over the extra points μ, μ', ρ, \dots needed for the resolution and the coefficients $c_{r,q,l}$ are integers and satisfy $\sum_{l=1}^r c_{r,q,l} = k$. For example, in the case $d = 5$ and $r = 2$, *i.e.* Calabi–Yau threefolds, and $\text{Vol}(\sigma) = 2$ only an even number of the ν_i^* , $i = 0, \dots, 3$ in (2.9) can belong to one E_l , and therefore $(c_{r,1}, c_{r,2})$ is either $(2, 0)$, $(1, 1)$, or $(0, 2)$ (we dropped the index $q = 1$).

One last point concerns the toric quotients of section 2.2. If the variety is a quotient, the volumes of all the simplices will be multiples of the index $N' : N_0$. In this case it is much

simpler to work on the simply connected covering space so that we only need to resolve the singularities of its ambient toric variety.

2.4 Fibrations

We will now discuss some properties of fibrations. Again, we restrict ourselves where the combinatorial data of the polytopes contain the relevant information. For general, also non-toric K3 surfaces and Calabi–Yau 3-folds there exists a criterion by Oguiso for the existence of elliptic and K3 fibrations in terms of intersection numbers [8]. We will state it in Section 3.2.2. Like the latter, fibration properties thus depend on the triangulation, or in other words, on the choice of the phase in the extended Kähler moduli space.

For toric Calabi–Yau spaces there is, however, a more direct way to search for fibrations that manifest themselves in the geometry of the polytope and to single out appropriate triangulations [39], [40], [41], [28]. These fibrations descend from toric morphisms of the ambient space [12, 42]: Let Σ and Σ_b be fans in N and N_b , respectively, and let $\phi : N \rightarrow N_b$ be a lattice homomorphism that induces a map of fans $\phi : \Sigma \rightarrow \Sigma_b$ such that for each cone $\sigma \in \Sigma$ there is a cone $\sigma_b \in \Sigma_b$ that contains the image of σ . Then there is a T -equivariant morphism $\tilde{\phi} : V_\Sigma \rightarrow V_{\Sigma_b}$ and the lattice N_f for the fibers is the kernel of ϕ in N .

For our construction of a fibered Calabi–Yau variety we require the existence of a reflexive section $\Delta_f^* \subset \Delta^*$ of the polytope $\Delta^* \subset N_\mathbb{R}$. The toric morphism ϕ is then given by the projection along the linear space spanned by Δ_f^* and N_b is defined as the image of N in the quotient space $N_\mathbb{R}/\langle \Delta_f^* \rangle_\mathbb{R}$. In order to guarantee the existence of the projection we choose a triangulation of Δ_f^* and then extend it to a triangulation of Δ^* . For each such choice we can interpret the homogeneous coordinates that correspond to rays in Δ_f^* as coordinates of the fiber and the others as parameters of the equations and hence as moduli of the fiber space. Reflexivity of the fiber polytope Δ_f^* ensures that the fiber also is a CICY because a nef partition of Δ^* automatically induces a nef partition of Δ_f^* . This follows immediately from the definition by restriction of the convex piecewise linear functions defining the partition to $(N_f)_\mathbb{R}$.

For hypersurfaces the geometry of the resulting fibration has been worked out in detail in [41]. The codimension r_f of the fiber generically coincides with the codimension r of the fibered space also for complete intersections. For $r > 1$ it may happen, however, that Σ_f^1 does not intersect one (or more) of the E_l 's, in which case the codimension decreases. An example of that type is the model

$$\mathbb{P} \left(\begin{array}{cccccccc} 2 & 2 & 2 & 4 & 1 & 1 & 0 \\ 0 & 0 & 0 & 4 & 1 & 1 & 2 \end{array} \right) \left[\begin{array}{c} 8 \\ 8 \end{array} \middle| \begin{array}{c} 4 \\ 0 \end{array} \right] / \mathbb{Z}_2 : 1 \ 1 \ 0 \ 1 \ 1 \ 0 \ 0 \quad (2.13)$$

with $h^{11} = 3$ and $h^{12} = 43$, which is a free \mathbb{Z}_2 quotient of a blowup of \mathbb{P}_{222411}^5 with the position of the additional vertex $\nu_7^* = -\frac{1}{2}(4\nu_4^* + \nu_5^* + \nu_6^*)$ given by the second linear relation, i.e. the bottom line in the parenthesis. (This notation will be explained in more detail in the next subsection.) This polytope has one nef partition with $E_1 = \{\nu_3^*, \nu_4^*, \nu_5^*, \nu_6^*, \nu_7^*\}$ and $E_2 = \{\nu_1^*, \nu_2^*\}$. The corresponding bidegrees are separated by a vertical line in the bracket

(they are given by the sums of the gradings of the homogeneous coordinates that correspond to the vertices that belong to E_l). The codimension two fiber polytope Δ_f^* that is spanned by ν_4^*, \dots, ν_7^* has all of its vertices in E_1 so that we obtain a K3 fibration with the generic fiber being a degree 8 hypersurface in \mathbb{P}_{4112}^3 instead of an elliptic codimension two fiber that would naively be expected.

In our searches for fiber spaces with certain properties we mostly restricted attention to the generic case where $r = r_f$. We also analyzed the intersection numbers of many spaces and found no example where a fibration has no toric realization, provided that the possible change of the codimension is taken into account. There are, however, cases where the fibration does not lift to a toric morphism of the ambient space. An example is the polytope (3.17) which will be discussed in subsection 3.2.3. Reflexivity of the Δ_f^* is thus sufficient but not necessary for a fibration structure of a complete intersection.⁷

2.5 The (2,30) example

In this subsection we will discuss a set of examples of CICYs in great detail. We will exhibit their non-trivial fundamental group, their fibrations, and their partitions.

In our analysis of the geometry and of applications of complete intersections it was natural to start with models with a small number h^{11} of Kähler moduli. In this realm it is quite likely that our lists of toric CICYs is fairly complete, at least for codimension two. Among the one-parameter models we found only two new Hodge numbers, namely $h^{12} = 25$ for the free \mathbb{Z}_3 quotient of the degree (3,3) CICY in \mathbb{P}^5 and $h^{12} = 37$ for the free \mathbb{Z}_2 quotient of the degree (4,4) CICY in \mathbb{P}_{111122}^5 . The Picard–Fuchs equations of the respective universal covers were both analyzed in [43].

We therefore turn to the list of 2-parameter examples, the first of which have Hodge numbers (2,30). They will serve as our main examples in this and the next section.⁸ In the appendix we compile a brief overview of toric CICYs with small h^{11} .

There are three different polytopes which allow for codimension two complete intersections with Hodge numbers (2,30). These have eight or nine vertices and no additional boundary points. In a convenient basis the coordinates of the vertices of the first of these polytopes are given by the column vectors

$$\Delta_{(A)}^* \ni \{\nu_i^*\} = \left\{ \begin{array}{cccccccc} 1 & 0 & 0 & 0 & -2 & 1 & -1 & -1 \\ 0 & 1 & 0 & 0 & -1 & 1 & -1 & 0 \\ 0 & 0 & 1 & 0 & -1 & 1 & -1 & 0 \\ 0 & 0 & 0 & 1 & -1 & 0 & 0 & 0 \\ 0 & 0 & 0 & 0 & 0 & 2 & -2 & 0 \end{array} \right\} \quad (2.14)$$

If the number of vertices is close to the simplex case it is most economical to describe a polytope in a coordinate independent way by the linear relations among the vertices. This data

⁷Note that Δ_f^* is the intersection of Δ^* with the linear fiber space $(N_f)_{\mathbb{R}}$ which need not be a lattice polytope and thus can be larger than the convex hull of $\Delta^* \cap N_f$.

⁸The first hypersurfaces example (2,29) is the free \mathbb{Z}_3 quotient of the degree (3,3) hypersurface in $\mathbb{P}^2 \times \mathbb{P}^2$.

is sufficient if the lattice N is generated by the vertices. Otherwise it has to be supplemented by an abelian group action that defines the lattice. The toric variety corresponding to the polytope $\Delta_{(A)}^*$, generalizing the notation \mathbb{P}_w^n or $\mathbb{P}^n(w)$ in the simplex case, is thus

$$\mathbb{P}_{\Delta_{(A)}^*} = \mathbb{P} \left(\begin{array}{cccccccc} 2 & 1 & 1 & 1 & 1 & 0 & 0 & 0 \\ 0 & 0 & 0 & 0 & 0 & 1 & 1 & 0 \\ 1 & 0 & 0 & 0 & 0 & 0 & 0 & 1 \end{array} \right) / \mathbb{Z}_2 : 1 \ 1 \ 1 \ 0 \ 0 \ 1 \ 0 \ 0 \quad (2.15)$$

The lines in the parenthesis indicate the linear relations among the vertices. The first two tell us that the toric variety corresponds to a product space $\mathbb{P}_{21111}^4 \times \mathbb{P}^1$, while the third linear relation $\nu_1^* + \nu_8^* = 0$ amounts to a blow-up of \mathbb{P}_{21111}^4 by the last vertex ν_8^* . Finally, the group action indicates that the lattice N is not generated by the vertices alone. It requires, as an additional generator, the lattice point $\frac{1}{2}(\nu_1^* + \nu_2^* + \nu_3^* + \nu_6^*)$, *i.e.* the linear combination of vertices that corresponds to the phases of the \mathbb{Z}_2 action on the homogeneous coordinates.

The coordinates displayed in (2.14), with the last line divisible by 2 for *all* lattice points, shows that the CICY is a free quotient. The group action can be recovered by finding an integer linear combination ν^* of the column vectors with coefficients in $\frac{1}{2}\mathbb{Z}$ whose last coordinate is odd (thus refining the lattice). The resulting generator for the \mathbb{Z}_2 action is unique only up to linear combinations with the weight vectors modulo 2, which corresponds to a different choice $\nu^* \rightarrow \nu^* + \Delta\nu^*$ with $\Delta\nu^* = \frac{1}{2}(\nu_2^* + \nu_3^* + \nu_4^* + \nu_5^*) = -\nu_1^*$, $\frac{1}{2}(\nu_6^* + \nu_7^*) = 0$ or $\frac{1}{2}(\nu_1^* + \nu_8^*) = 0$.

Next, we have to look at the possible nef-partitions for $\Delta_{(A)}^*$. It turns out that, up to symmetries,⁹ there is a unique nef partition, given by $E_1 = \{\nu_1^*, \nu_2^*, \nu_4^*, \nu_8^*\}$ and $E_2 = \{\nu_3^*, \nu_5^*, \nu_6^*, \nu_7^*\}$ with the Hodge numbers (2,30). This leads to the partitioning $6 = 4 + 2$, $2 = 2 + 0$ and $2 = 2 + 0$ of the total degrees of the complete intersection X into multidegrees. We will augment the previous notation by a bracket indicating these multidegrees and write

$$X_{(A)} = \mathbb{P} \left(\begin{array}{cccccccc} 2 & 1 & 1 & 1 & 1 & 0 & 0 & 0 \\ 0 & 0 & 0 & 0 & 0 & 1 & 1 & 0 \\ 1 & 0 & 0 & 0 & 0 & 0 & 0 & 1 \end{array} \right) \left[\begin{array}{c} 4 \\ 2 \\ 2 \end{array} \right] / \mathbb{Z}_2 : 1 \ 1 \ 1 \ 0 \ 0 \ 1 \ 0 \ 0 \quad (2.16)$$

In general these degrees do not specify the partition uniquely. We observed, however, in all examples that equal multidegrees of different partitions always lead to the same Hodge numbers. The \mathbb{Z}_2 quotient now indicates that the lattice M is replaced by the sublattice corresponding to monomials that are invariant under the given phase symmetry. Since this quotient does not lead to additional lattice points in $\Delta_{(A)}^*$ the corresponding group action is free on the CICY, *i.e.* $\pi_1(X) = \mathbb{Z}_2$.

In the present example the ambient space is a product space with a \mathbb{P}^1 factor. The CICY is, nevertheless, a nontrivial K3-fibration over \mathbb{P}^1 because the coefficients of the equations defining the K3 fiber X_f depend on the coordinates of the base. The K3 family containing the generic fibers is obtained by dropping the second line and the columns corresponding to ν_6^* and ν_7^* ,

$$X_f = \mathbb{P} \left(\begin{array}{cccccc} 2 & 1 & 1 & 1 & 1 & 0 \\ 1 & 0 & 0 & 0 & 0 & 1 \end{array} \right) \left[\begin{array}{c} 4 \\ 2 \end{array} \right] \quad (2.17)$$

⁹The symmetry group has order 16 and is generated by the transpositions $\nu_2^* \leftrightarrow \nu_3^*$, $\nu_4^* \leftrightarrow \nu_5^*$, $\nu_6^* \leftrightarrow \nu_7^*$ and by the exchange $(\nu_2^*, \nu_3^*) \leftrightarrow (\nu_4^*, \nu_5^*)$.

Note that the \mathbb{Z}_2 quotient does not change the fiber lattice because it also acts on \mathbb{P}^1 , effectively dividing the base by 2. Over the two fixed-points on the base we obtain, however, an Enriques fiber. (Since K3 only admits free \mathbb{Z}_2 quotients and since the group action on the base \mathbb{P}^1 always has fixed points, a free quotient of a K3 fibration can only have order 2.) The induced nef partition is obtained by dropping ν_6^* and ν_7^* from E_2 . It does, of course, lead to the bi-degrees of the divisors given in (2.17).

The lines in the parenthesis of our notation for toric varieties, as in (2.15), (2.16), or (2.17), generate the cone of non-negative linear relations among the points in N . We will often call them *weight vectors*. The definition of the polytope only requires the linear relations among the vertices (and possibly the group action defining a sublattice). For the discussion of fibrations and other geometrical data it is, however, often convenient to include the linear relations among all lattice points of Δ^* . When the partitioning of the total degree $d = \sum w_i$ of a weight vector by the nef partition is specified as $(-d_1, -d_2; w_1, \dots, w_N)$ with $d = d_1 + d_2$ we may also call them *charge vectors* because this is the data that characterizes part of the gauged linear sigma model realization of these geometries [44]. Note that for the definition of the polytope and for the degree data of the nef partition, it is sufficient to give the charge vectors that correspond to the linear relations among the vertices. A more redundant description may, nevertheless, be useful to make fibrations or non-free lattice quotients visible. A complete definition of the model, on the other hand, may require a resolution of singularities through triangulations and the inclusion of additional points. In the weighted projective case the (single) weight vector coincides with the generator of the Mori cone of the ambient space. In general, however, the Mori cone will be larger than the cone that is spanned by the charge vectors.

The other realizations of the (2,30) model are

$$X_{(B)} = \mathbb{P} \left(\begin{array}{cccccccc} 2 & 1 & 1 & 1 & 1 & 0 & 0 & 0 \\ 2 & 2 & 1 & 0 & 1 & 1 & 1 & 0 \\ 1 & 0 & 0 & 0 & 0 & 0 & 0 & 1 \end{array} \right) \left[\begin{array}{c|c} 4 & 2 \\ 4 & 4 \\ 2 & 0 \end{array} \right] / \mathbb{Z}_2 : 111100100 \quad (2.18)$$

with nef partitions $E_1 \cup E_2 = \{\nu_1^*, \nu_3^*, \nu_5^*, \nu_8^*\} \cup \{\nu_2^*, \nu_4^*, \nu_6^*, \nu_7^*\}$, $\{\nu_1^*, \nu_3^*, \nu_4^*, \nu_7^*, \nu_8^*\} \cup \{\nu_2^*, \nu_5^*, \nu_6^*\}$, or $\{\nu_1^*, \nu_2^*, \nu_4^*, \nu_8^*\} \cup \{\nu_3^*, \nu_5^*, \nu_6^*, \nu_7^*\}$ and

$$X_{(C)} = \mathbb{P} \left(\begin{array}{cccccccc} 2 & 1 & 1 & 1 & 1 & 0 & 0 & 0 \\ 2 & 2 & 1 & 0 & 1 & 1 & 1 & 0 \\ 1 & 0 & 0 & 0 & 0 & 0 & 0 & 1 \\ 0 & 1 & 0 & 0 & 0 & 0 & 0 & 1 \end{array} \right) \left[\begin{array}{c|c} 4 & 2 \\ 4 & 4 \\ 2 & 0 \\ 0 & 2 \end{array} \right] / \mathbb{Z}_2 : 1111001000 \quad (2.19)$$

with two possible nef partitions $E_1 \cup E_2 = \{\nu_1^*, \nu_3^*, \nu_4^*, \nu_7^*, \nu_8^*\} \cup \{\nu_2^*, \nu_5^*, \nu_6^*, \nu_9^*\}$ or $\{\nu_1^*, \nu_3^*, \nu_5^*, \nu_8^*\} \cup \{\nu_2^*, \nu_4^*, \nu_6^*, \nu_7^*, \nu_9^*\}$. The polytope $\Delta_{(B)}^*$ for $X_{(B)}$ has the same ‘‘K3 fiber’’ polytope as $\Delta_{(A)}^*$, but the two points above and below the fiber-hyperplane are shifted along the fiber as can be seen by the non-zero entries $(2, 2, 1, 0, 1)$ in the second line, below the weights of the fiber. The ambient space looks, at first sight, like a non-trivial fibration over the \mathbb{P}^1 with homogeneous coordinates $(x_6 : x_7)$. This is, however, not true because the line $\overline{\nu_6^* \nu_7^*}$ now intersects the fiber hyperplane outside the convex hull of the other lattice points. This line thus becomes an edge of any star triangulation of $\Delta_{(B)}^*$ so that the points in the intersection $D_6 \cap D_7$, which have homogeneous coordinates $x_6 = x_7 = 0$, have no image in the base \mathbb{P}^1 .

We will see in the next section that $X_{(A)}$ and $X_{(B)}$ are nevertheless diffeomorphic and that their Picard–Fuchs equations are related by a change of variables. In particular, also $X_{(B)}$ is a K3 fibration. This is only possible if $D_6 \cap D_7$ does not intersect the CICY (as is indeed the case).

The polytope $\Delta_{(C)}^*$ is similar to $\Delta_{(B)}^*$ except for an additional blowup of the fiber polytope with an exceptional divisor D_9 that, as we will see in subsection 3.2.3, does not intersect the Calabi–Yau threefold. The additional point does, however, make the K3 fibration manifest, because $\Delta_{(C),f}^*$ is again reflexive.

In the next section we will discuss in more detail how different partitions or different polytopes leading to CICYs with the same topological data may be related. We conclude this section with a slight digression. We show how the nef-partition for $\Delta_{(A)}^*$ can be obtained from the Newton polytopes of the degree (4,0) and (2,2) polynomials in the double cover of the ambient space. The rest of this section will not be used below and can be skipped.

In order to arrive at the polytope (2.14) we observe that the ambient space of the double cover is closely related to the product space $\mathbb{P}_{21111}^4 \times \mathbb{P}^1$. We thus start with the Newton polytope $\hat{\Delta}$ of a degree (6,2) equation in that space. It has 10 vertices corresponding to the monomials

$$x_0^3 y_j^2, x_i^6 y_j^2 \quad \text{with } 1 \leq i \leq 4, 0 \leq j \leq 1$$

where x_i and y_j are the homogeneous coordinates in \mathbb{P}_{21111}^4 and \mathbb{P}^1 , respectively. The degree (4,0) and (2,2) polynomials correspond to the Newton polytopes

$$\hat{\Delta}_1 = \langle x_0^2, x_i^4 \rangle, \quad \hat{\Delta}_2 = \langle x_0 y_j^2, x_i^2 y_j^2 \rangle$$

so that $\hat{\Delta} = \hat{\Delta}_1 + \hat{\Delta}_2$. The \mathbb{Z}_2 quotient acting with signs $(--- ++, -+)$ kills the two vertices $x_0^3 y_j^2$ and generates 9 additional ones:

$$x_0^3 y_0 y_1, x_0^2 x_i^2 y_j^2 \quad \text{with } 1 \leq i \leq 4, 0 \leq j \leq 1 \tag{2.20}$$

The resulting polyhedron is not reflexive, has 196 points, 17 vertices and 9 facets, but can be made reflexive by dropping the vertex $x_0^3 y_0 y_1$. This yields a polyhedron $\Delta_{(A)}$ with 195 points and 16 vertices that possesses a nef partition with Hodge numbers $h^{11} = 2$ and $h^{21} = 30$ (up to automorphisms there is only one additional nef partition whose Hodge numbers are $h^{11} = 4$ and $h^{21} = 44$). The dual polyhedron $\Delta_{(A)}^*$ has 9 points and (in an appropriate basis) the 8 vertices given in eq. (2.14), as can be checked using (2.2). The linear relations are $2\nu_1^* + \nu_2^* + \nu_3^* + \nu_4^* + \nu_5^* = 0 = \nu_6^* + \nu_7^*$ and the facet equation corresponding to the last vertex $\nu_8^* = -\nu_1^*$ is the one that eliminates $x_0^3 y_0 y_1$ and makes $\Delta_{(A)}$ reflexive.

The nef partition of $X_{(A)}$ is now constructed from the Newton polyhedra $\hat{\Delta}_i$ as follows: In order to get $\Delta_{(A)} = \Delta_1 + \Delta_2$ we drop the point $x_0 y_0 y_1$ (which becomes a vertex on the sublattice) from $\hat{\Delta}_2$ and obtain

$$\Delta_1 = \langle x_0^2, x_i^4 \rangle, \quad \Delta_2 = \langle x_i^2 y_j^2 \rangle$$

With $v_0 = x_0^2$, $v_i = x_i^4$ and $w_{ij} = x_i^2 y_j^2$ we thus find $\Delta_{(A)} = \Delta_1 + \Delta_2 = \langle v_0 w_{ij}, v_i w_{ij} \rangle$ for the decomposition of the $8+8=16$ vertices of $\Delta_{(A)}$. Shifting Δ_1 and Δ_2 by the exponent vectors of $1/(x_0 x_1 x_3 x_4)$ and $1/(x_2 y_0 y_1)$ and dropping the redundant exponents of x_4 and y_1 we obtain the vertex-matrices

$$\Delta_1^\sigma = \begin{Bmatrix} 1 & -1 & -1 & -1 & -1 \\ -1 & -1 & -1 & 3 & -1 \\ 0 & 4 & 0 & 0 & 0 \\ -1 & -1 & 3 & -1 & -1 \\ 0 & 0 & 0 & 0 & 0 \end{Bmatrix} \quad \Delta_2^\sigma = \begin{Bmatrix} 0 & 0 & 0 & 0 & 0 & 0 & 0 & 0 \\ 2 & 0 & 0 & 2 & 0 & 0 & 0 & 0 \\ -1 & 1 & -1 & -1 & -1 & -1 & -1 & 1 \\ 0 & 0 & 0 & 0 & 2 & 0 & 2 & 0 \\ 1 & 1 & 1 & -1 & 1 & -1 & -1 & -1 \end{Bmatrix} \quad (2.21)$$

with $\sigma_1^T = (1, 1, 0, 1, 0)$, $\sigma_2^T = (0, 0, 1, 0, 1)$ and $\Delta_l^\sigma \sim \Delta_l - \sigma_l$. The shifted Newton polytopes Δ_i^σ can be separated by a hyperplane, $\langle \rho, D_1^\sigma \rangle \leq 0 \leq \langle \rho, D_2^\sigma \rangle$, with $\rho = (2, 1, 0, 1, 0)$. The points of D_1^σ and those of D_2^σ on that hyperplane have no common non-zero coordinates, which implies that $\Delta_1^\sigma \cap \Delta_2^\sigma = \{0\}$ and thus establishes the nef property. (Up to symmetries of $\hat{\Delta}$ there is only one other choice of the nonnegative integral shift vectors σ_i with $\Delta_1^\sigma \cap \Delta_2^\sigma = \{0\}$, which leads to the same nef partition.) Converting to the basis

$$B = \begin{pmatrix} 1 & 0 & 0 & 0 & 0 \\ 0 & 1 & 0 & 0 & 0 \\ 0 & 0 & 1 & 0 & 0 \\ 0 & 0 & 0 & 1 & 0 \\ 1 & 1 & 1 & 0 & 2 \end{pmatrix}$$

of the \mathbb{Z}_2 quotient of the original lattice we find the nef partition $\Delta_l^{(A)} = B^{-1} \Delta_l^\sigma$,

$$E_1^* = \begin{Bmatrix} 1 & -1 & -1 & -1 & -1 \\ -1 & -1 & -1 & 3 & -1 \\ 0 & 4 & 0 & 0 & 0 \\ -1 & -1 & 3 & -1 & -1 \\ 0 & -1 & 1 & -1 & 1 \end{Bmatrix} \quad E_2^* = \begin{Bmatrix} 0 & 0 & 0 & 0 & 0 & 0 & 0 & 0 \\ 2 & 0 & 0 & 2 & 0 & 0 & 0 & 0 \\ -1 & 1 & -1 & -1 & -1 & -1 & -1 & 1 \\ 0 & 0 & 0 & 0 & 2 & 0 & 2 & 0 \\ 0 & 0 & 1 & -1 & 1 & 0 & 0 & -1 \end{Bmatrix},$$

which is dual to the partition

$$E_1 = \begin{Bmatrix} 1 & 0 & 0 & -1 \\ 0 & 1 & 0 & 0 \\ 0 & 0 & 0 & 0 \\ 0 & 0 & 1 & 0 \\ 0 & 0 & 0 & 0 \end{Bmatrix} \quad E_2 = \begin{Bmatrix} 0 & -2 & 1 & -1 \\ 0 & -1 & 1 & -1 \\ 1 & -1 & 1 & -1 \\ 0 & -1 & 0 & 0 \\ 0 & 0 & 2 & -2 \end{Bmatrix} \quad (2.22)$$

of the convex hull $\Delta_{(A)}^* = \langle \nabla_1, \nabla_2 \rangle = \langle E_1, E_2 \rangle$.

3 The geometry of toric CICYs

It is well-known that the same Hodge numbers can come from different polyhedra and even at different codimensions, so it is important to identify constructions that actually give equivalent CYs. First note that any hypersurface or complete intersection can be reconstructed at higher codimension: Just multiply with an interval $[-1, 1]$ and take the corresponding product nef

partition.¹⁰ A less obvious redundancy is due to partitions where one of the Δ_i consists of a single vertex, say ν_1^* : In that case the nef condition implies that the projection of Δ^* along ν_1^* is reflexive. Moreover, the CY is given by the intersection of the toric divisor D_1 with the remaining divisor(s) defined by the partition of the vertices. Since D_1 can only intersect the toric divisors that correspond to points bounding the reflexive projection along V_1 we conclude that we can construct the same CY variety in the ambient space that is given by that projection of Δ^* . We will call such a nef partition trivial.

An important but expensive calculational tool to settle the question about equivalences is the classification of real six manifolds by C. T. C. Wall [45]. Specialized to Calabi–Yau manifolds it states that two simply connected manifolds X and X' are of the same topological type, i.e. they are diffeomorphic, if besides the Hodge numbers the triple intersection numbers $\kappa_{abc} = \int_X J_a \wedge J_b \wedge J_c$ and the linear forms $\int_X c_2 \wedge J_a$ are the same, possibly up to an integer linear basis transformation $\underline{J} = M\underline{J}'$ in the Kähler cone of X and X' . If the basis can only be related by a rational linear transformation the spaces are rational homotopy equivalent. Only finitely many diffeomorphic types can exist in a rational homotopy equivalence class.

Gromov–Witten invariants have a modest history as symplectic invariants in the Calabi–Yau threefold case, and in general, we indeed find that symplectic families with large volume limits of the same topological type have the same Gromov–Witten invariants, but the toric mirror may have a different natural parametrization of the complex structure deformation space, which leads to different Picard–Fuchs equations and mirror maps.

In some cases, see Section 6.5, we find that rational homotopy equivalent pairs can have different Gromov–Witten invariants, and in Section 6.6 we discuss the situation of diffeomorphic manifolds with different symplectic structures.

In this section we explain in the example of the (2,30) model introduced in Section 2.5 how Calabi–Yau complete intersections coming from different polytopes and/or from different nef partitions can be related. Further examples are summarized in Appendix B.

3.1 Equivalence of different nef-partitions

As our example for different nef partitions we have chosen one of the nine polytopes in our list of models with Hodge numbers (2,44),

$$\mathbb{P} \left(\begin{array}{cccccccc} 4 & 2 & 2 & 2 & 1 & 1 & 0 \\ 1 & 0 & 0 & 0 & 0 & 0 & 1 \end{array} \right) \left[\begin{array}{c|c} 8 & 4 \\ \hline 2 & 0 \end{array} \right] / \mathbb{Z}_2 : 111010, \quad (3.1)$$

and its double cover, which we will relate to two different hypersurface polytopes. The polytope Δ of the quotient and its dual Δ^* have $(P_V, P_{V^*}) = (232_{10}, 9_7)$ points P and vertices V . The polytope for the double cover has $(461_{10}, 9_7)$, so that the \mathbb{Z}_2 quotient is free (the number P^* of points in Δ^* does not change). This model is again a K3 fibration, but this time the

¹⁰In the formulas for the Hodge numbers [20] this leads to a doubling because a quadratic equation in \mathbb{P}^1 is solved by two points.

fiber polytope has an additional vertex, namely $\nu_8^* = \frac{1}{2}(\nu_5^* + \nu_6^*)$, which is a lattice point on an edge of Δ^* . Anticipating the structure of the nef partitions, the corresponding relation $2\nu_1^* + \nu_2^* + \nu_3^* + \nu_4^* + \nu_8^* = 0$ shows that the fiber is again X_f in (2.17). Up to permutation symmetries this polyhedron only admits two nef partitions, $\{\nu_1^*, \nu_4^*, \nu_5^*, \nu_6^*, \nu_7^*\} \cup \{\nu_2^*, \nu_4^*\}$ and $\{\nu_1^*, \nu_3^*, \nu_4^*, \nu_7^*\} \cup \{\nu_2^*, \nu_5^*, \nu_6^*\}$. Both lead to the same partitioning of the degrees, $12 = 8 + 4$ and $2 = 2 + 0$, as indicated above. Note that non-vertices always belong to one of the ∇_l 's of a partition.¹¹ In our example this implies that ν_5^* and ν_6^* always have to belong to the same ∇_l . More cases with Hodge numbers (2,44) will be discussed in Appendix B.

Since the reflexivity constraint on $\nabla_1 + \nabla_2$ is weaker on a sublattice all of our partitions must lift to the double cover, but additional ones can show up. Indeed, up to automorphisms, we find a total of nine nef partitions with four different degrees and three different sets of Hodge numbers:

$$\mathbb{P} \left(\begin{array}{cccccccc} 4 & 2 & 2 & 2 & 1 & 1 & 0 & \\ 1 & 0 & 0 & 0 & 0 & 0 & 1 & \end{array} \right) \left[\begin{array}{c|c} 8 & 4 \\ \hline 2 & 0 \end{array} \right] \begin{array}{l} 2,86 \\ -168 \end{array} \quad \begin{array}{l} \{\nu_1^*, \nu_2^*, \nu_5^*, \nu_6^*, \nu_7^*\} \cup \{\nu_3^*, \nu_4^*\} \\ \{\nu_1^*, \nu_2^*, \nu_3^*, \nu_7^*\} \cup \{\nu_4^*, \nu_5^*, \nu_6^*\} \end{array} \quad (3.2)$$

$$\mathbb{P} \left(\begin{array}{cccccccc} 4 & 2 & 2 & 2 & 1 & 1 & 0 & \\ 1 & 0 & 0 & 0 & 0 & 0 & 1 & \end{array} \right) \left[\begin{array}{c|c} 8 & 4 \\ \hline 1 & 1 \end{array} \right] \begin{array}{l} 2,86 \\ -168 \end{array} \quad \begin{array}{l} \{\nu_2^*, \nu_3^*, \nu_4^*, \nu_5^*, \nu_6^*, \nu_7^*\} \cup \{\nu_1^*\} \\ \{\nu_1^*, \nu_2^*, \nu_3^*\} \cup \{\nu_4^*, \nu_5^*, \nu_6^*, \nu_7^*\} \\ \{\nu_1^*, \nu_2^*, \nu_5^*, \nu_6^*\} \cup \{\nu_3^*, \nu_4^*, \nu_7^*\} \end{array} \quad (3.3)$$

$$\mathbb{P} \left(\begin{array}{cccccccc} 4 & 2 & 2 & 2 & 1 & 1 & 0 & \\ 1 & 0 & 0 & 0 & 0 & 0 & 1 & \end{array} \right) \left[\begin{array}{c|c} 6 & 6 \\ \hline 1 & 1 \end{array} \right] \begin{array}{l} 3,69 \\ -132 \end{array} \quad \begin{array}{l} \{\nu_1^*, \nu_5^*, \nu_6^*\} \cup \{\nu_2^*, \nu_3^*, \nu_4^*, \nu_7^*\} \\ \{\nu_1^*, \nu_2^*\} \cup \{\nu_3^*, \nu_4^*, \nu_5^*, \nu_6^*, \nu_7^*\} \end{array} \quad (3.4)$$

$$\mathbb{P} \left(\begin{array}{cccccccc} 4 & 2 & 2 & 2 & 1 & 1 & 0 & \\ 1 & 0 & 0 & 0 & 0 & 0 & 1 & \end{array} \right) \left[\begin{array}{c|c} 10 & 2 \\ \hline 2 & 0 \end{array} \right] \begin{array}{l} 3,99 \\ -192 \end{array} \quad \begin{array}{l} \{\nu_1^*, \nu_3^*, \nu_4^*, \nu_5^*, \nu_6^*, \nu_7^*\} \cup \{\nu_2^*\} \\ \{\nu_1^*, \nu_2^*, \nu_3^*, \nu_4^*, \nu_7^*\} \cup \{\nu_5^*, \nu_6^*\} \end{array} \quad (3.5)$$

For the double cover we thus find two trivial partitions, for which we can construct the corresponding hypersurfaces: It is quite easy to work this out in terms of the weight data: A projection along ν_1^* , as required by the third partition in (3.3), just amounts to dropping that vertex from the linear relations. Since $\nu_7^* = -\nu_1^*$ the last vertex is projected onto the origin and we find the weighted projective space $\mathbb{P}_{22211}^4[8]$, whose degree 8 hypersurface indeed has Hodge data (2,86). For the trivial partition in (3.5) we project along ν_2^* and find the CY hypersurface $\mathbb{P} \left(\begin{array}{cccccccc} 4 & 2 & 2 & 1 & 1 & 0 & \\ 1 & 0 & 0 & 0 & 0 & 1 & \end{array} \right) \left[\begin{array}{c} 10 \\ 2 \end{array} \right]$, again with the expected Hodge numbers (3,99).

We also observe that the partitioning indeed fixes the Hodge numbers, *i.e.* equal charge vectors always lead to the same spectrum. This could be expected because for weighted projective intersections the degrees contain all information. How this result comes about in the toric context will be seen explicitly in the examples below. The converse is, however, not true: The first two partitions with Euler number $\chi = -168$ are the ones that survive the \mathbb{Z}_2 quotient, but there is now a different realization of the same Hodge numbers. The difference in the charge vectors is, however, only due to the contribution of ν_7^* and it turns out that the corresponding divisor D_7 does not intersect the CICY. All spaces with equal Hodge numbers turn out to be topologically equivalent so that there do not seem to be any phase boundaries associated with a transition among the respective partitions.

¹¹ The piecewise linear functions ψ_l defining the nef partition are integral on lattice points with values 0 or 1 on the vertices. The facets of Δ^* thus cannot contain lattice points with other values.

3.2 Equivalence of different polyhedra: the (2,30) model

We now take the main example introduced in subsection 2.5 and show that the three different models $X_{(A)}$, $X_{(B)}$, and $X_{(C)}$ are topologically equivalent.

3.2.1 The Mori cone, topological data and fibration structure

For the ambient space the Kähler cone is given purely combinatorial in terms of the secondary fan of the dual polyhedron Δ^* . One works conveniently with its dual cone called the Mori cone, which is generated by a certain basis of linear relations $\tilde{l}^{(a)}$ of the points in Δ^* . Their entries can be interpreted as the intersection of the divisors D_i corresponding to the points ν_i^* with the curves $c^{(a)}$ bounding the dual face of the Kähler cone. If the $2n$ -cycles of the ambient space, whose positivity $\int_{C_{2n}} J^n > 0$ w.r.t. to the Kähler form J defines the boundary of the Kähler cone of the ambient space do not descend to curves or divisors of the Calabi–Yau complete intersection, the Kähler cone of the Calabi–Yau X is bigger. A straightforward analysis of the intersection calculation yields for hypersurfaces that those divisors, which correspond to points on codimension one faces of the dual polyhedron, do not intersect the Calabi–Yau X as divisors and are therefore not involved in the linear relations spanning the Mori cone of X . By homology and cohomology pairing and Poincaré duality they would give rise to elements in $H^{1,1}$ and above is the reason for their absence in (2.8).

Even in the hypersurface case the lower dimensional toric cycles of the ambient space can or cannot descend to cycles in the Calabi–Yau. This phenomenon was first described in [46] and requires a detailed calculation of the intersection ring to determine the Kähler cone of X . It is not surprising that this phenomenon becomes more severe with higher codimension of X and in absence of a simple rule the analysis must start with the question which of the divisors of the ambient space become divisors of X . Details and some systematics are discussed in the present section.

Once the Mori cone generators $\tilde{l}^{(a)}$ of the ambient space are known we add to each of them as first entries the negatives of the intersections $l_{0,m}^{(a)}$ of the r constraints $D_{0,m}$ in (2.3), with the curve $c^{(a)}$, such that the general form of the Mori generators $l^{(a)}$ for the embedded Calabi–Yau manifold becomes

$$l^{(a)} = (l_{0,1}^{(a)}, \dots, l_{0,r}^{(a)}; l_1^{(a)}, \dots, l_n^{(a)}), \quad \text{for } a = 1, \dots, h. \quad (3.6)$$

Note that by construction $\sum_{m=1}^r l_{0,m}^{(a)} + \sum_{i=1}^n l_i^{(a)} = 0$, $\forall a$, which ensures the vanishing of the first Chern class of X . The knowledge of the Mori cone is important for several reasons. In Section 3.2.4 we will use it to determine the phase diagram of the (2,30) model. More importantly, in Section 4.3 it is needed to define the local coordinates on the complex structure moduli space of the mirror X^* near the point of maximal unipotent monodromy. Moreover, the generators enter the coefficients of the fundamental period in (4.5) which is a solution of the Picard–Fuchs equations. The latter are most easily obtained from the Mori cone as is reviewed in Appendix A.

3.2.2 The first realization of the (2,30) model

We first discuss the model $X_{(A)}$ in detail. Recall that the intersection ring of the ambient space is obtained as the quotient of the polynomial ring $\mathbb{C}[D_1, \dots, D_n]$ by the ideal generated by the linear relations among the points, and by the Stanley–Reisner ideal. The latter is obtained from the primitive collections which are collections of vertices that do not form a cone but any proper subset forms a cone [47]. The intersection ring of the Calabi–Yau is then an ideal quotient of the above ring by the ideal generated by $D_{0,l}$.

In the present example these primitive collections can easily be seen in the geometry of the polyhedron $\Delta_{(A)}^*$. As discussed in subsection 2.5, the section in the lattice N that corresponds to the K3 fiber is a blowup of \mathbb{P}_{21111}^4 by the vertex $\nu_8^* = -\nu_1^*$, hence it is a double pyramid over the tetrahedron $\langle \nu_2^*, \nu_3^*, \nu_4^*, \nu_5^* \rangle$. Subsequently, we will identify faces with their index sets and simply write the indices of the points ν_i^* of the faces, e.g. here $\langle 2345 \rangle$. This implies the relations $D_1 \cdot D_8 = 0 = D_2 \cdot D_3 \cdot D_4 \cdot D_5$ because the respective vertices never can belong to the same cone of any (triangulated) fan over the polyhedron. The complete polyhedron is a double pyramid over that 4-dimensional double pyramid. As $\nu_6^* + \nu_7^* = 0$ this leads to the additional relation $D_6 \cdot D_7 = 0$, which completes the generators of the Stanley–Reisner ideal. The polyhedron is simplicial and has the 16 facets $\langle \widehat{18234567} \rangle$, where a hat above a sequence of numbers indicates to take all simplices that arise by dropping one of the respective vertices. The linear equivalences (up to principal divisors) follow from the lines of (2.14) and we find altogether

$$D_1 \sim 2D_5 + D_8, \quad D_2 \sim D_3 \sim D_4 \sim D_5, \quad D_6 \sim D_7, \quad (3.7)$$

$$D_1 \cdot D_8 = 0 \quad D_2 \cdot D_3 \cdot D_4 \cdot D_5 = 0, \quad D_6 \cdot D_7 = 0. \quad (3.8)$$

According to the nef partition (2.22) the complete intersection $X_{(A)}$ is given by $D_{0,1} \cdot D_{0,2}$ (cf. (2.3)) with

$$D_{0,1} = D_1 + D_2 + D_4 + D_8 \sim 2D_1, \quad D_{0,2} = D_3 + D_5 + D_6 + D_7 \sim 2D_2 + 2D_6, \quad (3.9)$$

so that D_8 does not intersect the Calabi–Yau and the Kähler moduli correspond to the volumes of, for example, D_3 and D_6 .

The unique star triangulation of the simplicial polytope (2.14) fixes the toric intersection numbers and therefore the Mori cone of the ambient space $\mathbb{P}_{\Delta_{(A)}^*}$. We determine this Mori cone as

$$\begin{aligned} \hat{l}^{(1)} &= (0, 0, 0, 0, 0, 1, 1, 0) \\ \tilde{l}^{(2)} &= (0, 1, 1, 1, 1, 0, 0, -2) \\ \hat{l}^{(3)} &= (1, 0, 0, 0, 0, 0, 0, 1). \end{aligned} \quad (3.10)$$

As mentioned above the divisor D_8 of $\mathbb{P}_{\Delta_{(A)}^*}$ does not intersect the complete intersection. All other divisors descend to divisors on the hypersurface. The entries in the Mori vectors are the intersections of the curves $c^{(a)}$, which have positive volume inside the Kähler cone, with the corresponding divisor. The Mori vectors of the complete intersection must therefore have a zero in the eighth entry. Besides $\hat{l}^{(1)}$ there is the unique minimal length combination $l^{(2)} =$

$\tilde{l}^{(2)} + 2\hat{l}^{(3)} = (2, 1, 1, 1, 1, 0, 0, 0)$ with this property. We drop the eighth entry and add the negative value of the intersection of the $c^{(a)}$ with $D_{0,1}$ and $D_{0,2}$ as the first entries (these numbers correspond to the negative degrees in the charge vectors). Thus we get the Mori vectors for the complete intersection $X_{(A)}$

$$\begin{aligned} l^{(1)} &= (-4, -2; 2, 1, 1, 1, 1, 0, 0) \\ l^{(2)} &= (0, -2; 0, 0, 0, 0, 0, 1, 1) . \end{aligned} \tag{3.11}$$

(in the present example they coincide with the charge vectors because, propping the non-intersecting vertex, the ambient space is a product of weighted projective spaces, but generically the Mori vectors span a larger cone). This way of summarizing the Mori generators becomes particularly useful, when we discuss the Picard–Fuchs system.

It is convenient to summarize all the relevant information for $X_{(A)}$ in the following table:

| | | | | | | | | | | |
|-----------|---|---|----|----|----|----|----|-----------|-----------|------|
| | | | | | | | | $c^{(1)}$ | $c^{(2)}$ | |
| $D_{0,1}$ | 1 | 0 | 0 | 0 | 0 | 0 | 0 | -4 | 0 | |
| $D_{0,2}$ | 0 | 1 | 0 | 0 | 0 | 0 | 0 | -2 | -2 | |
| D_1 | 1 | 0 | 1 | 0 | 0 | 0 | 0 | 2 | 0 | $2H$ |
| D_2 | 1 | 0 | 0 | 1 | 0 | 0 | 0 | 1 | 0 | H |
| D_3 | 0 | 1 | 0 | 0 | 1 | 0 | 0 | 1 | 0 | H |
| D_4 | 1 | 0 | 0 | 0 | 0 | 1 | 0 | 1 | 0 | H |
| D_5 | 0 | 1 | -2 | -1 | -1 | -1 | 0 | 1 | 0 | H |
| D_6 | 0 | 1 | 1 | 1 | 1 | 0 | 2 | 0 | 1 | L |
| D_7 | 1 | 0 | -1 | -1 | -1 | 0 | -2 | 0 | 1 | L |

(3.12)

On the left-hand side of the vertical line we have listed from top to bottom the points ν_i^* of the polyhedron Δ^* , where the first two entries refer to the nef-partition $E_l, l = 1, 2$, and the next five entries are their coordinates in $N = \mathbb{Z}^5$. Together they form the coordinates of the generators of the 7-dimensional Gorenstein cone $\Gamma(\Delta^*)$ that was defined below (2.7). To each point ν_i^* we have associated the corresponding divisor D_i . The first two rows, *i.e.* $D_{0,1}$ and $D_{0,2}$ correspond to the interior point appearing once in either partition. The two columns labeled by $c^{(a)}$ on the right-hand side of the vertical line denote the Mori generators. Its entries are the intersection numbers of the restrictions of the divisors D_i to X with the curves $c^{(a)}$. The data only refer to the Calabi–Yau manifold, *i.e.* we dropped the non-intersecting divisors and the curves that do not descend to the complete intersection.

Let us denote the independent divisors of the complete intersection by H and L . In our example we can choose $H = D_3 D_{0,1} D_{0,2}$ and $L = D_6 D_{0,1} D_{0,2}$, as is indicated on the right in (3.12). The classical intersection numbers are defined as

$$\kappa_{abc} = \int_X J_a \wedge J_b \wedge J_c = D_a \cap D_b \cap D_c \tag{3.13}$$

where $J_a \in H^2(X, \mathbb{Z})$ and $D_a \in H_4(X, \mathbb{Z})$. Here, J_1 and J_2 are the Kähler forms dual to H and L , respectively. They can be easily evaluated from the intersections on $\mathbb{P}_{\Delta(A)}$, *e.g.* $D_1 D_2 D_3 D_4 D_6 = \text{Vol}\langle \nu_1^*, \nu_2^*, \nu_3^*, \nu_4^*, \nu_6^* \rangle = 2$, and the relations in (3.7) and (3.8). The fact that

we are dealing with a free \mathbb{Z}_2 quotient is accounted for by a division by 4. Therefore, the intersection numbers are

$$\begin{aligned}\kappa_{111} &= \kappa_{112} = 2 \\ \kappa_{122} &= \kappa_{222} = 0.\end{aligned}\tag{3.14}$$

According to Oguiso [8], a Calabi–Yau threefold admits a K3-fibration if there exists an effective divisor L such that

$$L \cdot c \geq 0 \text{ for all curves } c \in H_2(X, \mathbb{Z}), \quad L^2 \cdot D = 0 \text{ for all divisors } D \in H_4(X, \mathbb{Z}).\tag{3.15}$$

Therefore, we conclude from (3.14) that the geometry of the Calabi–Yau space $X_{(A)}$ is a fibration with J_1 the Kähler class of the fiber and J_2 the Kähler class of the base. This is in agreement with the purely combinatorial argument in (2.17). Normally, one expects in such cases the fiber to be K3 and $\int_X c_2 J_2 = 24$ [7, 8, 48]. That is because the integral of J_2 over the base \mathbb{P}^1 gives 1, the rest of the integral extends over the fiber and yields $\int_{\text{K3}} c_2 = 24$. Instead one has here

$$c_2 L = \int_X c_2 J_2 = 12 \quad c_2 H = \int_X c_2 J_1 = 20,\tag{3.16}$$

which indicates that the \mathbb{Z}_2 quotient has divided the volume of the \mathbb{P}^1 by two. Indeed, we know that the model is a free \mathbb{Z}_2 quotient of an ordinary K3 fibration, which might be represented as the complete intersection of degree $(4, 0)$ and $(2, 2)$ in $\mathbb{P}_{21111}^4 \times \mathbb{P}^1$ with Euler number $\chi = -112$ and the same $l^{(a)}$ vectors as in (3.11). Now recall our extensive discussion of the properties of $X_{(A)}$ in subsection 2.5. With the homogeneous coordinates x_i for \mathbb{P}_{21111}^4 and y_j for \mathbb{P}^1 , respectively, the polynomials f_1 and f_2 in (2.6) are

$$\begin{aligned}f_1 &= x_0^2 + x_1^4 + x_2^4 + x_3^4 + x_4^2 + \dots \\ f_2 &= x_0^2(y_0^2 + y_0 y_1 + y_2^2) + \dots\end{aligned}$$

For any choice $(y_0 : y_1)$ in \mathbb{P}^1 the fiber is the complete intersection K3 X_f in (2.17). The \mathbb{Z}_2 acts on the coordinates by $(x_0, x_1, x_2, x_3, x_4; y_0, y_1) \rightarrow (-x_0, x_1, -x_2, x_3, -x_4; y_0, -y_1)$. Hence the \mathbb{P}^1 gets folded with fixed points $(1 : 0)$ and $(0 : 1)$, which explains the division of $\int_X c_2 J_a$ by 2, while the \mathbb{Z}_2 action leads to an Enriques fiber over the fixed points in the base. Note that, therefore, only \mathbb{Z}_2 can act freely on K3 fibered Calabi–Yau manifolds. We will come back to this observation in Section 7.2.

3.2.3 Other realizations of the (2,30) model

One difficulty with complete intersection realizations is a high redundancy in the description of a given family of Calabi–Yau spaces. For example, we know from subsection 2.5 that there are two more polyhedra with three and two nef-partitions respectively, which lead to complete intersections with Hodge numbers $(2, 30)$. In addition, these polyhedra admit two and five different star triangulations respectively, which could potentially lead to different large volume phases of the families.

We first consider the second realization of the Hodge numbers $(2,30)$, $X_{(B)}$. In this case the dual polyhedron $\Delta_{(B)}^*$ has vertices

$$\Delta_{(B)}^* \ni \{\nu_i^*\} = \left\{ \begin{array}{cccccccc} 1 & 0 & 0 & 0 & -2 & 1 & -1 & -1 \\ 0 & 1 & 0 & 0 & -1 & 1 & -2 & 0 \\ 0 & 0 & 1 & 0 & -1 & 1 & -1 & 0 \\ 0 & 0 & 0 & 1 & -1 & 0 & 1 & 0 \\ 0 & 0 & 0 & 0 & 0 & 2 & -2 & 0 \end{array} \right\} \quad (3.17)$$

and admits the three nef-partitions given below eq. (2.18). In order to find the triangulations we observe that the shift of ν_7^* , as compared to its position in $\Delta_{(A)}^*$, moves the intersection point of the line $\overline{\nu_6^* \nu_7^*}$ with the fiber hyperplane through the facet $\langle 1345 \rangle$ of Δ_f^* till it reaches the linear span of $\langle 3458 \rangle$ outside of that facet of the fiber polytope. This kills the 4 simplices $\langle \widehat{1834567} \rangle$ of $\Delta_{(A)}^*$ and replaces them by the 3 triangles $\langle \widehat{134567} \rangle$ and by the 16th facet $\langle 345678 \rangle$. The vertices of the non-simplicial facet form a circuit, $\nu_3^* + 2\nu_4^* + \nu_5^* = \nu_6^* + \nu_7^* + 2\nu_8^*$, for which we introduce the short hand notation $\langle 3_1 4_2 5_1 | 6_1 7_1 8_2 \rangle$. It indicates the labels m of the involved vertices ν_m^* and, as subscripts, their coefficients c_m in the linear relation (2.11). Therefore, it can be triangulated in the two different ways: $\langle \widehat{345678} \rangle$ or $\langle 345\widehat{678} \rangle$, so that we find two different triangulations with 18 simplices:

$$\begin{aligned} T_1 &= \{ \langle \widehat{18234567} \rangle, \langle \widehat{1834567} \rangle \} \\ T_2 &= \{ \langle \widehat{18234567} \rangle, \langle \widehat{134567} \rangle, \langle 345\widehat{678} \rangle \} \end{aligned} \quad (3.18)$$

Since we deal with a free \mathbb{Z}_2 quotient, the volume of each simplex is divisible by two. Because of the coefficient 2 of ν_4^* and ν_8^* in the circuit the simplices that do not contain one of these vertices, i.e. $\langle 35678 \rangle \in T_1$ and $\langle 34567 \rangle \in T_2$, have volume 4. We thus need to resolve the singularities of the ambient space by adding points at higher degree, following the general discussion given in Section 2.3. From that we expect another simplex of volume 4, sharing a facet, which has to be the same for both triangulations. The only possibility is the facet $\langle 13567 \rangle$, which indeed has volume 4. The additional point in degree two, which resolves all singularities is $\nu_r^* = \frac{1}{2}(\nu_3^* + \nu_5^* + \nu_6^* + \nu_7^*)$. The corresponding triangulations are

$$\begin{aligned} T_1 &= \{ \langle \widehat{18234567} \rangle, \langle \widehat{1835467} \rangle, \langle \widehat{183567r} \rangle \} \\ T_2 &= \{ \langle \widehat{18234567} \rangle, \langle \widehat{146735} \rangle, \langle 3458\widehat{67} \rangle, \langle \widehat{143567r} \rangle \} \end{aligned} \quad (3.19)$$

The linear relations are

$$D_6 \sim D_7, \quad D_1 \sim 2D_5 + D_8 + D_r, \quad D_3 \sim D_5 \sim D_4 + D_6 \sim D_2 - D_6 - D_r \quad (3.20)$$

For the first two nef-partitions in (2.18), the face $\langle 3, 5, 6, 7 \rangle$ belongs to both sets of vertices, therefore (2.12) becomes for the first nef-partition

$$D_{0,1} = D_1 + D_3 + D_5 + D_8 + D_r = 2D_1 \quad D_{0,2} = D_2 + D_4 + D_6 + D_7 + D_r = 2D_2 \quad (3.21)$$

The second nef-partition is analogous and yields the same result. For the third one, however, this face lies entirely in the second set of vertices, so that

$$D_{0,1} = D_1 + D_2 + D_4 + D_8 = 2D_1 \quad D_{0,2} = D_3 + D_5 + D_6 + D_7 + 2D_r = 2D_2 \quad (3.22)$$

yields again the same result. We discuss the triangulations for a single nef-partition, say, the first one, in detail. The Stanley–Reisner ideal, of course, always contains the generator $D_1 \cdot D_8$ because antipodal points can never belong to the same simplex. The divisor D_8 thus never intersects the Calabi–Yau manifold $X_{(B)}$, whose first defining equation is a section of $\mathcal{O}(D_{0,1}) = \mathcal{O}(2D_1)$. Furthermore, since ν_2^* and ν_r^* never belong to the same simplex, the divisor D_r coming from the blow-up of the ambient space never intersects $X_{(B)}$ because its second defining equation is a section of $\mathcal{O}(D_{0,2}) = \mathcal{O}(2D_2)$. Otherwise it depends on the triangulation, and we find, using a similar argument, from (3.19)

$$\begin{aligned} \mathcal{I}_{SR}(T_1) &= \{D_1 D_8, D_2 D_6 D_7, D_3 D_4 D_5, \\ &\quad D_3 D_5 D_6 D_7, D_2 D_r, D_4 D_r\} \\ \mathcal{I}_{SR}(T_2) &= \{D_1 D_8, D_2 D_6 D_7, D_6 D_7 D_8, D_1 D_3 D_4 D_5, D_2 D_3 D_4 D_5, \\ &\quad D_3 D_5 D_6 D_7, D_2 D_r, D_8 D_r, D_1 D_4 D_r\} \end{aligned} \quad (3.23)$$

Note that the first lines in (3.23) correspond to the Stanley–Reisner ideal of the unresolved toric variety $\mathbb{P}_{\Delta_{(B)}^*}$. Next, we determine the Mori cone of the resolved ambient space and find

$$\begin{aligned} \hat{l}_{T_1} &= \begin{pmatrix} 0 & 1 & 0 & -1 & 0 & 1 & 1 & 0 & 0 \\ 0 & 0 & 1 & 0 & 1 & 1 & 1 & 0 & -2 \\ 1 & 0 & 0 & 0 & 0 & 0 & 0 & 1 & 0 \\ 0 & 0 & 0 & 1 & 0 & -1 & -1 & -1 & 1 \end{pmatrix} \\ \hat{l}_{T_2} &= \begin{pmatrix} 1 & 0 & 0 & 1 & 0 & -1 & -1 & 0 & 1 \\ 0 & 1 & 1 & 1 & 1 & 0 & 0 & -2 & 0 \\ 0 & 0 & -1 & -1 & -1 & 0 & 0 & 1 & 1 \\ 0 & 0 & 1 & 0 & 1 & 1 & 1 & 0 & -2 \end{pmatrix} \end{aligned}$$

Since D_8 and D_r do not intersect the Calabi–Yau space, we consider the linear combinations of the vectors above for which the eighth and the ninth entry vanishes, and adding the intersections of $-D_{0,l}$ with $c^{(a)}$ as before, we get for both triangulations the two Mori generators

$$\begin{aligned} \tilde{l}^{(1)} &= (-4, 0; 2, 0, 1, 2, 1, -1, -1, 0, 0) \\ l^{(2)} &= (0, -2; 0, 1, 0, -1, 0, 1, 1, 0, 0). \end{aligned} \quad (3.24)$$

Now we have to check that the curves which bound the corresponding Kähler cones in $\mathbb{P}_{\Delta_{(B)}^*}$ descend to the Calabi–Yau space $X_{(B)}$. As mentioned above these curves have intersection $c^{(a)} \cdot D_i = l_i^{(a)}$. In particular $c^{(1)}$ has negative intersection with both D_6 and D_7 . Negative intersection numbers indicate that the curves are actually contained in the corresponding divisors. Since by (3.23), $D_6 D_7 = 0$ on the Calabi–Yau space, we conclude that $c^{(1)}$ does not descend to $X_{(B)}$. For this reason the Mori cone must become smaller and the Kähler cone becomes bigger due to the absence of the bounding curve in $X_{(B)}$. The minimal positive integer linear combination of $\tilde{l}^{(1)}$ and $l^{(2)}$ without two negative entries is $l^{(1)} = \tilde{l}^{(1)} + l^{(2)}$

$$\begin{aligned} l^{(1)} &= (-4, -2; 2, 1, 1, 1, 1, 0, 0, 0, 0) \\ l^{(2)} &= (0, -2; 0, 1, 0, -1, 0, 1, 1, 0, 0). \end{aligned} \quad (3.25)$$

We can then pick $H = D_3 D_{0,1} D_{0,2}$ and $L = D_6 D_{0,1} D_{0,2}$ and observe exactly the same classical intersections as in (3.14) and (3.16). According to the theorem of Wall the Calabi–Yau manifolds

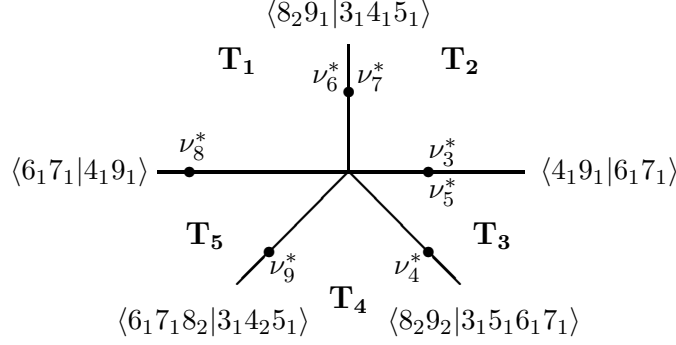


Figure 1: Secondary fan of the facet $\langle 3456789 \rangle$ of $\Delta_{(C)}^*$ with circuits relating its triangulations.

are then of the same topological type. It turns out that the world sheet instanton numbers on both Calabi–Yau spaces are the same. However, as we will see in subsection A, the slightly different vectors $l^{(i)}$ lead to a different parametrization of the complex structure moduli space. Since these arguments used only the triangulations, which are independent of the nef-partition, they show that the other two nef-partitions lead to the same topological type of the Calabi–Yau space.

The third model with Hodge numbers $(2, 30)$ has the dual polyhedron

$$\Delta_{(C)}^* \ni \{\nu_i^*\} = \left\{ \begin{array}{cccccccc} 1 & 0 & 0 & 0 & -2 & 1 & -1 & -1 & 0 \\ 0 & 1 & 0 & 0 & -1 & 1 & -2 & 0 & -1 \\ 0 & 0 & 1 & 0 & -1 & 1 & -1 & 0 & 0 \\ 0 & 0 & 0 & 1 & -1 & 0 & 1 & 0 & 0 \\ 0 & 0 & 0 & 0 & 0 & 2 & -2 & 0 & 0 \end{array} \right\} \quad (3.26)$$

and admits the two nef-partitions given below (2.19). The star triangulations of $\Delta_{(C)}^*$ again contain the twelve simplices $\langle \widehat{18234567} \rangle$ of $\Delta_{(A)}^*$, but now there are 5 additional facets, namely the two simplices $\langle 135\widehat{6}79 \rangle$, and the facets $\langle 143\widehat{5}679 \rangle$ and $\langle 3456789 \rangle$. The circuit $\nu_6^* + \nu_7^* = \nu_4^* + \nu_9^*$ shows that the additional vertex ν_9^* restores the possibility of a fibered ambient space. Namely, if we triangulate this circuit as $\langle 4\widehat{6}79 \rangle$, we avoid the edge $\overline{\nu_6^* \nu_7^*}$. The triangulations of $\Delta_{(C)}^*$ that are consistent with the fibration are easily found by triangulating the reflexive section $\Delta_{(C),f}^*$, which is spanned by $\nu_1^*, \dots, \nu_5^*, \nu_8^*, \nu_9^*$. Its single non-simplicial facet, $\langle 34589 \rangle$, yields a circuit $\langle 3_1 4_1 5_1 | 8_2 9_1 \rangle$. One triangulation, $\langle \widehat{345}89 \rangle$, leads to a regular ambient space while the other contains the simplex $\langle 3459 \rangle$ of volume 2. In the 4-dimensional ambient space of the fiber we expect a resolution of the singularity by a point in degree 2 in the interior of the cone. Indeed, $\nu_r^* = \frac{1}{2}(\nu_3^* + \nu_4^* + \nu_5^* + \nu_9^*)$ is a lattice point (which actually is identical to the point ν_r^* that resolved the singularities in the previous example). Extending these subdivisions to a triangulation of the complete polytope we thus obtain the first two triangulations T_2 and T_1 below. T_2 is regular while T_1 requires the subdivision of the two triangles $\langle 3459\widehat{6}7 \rangle$ through ν_r^* .

The complete set of triangulations can be found by constructing the secondary fan [22] for the facet $\langle 3456789 \rangle$: Let A denote the matrix consisting of the coordinates of the respective

vertices ν_3^*, \dots, ν_9^* and compute its Gale transform [22, 49]

$$B = \begin{pmatrix} 1 & 1 & 1 & 0 & 0 & -2 & -1 \\ 0 & -1 & 0 & 1 & 1 & 0 & -1 \end{pmatrix}, \quad (3.27)$$

which is the transpose of its kernel, i.e. $AB^T = 0$, where we have chosen the two circuits $\langle 3_1 4_1 5_1 | 8_2 9_1 \rangle$ and $\langle 6_1 7_1 | 4_1 9_1 \rangle$ as generators of the kernel. The rays of the secondary fan are generated by the column vectors of B , which we label by the respective vertices of $\Delta_{(C)}^*$. The triangulations T_i can then be read off as indicated in figure 1: The vertices of the simplices $\sigma \in T_i$ are obtained as complements of the vertices of an appropriate number of points that span cones containing the phases labeled by T_i (see Lemma 4.3 of [49]). As an example consider T_4 , where these complements are $\{48, 39, 49, 59\}$, yielding the triangulation $\{\langle 35679 \rangle, \langle \widehat{345678} \rangle\}$. Adjacent triangulations are connected by (bistellar flips for) circuits involving, on either side, vertices that can form a strictly convex cone with the ray that separates the corresponding phases (see Proposition 2.12 in chapter 7 of [22]).

A triangulation of $\langle 3456789 \rangle$ induces a triangulation of the other two non-simplicial facets $\langle 14\widehat{35679} \rangle$. Writing the triangulations as a union of the simplices of the big facet $\langle 3456789 \rangle$, simplices of the induced triangulations of the circuits $\langle 14\widehat{35679} \rangle$, and simplicial facets of $\Delta_{(C)}^*$, respectively, we obtain

$$T_1 = \{\langle 3456\widehat{789} \rangle\} \cup \{\langle 14\widehat{35679} \rangle\} \cup \{\langle \widehat{18234567} \rangle, \langle 135679 \rangle\} \quad (3.28)$$

$$T_2 = \{\langle \widehat{3456789} \rangle\} \cup \{\langle 14\widehat{35679} \rangle\} \cup \{\langle \widehat{18234567} \rangle, \langle 135679 \rangle\} \quad (3.29)$$

$$T_3 = \{\langle \widehat{3549678} \rangle, \langle 356789 \rangle\} \cup \{\langle 14\widehat{93567} \rangle\} \cup \{\langle \widehat{18234567} \rangle, \langle 135679 \rangle\} \quad (3.30)$$

$$T_4 = \{\langle \widehat{345678} \rangle, \langle 35679 \rangle\} \cup \{\langle 14\widehat{93567} \rangle\} \cup \{\langle \widehat{18234567} \rangle, \langle 135679 \rangle\} \quad (3.31)$$

$$T_5 = \{\langle 3456\widehat{78} \rangle, \langle 35679 \rangle\} \cup \{\langle 14\widehat{93567} \rangle\} \cup \{\langle \widehat{18234567} \rangle, \langle 135679 \rangle\} \quad (3.32)$$

T_2 and T_3 have 24 regular simplices. The triangulations T_1 , T_4 and T_5 have 22 simplices, two of which have volume 2. Inspection of the coefficients in the circuits connecting the phases shows that these are $\langle 3459\widehat{67} \rangle$, $\langle 3567\widehat{49} \rangle$ and $\langle 3567\widehat{49} \rangle$, respectively, so that the refinement induced by adding

$$\nu_r^* = \frac{1}{2}(\nu_3^* + \nu_4^* + \nu_5^* + \nu_9^*) = \frac{1}{2}(\nu_3^* + \nu_5^* + \nu_6^* + \nu_7^*) \quad (3.33)$$

resolves the singularities in all cases. Note that star triangulations are refinements of the polyhedral subdivision induced by the cones over the facets of Δ^* . Figure 1 is therefore a face of the complete secondary fan that describes all triangulations of $\Delta_{(C)}^*$ (see Theorem 2.4 in chapter 7 of [22]).

We list here the data for the ambient space only for two triangulations, T_2 and T_1 . For T_2 we do not need ν_r^* . Therefore, the linear relations are

$$D_6 \sim D_7, \quad D_1 \sim 2D_5 + D_8, \quad D_2 - D_6 - D_9 \sim D_3 \sim D_4 + D_6 \sim D_5 \quad (3.34)$$

and the Stanley-Reisner ideal is

$$I_{SR}(T_2) = \{D_1 D_8, D_2 D_9, D_6 D_7, D_3 D_4 D_5\} \quad (3.35)$$

The Mori generators associated to the triangulation T_2 are

$$\hat{l}_{T_2} = \begin{pmatrix} 0 & 1 & 0 & 0 & 0 & 0 & 0 & 0 & 1 \\ 1 & 0 & 0 & 0 & 0 & 0 & 0 & 1 & 0 \\ 0 & 0 & 1 & 1 & 1 & 0 & 0 & -2 & -1 \\ 0 & 0 & 0 & -1 & 0 & 1 & 1 & 0 & -1 \end{pmatrix} \quad (3.36)$$

The complete intersection $X_{(C)}$ for the first nef-partition below (2.19) is defined by

$$D_{0,1} = D_1 + D_3 + D_4 + D_7 + D_8, \quad D_{0,2} = D_2 + D_5 + D_6 + D_9$$

For T_1 the linear relations involve ν_r^*

$$D_6 \sim D_7, \quad D_1 \sim 2D_5 + D_8 + D_r, \quad D_2 - D_6 - D_9 - D_r \sim D_3 \sim D_4 + D_6 \sim D_5 \quad (3.37)$$

and so does the Stanley-Reisner ideal

$$I_{SR}(T_1) = \{D_1D_8, D_1D_r, D_2D_9, D_2D_r, D_6D_7, D_8D_9, D_8D_r, D_1D_3D_4D_5, D_2D_3D_4D_5, D_3D_4D_5D_9\} \quad (3.38)$$

The Mori generators become accordingly

$$\hat{l}_{T_1} = \begin{pmatrix} 0 & 1 & 1 & 1 & 1 & 0 & 0 & -2 & 0 & 0 \\ 1 & 0 & 0 & 0 & 0 & 0 & 0 & 0 & -1 & 1 \\ 0 & 0 & 1 & 1 & 1 & 0 & 0 & 0 & 1 & -2 \\ 0 & 0 & -1 & -1 & -1 & 0 & 0 & 1 & 0 & 1 \\ 0 & 0 & 0 & -1 & 0 & 1 & 1 & 0 & -1 & 0 \end{pmatrix} \quad (3.39)$$

The complete intersection for the first nef partition below (2.19) is defined by

$$D_{0,1} = D_1 + D_3 + D_4 + D_7 + D_8 + D_r, \quad D_{0,2} = D_2 + D_5 + D_6 + D_9 + D_r$$

We find for all triangulations (and all partitions) that D_8 and D_9 do not intersect the Calabi–Yau space $X_{(C)}$. Taking linear combinations for which the corresponding components of the Mori vectors vanish and going to a basis where curves on X bound the Kähler cone yields again

$$\begin{aligned} l^{(1)} &= (-4, -2; 2, 1, 1, \quad 1, 1, 0, 0, 0) \\ l^{(2)} &= (\quad 0, -2; 0, 1, 0, -1, 0, 1, 1, 0) . \end{aligned} \quad (3.40)$$

With $H = D_3D_{0,1}D_{0,2}$ and $L = D_6D_{0,1}D_{0,2}$ we find the same intersections as (3.14) and (3.16). The same conclusions arise for the other star triangulations.

To summarize all representations of the (2,30) model, be it different polyhedra, different nef-partitions, or different triangulations, are equivalent. Some of them exhibit, however, different parametrizations of the complex moduli space of the mirror.

3.2.4 The phase diagram

In the case of hypersurfaces it is well-known [50] that points in the interior of codimension one faces correspond to nonlinear automorphisms of the ambient space. A generic Calabi–Yau

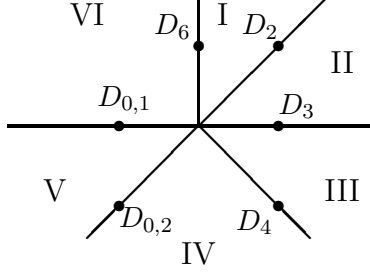


Figure 2: Secondary fan of the CICYs with $(h^{1,1}, h^{2,1}) = (2, 30)$.

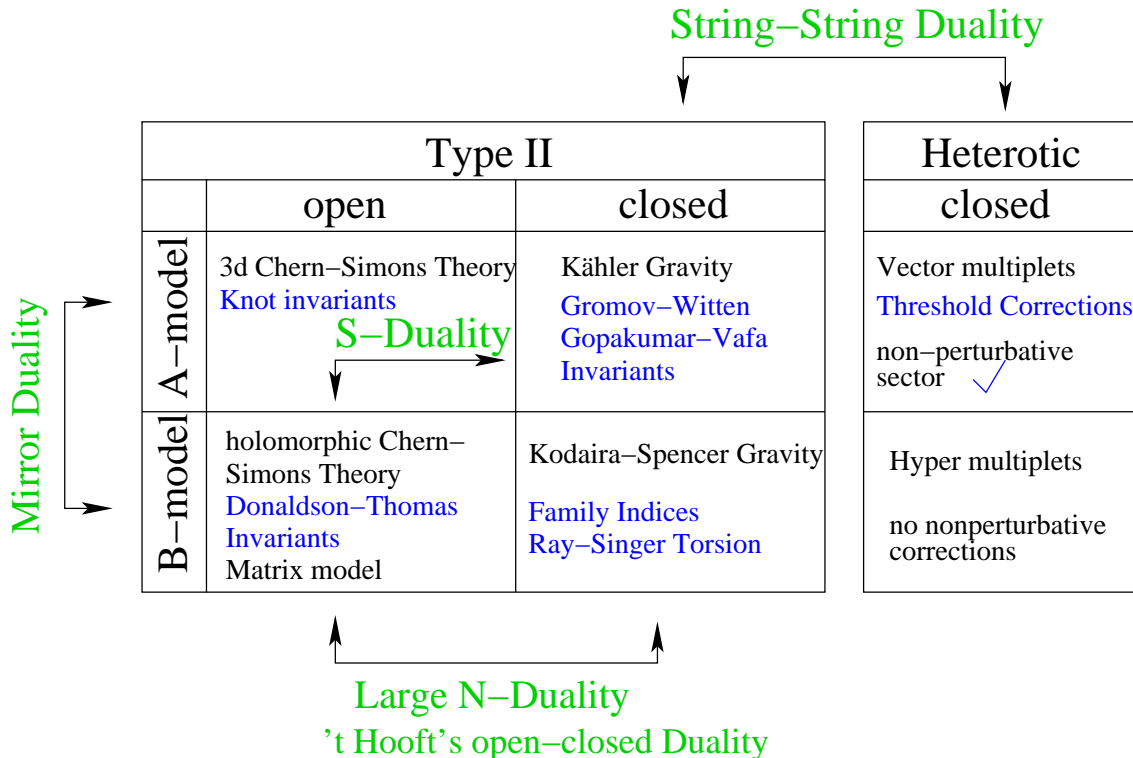
hypersurface does not intersect the divisors corresponding to these points, and can, therefore, be neglected for most purposes, e.g. for computing the intersection ring and the phase diagram. In the case of complete intersections of codimension $r > 1$ we have seen in the previous subsections that there are also vertices whose corresponding divisors do not intersect the generic complete intersection. We will now argue that these can be neglected a priori. We consider the example $X_{(C)}$ where D_8 and D_9 do not intersect $D_{0,1}D_{0,2}$. If we look for *all* the triangulations of $\langle 0_1 0_2 1234567 \rangle$ we find using the prescription given after (3.27)

$$\begin{aligned}
T_I &= \{ \langle 0_2 134567 \rangle, \langle 0_1 0_2 13457 \rangle, \langle 0_1 0_2 13456 \rangle, \langle 0_1 0_2 12347 \rangle, \langle 0_1 0_2 23457 \rangle, \langle 0_1 0_2 12457 \rangle, \\
&\quad \langle 0_1 0_2 12357 \rangle, \langle 0_1 0_2 12356 \rangle, \langle 0_1 0_2 12456 \rangle, \langle 0_1 0_2 12346 \rangle, \langle 0_1 0_2 23456 \rangle \} \\
T_{II} &= \{ \langle 0_1 0_2 13467 \rangle, \langle 0_1 0_2 12347 \rangle, \langle 0_1 0_2 23457 \rangle, \langle 0_1 0_2 12457 \rangle, \langle 0_1 0_2 12357 \rangle, \langle 0_1 0_2 34567 \rangle, \\
&\quad \langle 0_1 0_2 14567 \rangle, \langle 0_1 0_2 13567 \rangle, \langle 0_1 0_2 12356 \rangle, \langle 0_1 0_2 12456 \rangle, \langle 0_1 0_2 12346 \rangle, \langle 0_1 0_2 23456 \rangle \} \\
T_{III} &= \{ \langle 0_1 124567 \rangle, \langle 0_1 123467 \rangle, \langle 0_1 234567 \rangle, \langle 0_1 0_2 12367 \rangle, \langle 0_1 0_2 23567 \rangle, \langle 0_1 0_2 12567 \rangle, \\
&\quad \langle 0_1 0_2 12357 \rangle, \langle 0_1 0_2 13567 \rangle, \langle 0_1 0_2 12356 \rangle \} \\
T_{IV} &= \{ \langle 0_1 123457 \rangle, \langle 0_1 123456 \rangle, \langle 0_2 123567 \rangle, \langle 1234567 \rangle \} \\
T_V &= \{ \langle 0_1 123457 \rangle, \langle 0_1 123456 \rangle, \langle 0_2 123456 \rangle, \langle 0_2 123457 \rangle, \langle 0_2 134567 \rangle \} \\
T_{VI} &= \{ \langle 0_1 124567 \rangle, \langle 0_1 123567 \rangle, \langle 0_1 123467 \rangle, \langle 0_1 234567 \rangle, \langle 0_2 123567 \rangle \}
\end{aligned}$$

Here 0_1 and 0_2 denote the two “interior points” corresponding to $D_{0,1}$ and $D_{0,2}$, respectively. One can check that if we identified 0_1 with 0_2 and triangulated the polyhedron Δ^* instead of the Gorenstein cone $\Gamma(\Delta^*)$, then we would find 2 more triangulations. Looking at the columns of the Mori vectors in (3.40) we see, however, that we indeed expect only six triangulations. This confirms the statement that the phases are obtained by triangulating the Gorenstein cone instead of the polyhedron only. The corresponding phase diagram is drawn in figure 2. We see that the Kähler cone that we determined to be spanned by D_3 and D_6 in the previous subsections contains two phases. This is due to the fact that for $X_{(B)}$ and $X_{(C)}$ we needed to add ν_r^* in order to resolve all the singularities. This is also reflected in the different Mori cones (3.11) for $X_{(A)}$ on one hand, and respectively (3.25), (3.40) for $X_{(B)}$ and $X_{(C)}$ on the other hand. For $X_{(A)}$ we did not have to add a point in degree 2, so that the ray corresponding to D_2 points in the same direction as D_3 .

4 Topological strings on compact Calabi–Yau threefolds

All genus topological string amplitudes are non-trivial precisely on Calabi–Yau 3-folds. In the figure we give an overview over the various techniques to solve for these amplitudes in practice and we will discuss their applications and limitations below.



We want to emphasize that in this figure mirror symmetry is a map from the A–model on X to the B–model on its mirror X^* , while S–duality maps the A–model on X to the B–model on the *same* space. Furthermore, in the present work, we will use the latter to compute the Donaldson–Thomas invariants as an expansion of closed string amplitudes.

Easy generalizations of localization w.r.t. the torus action or the use of large N-transition, two techniques that are successful for non-compact toric varieties, fail for the compact case. In the first case the strata of the moduli space of higher genus maps to the compact Calabi–Yau are not restrictions of the moduli space of maps to the ambient space. Using the induced torus action of the ambient space on the moduli space of maps for localization with the Atiyah–Bott fixed point theorem will therefore not work. The topological vertex [51] is a tool which implements the large N transition idea systematically for all non-compact toric Calabi–Yau spaces and solves the open/closed topological string in these backgrounds. It relies likewise on the localization to equivariant maps under the torus action and does not generalize straightforwardly to the compact case. The remaining tools are the B-model, heterotic type II string duality [52] and direct calculation of the cohomology of D-brane moduli spaces. Unlike localizations and large N duality, the first two methods will give the holomorphic and the antiholomorphic de-

pendence of the amplitudes. So far the second one gives only the amplitudes for K3 fibrations in the limit of large \mathbb{P}^1 base. Like localizations and large N techniques the last method calculates the holomorphic limit. But it seems that the calculational methods developed in [2] will become mathematically rigorous using the newly discovered relation between Gromov–Witten and Donaldson–Thomas invariants. For a recent comparison between Gromov–Witten, Gopakumar–Vafa and Donaldson–Thomas invariants see also [53].

4.1 Solution of the B-model on compact multi parameter Calabi–Yau spaces

The main physical application of mirror symmetry, manifest in the toric complete intersections, is the exact calculation of terms in the effective action of string compactification on the Calabi–Yau manifolds, by the variation of the Hodge structure under complex structure deformations. These deformations are unobstructed on Calabi–Yau spaces and the physical interpretation of Kodaira deformation theory leads to the topological B-model expansion in orders λ^{2g-2} of the topological string coupling λ . The simplest application is to the vector multiplet moduli space \mathcal{M} in type IIB compactification on the Calabi–Yau manifold X^* . \mathcal{M} is a Kähler manifold with special geometry, which is directly identified with the complex structure moduli space of the Calabi–Yau space X^* . In the resulting four dimensional $N = 2$ supergravity theory the calculation yields at genus $g = 0$ the exact Kähler potential for the vector moduli fields including the exact gauge couplings, as well as the moduli dependent BPS masses and the triple couplings, in lowest order in λ^{2g-2} at genus $g = 0$. The higher order terms $g > 0$ give the exact moduli dependence of the coupling of the selfdual part of the Riemann curvature to the selfdual part of the graviphoton field strength $R_+^2 F_+^{2g-2}$. If X and X^* are mirror pairs, mirror symmetry extends the application of the above calculation to the vector multiplet moduli space of type IIA on X , where the couplings are world-sheet instanton corrected and therefore Kähler structure dependent. (For a review and further references, see e.g. [54].) The calculation gives only limited information about the hypermultiplet moduli space of both type II theories, because the latter is doubled by RR field background values to a quaternionic manifold, which is hard to access by worldsheet methods. On the other hand string/string duality and flux compactifications extend the relevance of our analysis to vector multiplets of the $N = 2$ heterotic string and the superpotential of chiral multiplets in $N = 1$ compactifications.

In this chapter we will outline the techniques necessary to obtain the effective action for the general class of complete intersections described above. Calabi–Yau hypersurfaces in torically resolved ambient spaces have been treated in some generality. The cases of complete intersections that were discussed in the literature, however, avoided the singularities of the ambient space apart from one class of examples with \mathbb{Z}_2 curve singularities in [6]. One aim of the present investigation is to overcome various technical complications in finding the Picard–Fuchs operators, good coordinates and an integral basis of solutions corresponding to the geometric periods for the general complete intersection Calabi–Yau in toric ambient spaces. This will be described in Appendix A. Our main progress however is the construction of the propagators of the Kodaira–Spencer Gravity for the compact multi moduli case.

4.2 $N = 2$ special geometry

The B-model twist [55] modifies the spin operator of the $N = (2, 2)$ world sheet theory by the axial $U(1)_A$ operator¹² so that $Q_B = \bar{Q}_+ + \bar{Q}_-$ becomes a scalar BRST operator, well defined for all world-sheet genus. The cohomology of local observables is isomorphic to $\oplus_{p,q} H^p(X^*, \wedge^q TX^*)$ and the marginal deformations, *i.e.* $p = q = 1$, of the B-model are identified with the complex structure deformations¹³ of X^* .

The genus g correlators with n marginal B-model observables inserted $C_{i_1, \dots, i_n}^{(g)}$ are derivable from generating functions $\mathcal{F}^{(g)}$ as

$$\begin{aligned} C_{i_1, \dots, i_n}^{(g)} &= D_{i_1} \dots D_{i_n} \mathcal{F}^{(g)}, \quad \text{with} \\ D_i &= \partial_{t^i} - \Gamma_i - (2 - 2g) \partial_{t^i} K. \end{aligned} \quad (4.1)$$

The D_i are covariant w.r.t. the metric connection on the moduli space as well as w.r.t. Kähler transformations, *i.e.* Γ_{jk}^i is the connection of the special Kähler metric on the vector multiplet moduli space. This metric is identified with the Weil–Petersson metric of the complex structure moduli space \mathcal{M} of X^* . Its Kähler potential $K(t, \bar{t})$ is derivable from $\mathcal{F}^{(0)}$, the generating function of the genus zero Gromov–Witten invariants of X^* , which is called prepotential. It is a section of a holomorphic line bundle \mathcal{L}^2 over \mathcal{M} , where the power 2 indicates the transformation, multiplication by $e^{2f(t)}$, under a holomorphic change of the unique $(3, 0)$ form $\Omega \rightarrow \Omega e^{f(t)}$ of the Calabi–Yau manifold. More generally, the $\mathcal{F}^{(g)}$ transform as a section of \mathcal{L}^{2-2g} .

We set $h = h^{2,1}(X^*) = h^{1,1}(X)$. In inhomogeneous variables $t^i = \frac{X^i}{X^0}$, $i = 1, \dots, h$, with the A-periods $X^I = \int_{A^I} \Omega$, $I = 0, \dots, h$, one has

$$\exp(-K(t, \bar{t})) = (t^i - \bar{t}^{\bar{i}})(\partial_{t^i} \mathcal{F}^{(0)} + \partial_{\bar{t}^{\bar{i}}} \bar{\mathcal{F}}^{(0)}) - 2(\mathcal{F}^{(0)} - \bar{\mathcal{F}}^{(0)}). \quad (4.2)$$

Note that $\Omega \rightarrow e^{f(t)} \Omega$ induces a transformation of the Kähler potential, $K \rightarrow K - f(t) - \bar{f}(\bar{t})$, leaving the metric $G_{\bar{i}j} = \partial_{\bar{t}^{\bar{i}}} \partial_{t^j} K$ invariant. The special Kähler property of \mathcal{M} manifests itself also in the special relation between the Riemann curvature and the genus 0 correlators¹⁴

$$R_{i\bar{k}j}^l = -\bar{\partial}_{\bar{k}} \Gamma_{ij}^l = [D_i, \partial_{\bar{k}}]_j^l = G_{\bar{k}i} \delta_j^l + G_{\bar{k}j} \delta_i^l - C_{ijm} \bar{C}_{\bar{k}}^{ml} \quad (4.3)$$

4.3 The genus zero sector

The genus zero sector is derived from the period integrals of X^* , which can be partly obtained by direct computation and more systematically by solving the Picard–Fuchs equations. The large complex structure limit in \mathcal{M} can be defined from the Kähler cone of the original manifold X .

¹²This current is anomalous unless the target space X^* is a Calabi–Yau manifold.

¹³The extended deformation space w.r.t. all operators in $\oplus_{p,q} H^p(X^*, \wedge^q TX^*)$ has been considered in [56].

¹⁴To simplify notations quantities with no superscript ⁽⁰⁾ refer also to the genus zero sector.

If $\Pi = (\int_{A_i} \Omega, \int_{B_i} \Omega) = (X^i, F_i)$ is a symplectic¹⁵ basis of the periods one has

$$\begin{aligned} e^{-K} &= -i \int_{X^*} \Omega \wedge \bar{\Omega} = i \Pi^\dagger \Sigma \Pi \\ C_{ijk}^{(0)} &= D_i D_j D_k \mathcal{F}^{(0)} = \int_{X^*} \Omega \wedge \partial_i \partial_j \partial_k \Omega . \end{aligned} \quad (4.4)$$

The special Kähler equation (4.3) guarantees that $\mathcal{F}^{(0)}$ can be integrated compatibly with (4.2).

Given the data for the Mori cone (3.6) and the classical intersections numbers κ_{abc} we can follow [6] and write down a local expansion of the periods convergent near the large complex structure point, which is characterized by its maximal unipotent monodromy. We review in the following just the essentials and refer to [6] for further details.

A particular set of local coordinates z_a on the complex structure moduli space on X^* is defined by $z_b = \prod_{i=1}^n a_i^{l_i^{(b)}}$, $b = 1, \dots, h$ in terms of a_i , the coefficients in the polynomial constraints of the complete intersection in the torus variables (2.6). A point of maximal unipotent monodromy is then always at $z_b = 0$. Let ϖ_{a_1, \dots, a_s} be obtained by the Frobenius method¹⁶ [6] from the coefficients of the holomorphic function $\varpi(\vec{z}, \vec{\rho})$ defined as

$$\begin{aligned} \varpi(z_1, \dots, z_h, \rho_1, \dots, \rho_h) &= \sum_{\{n_a\}} c(n_1 \dots n_h, \rho_1 \dots \rho_h) \prod_{a=1}^h z_a^{n_a + \rho_a} \\ c(n_1, \dots, n_h, \rho_1, \dots, \rho_h) &= \frac{\prod_{m=1}^r \Gamma(1 - \sum_{a=1}^h \tilde{l}_m^{(a)}(n_a + \rho_a))}{\prod_{i=1}^n \Gamma(1 + \sum_{a=1}^h l_i^{(a)}(n_a + \rho_a)} \\ \varpi_{a_1, \dots, a_s}(z_1, \dots, z_h) &= \left(\frac{1}{2\pi i}\right)^s \partial_{\rho_{a_1}} \dots \partial_{\rho_{a_s}} \varpi(z_1, \dots, z_h, \rho_1, \dots, \rho_h) \Big|_{\{\rho_a=0\}} . \end{aligned} \quad (4.5)$$

Define also $\sigma_{a_1, \dots, a_s} = (\varpi_{a_1, \dots, a_s}(z_1, \dots, z_h) \Big|_{\log(z_a)=0}) / \varpi(z_1, \dots, z_h, \rho_1, \dots, \rho_h) \Big|_{\{\rho_a=0\}}$. At the large complex structure point the mirror map defines natural flat coordinates on the Kähler moduli space of the original manifold X

$$t^a = \frac{X^a}{X^0} = \frac{1}{2\pi i} (\log(z_a) + \sigma_a), \quad a = 1, \dots, h , \quad (4.6)$$

where $X^0 = \varpi(z_1, \dots, z_h, \rho_1, \dots, \rho_h) \Big|_{\rho=0}$ is the unique holomorphic period at $z_a = 0$ and $X^a = \varpi_a$ are the logarithmic periods. Double and triple logarithmic solutions are given by

$$w_a^{(2)} = \frac{1}{2} \sum_{b,c=1}^h \kappa_{abc} \varpi_{bc}(z_1, \dots, z_h), \quad a = 1, \dots, h. \quad (4.7)$$

$$w^{(3)} = \frac{1}{6} \sum_{a,b,c=1}^h \kappa_{abc} \varpi_{abc}(z_1, \dots, z_h) , \quad (4.8)$$

¹⁵W.r.t. $\Sigma = \begin{pmatrix} 0 & \mathbf{1} \\ -\mathbf{1} & 0 \end{pmatrix}$.

¹⁶The holomorphic period $\varpi(z_1, \dots, z_h)$ can also be directly integrated using a residuum expression for the holomorphic (3, 0) form. An illustrative example for a complete intersection is given in Appendix A.

where κ_{abc} are the classical intersection numbers in (3.13). The prepotentials $F^{(0)}(X^I)$ in homogeneous or $\mathcal{F}^{(0)}(t^a)$ in inhomogeneous coordinates can now be written as

$$\begin{aligned} F^{(0)} &= -\frac{\kappa_{abc}X^aX^bX^c}{3!X^0} + A_{ab}\frac{X^aX^b}{2} + c_aX^aX^0 - i\chi\frac{\zeta(3)}{2(2\pi)^3}(X^0)^2 + (X^0)^2f(q) \\ &= (X^0)^2\mathcal{F}^{(0)} = (X^0)^2\left[-\frac{\kappa_{abc}t^at^bt^c}{3!} + A_{ab}t^at^b + c_at^a - i\chi\frac{\zeta(3)}{2(2\pi)^3} + f(q)\right] \end{aligned} \quad (4.9)$$

where $q_a = \exp(2\pi it^a)$, $c_a = \frac{1}{24}\int_X c_2 J_a$ and χ is the Euler number of X . The real coefficients A_{ab} are not completely fixed. They are unphysical in the sense that $K(t, \bar{t})$ and $C_{abc}(q)$ do not depend on them. A key technical problem¹⁷ in the calculation is to invert the exponentiated mirror map (4.6) to obtain $z_i(\underline{t})$. An integral symplectic basis for the periods is given by

$$\Pi = X^0 \begin{pmatrix} 1 \\ t^a \\ 2\mathcal{F}^{(0)} - t^a\partial_{t^a}\mathcal{F}^{(0)} \\ \partial_{t^a}\mathcal{F}^{(0)} \end{pmatrix} = X^0 \begin{pmatrix} 1 \\ t^a \\ \frac{\kappa_{abc}t^at^bt^c}{3!} + c_at^a - i\chi\frac{\zeta(3)}{(2\pi)^3} + 2f(q) - t^a\partial_{t^a}f(q) \\ -\frac{\kappa_{abc}t^bt^c}{2} + A_{ab}t^b + c_a + \partial_{t^a}f(q) \end{pmatrix} \quad (4.10)$$

This period vector can be uniquely given in terms of (4.8),(4.5) by adapting the leading log behaviour. The A_{ab} are further restricted by the requirement that the Peccei-Quinn symmetries $t^a \rightarrow t^a + 1$ act as integral $\mathrm{Sp}(2h^{11} + 2, \mathbb{Z})$ transformations on Π . Note that $\mathcal{F}^{(0)}$ can be read off from the periods and since t^a are flat coordinates, we have

$$C_{abc}(q) = \partial_{t^a}\partial_{t^b}\partial_{t^c}\mathcal{F}^{(0)} = \kappa_{abc} + \sum_{d_a, d_b, d_c \geq 0} n_d^{(0)} d_a d_b d_c \frac{q^d}{1 - q^d}, \quad (4.11)$$

where the sum counts the contribution of the genus zero worldsheet instantons. We defined $q^d = \prod_a e^{-2\pi i d_a t^a}$ where the tuple (d_1, \dots, d_h) specifies a class Q in $H^2(X, \mathbb{Z})$.

An alternative way of obtaining $C_{abc}(q)$ is to first calculate $Y_{ijk} := C_{ijk}(z)$ from the last equation in (4.4) and the Picard-Fuchs operators (A.8). This leads to linear differential equations, which determine Y_{ijk} up to a common constant, see again [6] for details. $C_{abc}(q)$ follows from $Y_{ijk}(z)$ using the inverse mirror map (4.6) $z = z(t)$ in a special gauge w.r.t. \mathcal{L}^2 as

$$C_{abc}(q) = \frac{1}{X_0^2} \frac{\partial z_i}{\partial t^a} \frac{\partial z_j}{\partial t^b} \frac{\partial z_k}{\partial t^c} Y_{ijk}(z(q)). \quad (4.12)$$

Knowledge of the $Y_{ijk}(z)$ will be essential for determining the B-model propagators in the next subsection.

4.4 Multi parameter B-model propagators

The key to the solution of the B-model are the holomorphic anomaly equations [57]. The derivatives of $\mathcal{F}^{(g)}$ or $C_{i_1, \dots, i_n}^{(g)}$ w.r.t. the antiholomorphic coordinates lead to an integral over an

¹⁷We wrote an improved code for that [11].

exact form over the moduli space $\mathcal{M}_{g,n}$ of the world sheet curve Σ_g , which receives contributions only from the boundary of $\mathcal{M}_{g,n}$. In particular, C_{abc} is holomorphic because the sphere is rigid and three points can be fixed by $\text{SL}(2, \mathbb{C})$, and therefore the boundary of the moduli space is empty. In the other cases the boundary contributions leads to recursive differential equations, the so called holomorphic anomaly equations [57], which read for $g > 1$

$$\bar{\partial}_{\bar{k}} \mathcal{F}^{(g)} = \frac{1}{2} \bar{C}_{\bar{k}}^{ij} \left(D_i D_j \mathcal{F}^{(g-1)} + \sum_{r=1}^{g-1} D_i \mathcal{F}^{(r)} D_j \mathcal{F}^{(g-r)} \right) \quad (4.13)$$

and for $g = 1$ [58]

$$\bar{\partial}_{\bar{k}} \partial_m \mathcal{F}^{(1)} = \frac{1}{2} \bar{C}_{\bar{k}}^{ij} C_{mij} + \left(\frac{\chi}{24} - 1 \right) G_{\bar{k},m} . \quad (4.14)$$

Both terms in (4.13) have an obvious interpretation as coming from boundary components of $\mathcal{M}_{g,n}$; the first from pinching a handle and the second from pinching the connection between two irreducible components of genus r and $g-r$. In (4.14) the first and second term correspond, respectively, to also pinching a handle and to a contact term which arises when the locations of the two operators needed to fix the conformal symmetry coincide.

Here $\bar{C}_{\bar{k}}^{ij} = e^{2K} G^{i\bar{i}} G^{j\bar{j}} \bar{C}_{i\bar{j}\bar{k}}$ is related to the antiholomorphic coupling $\bar{C}_{i\bar{j}\bar{k}}$, which is symmetric in its indices and fulfils an integrability condition, known as the WDVV equations, $D_i \bar{C}_{j\bar{k}\bar{l}} = D_j \bar{C}_{i\bar{k}\bar{l}}$. It can therefore be derived from a section S of \mathcal{L}^{-2} as

$$\bar{C}_{i\bar{j}\bar{k}} = e^{-2K} D_{\bar{i}} D_{\bar{j}} D_{\bar{k}} S . \quad (4.15)$$

One of the main prerequisites to solve (4.13) recursively is the construction of S . It is convenient to define as intermediate steps of the above integration $S_{\bar{j}}$, $S_{\bar{j}}^i$, S^i and S^{ij} by

$$\begin{aligned} S^i &= G^{i\bar{j}} S_{\bar{j}} = G^{i\bar{j}} \bar{\partial}_{\bar{j}} S \\ S^{ik} &= G^{k\bar{k}} S_{\bar{k}}^i = G^{k\bar{k}} \bar{\partial}_{\bar{k}} S^i \\ \bar{C}_{\bar{k}}^{ij} &= \bar{\partial}_{\bar{k}} S^{ij} . \end{aligned} \quad (4.16)$$

These are used in rewriting the right hand side of (4.13) in successive steps as $\partial_{\bar{k}}[\dots]$. I.e. one gets in the first step $\partial_{\bar{k}} \frac{1}{2} S^{ij}(\dots) - \frac{1}{2} S^{ij} \partial_{\bar{k}}(\dots)$ on the right hand side. Using the commutator (4.3) from special geometry and (4.13), (4.14) in the second term one gets again terms in which antiholomorphic derivatives of S, S^i, S^{ij} can be substituted using (4.16). Repeating the partial integration and the application of $[\partial_{\bar{k}}, D_i]$ and (4.13), (4.14) one gets after g steps the desired total derivative $\partial_{\bar{k}}[\dots]$. In the final expression we set $K^{\phi\phi} := -S$, $K^{i,\phi} := -S^i$ and $K^{ij} := -S^{ij}$ which can be interpreted as propagators of a Feynman expansion, where i labels moduli fields and ϕ the dilaton. Using the formula for the Ricci tensor in Kähler geometry $R_{i\bar{i}} = -\frac{1}{2} \partial_i \partial_{\bar{i}} \log \det(G)$ and (4.3) one can integrate the anomaly (4.14) to ¹⁸

$$\mathcal{F}^{(1)} = \frac{1}{2} \log \left(\det(G^{-1}) \exp \left(K \left(3 + h^{11} - \frac{\chi}{12} \right) \right) |f_1| \right) . \quad (4.17)$$

¹⁸The normalization of $\mathcal{F}^{(1)}$ differs from the normalization of $\mathcal{F}^{(1),\text{het}}$ by $\frac{16\pi^2}{24}$ [7]. This will be taken up in the discussion of free quotients in Section 7.2

Here $f_1 = \prod_i \Delta_i^{r_i}$ is a function on the moduli space \mathcal{M} , which encodes the behaviour of $\mathcal{F}^{(1)}$ at the various components Δ_i of the discriminant loci. We can alternatively use the propagator S^{ij} to write

$$\partial_k \mathcal{F}^{(1)} = \frac{1}{2} S^{ij} C_{ijk} + \left(\frac{\chi}{24} - 1 \right) \partial_k (K + \log f_1). \quad (4.18)$$

Here no partial integration was required since C_{ijk} is holomorphic. For the same reason one can rewrite (4.3) as $\bar{\partial}_k [S^{ij} C_{jkl}] = \bar{\partial}_k [\delta_l^i \partial_k K + \delta_k^i \partial_l K + \Gamma_{kl}^i]$. At the expense of introducing a holomorphic ambiguity A_{ij}^p , the $\bar{\partial}_k$ derivative can be removed and the equation is solved for S^{ij}

$$S^{ij} = (C_k^{-1})^{jl} \left((\delta_k^i \partial_l + \delta_l^i \partial_k) K + \Gamma_{kl}^i + A_{kl}^i \right) =: (C_k^{-1})^{jl} (Q_{kl}^i + A_{kl}^i), \quad k = 1, \dots, h \quad (4.19)$$

In this last step we must assume that the matrix $(C_k)_{ij} = C_{ijk}$ is invertible, see below. The left hand side S^{ij} should be a unique and globally defined section of $\text{Sym}^2 T^* \mathcal{M}_{g,n} \times \mathcal{L}^{-2}$. This has three important consequences: First A_{kl}^i is not a tensor but has to compensate for the non covariant transformation of Q_{kl}^i , i.e.

$$A_{kl}^i = \delta_k^i \partial_l \log(f) + \delta_l^i \partial_k \log(f) - v_{l,a} \partial_k v^{i,a} + T_{kl}^i, \quad (4.20)$$

where $f \in \mathcal{L}$, $v_{i,a}$ are h sections of $T\mathcal{M}_{g,n}$ and T_{kl}^i does transform as a tensor. Secondly we must satisfy the compatibility

$$(C_\kappa^{-1})^{il} (Q_{\kappa l}^i + A_{\kappa l}^i) = (C_\mu^{-1})^{il} (Q_{\mu l}^i + A_{\mu l}^i) \quad \forall \mu \neq \kappa, \quad \mu, \kappa = 1, \dots, h \quad (4.21)$$

and finally ensure the symmetry

$$(C_\kappa^{-1})^{jl} (Q_{\kappa l}^i + A_{\kappa l}^i) = (C_\kappa^{-1})^{il} (Q_{\kappa l}^j + A_{\kappa l}^j) \quad \forall i \neq j, \quad i, j = 1, \dots, h. \quad (4.22)$$

We solve the equations (4.21), (4.22) by first finding A_{jk}^i algebraically. It turned out that one could always make the solution covariant by finding $v_{i,a}$ and f and that T_{jk}^i could be set to zero. From $\partial_i S^j = G_{i\bar{i}} S^{j\bar{i}}$ and $S^{ij} C_{jkl} = Q_{kl}^i + A_{kl}^i$ we get

$$S^i C_{ikl} = (\partial_k K \partial_l K - \partial_k \partial_l K + A_{kl}^i \partial_i K) + A_{kl} =: Q_{kl} + A_{kl}. \quad (4.23)$$

If A_{kl}^i transforms as in (4.20), which we always could achieve, then A_{ij} transforms as $\text{Sym}^2 T\mathcal{M}_{g,n}$. We get again constraints on the A_{jk} from the uniqueness of $S^i = (C_\kappa^{-1})^{ij} (Q_{\kappa j} + A_{\kappa j})$, $\kappa = 1, \dots, h$, namely

$$(C_\kappa^{-1})^{ij} (Q_{\kappa j} + A_{\kappa j}) = (C_\mu^{-1})^{ij} (Q_{\mu j} + A_{\mu j}), \quad \mu \neq \kappa, \quad \mu, \kappa = 1, \dots, h \quad (4.24)$$

In this step we found the necessity of non zero rational A_{ij} in some cases. The last propagator S involves no further algebraic consistency conditions and a special solution is given by [57]

$$S = \frac{1}{2h^{11}} [(h^{11} + 1) S^i - D_j S^{ij} - S^{ij} S^{kl} C_{jkl}] \partial_i (K + \log(|f|)/2) + \frac{1}{h^{11}} (D_i S^i + S^i S^{jk} C_{ijk}). \quad (4.25)$$

4.5 Compatibility constraints on the multi parameter mirror maps

So far (4.21), (4.22) and (4.24) have not been solved for global multi parameter Calabi–Yau manifolds. The one parameter case is of course trivial in this respect. What we have found is that the conditions (4.21) to (4.24) are in general non-trivial and can nevertheless be solved with rational functions A_{kl}^i, A_{kl} over the complex structure moduli space \mathcal{M} . In the holomorphic limit $\bar{t}^i \rightarrow 0$, one has

$$\begin{aligned} G_{\bar{p}j} &= \delta_{\bar{p}p} \frac{\partial t_j}{\partial z_p}, & G^{j\bar{p}} &= \delta^{\bar{p}p} \frac{\partial z_p}{\partial t_j}, \\ \Gamma_{kj}^i &= -\frac{\partial z^i}{\partial t_p} \frac{\partial}{\partial z_k} \frac{\partial t_p}{\partial z_j} = \frac{\partial t_p}{\partial z_j} \frac{\partial}{\partial z_k} \frac{\partial z^i}{\partial t_p}, \\ K &= \log(X^0). \end{aligned} \tag{4.26}$$

The equations (4.21) to (4.24) and the fact that we can find rational A_{kl}^i, A_{ij} in z do therefore constitute non-trivial relations for the derivatives of the mirror maps and derivatives of X^0 . This generalizes in an interesting way observations that the mirror maps of local multi parameter Calabi–Yau manifolds fulfil rational relations $Q(z_1, \dots, z_h; t^1, \dots, t^h) = 0$. For example, in the case of the local Calabi–Yau $\mathcal{O}(-2, -2) \rightarrow \mathbb{P}^1 \times \mathbb{P}^1$ it was found in [59] that the relation $t_1 z_2 = z_1 t_2$ holds and with $X^0 = 1$ in the local case, one can use the rational relation to find a solution of (4.21), (4.22). In the local case (4.24) is always trivial as was shown in [60]. Here we find that (4.24) is in general non-trivial, while rational expressions in z for A_{ij} could always be found.

The number of constraints does depend furthermore on the fibration structure of X . We found e.g. that for elliptically fibered Calabi–Yau manifolds such as $\mathbb{P}_{1,1,1,6,9}$ [18] and $\mathbb{P}_{1,1,2,8,12}$ [24] the $(C_k)_{ij}$ are not invertible over the index k that corresponds to the class of the elliptic fiber, hence there are $h - 1$ constraints less in (4.21).

4.6 The solutions to the holomorphic anomaly equations

Solutions to the holomorphic anomaly equations (4.13) have been constructed in [57] for genus two and in [2] up to genus four for the compact and genus seven for the non-compact case. As an example we quote from [57] the solution of (4.13) for $g = 2$, which we will compute in the examples below:

$$\begin{aligned} \mathcal{F}^{(2)}(t, \bar{t}) &= \frac{1}{2} S^{ij} C_{ij}^{(1)} + \frac{1}{2} C_i^{(1)} S^{ij} C_j^{(1)} - \frac{1}{8} S^{ij} S^{kl} C_{ijkl} \\ &\quad - \frac{1}{2} S^{ij} C_{ijk} S^{kl} C_l^{(1)} + \frac{\chi}{24} S^i C_i^{(1)} \\ &\quad + \frac{1}{8} S^{ij} C_{ijk} S^{kl} C_{lmn} S^{mn} + \frac{1}{12} S^{il} S^{jm} S^{kn} C_{ijk} C_{lmn} \\ &\quad - \frac{\chi}{48} S^i C_{ijk} S^{jk} + \frac{\chi}{24} \left(\frac{\chi}{24} - 1 \right) S + f_2(t) \end{aligned} \tag{4.27}$$

where $f_2(t)$ is the holomorphic ambiguity coming from the integration of (4.13). We should stress that the solutions for $\mathcal{F}^{(g)}$ in [57], [2] together with the Kähler potential and the Weil–Peterson metric (4.3) are sufficient to obtain the full (t, \bar{t}) dependence of $\mathcal{F}^{(g)}$. However the

determination of $f_g(t)$ is the main difficulty in finding an explicit solution for a given X . The general form of $f_g(t)$, $g > 0$ is expected to be, written in terms of the complex structure moduli $z = z(t)$,

$$f_g(z) = \sum_{i=1}^D \sum_{k=0}^{2g-2} \frac{p_i^{(k)}(z)}{\Delta_i^k} \quad (4.28)$$

where D is the number of components Δ_i of the discriminant, and $p_i^{(k)}(z)$ are polynomials of degree k . At present, it is not known how to determine the $p_i^{(k)}(z)$ a priori. Their structure is presumably related to the compactification of the complex structure moduli space \mathcal{M} , i.e. it is encoded in the boundary of \mathcal{M} . It would be interesting to make this relation precise. For our purpose, we will make an ansatz and try to constrain this ansatz by using all the knowledge about the $\mathcal{F}^{(g)}$ that is already available. We will address this point in detail in Section 5.3.

5 Topological free energy and partition function

The only currently known way to derive the free energy of the topological A-model on a Calabi–Yau manifold X

$$\mathcal{F}(\lambda, t, \bar{t}) = \sum_{\lambda=0}^{\infty} \lambda^{2g-2} \mathcal{F}^{(g)}(t, \bar{t}) \quad (5.1)$$

is to use mirror symmetry and the solutions to the holomorphic anomaly equation described in the last section. The topological partition function

$$Z(\lambda, t, \bar{t}) = e^{\mathcal{F}(\lambda, t, \bar{t})} \quad (5.2)$$

has a very elegant interpretation essentially as a wave function Ψ in an auxiliary Hilbert space, which arises by geometric quantization of $H^3(X, \mathbb{Z})$ [61]. The holomorphic anomaly equations are interpreted as granting the independence of Ψ on the choice of the symplectic structure on $H^3(X, \mathbb{Z})$ relative e.g. to the symplectic structure induced by a given complex structure on X . To specify the state Ψ , which corresponds to the topological string, a huge amount of holomorphic boundary data are needed, namely the holomorphic $f^{(g)}$. To make progress here, we discuss what is known in various holomorphic limits of $\mathcal{F}^{\text{hol}}(\lambda, t) = \lim_{\bar{t} \rightarrow \infty} \mathcal{F}(\lambda, t, \bar{t})$.

5.1 Holomorphic free energy and partition function

In this limit $\mathcal{F}^{\text{hol}}(\lambda, t)$ has a conjectured expansion in terms of BPS states associated to M2 branes wrapped around a holomorphic curve C and the M-theory circle. The charge Q of the BPS state is labelled by the homology class of the curve, i.e. $Q \in H_2(X, \mathbb{Z})$. The genus of the curve is related to the $SU(2)_L$ spin [62], [63].

More precisely, the authors of [63] consider an M-theory compactification on X to five dimensions. The space time BPS states fall into representations of the little group of the 5d

Lorentz group $L = \text{SO}(4) \simeq \text{SU}(2)_L \times \text{SU}(2)_R$. The low energy interpretation of the free energy F in 4d relates it to the 5d BPS spectrum through a Schwinger one loop calculation of the 4d $R_+^2 F_+^{2g-2}$ effective terms. A similar one loop calculation corrects the effective gauge coupling $\frac{1}{g^2(G,p^2)}$ through threshold effects [64]. Note that these 4d calculations are sensitive to the off shell quantum numbers, i.e. to $\text{SU}(2)_L \times \text{SU}(2)_R$. Only BPS particles annihilated by the supercharges in the $(\mathbf{0}, \frac{1}{2})$ representation contribute to the loop. They couple to the anti-selfdual graviphoton field strength F_+ and the anti-selfdual curvature R_+ only via their left spin eigenvalues of their representation under L . The right representation content enters solely via its multiplicity and a sign $(-1)^{2j_R^3}$, in particular any contribution of long multiplets is projected out by these signs. To summarize, the dependence of \mathcal{F} on the BPS spectrum is via a supersymmetric index

$$I(\alpha, \beta) = \text{Tr}_{\mathcal{H}} (-1)^{2j_L^3 + 2j_R^3} e^{-\alpha j_L^3 - \beta H} \quad (5.3)$$

and all information entering \mathcal{F} is carried by the following combination

$$\sum_{j_L^3, j_R^3} (-1)^{2j_R^3} (2j_R^3 + 1) N_{j_R^3, j_L^3}^Q[\mathbf{j}_L] = \sum_{g=0}^{\infty} n_Q^{(g)} I_g \quad (5.4)$$

of the multiplicities of the BPS states $N_{j_R^3, j_L^3}^Q$. The last basis change of the left spin from $[\mathbf{j}_L]$ to

$$I_g = \left[\left(\frac{\mathbf{1}}{\mathbf{2}} \right)_L + 2(\mathbf{0})_L \right]^{\otimes g} \quad (5.5)$$

relates the left spin to the genus g of C and defines the integer Gopakumar-Vafa invariants $n_Q^{(g)}$ associated to a holomorphic curve C of genus g in the class $Q = [C] \in H^2(X, \mathbb{Z})$. In contrast to the $n_Q^{(g)}$, the $N_{j_R^3, j_L^3}^Q$ are no symplectic invariants. They change when lines of marginal stability in the complex moduli space are crossed¹⁹ [2]. The $N_{j_R^3, j_L^3}^Q$ are interpreted as the dimension of $\text{SU}(2)_L \times \text{SU}(2)_R$ representations w.r.t. a natural action of this group on the cohomology of the moduli space of the M2 brane. This moduli space is given by the moduli of flat $\text{U}(1)$ connections on C and the moduli of the curve. A model for this space is the Jacobian fibration over the moduli space of the curve C in Q . The expansion of \mathcal{F}^{hol} in terms of these BPS state sums is obtained by performing the Schwinger loop calculation [65], [63] as

$$\begin{aligned} \mathcal{F}^{\text{hol}}(\lambda, t) &= \sum_{g=0}^{\infty} \lambda^{2g-2} \mathcal{F}^{(g)}(t) \\ &= \frac{c(t)}{\lambda^2} + l(t) + \sum_{g=0}^{\infty} \sum_{Q \in H_2(X, \mathbb{Z})} \sum_{m=1}^{\infty} n_Q^{(g)} \frac{1}{m} \left(2 \sin \frac{m\lambda}{2} \right)^{2g-2} q^{Qm} \\ &= \frac{c(t)}{\lambda^2} + l(t) + \sum_{g=0}^{\infty} \sum_{Q \in H_2(X, \mathbb{Z})} \sum_{m=1}^{\infty} n_Q^{(g)} (-1)^{g-1} \frac{[m]^{(2g-2)}}{m} q^{Qm}, \end{aligned} \quad (5.6)$$

¹⁹Notice that the successful microscopic interpretation of the 5d black hole entropy requires deformation invariance and relies on the index-like quantity and not on the total number of BPS states.

with

$$q^Q = e^{i \sum_{i=1}^{h^{1,1}} t_i \int_Q J_i}, \quad [x] := q_\lambda^{\frac{x}{2}} - q_\lambda^{-\frac{x}{2}}, \quad q_\lambda = e^{i\lambda}.$$

The cubic term $c(t)$ in the Kähler parameters t_i is the classical part of the prepotential $\mathcal{F}^{(0)}$ given in (4.9) without the constant term, and $l(t) = \sum_{i=1}^h \frac{t_i}{24} \int_X c_2 J_i$ is the classical part of $\mathcal{F}^{(1)}$. Using the expansion

$$\frac{1}{m} \frac{1}{\left(2 \sin \frac{m\lambda}{2}\right)^2} = \sum_{g=0} \lambda^{2g-2} (-1)^{g+1} \frac{B_{2g}}{2g(2g-2)!} m^{2g-3}$$

and a $\zeta(x) = \sum_{m=1}^{\infty} \frac{1}{m^x}$ regularization of the sum over m with $\zeta(-n) = -\frac{B_{n+1}}{n+1}$, we see that for $g \geq 2$ the $Q = 0$ constant map terms from localization [66]

$$\langle 1 \rangle_{g,0}^X = (-1)^g \frac{\chi}{2} \int_{\mathcal{M}_g} c_{g-1}^3 = (-1)^g \frac{\chi}{2} \frac{|B_{2g} B_{2g-2}|}{2g(2g-2)(2g-2)!} \quad (5.7)$$

are reproduced if we set $n_0^{(0)} = -\frac{\chi}{2}$. This choice also reproduces the constant term proportional to $\zeta(3)$ in $\mathcal{F}^{(0)}$. In $\mathcal{F}^{(1)}$ there is a $\zeta(1)$ term which requires an additional regularization.

In terms of the invariants $n_Q^{(g)}$ the partition function $Z^{\text{hol}} = \exp(\mathcal{F}^{\text{hol}})$ has the following product form²⁰

$$Z_{\text{GV}}^{\text{hol}}(X, q_\lambda, q) = \prod_Q \left[\left(\prod_{r=1}^{\infty} (1 - q_\lambda^r q^Q)^{r n_Q^{(0)}} \right) \prod_{g=1}^{\infty} \prod_{l=0}^{2g-2} (1 - q_\lambda^{g-l-1} q^Q)^{(-1)^{g+r} \binom{2g-2}{l} n_Q^{(g)}} \right]. \quad (5.8)$$

This product form resembles the Hilbert scheme of symmetric products written in terms of partition sums over free fermionic and bosonic fields with an integer $U(1)$ charge as well as the closely related product form for the elliptic genus of symmetric products. As it has already been pointed out in [62], it is also reminiscent of the Borcherds product form of automorphic forms of $O(2, n, \mathbb{Z})$, see [67] and [68] for a review. Here the idea is that integrality of the $n_Q^{(g)}$ is related to the fact that they are Fourier coefficients of other (quasi)automorphic forms, see also [69].

5.2 Donaldson–Thomas expansion

Another way to obtain BPS states is by wrapping D-branes on supersymmetric cycles in X . In particular, we can wrap Euclidean 6-branes on X itself and Euclidean 2-branes on a curve $C \subset X$, possibly bound to some 0-branes. At the level of RR charges such a configuration can be cast into a short exact sequence of the form

$$0 \longrightarrow \mathcal{I} \longrightarrow \mathcal{O}_X \longrightarrow \mathcal{O}_Z \longrightarrow 0 \quad (5.9)$$

²⁰Here we dropped the $\exp(\frac{c(t)}{\lambda^2} + l(t))$ factor of the classical terms at genus 0, 1.

where \mathcal{I} is the ideal sheaf describing this configuration and Z is the subscheme of X consisting of the curve C and the points at which the 0-branes are supported. Counting BPS states therefore leads to the study of the moduli space $I_m(X, Q)$ of such ideal sheaves \mathcal{I} , which has two discrete invariants: the class $Q = [Z] \in H_2(X, \mathbb{Z})$ and, roughly speaking, the number of 0-branes $m = \chi(\mathcal{O}_Z)$. Due to the Calabi–Yau condition the virtual dimension of $I_m(X, Q)$ is zero, and the number of BPS states with these charges is therefore obtained by counting the points in $I_m(X, Q)$. It is, however, not quite as simple as that because as is well-known from Gromov–Witten theory, these configurations can appear in families, and one has to work with the virtual fundamental class. Putting this important subtlety aside, this number is called the Donaldson–Thomas invariant $\tilde{n}_Q^{(m)}$ [70], [71]. These invariants are expected to be integral as they count BPS states.

Since both invariants, Gopakumar–Vafa and Donaldson–Thomas, keep track of the number of BPS states, they should be related. The relation is in fact a consequence of the S–duality in topological strings [72], and takes the following form. The factor in (5.8) coming from the constant maps gives the McMahon function $M(q_\lambda) = \prod_{n \geq 0} \frac{1}{(1-q_\lambda^n)^n}$ to the power $\frac{\chi}{2}$. This function appears also in Donaldson–Thomas theory [73], calculable on local toric Calabi–Yau spaces e.g. with the vertex [51]. However, in Donaldson–Thomas theory the power of the McMahon function is²¹ χ . Note also that if (5.6) holds then \mathcal{F} or Z restricted to this class is always a finite degree rational function in q_λ symmetric in $q_\lambda \rightarrow \frac{1}{q_\lambda}$, since the genus is finite in a given class Q . Thanks to this observation one can read from the comparison of the expansion of Z^{hol} in terms of Donaldson–Thomas invariants $\tilde{n}_Q^{(m)} \in \mathbb{Z}$

$$Z_{\text{DT}}^{\text{hol}}(X, q_\lambda, q) = \sum_{Q, m \in \mathbb{Z}} \tilde{n}_Q^{(m)} q_\lambda^m q^Q \quad (5.10)$$

with the expansion in terms of Gopakumar–Vafa invariants [73]

$$Z_{\text{GV}}^{\text{hol}}(X, q_\lambda, q) M(q_\lambda)^{\frac{\chi(X)}{2}} = Z_{\text{DT}}^{\text{hol}}(X, -q_\lambda, q) \quad (5.11)$$

the precise relation between $\tilde{n}_Q^{(m)}$ and $n_Q^{(g)}$. Eq. (5.6) and (5.8) then relate the two types of invariants to the Gromov–Witten invariants $r_Q^{(g)} \in \mathbb{Q}$ as in

$$\mathcal{F}_{\text{GW}}^{\text{hol}}(\lambda, q) = \sum_{g=0}^{\infty} \lambda^{2g-2} \sum_Q r_Q^{(g)} q^Q .$$

5.3 Constraints on the Ansatz

If we expand (5.6) we find for the genus 2 contribution

$$\mathcal{F}^{(2)}(t) = \frac{\chi}{5760} + \sum_Q \left(\frac{1}{240} n_Q^{(0)} + n_Q^{(2)} \right) \text{Li}_{-1}(q^Q) \quad (5.12)$$

²¹We would like to thank Jim Bryan for discussion on this point. The formula (5.8) has been independently derived by him, S. Katz and us.

We can compare this expression with the $\bar{t} \rightarrow 0$ limit of (4.27). However, in order to find the genus 2 instanton numbers $n_Q^{(2)}$ we need in general additional information. We have seen in the previous section that the system of equations determining $\mathcal{F}^{(2)}$ is overdetermined, and we have solved it using an ansatz. Furthermore, we made an ansatz for the holomorphic ambiguity $f_2(t)$ in (4.28). We therefore need additional consistency checks in order to fix all the ambiguities. We can obtain them from the following six sources.

- For low degrees Q , some of the $n_Q^{(g)}$ can be computed using classical algebraic geometry, in particular Castelnuovo theory, as is explained in [2].
- Next, the authors of [74] have given an argument for the expected behaviour of the $\mathcal{F}^{(g)}$ near the conifold locus in \mathcal{M} , described by the vanishing of Δ_{con} . It is given by the asymptotic expansion of the $c = 1$ string at the selfdual radius

$$\mathcal{F}(\mu) = \frac{1}{2}\mu^2 \log \mu - \frac{1}{12} \log \mu + \sum_{g=2}^{\infty} \frac{B_{2g}}{(2g-2)2g} \mu^{2-2g} + \dots \quad (5.13)$$

The leading coefficient in $f_2(z)$ in (4.28), $a_2 = p_{con}^{(2g-2)}(0)|_{g=2}$ is $a_2 = s \frac{1}{240}$. The factor $\frac{1}{240} = B_{2g}/(2g-2)(2g)|_{g=2}$ comes from (5.13) while the scaling factor $s = \frac{\prod_{i=1}^r d_i}{\prod_{i=1}^k w_i}$ of the natural coordinate in terms of the degrees d_i of the constraints of X and the weights w_i of the ambient weighted projective space \mathbb{P}_w^4 was already observed in [2]. In the case of general toric ambient spaces, we expect s to be given in terms of the generators of the Mori cone (3.6).

- Furthermore, at other singularities in the moduli space, a Calabi–Yau manifold X can degenerate to another Calabi–Yau manifold X' , having less moduli in general. This degeneration is typically described via a birational map $f : X \dashrightarrow X'$. The instanton numbers in this case are related by

$$n_{Q'}^{(g)}(X') = \sum_{Q:f(Q)=Q'} n_Q^{(g)}(X) \quad (5.14)$$

An example is the curve of \mathbb{Z}_2 singularities discussed in detail in [75].

- Fourth, if X admits an elliptic fibration, we can take the local limit of a large elliptic fiber, and obtain a non-compact Calabi–Yau manifold Y . Therefore, we can use the results for local Calabi–Yau manifolds from [60], [2], [76] and [59] to check that for $Q \in H_2(Y) \subset H_2(X)$ we have

$$n_Q^{(g)}(X) = n_Q^{(g)}(Y) \quad (5.15)$$

- On the other hand, if X admits a K3 fibration \mathcal{F}^{hol} has been evaluated using the heterotic-type II duality in the limit where the base of the fibration is large by [65] and [77]. We will extend their argument in several directions, and discuss it in detail in Section 6.

- Finally, closely related to the last result, as well as to the birational maps above, is the fact that one can in principle use the information contained in the monodromies about the singularities in the complex structure moduli space \mathcal{M} . For example, if Q and Q' are related by a Weyl reflection of the form $Q' = Q + \langle Q, D \rangle [C]$ for some divisor D and a rational curve C such that $D \cdot C < 0$ then [75], [78], [79]

$$n_Q^{(g)} = n_{Q'}^{(g)} \quad (5.16)$$

We will apply these additional consistency checks, where applicable, in the examples in the next sections.

6 Higher genus calculations for regular K3 fibrations

In this section we solve the higher genus amplitudes for K3 fibrations without reducible fibers, which we call regular. For simplicity we also assume that there is no monodromy on the algebraic cycles in the fiber, even though we expect that the general form of the formulas for \mathcal{F} below will not be affected by lifting this restriction.

6.1 $K3 \times T^2$

For C a curve in the class $[C]$ in the K3 with $C^2 = 2g - 2$ a formula for the topological free energy was given in [2]. It is based on a specific model of the moduli space of M2 branes, which leads to the Hilbert scheme of points on K3

$$\mathcal{H}^{\text{hol}}(\lambda, t) = \left(\frac{1}{2 \sin(\frac{\lambda}{2})} \right)^2 \prod_{n \geq 1} \frac{1}{(1 - e^{i\lambda} q^n)^2 (1 - q^n)^{20} (1 - e^{-i\lambda} q^n)^2} . \quad (6.1)$$

As we will review below, this formula is basically a reorganization of the formula of [80] keeping track of the $\mathfrak{su}(2)_L \times \mathfrak{su}(2)_R$ quantum numbers. Closely related situations on $T^4 \times S^1$ were discussed in [1] and a very similar logic for the counting of the BPS states in the $Q = [B] + g[F]$ class, in an elliptic del Pezzo surface with base B and fiber F , appeared in [81]. In the latter case there is no complex structure deformation and one could in principle calculate $N_{j_L^3, j_R^3}^Q$. A generalization of (6.1) for classes wrapping the T^2 base involving the elliptic genus of $\text{Hilb}^n(\text{K3})$ was also given in [2].

As it stands (6.1) is not very useful, because in the $N = 4$ supersymmetry preserving geometry $T^2 \times \text{K3}$ the index calculating \mathcal{F} vanishes, since the factor from the torus involving $(\frac{1}{2})_R + 2(\mathbf{0})_R$ vanishes under the sum $\sum_R (-1)^{2j_R^3} (2j_R^3 + 1)$ over the right $\text{SU}(2)_R$ representations. There are three possibilities to make it applicable to $N = 2$ geometries.

- Use the deformation invariance to make predictions for classes in the K3 fiber of regular K3 fibrations. This will be done in the next section.

- Consider a local model $\mathcal{O}(K) \rightarrow S$ where S is an elliptic del Pezzo surface as in [81].
- Closely related to the first one, one can mod out the \mathbb{Z}_2 which converts $K3 \times T^2$ to a special K3 fibration over \mathbb{P}^1 with 4 Enriques fibers, a Calabi–Yau manifold which has $SU(2) \times \mathbb{Z}_2$ holonomy. Such a manifold has been constructed in [9]. A first step for this model will be taken in Section 6.11.

6.2 Regular K3 fibrations

Extending the argument in [2] for $T^2 \times K3$ we will argue in this section that for regular K3 fibrations the higher genus invariants in the fiber classes are given by

$$\mathcal{F}_{K3}^{\text{hol}}(\lambda, t) = \frac{\Theta(q)}{q} \left(\frac{1}{2 \sin(\frac{\lambda}{2})} \right)^2 \prod_{n \geq 1} \frac{1}{(1 - e^{i\lambda} q^n)^2 (1 - q^n)^{20} (1 - e^{-i\lambda} q^n)^2}, \quad (6.2)$$

where the subscript K3 indicates that only maps into fiber classes are counted. $\Theta(q)$ is determined from the lattice embedding of

$$i : \text{Pic}(K3) \hookrightarrow H^2(X, \mathbb{Z}). \quad (6.3)$$

As such it depends on global properties of the fibration and in particular not only on $\text{Pic}(K3)$. (6.2) is clearly inspired by the results of heterotic-type II duality [82], [77], which are reviewed below. However we can construct $\Theta(q)$ purely from the geometric data of the fibration and in particular in cases where the heterotic dual is not known.

As explained above the BPS states are counted by complex structure deformation invariant indices related to the cohomology of the M2 brane moduli space, i.e. the deformation space of the genus g curves in the class $[C]$ of the K3 together with the flat $U(1)$ bundle moduli. Global issues of the fibration affect only the $\Theta(q)$ part and can be ignored for the sake of determining the BPS moduli space of a genus g curve in a generic class $[C]$ in the K3 fiber with $C^2 = 2g - 2$. In particular, one can ignore the global embedding into X and vary the complex structure of the K3 fiber so that it admits an elliptic fibration with base B and fiber F [83]. Further by a diffeomorphism on the fiber, $[C]$ can be brought into the class $[B] + g[F]$. In fact, this argument applies even to fibers which have Picard number one, however, not all classes $[B] + g[F]$ can be related to classes in the image of $i : \text{Pic}(K3) \hookrightarrow H^2(X, \mathbb{Z})$. A degenerate configuration of the curve which has g fiber components over g points on the \mathbb{P}^1 section is a sufficient model to determine the relevant cohomology of the moduli space. The $U(1)$ bundle modulus over each fiber T^2 corresponds to a choice of a point in the dual T^2 fiber. Hence the unresolved moduli space of a genus g curve is given by the choice of $n = g$ points on the dual $K3 = Y$, irrespectively of their ordering, i.e. by $\text{Sym}^n(X) = X^n / \text{Sym}_n$, where Sym_n is the symmetric group. It is convenient to define the formal sum of vector spaces such as $V = H^*(Y)$ by $S_q V = \bigoplus_{n \geq 0} q^n \text{Sym}^n(V)$ [84]. The relevant model of the moduli space \mathcal{M}_n is given by the orbifold resolution of $\text{Sym}^n(Y)$, i.e. $\mathcal{M}_n = \text{Hilb}^n(Y)$. In general, for a surface X with Euler number $\chi(Y) = \sum_i (-1)^i b_i(Y)$ one can write a generating function for $\chi(\mathcal{M}_n)$ by using the

partition function of $\chi(Y)$ free fields $\chi_{orb}(S_p Y) = \sum_n q^n \text{sdim} H^*(\mathcal{M}_n) = \prod_k \frac{1}{(1-q^k)} \chi(Y)$. One can get more detailed information about the individual cohomology groups. In particular [85] obtain for the Poincaré polynomial $P(Y, y) = \sum_{0 \leq k \leq d} (-1)^k y^k b_k(Y)$, $d = \dim Y$, of the orbifold resolution

$$P_{orb}(S_q Y, y) = \prod_{\substack{n > 0 \\ 0 \leq k \leq d}} (1 - y^{k - \dim_{\mathbb{C}}(X)} q^n)^{-(-1)^k b_k}. \quad (6.4)$$

The principle to obtain this finer information is to assign to the bosonic and fermionic free field oscillators the $\mathfrak{su}(2)$ eigenvalues of the natural Lefschetz action on the cohomology of Y as their zero modes. For the K3 one has only bosonic operators and the cohomology decomposes into $21(\mathbf{0}) + \mathbf{1}$ under this $\mathfrak{su}(2)$ action.

The eigenvalues of the cohomology of \mathcal{M}_g under the $\mathfrak{su}(2)_L \times \mathfrak{su}(2)_R$ Lefschetz action [63] on the cohomology of \mathcal{M}_n can similarly be recovered by assigning to each of the oscillators of the bosons ($b_{\text{odd}} = 0$) the representations of the unique splitting of the K3 cohomology, i.e. the ones of their zero modes,

$$[\alpha_n^i] = 20(\mathbf{0}, \mathbf{0}) + \left(\frac{\mathbf{1}}{\mathbf{2}}, \frac{\mathbf{1}}{\mathbf{2}} \right).$$

Summing now over the right $\mathfrak{su}(2)_R$ eigenvalues with $(-1)^{2j_R^3} (2j_R^3 + 1)$ yields formula (6.2). Note that the knowledge of the genus zero invariants on the Calabi–Yau manifold in the fiber direction alone is in general not sufficient to determine $\Theta(q)$. We need in addition the information of the embedding of the Picard lattice of Y into the Picard lattice of X and global properties of X , in particular the Euler number. Let us assume for simplicity that a heterotic dual does exist. The Narain lattice is then

$$\Gamma_{2,r} = H \oplus \Lambda, \quad (6.5)$$

with H being the even unimodular lattice of signature $(1, 1)$, Λ a rational lattice of signature $(1, r)$. $\Gamma_{2,r}$ can be identified in the stringy K3 cohomology lattice $\Gamma_{4,20}$. In particular, Λ gets identified with the Picard lattice of the K3 fiber. (6.2) counts the index of BPS states. To relate it to $n_Q^{(g)}$ of (5.6), (5.8) one has to change the basis of the left sum according to (5.4). Furthermore, to actually write down the free energy of the topological string for the classes in the image of i one must replace powers of λ, q by

$$\lambda^{2g-2} q^l \rightarrow \frac{1}{(2\pi i)^{3-2g}} \sum_{\alpha^2/2=l} \text{Li}_{3-2g}(e^{2\pi i(\alpha \cdot t)}), \quad (6.6)$$

where α is an element of $\text{Pic}(\text{K3}) \cong \Lambda$ and t stands for the associated complex volumes. We can determine $\Theta(q)$ from the spacing of the exponents in $\Theta(q)$ determined by (6.6) and the genus 0 results.

It is noticeable that this formula makes sense even for $\alpha^2 = 0$. The q^0 coefficient of Θ/η^{24} is always the Euler number of X . In the heterotic string this is related to the one loop contribution to the gravitational coupling. Focusing on genus zero first, and using $\text{Li}_3(1) = \zeta(3)$ the replacement gives $\frac{\zeta(3)\chi(X)}{(2\pi i)^2}$. This is up to a factor $-1/2$ the constant map contribution to \mathcal{F}^0 from the famous 4-loop σ model calculation. The factor can eventually be explained as

follows. For the moduli space of the curves in K3 the total moduli space contains an additional factor from the \mathbb{P}^1 for which the sum over $(-1)^{2J_R^3}(2J_R^3 + 1)$ is -2 . For this reason the modular forms in (6.58) etc. below contain a factor of 2. However, this factor is not appropriate for the constant maps as their moduli space does not factorize. The same regularization which lead from (5.6) to (5.8) will reproduce the constant map term for the higher genus $\mathcal{F}^{(g)}$ for $g > 1$. It has been noticed in [82] that the correct normalization comes out naturally from the integral $\tilde{I}_{2,2}$.

In order to see the effect of topologically different types of fibrations with the same K3 fiber we determine the higher genus numbers for the three fibrations

$$A = \mathbb{P}_{1,1,2,2,2}^4[8], \quad B = \mathbb{P} \begin{pmatrix} 1 & 1 & 1 & 1 & 2 & 0 & 0 \\ 0 & 0 & 0 & 0 & 0 & 1 & 1 \end{pmatrix} \begin{bmatrix} 4 \\ 2 \\ 2 \end{bmatrix}, \quad C = \mathbb{P} \begin{pmatrix} 1 & 1 & 1 & 1 & 1 & 0 & 0 \\ 0 & 0 & 0 & 0 & 0 & 1 & 1 \end{pmatrix} \begin{bmatrix} 4 \\ 1 \\ 1 \end{bmatrix}$$

A is a hypersurface of degree 8 in the weighted projective space $\mathbb{P}_{1,1,2,2,2}$ and B a complete intersection of degree (4, 0) and (2, 2) in $\mathbb{P}_{1,1,1,1,2}^4 \times \mathbb{P}^1$ with Hodge numbers $(h^{11}, h^{21}) = (2, 58)$. Both fibres $\mathbb{P}_{1,1,1,1}^3[4]$ and $\mathbb{P}_{1,1,1,1,2}^4[2, 4]$ have a one dimensional Picard lattice with self intersection $E^2 = 4$ and the same modular properties of the mirror map, but $\Theta(q)$ will be different. The fibration C , with $(h^{11}, h^{21}) = (2, 86)$, has the same generic fibers and the same type of degenerate fibers as the first one. Nevertheless, the fibration turns out to be topologically different. We next discuss these fibrations as well as a closely related fibration that was treated in [86] in detail.

6.3 The $\mathbb{P}_{1,1,2,2,2}^4[8]$ model

This is a K3 fibration whose heterotic dual has not yet been precisely identified. Its topological data are $\chi = -168$, $h^{1,1} = 2$, $h^{2,1} = 86$, $\mathcal{R} = 8t_1^3 + 4t_1^2t_2$, $\int_X c_2 J_1 = 56$ and $\int_X c_2 J_2 = 24$. The Kähler class $t_1 = T$ is identified with the unique class of the K3 fiber and $t_2 = 4\pi i S$ is the size of the base, which, in leading order, would be proportional to the heterotic dilaton S . The generic manifold X is defined as the vanishing locus of $p = x_1^8 + x_2^8 + x_3^4 + x_4^4 + x_5^4 + \sum_{\sum w_i d_i = 8} a_{\underline{d}} x_{\underline{d}}$ in $\mathbb{P}_{1,1,2,2,2}^4$, where $a_{\underline{d}}$ are the complex structure moduli, $d_1, d_2 \leq 6$, $d_3, d_4, d_5 \leq 2$ and w_i are the weights of the ambient space. X^* can be described by the same equation in $\mathbb{P}_{1,1,2,2,2}^4/\mathbb{Z}_4^3$ where the only invariant perturbations are $ax_1x_2x_3x_4x_5$ and $bx_1^4x_2^4$. Clearly, the Euler number of X is determined by the singular fibres. X admits a contraction along a K3 to a \mathbb{P}^1 , which is defined by the first two coordinates. The dependence of a smooth K3 fiber on the \mathbb{P}^1 coordinate μ is given by

$$(1 + \mu^8)z^4 + x_3^4 + x_4^4 + x_5^4 = 0$$

which is a quartic in \mathbb{P}^3 . This quartic degenerates for $\mu^8 = -1$ to a complex cone over the genus 3 curve $\mathbb{P}^2[4]$ with Euler number $-4 + 1$. The Euler number of X hence is $\chi(X) = 2(24) - 8(24) + 8(-3) = -168$.

The complex structure moduli of the mirror X^* with $\log(x = b/a^4) \sim t_1$ and $\log(y = 1/b^2) \sim$

t_2 at the large complex structure limit are suitably rescaled so that the Yukawa couplings read [5]

$$\begin{aligned} Y_{111} &= \frac{4}{x^3 \Delta_{con}}, & Y_{112} &= \frac{2(1-x)}{x^2 y \Delta_{con}} \\ Y_{122} &= \frac{1-2x}{xy \Delta_{con} \Delta_s}, & Y_{222} &= \frac{1-y+x(1+3y)}{2y^2 \Delta_{con} \Delta_s} \end{aligned} \quad (6.7)$$

where the discriminants are $\Delta_{con} = 1 - 2x + x^2(1 - y)$ and $\Delta_s = 1 - y$. In contrast to elliptic toric fibrations Y_{1jk} and Y_{2jk} are invertible at a generic point in the moduli space away from $\Delta_{con} = 0, \Delta_s = 0, x = 0$ and $y = 0$.

The first task is to fulfil the algebraic compatibility conditions (4.21) and (4.22) for the ambiguity A_{kl}^i inherent in the two ways of constructing the topological propagators S^{ij} . With

$$\begin{aligned} A_{1,1}^1 &= -\frac{1}{x}, & A_{1,2}^1 &= -\frac{1}{4y}, & A_{2,2}^1 &= 0 \\ A_{1,1}^2 &= 0, & A_{1,2}^2 &= \frac{1}{2x}, & A_{2,2}^2 &= -\frac{1}{y} \end{aligned} \quad (6.8)$$

we find the leading behaviour

$$\begin{aligned} S^{11} &= -\frac{1}{16} - 44q_1 q_2 + O(q^3), \\ S^{12} &= \frac{1}{8} - 22q_1 + 214q_1^2 + 22q_1 q_2 + O(q^3) \\ S^{22} &= -\frac{1}{4} - 1272q_1^2 + O(q^3). \end{aligned} \quad (6.9)$$

We checked (4.18) and found that

$$\partial_{t_k} \mathcal{F}^{(1)} = \frac{1}{2} C_{k,j,i} S^{ij} + \partial_{t_k} \left(\frac{1-\chi}{24} \log(\omega) - \frac{1}{12} \log(\Delta_{con}) - \frac{5}{12} \log(\Delta_s) - \frac{31}{12} \log(x) - \frac{7}{8} \log(y) \right)$$

in accordance with the expected behaviour of $\mathcal{F}^{(g)}$ near the conifold coming from the 1-loop β -function of one hypermultiplet [87], [88]. The $-\frac{5}{12} \log(\Delta_s)$ is the same behaviour as in the conventional calculation of $\mathcal{F}^{(1)}$ [75]²². The total leading coefficient is $\mathcal{F}^{(1)} = -\frac{1}{12} \log(\Delta_s) + O(\Delta_s)$ coming from the 1-loop β -function of 3 massless hypermultiplets and a non-contributing massless $N = 4$ -like spectrum of an $SU(2)$ gauge symmetry enhancement [78]. This implies that the S^{ij} terms contribute $\frac{1}{4} \log(\Delta_s)$. The S^i can also be derived in two ways. We find that with the choice (6.8)

$$A_{1,1} = 0, \quad A_{2,1} = 0, \quad A_{2,2} = 0 \quad (6.10)$$

is a possible solution to the constraints (4.24). The leading behaviour of S^i, S is then

$$\begin{aligned} S^1 &= \frac{3}{2} q_1 - 33q_1^2 + \frac{9}{2} q_1 q_2 + O(q^3), \\ S^2 &= 3q_1 + 186q_1^2 - 3q_1 q_2 + O(q^3) \\ S &= -18q_1^2 + 792q_1^3 - 180q_1 q_2 + O(q^4). \end{aligned} \quad (6.11)$$

²²The difference by a factor of 2 w.r.t. [75] originates in the different normalization of $\mathcal{F}^{(1)}$ between [58] and [57].

We found the following ansatz for the holomorphic ambiguity f_2

$$f_2(x, y) = \left(\frac{107}{9216} + \frac{193}{1280}y - 2x(1 - 4y) \right) \frac{1}{\Delta_s} + \frac{(831 - 199936x)(1 - 2^8x)}{46080\Delta_{con}} + \frac{(1 - 2^8x)^3}{240\Delta_{con}^2} \quad (6.12)$$

in (4.28), which satisfies the integrability constraints as well as the vanishing of some low degree invariants as mentioned in Section 5.3. With this ansatz we get integral genus 2 invariants. For comparison we list the genus 0 and 1 invariants first.

$g = 0$

| d_1 | $d_2 =$ | 0 | 1 | 2 | 3 | 4 | 5 | 6 |
|-------|-----------|---|-------------|--------------|--------------|-------------|-----------|---|
| 0 | | | 4 | | | | | |
| 1 | 640 | | 640 | | | | | |
| 2 | 10032 | | 72224 | 10032 | 0 | 0 | 0 | 0 |
| 3 | 288384 | | 7539200 | 7539200 | 288384 | 0 | 0 | 0 |
| 4 | 10979984 | | 757561520 | 2346819520 | 757561520 | 10979984 | 0 | 0 |
| 5 | 495269504 | | 74132328704 | 520834042880 | 520834042880 | 74132328704 | 495269504 | 0 |

$g = 1$

| d_1 | $d_2 =$ | 0 | 1 | 2 | 3 | 4 | 5 | 6 |
|-------|-------------|---|-------------|---------------|----------------|---------------|-------------|-------------|
| 2 | | | | | | | | |
| 3 | -1280 | | 2560 | 2560 | -1280 | | | |
| 4 | -317864 | | 1047280 | 15948240 | 1047280 | -317864 | | |
| 5 | -36571904 | | 224877056 | 12229001216 | 12229001216 | 224877056 | -36571904 | |
| 6 | -3478899872 | | 36389051520 | 4954131766464 | 13714937870784 | 4954131766464 | 36389051520 | -3478899872 |

$g = 2$

| d_1 | $d_2 =$ | 0 | 1 | 2 | 3 | 4 | 5 | 6 |
|-------|-----------|---|-------------|-------------|--------------|-------------|-------------|-----------|
| 2 | | | | | | | | |
| 3 | | | | | | | | |
| 4 | 472 | | -1232 | 848 | -1232 | 472 | | |
| 5 | 875392 | | -2540032 | 9699584 | 9699584 | -2540032 | 875392 | |
| 6 | 220466160 | | -1005368448 | 21816516384 | 132874256992 | 21816516384 | -1005368448 | 220466160 |

It should be stressed that (6.12) is only the simplest ansatz in the sense that it matches all known properties of the $n_{i,j}^{(g)}$, as discussed in Section 5.3. In particular, we find that in the strong coupling limit [78] this model has a non-conifold transition at $\Delta_s = 0$ to the complete intersection $X' = \mathbb{P}^5[2, 4]$ with the topological data $\chi = -176$, $h^{1,1} = 1$. This transition occurs for $x_2 = q_2 = 1$ and (5.14) yields

$$n_d^{(g)} = \sum_{i=0}^{2d+1} n_{d,i}^{(g)}$$

for the invariants with one modulus, which is consistent with the $n_d^{(2)}(X')$ in the following table

| | | | | | |
|---------|---|---|------|----------|--------------|
| $d = 1$ | 2 | 3 | 4 | 5 | 6 |
| 0 | 0 | 0 | -672 | 16069888 | 174937485184 |

As we mentioned we can reconstruct $\Theta(q)$ from the lattice embedding and $g = 0$ results. We use the fact that $E^2 = 4$ and since the one dimensional Picard lattice is generated by δ with $\delta^2 = \frac{1}{4}$, the embedding of the Picard lattice of the K3 into $H^2(X, \mathbb{Z})$ in (6.6) is

$$\lambda^{2g-2} q^l \rightarrow \frac{1}{(2\pi i)^{3-2g}} \sum_{n^2/8=l} \text{Li}_{3-2g}(e^{2\pi i nT}), \quad (6.13)$$

which yields

$$\frac{\Theta}{\eta^{24}} = -\frac{2}{q} + 168 + 640 q^{\frac{1}{8}} + 10032 \sqrt{q} + 158436 q + 288384 q^{\frac{9}{8}} + 1521216 q^{\frac{3}{2}} + 10979984 q^2 + \dots \quad (6.14)$$

Now we can realize Θ as a modular form of $\Gamma^0(8)$ with weight $\frac{21}{2}$ in terms of

$$U = \theta_3\left(\frac{\tau}{4}\right), \quad V = \theta_4\left(\frac{\tau}{4}\right) \quad (6.15)$$

with $\theta_3(\tau) = \sum_{n \in \mathbb{Z}} q^{\frac{n^2}{2}}$ and $\theta_4(\tau) = \sum_{n \in \mathbb{Z}} (-1)^n q^{\frac{n^2}{2}}$,

$$\begin{aligned} \Theta = & 2^{-21} (3U^{21} - 81U^{19}V^2 - 627U^{18}V^3 - 14436U^{17}V^4 - 20007U^{16}V^5 - 169092U^{15}V^6 \\ & - 120636U^{14}V^7 - 621558U^{13}V^8 - 292796U^{12}V^9 - 1038366U^{11}V^{10} - 346122U^{10}V^{11} \\ & - 878388U^9V^{12} - 207186U^8V^{13} - 361908U^7V^{14} - 56364U^6V^{15} - 60021U^5V^{16} \\ & - 4812U^4V^{17} - 1881U^3V^{18} - 27U^2V^{19} + V^{21}). \end{aligned} \quad (6.16)$$

It is quite remarkable that we reconstruct the threshold correction of a not yet identified heterotic string from the higher genus calculation on the K3 fibration.

In fact, compatibility with (6.2) gives us consistency checks on the genus 2 invariants in the first column and allows to predict all higher genus numbers $n_{d,0}^{(g)}$ such as

| g | $d = 1$ | 2 | 3 | 4 | 5 | 6 | 7 | 8 |
|-----|---------|-------|--------|----------|-----------|-------------|---------------|-----------------|
| 0 | 640 | 10032 | 288384 | 10979984 | 495269504 | 24945542832 | 1357991852672 | 78313183960464 |
| 1 | 0 | 0 | -1280 | -317864 | -36571904 | -3478901152 | -306675842560 | -26077193068200 |
| 2 | 0 | 0 | 0 | 472 | 875392 | 220466160 | 36004989440 | 4824769895208 |
| 3 | 0 | 0 | 0 | 8 | -2560 | -6385824 | -2538455296 | -599694313488 |
| 4 | 0 | 0 | 0 | 0 | 0 | 50160 | 101090432 | 51094399168 |
| 5 | 0 | 0 | 0 | 0 | 0 | 0 | -1775104 | -2848329800 |
| 6 | 0 | 0 | 0 | 0 | 0 | 0 | 4480 | 92179128 |
| 7 | 0 | 0 | 0 | 0 | 0 | 0 | 0 | -1286576 |
| 8 | 0 | 0 | 0 | 0 | 0 | 0 | 0 | 1192 |
| 9 | 0 | 0 | 0 | 0 | 0 | 0 | 0 | 20 |

Some predictions of this table can be checked with the methods²³ described in [2] as follows. We denote the divisors dual to t_1, t_2 by $H = \mathcal{O}(2)$ and $L = \mathcal{O}(1)$, i.e. $H^3 = 8$ and $H^2L = 4$ are the non vanishing intersection numbers. The authors of [2] use a Jacobian fibration over the universal curve as model for the moduli space of M2 branes and construct the mixed sums of dimensions of the cohomology groups of this moduli space $n_Q^{(g)}$ with the Abel-Jacobi map. It follows from [2] that the $n_Q^{(g-\delta)}$ of a curve C_g of genus g with δ nodes can be computed by $n_Q^{(g-\delta)} = (-1)^{\dim(\mathcal{M}_\delta)} e(\mathcal{M}_\delta)$. In particular, if C_g is a smooth curve of genus g in a class in $H^2(X, \mathbb{Z})$, i.e. $\delta = 0$, one obtains

$$n_Q^{(g)} = (-1)^{\dim(\mathcal{M}_0)} e(\mathcal{M}_0), \quad (6.17)$$

where \mathcal{M}_0 is the moduli space of the smooth curve C_g .

We therefore first look at smooth curves of higher genus in the K3 fiber. If such a curve is a complete intersection $C = (kH)L$, its canonical class is $K_C = kH + L$ and its genus is given by adjunction as

$$\frac{K_C C}{2} + 1 = g. \quad (6.18)$$

Such a curve hence has genus $g = 2k^2 + 1$, degree 0 w.r.t. L and degree $4k$ w.r.t. H . Its moduli space is given by a fibration of $\mathbb{P}H^0(\mathcal{O}(2kH))$ over \mathbb{P}^1 . The dimensions $p(n) = \dim \mathbb{P}H^0(\mathcal{O}(nH))$ can be described for a general hypersurface in a weighted projective space by

$$\sum_{n=0}^{\infty} p(n) q^n = (1-q) \prod_{i=1}^5 \frac{1}{1-q^{w_i}}, \quad (6.19)$$

which for $H \subset X = \mathbb{P}_{1,1,2,2,2}^4$ [8] becomes

$$\sum_{n=0}^{\infty} p(n) q^n = \frac{1}{(1-q)(1-q^2)^3} \quad (6.20)$$

and we conclude that

$$n_{4k,0}^{(2k^2+1)} = (-1)^{p(2k)} 2p(2k) \quad (6.21)$$

in perfect agreement with the table above. By a similar method one can count the $n_Q^{(g)}$ of smooth curves with degree 1 w.r.t. L and gets $n_{2k,1}^{(k^2+1)} = (-1)^{p(2k)-1} 4(p(2k) - 1)$.

Curves with one node in the class $(4k, 0)$ have genus $g = 2k^2$. The formula for the Euler number of moduli space with one node is [2]

$$e(\mathcal{M}_1) = e(\mathcal{C}) + (2g - 2)e(\mathcal{M}_0), \quad (6.22)$$

where \mathcal{C} is the universal curve $\pi : \mathcal{C} \rightarrow \mathcal{M}_0$, which in our case has $e(\mathcal{C}) = -168(p(2k) - 1)g$. Combining this with (6.22) and using the fact that we already calculated $e(\mathcal{M}_0)$ we obtain

$$n_{4k,0}^{(2k^2)} = (-1)^{p(2k)-1} (8k^2 p(2k) + 168(1 - p(2k))), \quad (6.23)$$

again in perfect agreement with the table.

²³We would like to thank Sheldon Katz for many explanations regarding the geometry of the instanton moduli spaces.

6.4 The fibration B

Comparing the fibrations A and B which have the same Picard lattice is very instructive. The model B has $h^{11} = 2$ and $h^{21} = 58$. Its intersection data are $\mathcal{R} = 4J_1^3 + 4J_1^2 J_2$ and $\int_X c_2 J_1 = 40$, $\int_X c_2 J_2 = 24$.

Again we can realize Θ as a modular form of $\Gamma^0(8)$ with weight $\frac{21}{2}$ in terms of $U = \theta_3(\frac{\tau}{4})$ and $V = \theta_4(\frac{\tau}{4})$, which has a quite similar, but different form than in the previous case

$$\begin{aligned} \Theta = & 2^{-21} (3U^{21} - U^{20}V - 60U^{19}V^2 - 580U^{18}V^3 - 14223U^{17}V^4 - 20027U^{16}V^5 - 169536U^{15}V^6 \\ & -120800U^{14}V^7 - 621858U^{13}V^8 - 292746U^{12}V^9 - 1037592U^{11}V^{10} - 345864U^{10}V^{11} \\ & -878238U^9V^{12} - 207286U^8V^{13} - 362400U^7V^{14} - 56512U^6V^{15} - 60081U^5V^{16} \\ & -4741U^4V^{17} - 1740U^3V^{18} - 20U^2V^{19} - 3UV^{20} + V^{21}), \end{aligned} \quad (6.24)$$

which yields

$$\frac{\Theta}{\eta^{24}} = \frac{-2}{q} + \frac{4}{\sqrt{q}} + 112 + 768 q^{\frac{1}{8}} + 9376 \sqrt{q} + 154820 q + 293632 q^{\frac{9}{8}} + 1505904 q^{\frac{3}{2}} + O(q^2) \quad (6.25)$$

From this we get the following higher genus numbers $n_{d,0}^{(g)}$ in the fiber direction

| g | $d=1$ | 2 | 3 | 4 | 5 | 6 | 7 | 8 |
|-----|-------|------|--------|----------|-----------|-------------|---------------|-----------------|
| 0 | 768 | 9376 | 293632 | 10924128 | 495966976 | 24935882144 | 1358136021760 | 78310908911200 |
| 1 | 0 | -8 | -1536 | -310296 | -36755968 | -3474708168 | -306768929792 | -26075148138264 |
| 2 | 0 | 0 | 0 | 304 | 893184 | 219647904 | 36034776064 | 4823807971056 |
| 3 | 0 | 0 | 0 | 8 | -3072 | -6305376 | -2544193024 | -599398380992 |
| 4 | 0 | 0 | 0 | 0 | 0 | 47072 | 101752576 | 51032102080 |
| 5 | 0 | 0 | 0 | 0 | 0 | -24 | -1815552 | -2839525176 |
| 6 | 0 | 0 | 0 | 0 | 0 | 0 | 5376 | 91402192 |
| 7 | 0 | 0 | 0 | 0 | 0 | 0 | 0 | -1250592 |
| 8 | 0 | 0 | 0 | 0 | 0 | 0 | 0 | 688 |
| 9 | 0 | 0 | 0 | 0 | 0 | 0 | 0 | 20 |

As the Picard lattice of the fiber is identical to the model discussed in the last section, i.e. $H^2L = 4$, we also get

$$n_{4k,0}^{(2k^2+1)} = (-1)^{p(2k)} 2p(2k), \quad (6.26)$$

but since $e(\mathcal{C}) = -112$ we now get

$$n_{4k,0}^{(2k^2)} = (-1)^{p(2k)-1} (8k^2 p(2k) + 112(1 - p(2k))). \quad (6.27)$$

6.5 The fibration C

The fibration C with intersection $\mathcal{R} = 5J_1^3 + 4J_1^2 J_2$ and $\int_X c_2 J_1 = 50, \int_X c_2 J_2 = 24$ is well known, as it has a transition to the quintic hypersurface in \mathbb{P}^4 , see [89]. This is reflected by the

fact that the GV invariants in the rows of the tables below sum up to the GV invariants of the quintic.

$g = 0$

| d_1 | $d_2 = 0$ | 1 | 2 | 3 | 4 | 5 | 6 | 7 | 8 | 9 |
|-------|-----------|----------|-----------|-----------|---------|----------|--------|---------|-------|--------|
| 0 | | 16 | | | | | | | | |
| 1 | 640 | 2144 | 120 | -32 | 3 | | | | | |
| 2 | 10032 | 231888 | 356368 | 14608 | -4920 | 1680 | -480 | 80 | -6 | |
| 3 | 288384 | 23953120 | 144785584 | 144051072 | 5273880 | -1505472 | 512136 | -209856 | 75300 | -21600 |

$g = 1$

| d_1 | $d_2 = 0$ | 1 | 2 | 3 | 4 | 5 | 6 | 7 | 8 | 9 | 10 | 11 | 12 |
|-------|-----------|-------|--------|--------|--------|-------|--------|-------|--------|------|------|-----|-----|
| 0 | | | | | | | | | | | | | |
| 1 | -1280 | 10240 | 356368 | 243328 | -15708 | 34320 | -32032 | 21840 | -10920 | 3920 | -960 | 144 | -10 |

The model admits a projection to \mathbb{P}^2 , which is visible in the instanton numbers as the $n_{k+2,4k}^{(g)}$ numbers agree with the local $\mathcal{O}(-3) \rightarrow \mathbb{P}^2$ numbers.

What is physically intriguing is that the BPS numbers $n_{k,0}^{(g)}$ and hence the $\Theta(q)$ coincide with the one of the fibration A , while the non-perturbative ones, i.e. $n_{k,m}^{(g)}$ for $m > 0$ do not coincide. This is geometrically expected as the generic fiber is the same and the degenerations of the fibres are the same in both cases. However, it shows that the degeneracy of BPS states as calculated by the gauge and gravitational threshold corrections, i.e. the indices of the perturbative $N = 2$ heterotic string associated to the vector multiplets, do not suffice to fix a unique non-perturbative completion. It should be stressed that globally the non-perturbative completions are very different. This might be surprising as the heterotic dilaton does not couple to the hypermultiplets, i.e. potential differences (which we have not controlled) in this sector between the two models should not affect the completion. However, the moduli space of the fibration A has been analyzed in sufficient detail [75] to exclude e.g. a transition to the quintic in \mathbb{P}^4 , which the fibration C admits. On the other hand, some local features of the perturbative region, in particular, the occurrence of the Seiberg-Witten theory [90] at the blow up of the point $T = i, S \rightarrow \infty$ does not differ for the different fibrations. The same conclusion will be reached in section 6.8 for a model where a heterotic dual is known.

Mathematically it is noticeable that the manifolds A and C are rational homotopy equivalent by the criterion of C.T.C. Wall [45]. Calling the Kähler classes of C J_1 and J_2 as above and the ones of A \tilde{J}_1 and \tilde{J}_2 the transformation $\tilde{J}_1 = J_1 + \frac{1}{4}J_2$, $\tilde{J}_2 = J_2$ identifies the topological data, i.e. these models are rational homotopy equivalent. The example shows that Gromov–Witten invariants can be different on rational homotopy equivalent manifolds.

| d_1 | $d_2 = 0$ | 1 | 2 | 3 | 4 |
|-------|-----------|-----|-------|--------|---------|
| 0 | | 20 | -2 | | |
| 1 | 1 | 640 | 6474 | 1152 | -1023 |
| 2 | | | 10032 | 733560 | 4458084 |

and use $n_{i,j-i}^{(0)} = \tilde{n}_{i,j}^{(0)}$ to relate them to the K3 fibration phase. The result is that the analytic continuation of Li_3

$$\text{Li}_3(e^x) = \text{Li}_3(e^{-x}) - \frac{x^3}{6} - \frac{\pi i}{2}x^2 + \frac{\pi^2 x}{3} \quad (6.28)$$

applied to the GV invariant $\tilde{n}_{1,0}^{(0)}$ contributes $\text{Li}_3(q_2/q_1)$ and a term $-\frac{(2\pi i)^3}{12}(2(t_1 - t_2)^3 + 3(t_1 - t_2)^2 + t_1 - t_2)$ that connects precisely the classical intersection data in $\mathcal{F}^{(0)}$ in the two phases. Similarly, the contribution from the analytic continuation of Li_1

$$\text{Li}_1(e^x) = \text{Li}_1(e^{-x}) + x \quad (6.29)$$

connects the $\int_X c_2 J_i$ terms in $\mathcal{F}^{(1)}$. The term $\text{Li}_3(q_2/q_1)$ vanishes in the polarization $B + NF$ with $N \gg 0$ chosen in [71]. The genus zero GV invariants in the K3 fibration phase are

| d_1 | $d_2 = 0$ | 1 | 2 | 3 | 4 |
|-------|-----------|--------|---------|---------|---------|
| 0 | 0 | 20 | -2 | | |
| 1 | 640 | 6474 | 1152 | -1023 | 1536 |
| 2 | 10032 | 733560 | 4458084 | 1080696 | -762128 |

They are clearly different from those on the diffeomorphic K3 fibration discussed first, which means that the two cases have disjoint families of symplectic structures. As in the cases *A* and *C* these cases have the same weak coupling limit when the base of the \mathbb{P}^1 goes to infinity. Our construction shows also that it is possible to put two different complex structures on mirrors of one topological type of K3 fibrations. Given the polyhedra it is possible to decide whether these mirrors have topologically equivalent phases, but we have not done this.

Our conclusion, however, is that the BPS numbers on the heterotic side fix the topology up to rational equivalence, but even on topologically equivalent manifolds they do not necessarily fix the symplectic family. The difference between the heterotic data is now even more subtle than in the comparison between the fibrations *A* and *C*. While the higher genus data agree, even the classical terms of $\mathcal{F}^{(1)}$, we see that there is an unconventional term $\text{Li}_3(q_2/q_1)$ in the genus zero prepotential. This term gets exponentially suppressed in the weak coupling limit $q_2 \sim \exp(-\frac{1}{g^2})$. One may already think of it as a non-perturbative effect, whose suppression can, however, be counterbalanced by tuning the geometrical modulus to the limit $T \rightarrow i\infty$ in which $q_1 \rightarrow 0$. The visibility of non-perturbative effects even at weak coupling at special points of the geometric moduli space is just as for small instantons.

6.7 Heterotic duals and threshold corrections

In this section we focus on the situation of Calabi–Yau manifolds X that admit a K3 fibration. For such an X with a known heterotic-type II dual, \mathcal{F}^{hol} has been evaluated in the limit where the base of the fibration is large. More specifically, for the STU model (see Section 6.10 below) [82], [77] have obtained results which can be summarized in the holomorphic limit as follows

$$\mathcal{F}_{\text{K3}}^{\text{hol}}(\lambda, t) = -\frac{\Theta(q)}{4\pi^2\eta^{24}} \sum_{g=0}^{\infty} S_g(G_2, \frac{1}{2}G_4, \dots, \frac{1}{g}G_{2g}) \left(\frac{\lambda}{2\pi}\right)^{2g-2}. \quad (6.30)$$

Here $G_k(\tau) = 2\zeta(k)E_k(\tau)^{24}$ and the Schur polynomials are obtained by $\sum_{k=0}^{\infty} S_k(x_1, \dots, x_k)z^k := \exp \sum_{k=1}^{\infty} x_k z^k$. The Eisenstein series are defined as

$$E_k(\tau) = \frac{1}{2} \sum_{\substack{n,m \in \mathbb{Z} \\ (n,m)=1}} \frac{1}{(m\tau + n)^k} = 1 - \frac{2k}{B_k} \sum_{n=1}^{\infty} \sigma_{k-1}(n)q^n, \quad (6.31)$$

where $q = e^{2\pi i\tau}$, B_k are the Bernoulli numbers defined through $\sum_{k=0}^{\infty} B_k \frac{x^k}{k!} := (e^x - 1)^{-1}$ and $\sigma_k(n) := \sum_{d|n} d^k$ is the σ divisor function. $\Theta(q)$ is related to an automorphic form of the classical duality group $\text{SO}(2, h-1, \mathbb{Z})$ by the Borchers lifting. The connection to the classes T, U_i in the fiber of the K3 is defined by an analog of (6.6).

The expression (6.30) was obtained from a one loop string calculation in the heterotic theory. The information at genus 0 and 1 is contained in the well known index calculation for the one loop threshold dependence of the gauge coupling [82], [92] ²⁵

$$\Delta(G) = -i \int_{\mathcal{F}} \frac{d^2\tau}{\text{Im}\tau} \frac{1}{\eta^2} \text{Tr}_{\mathcal{H}} F_L(-1)^{F_L} q^{H_L} q^{H_R} \left[Q^2 - \frac{k}{8\pi \text{Im}\tau} \right], \quad (6.32)$$

where k is the level and Q is the operator of the gauge group in \mathcal{H} . For the STU model the integrand is given by $-\frac{i}{12} \sum_{p \in \Gamma_{2,2}} q^{\frac{1}{2}P_L^2} \bar{q}^{\frac{1}{2}P_R^2} \left(\frac{E_4 E_6}{\eta^{24}} (E_2 - \frac{3}{\pi \text{Im}\tau}) - \frac{E_6^2}{\eta^{24}} \right)$. Only the first terms in the second bracket are relevant for the calculation²⁶ of $\mathcal{F}^{(0)}$ and $\mathcal{F}^{(1)}$. The $\hat{E}_2 = (E_2 - \frac{3}{\pi \text{Im}\tau})$ term has a beautiful generalization to all higher genus $\mathcal{F}^{(g)}$ found in [65], see also [94], to include the gravitational corrections to the gauge coupling. Using the identity

$$\frac{2\pi\eta^3(\tau)z}{\theta_1(z, \tau)} = -\exp \left[\sum_{k=1}^{\infty} \frac{\zeta(2k)}{k} E_{2k}(\tau) z^{2k} \right], \quad (6.33)$$

this generalization can be written as

$$\left(\frac{2\pi i \tilde{\lambda} \eta^3}{\theta_1(\lambda, \tau)} \right)^2 e^{-\frac{\pi \tilde{\lambda}^2}{\text{Im}\tau}} = -\sum_{k=0}^{\infty} \tilde{\lambda}^{2k} S_{2k} \left(\hat{G}_2, \frac{1}{2}G_4, \dots, \frac{1}{k}G_{2k} \right), \quad (6.34)$$

²⁴Note that $\zeta(2n) = -\frac{1}{(2n)!} (-1)^n 2^{2n-1} \pi^{2m} B_{2n}$.

²⁵Differences $\Delta(G_1) - \Delta(G_2)$ were first computed in [93], but for these the important non-holomorphic term proportional to $(\text{Im}\tau)^{-1}$ in the integrand drops out.

²⁶They constitute up to the constant 264 the integrand of $\tilde{I}_{2,2}$ evaluated in [82].

where $\tilde{\lambda} = \tau_2 \lambda f(T, U_i)$ with f given in [65]. The integration over the fundamental region was performed in [77] using techniques of [93], [82] and [67]. Evaluation of the integral leads to the full (t, \bar{t}) dependence of $\mathcal{F}(\lambda, t, \bar{t})$, but in the holomorphic limit there is a simplification which will help us to make contact with the geometry. With the Jacobi triple product identity ($q = \exp(2\pi i\tau)$, $y = \exp(2\pi iz)$)

$$\theta_1(z, \tau) = i(y^{-\frac{1}{2}} - y^{\frac{1}{2}})q^{\frac{1}{8}} \prod_{n=1}^{\infty} (1 - q^n)(1 - q^n y)(1 - q^n y^{-1}) \quad (6.35)$$

and the definition $\eta = q^{\frac{1}{24}} \prod_{n=1}^{\infty} (1 - q^n)$ the holomorphic limit (6.30) is rewritten in the form (6.2). Note the important difference that (6.34) is not holomorphic but decomposes into $(2k, 0)$ $\text{SL}(2, \mathbb{Z})$ forms, which is essential to perform the integrals, while (6.30) contains only quasimodular forms but is holomorphic. Also $\tilde{\lambda}$ is shifted w.r.t. λ , which introduces a non-holomorphic space time moduli dependence.

6.8 The ST model and dual type II K3 fibrations

Many aspects of the ST heterotic model on $\text{K3} \times T^2$ have been discussed in the context of the $N = 2$ heterotic-type II string duality. It has two vectors multiplets, the complexified size of the T^2 and the dilaton S . Because of the Hodge numbers the type II dual has been identified with the hypersurface $X = \mathbb{P}_{1,1,2,2,6}^4$ [12] with $\chi = -252$, $h^{1,1} = 2$ and $h^{2,1} = 128$ [52], which is a K3 fibration whose generic fiber has Picard number one and self intersection $E^2 = 2$. The significance of K3 fibrations in the context of heterotic-type II duality was first pointed out in [48]. Later a supergravity argument was given in [7]. The intersection ring of $X = \mathbb{P}_{1,1,2,2,6}^4$ [12] is $\mathcal{R} = 4t_1^3 + 2t_1^2 t_2$, and the heterotic modulus T is identified with the unique class of the K3 fiber $t_1 = T$, while the complexified size of the base t_2 is identified with the heterotic dilaton $t_2 = 4\pi i S$. Furthermore, $\int_X c_2 J_1 = 52$ and $\int_X c_2 J_2 = 24$.

The propagators and the higher genus amplitudes have very similar structure as for the model $\mathbb{P}_{1,1,2,2,2}^4$ [8] discussed in Section 6.3. In particular the Yukawa couplings are, after a suitable rescaling [5], identical to those in (6.7). The algebraic compatibility conditions (4.21) and (4.22) for the ambiguity A_{kl}^i can therefore be satisfied with (6.8). The leading behaviour of the propagators S^{ij} becomes

$$\begin{aligned} S^{11} &= -\frac{1}{8} - 552q_1q_2 + O(q^3), \\ S^{12} &= \frac{1}{4} - 276q_1^2 + 42732q_1^2 + 276q_1q_2 + O(q^3) \\ S^{22} &= -\frac{1}{2} - 77040q_1^2 + O(q^3). \end{aligned} \quad (6.36)$$

We checked (4.18) and found that

$$\partial_{t_k} \mathcal{F}^{(1)} = \frac{1}{2} C_{k,j,i} S^{ij} + \partial_{t_k} \left(\frac{1 - \chi}{24} \log(\omega) - \frac{1}{12} \log(\Delta_{con}) - \frac{1}{3} \log(\Delta_s) - \frac{29}{12} \log(x) - \frac{7}{8} \log(y) \right)$$

again in accordance with the expected behaviour of $\mathcal{F}^{(g)}$ near the conifold. The $-\frac{1}{3} \log(\Delta_s)$ is the same behaviour as in the conventional calculation of $\mathcal{F}^{(1)}$. The total leading coefficient is $\mathcal{F}^{(1)} =$

$-\frac{1}{12} \log(\Delta_s) + O(\Delta_s)$ coming from the 1-loop β -function of 2 massless hypermultiplets and a non-contributing massless $N = 4$ -like spectrum of an $SU(2)$ gauge symmetry enhancement. This implies that the S^{ij} terms contribute $\frac{1}{4} \log(\Delta_s)$. The ambiguity A_{ij} for the S^i can also be solved by (6.10). The leading behaviour of the S^i and S is then

$$\begin{aligned} S^1 &= 15q_1 - 3330q_1^2 + 45q_1q_2 + O(q^3), \\ S^2 &= 30q_1 + 5940q_1^2 - 30q_1q_2 + O(q^3) \\ S &= -900q_1^2 + 399600q_1^3 - 9000q_1q_2 + O(q^4). \end{aligned} \tag{6.37}$$

The ansatz for the holomorphic ambiguity f_2 in (4.28) satisfying all known constraints of Section 5.3 is

$$\begin{aligned} f_2(x, y) &= \left(\frac{2051}{103680} + \frac{965}{5184}y - \frac{615}{4}x(1-4y) \right) \frac{1}{\Delta_s} \\ &+ \frac{-2 + 6757x - 5643648x^2}{60\Delta_{con}} + \frac{(1-1728x)^3}{120\Delta_{con}^2} \end{aligned} \tag{6.38}$$

Observe that $p_{con}^{(3)}$ has a very simple form, similar to the one in (6.12). This leads to the following predictions for the invariants $n_{i,j}^{(2)}$ for curves of genus 2. We list for comparison the invariants $n_{i,j}^{(g)}$ for curves of genus $g = 0, 1, 2$.

$g = 0$

| d_1 | d_2 | = | 0 | 1 | 2 | 3 | 4 | 5 |
|-------|---------------|---|---|-----------------|------------------|------------------|-----------------|---------------|
| 0 | | | | 2 | | | | |
| 1 | 2496 | | | 2496 | | | | |
| 2 | 223752 | | | 1941264 | 223752 | | | |
| 3 | 38637504 | | | 1327392512 | 1327392512 | 38637504 | | |
| 4 | 9100224984 | | | 861202986072 | 2859010142112 | 861202986072 | 9100224984 | |
| 5 | 2557481027520 | | | 540194037151104 | 4247105405354496 | 4247105405354496 | 540194037151104 | 2557481027520 |

$g = 1$

| d_1 | d_2 | = | 0 | 1 | 2 | 3 | 4 | 5 |
|-------|---------------|---|---|---------------|-----------------|-----------------|---------------|---------------|
| 0 | | | | | | | | |
| 1 | | | | | | | | |
| 2 | -492 | | | 480 | -492 | | | |
| 3 | -1465984 | | | 2080000 | 2080000 | -1465984 | | |
| 4 | -1042943028 | | | 3453856440 | 74453838480 | 3453856440 | -1042943028 | |
| 5 | -595277880960 | | | 3900245149440 | 313232037949440 | 313232037949440 | 3900245149440 | -595277880960 |

$g = 2$

| | | | | | | | | |
|-------|-------------|---|---------------|---|---------------|---|---------------|-------------|
| d_1 | d_2 | = | 0 | 1 | 2 | 3 | 4 | 5 |
| 0 | | | | | | | | |
| 1 | | | | | | | | |
| 2 | -6 | | 8 | | -6 | | | |
| 3 | 7488 | | 0 | | 0 | | 7488 | |
| 4 | 50181180 | | -73048296 | | 32635544 | | -73048296 | |
| 5 | 72485905344 | | -194629721856 | | 2083061531520 | | 2083061531520 | |
| | | | | | | | -194629721856 | |
| | | | | | | | | 72485905344 |

In the strong coupling limit [78] this model has a non-conifold transition at $\Delta_s = 0$ to the complete intersection $X' = \mathbb{P}_{1,1,1,1,1,3}^5[2, 6]$ with the topological data $\chi = -256$, $h^{1,1} = 1$ whose invariants $n_d^{(2)}(X')$ are given by

| | | | | | |
|---------|----|-------|-----------|---------------|--------------------|
| $d = 1$ | 2 | 3 | 4 | 5 | 6 |
| 0 | -4 | 14976 | -13098688 | 3921835430016 | 128614837503143532 |

We therefore see that the $n_{i,j}^{(2)}$ and $n_d^{(2)}$ are in agreement with the constraint (5.14).

Moreover, we find a good consistency check in the weak coupling limit of the heterotic string dual to all orders in $n = d_1$ for $d_2 = 0$. Combining the results of [65], [95] and [77] we conclude that (6.2) extends the analysis of [95] to all genus with

$$\frac{\Theta(q)}{\eta^{24}} = -\frac{2\theta E_4 F_6}{\eta^{24}} = \frac{-2}{q} + 252 + 2496q^{\frac{1}{4}} + 223752q + \dots, \quad (6.39)$$

where

$$\theta(q) = \sum_{n \in \mathbb{Z}} q^{\frac{n^2}{4}}, \quad F_2(q) = \sum_{n \in \mathbb{Z}_{>0, \text{odd}}} \sigma_1(n) q^{\frac{n}{4}} \quad (6.40)$$

generate the ring of modular forms for the congruence subgroup $\Gamma^0(4)$ and $F_6 = E_6 - 2F_2(\theta^4 - 2F_2)(\theta^4 - 16F_2)$. The self intersection of the unique divisor class in the generic fiber is $E^2 = 2$ and the one dimensional Picard lattice is generated by δ with $\delta^2 = \frac{1}{2}$. Hence we get for the embedding of the Picard lattice of the K3 into $H^2(X, \mathbb{Z})$

$$\lambda^{2g-2} q^l \rightarrow \frac{1}{(2\pi i)^{3-2g}} \sum_{n^2/4=l} \text{Li}_{3-2g}(e^{2\pi i n T}). \quad (6.41)$$

For $g = 0$ this was already checked in [95]. For $g = 1$ the subtraction scheme used in [58], [95] involves the Möbius function for the covering of the torus to itself and differs from (6.2), (6.41). Our generalization to all genus is perfectly consistent with the above B-model one and two loop results and the lowest n non-vanishing genus g invariants can be checked to all g using [2] as we will do below. The predictions for the $n_{d,0}^{(g)}$, $g \geq 0$, are as follows

| g | $d = 1$ | 2 | 3 | 4 | 5 | 6 | 7 | 8 |
|-----|---------|--------|----------|-------------|---------------|------------------|-----------|------|
| 0 | 2496 | 223752 | 38637504 | 9100224984 | 2557481027520 | 805628041231176 | ... | ... |
| 1 | 0 | -492 | -1465984 | -1042943520 | -595277880960 | -316194812546140 | ... | ... |
| 2 | 0 | -6 | 7488 | 50181180 | 72485905344 | 70378651228338 | ... | ... |
| 3 | 0 | 0 | 0 | -902328 | -5359699200 | -10869145571844 | ... | ... |
| 4 | 0 | 0 | 0 | 1164 | 228623232 | 1208179411278 | ... | ... |
| 5 | 0 | 0 | 0 | 12 | -4527744 | -94913775180 | ... | ... |
| 6 | 0 | 0 | 0 | 0 | 17472 | 4964693862 | ... | ... |
| 7 | 0 | 0 | 0 | 0 | 0 | -152682820 | ... | ... |
| 8 | 0 | 0 | 0 | 0 | 0 | 2051118 | ... | ... |
| 9 | 0 | 0 | 0 | 0 | 0 | -2124 | ... | ... |
| 10 | 0 | 0 | 0 | 0 | 0 | -22 | 605915136 | ... |
| 11 | 0 | 0 | 0 | 0 | 0 | 0 | -9419904 | ... |
| 12 | 0 | 0 | 0 | 0 | 0 | 0 | 32448 | ... |
| 13 | 0 | 0 | 0 | 0 | 0 | 0 | 0 | ... |
| 14 | 0 | 0 | 0 | 0 | 0 | 0 | 0 | ... |
| 15 | 0 | 0 | 0 | 0 | 0 | 0 | 0 | ... |
| 16 | 0 | 0 | 0 | 0 | 0 | 0 | 0 | 3132 |
| 17 | 0 | 0 | 0 | 0 | 0 | 0 | 0 | 36 |

Repeating the discussion at the end of the subsection 6.3 with $H^3 = 4$ and $H^2L = 2$ we obtain

$$n_{2k,0}^{(k^2+1)} = (-1)^{\tilde{p}(2k)} 2\tilde{p}(2k) , \quad (6.42)$$

where we define \tilde{p} using (6.19) as

$$\sum_{n=0}^{\infty} \tilde{p}(n) q^n = \frac{1}{(1-q)(1-q^2)^2(1-q^6)} . \quad (6.43)$$

Furthermore, with $e(\mathcal{C}) = -252(\tilde{p}(2k) - 1)g$ we get for the $n_Q^{(g)}$ with one node

$$n_{2k,0}^{(k^2)} = (-1)^{\tilde{p}(2k)-1} (4k^2\tilde{p}(2k) + 252(1 - \tilde{p}(2k))) , \quad (6.44)$$

again in perfect agreement with the table. In a way very similar to the first calculation one can also calculate the Euler number of the moduli space of smooth curves in the class $(2k, 1)$ with the result

$$n_{2k,1}^{(k^2+1)} = (-1)^{\tilde{p}(2k)-1} 4(\tilde{p}(2k) - 1) . \quad (6.45)$$

What we have seen above is a very detailed perturbative check of heterotic-type II duality based on the BPS degeneracies for certain degrees to all genus. However, just as in the case of the fibration discussed in section 6.3, we find three fibrations with the same Hodge numbers as listed in table 1 below. From the dimension of the vector- and hypermultiplet moduli space they could be equally well type II duals of the ST model. The difference between these cases is in the classical intersection ring $\mathcal{F}^{(0)} = -\eta t_1^3/6 - t_1^2 t_2$ and in the classical terms in $\mathcal{F}^{(1)} \sim \frac{36+4\eta}{24} t_1 + t_2$.

We parameterized these by $\eta = 4, 2, 0$, so that $\eta = 4$ is the case presented above. The complete intersection with $\eta = 2$ has Picard–Fuchs operators

$$\begin{aligned}\mathcal{L}_1 &= \theta_1^2(\theta_1 - \theta_2) - 8(6\theta_1 + 2\theta_2 - 5)(6\theta_1 + 2\theta_2 - 3)(6\theta_1 + 2\theta_2 - 1)z_1 \\ \mathcal{L}_2 &= \theta_2^2 - 2(\theta_1 - \theta_2 + 1)(6\theta_1 + 2\theta_2 - 1)z_2\end{aligned}\quad (6.46)$$

from which we obtain, with suitably rescaled variables $a = \frac{z_1}{1728}$ and $b = \frac{z_2}{16}$, the B-model triple couplings

$$\begin{aligned}Y_{111} &= \frac{2(3(1+3b)^2 + a(3+13b+16b^2))}{3a^3\Delta_{con}}, & Y_{112} &= \frac{2((1+3b)^2 - a(1+9b+16b^2))}{a^2b\Delta_{con}} \\ Y_{122} &= \frac{2(3+9b+3a(5+16b))}{ab\Delta_{con}}, & Y_{222} &= \frac{18(1-a+b-16ab)}{b^2\Delta_{con}}\end{aligned}\quad (6.47)$$

where the conifold discriminant is

$$\Delta_{con} = (1-a)^2 - b(6+9b-2a(21+96b+128b^2)).$$

The fact that the fiber has $E^2 = 2$ guarantees that $\frac{1}{z_1}|_{z_2=0} = J(t_1)$, and together with the discriminant of the form $\Delta_{con} = (1-1728z_1)^2 - O(z_2)$ we get a clear hint of a $SU(2)$ gauge enhancement for the value $t_1 := T = i$, i.e. the gauge symmetry enhancement expected for the torus modulus of the heterotic torus in the weak coupling. Using the Picard–Fuchs operators transformed to the variables $x = (1-a) = \epsilon\tilde{u}$ and $y = \frac{a^2b}{3(1-a)^2} = \frac{1}{\tilde{u}^2}$ we have established that we get the embedding of the Seiberg–Witten non-perturbative completion of the rigid $N = 2$ $SU(2)$ gauge symmetry at this point. The Seiberg–Witten periods $a(u)$ and $a_D(u)$ with $\frac{1}{\tilde{u}^2} = \frac{\Lambda^4}{u^2}$ occur in the double scaling limit of the Calabi–Yau periods like in the work of [90], which considers the fibration $n = 4$. The Calabi–Yau periods for the various cases $\eta = 4, 2, 0$ differ in the ϵ corrections near the SW point.

The Seiberg–Witten enhancement, even though non-perturbative in the rigid theory, is an effect that is local near the weak coupling divisor $z_2 = 0$ of the moduli space. When we venture deeper into the non-perturbative regime of the full heterotic string we see a completely different picture. The easiest way to detect the differences is to look at the GV invariants in arbitrary classes. Here we see the different non-perturbative completions of the three theories.

$g = 0$

| d_1 | $d_2 = 0$ | 1 | 2 | 3 | 4 | 5 |
|-------|------------|---------------|-----------------|------------------|-------------------|--------------|
| 0 | | 24 | -2 | | | |
| 1 | 2496 | 24000 | 4544 | -4096 | 6144 | -8192 |
| 2 | 223752 | 17244192 | 92555600 | 22945824 | -12818168 | 24969216 |
| 3 | 38637504 | 11552340480 | 239152764672 | 911674812096 | 283693717248 | -89080677888 |
| 4 | 9100224984 | 7397501182992 | 387426434941992 | 4444162191527440 | 13387851546648736 | ... |

$g = 1$

| d_1 | d_2 | = | 0 | 1 | 2 | 3 | 4 | 5 |
|-------|-------|---|-------------|-------------|----------------|-----------------|------------------|-----------------|
| 0 | | | | | | | | |
| 1 | | | | | | | | |
| 2 | | | -492 | 5760 | 43080 | -108928 | 638420 | -2703360 |
| 3 | | | -1465984 | 23531520 | 3651733760 | 14152031872 | 2833959168 | 5870161920 |
| 4 | | | -1042943028 | 35586706080 | 21017735917528 | 346074753826240 | 1064755476016840 | 364053943057856 |

We have also checked with the B-model calculation that the $n_{d_1,0}^{(2)}$ genus 2 BPS numbers for the $\eta = 2, 0$ cases are the same as in the $\eta = 4$ case for a choice of the ambiguity. Since the discriminant is of higher order in b , it becomes harder to fix the ambiguity to uniquely determine the genus 2 numbers for general (d_1, d_2) classes in the $\eta = 2, 0$ cases. The agreement for all genus amplitudes for the perturbative classes $(d_1, 0)$ follows from formulae (6.2), (6.50), (6.51).

The complex structure data of the $\eta = 0$ case are

$$\begin{aligned}\mathcal{L}_1 &= \theta_1^3 - 8(6\theta_1 + 4\theta_2 - 5)(6\theta_1 + 4\theta_2 - 3)(6\theta_1 + 4\theta_2 - 1)z_1 \\ \mathcal{L}_2 &= \theta_2^2 - 4(6\theta_1 + 4\theta_2 - 1)(6\theta_1 + 4\theta_2 - 3)z_2\end{aligned}\quad (6.48)$$

and with $a = \frac{z_1}{1728}$, $b = \frac{z_2}{64}$ the B-model triple couplings are

$$\begin{aligned}Y_{111} &= \frac{4(3+b)}{3a^2\Delta_{con}}, & Y_{112} &= \frac{2((1-b)^2 - a(1+b))}{a^2b\Delta_{con}} \\ Y_{122} &= \frac{3(2+a-2b)}{ab\Delta_{con}}, & Y_{222} &= \frac{9(1-a+3b)}{2b^2\Delta_{con}}\end{aligned}\quad (6.49)$$

where the conifold discriminant is

$$\Delta_{con} = (1-a)^2 - b(3(1+2a) - b(3-b)).$$

Establishing the rigid SU(2) Seiberg-Witten embedding is very similar as in the case above and the non-perturbative BPS numbers are

$g = 0$

| d_1 | d_2 | = | 0 | 1 | 2 | 3 | 4 |
|-------|-------|---|------------|----------------|-------------------|----------------------|--------------------|
| 0 | | | | 288 | 252 | 288 | 252 |
| 1 | | | 2496 | 216576 | 6391296 | 104994816 | 1209337344 |
| 2 | | | 223752 | 152031744 | 19638646848 | 1180450842624 | 43199009739072 |
| 3 | | | 38637504 | 100021045248 | 34832157566976 | 4962537351009792 | 401057938191181824 |
| 4 | | | 9100224984 | 63330228232704 | 47042083144050624 | 13025847457256417280 | ... |

$g = 1$

| d_1 | d_2 | = | 0 | 1 | 2 | 3 | 4 |
|-------|-------------|--------------|------------------|---------------|---------------------|-----------------|-----------------------|
| 0 | | | | | 3 | | |
| 1 | | | | | -4992 | -433152 | -12797568 |
| 2 | -492 | | 69120 | | 104982288 | 11531535360 | 582562937232 |
| 3 | -1465984 | 265236480 | | 1257004076544 | | 351343656784896 | 42652659615054336 |
| 4 | -1042943028 | 360976775040 | 4290798245087472 | | 2287148665427369472 | | 506382335153204333472 |

To summarize, these three models have the same degeneracies of BPS states in the perturbative limit and these are the data on which the impressive checks of the duality [52] [96] [48] rely. The differences in the classical terms $\mathcal{F}^{(0)}$ and $\mathcal{F}^{(1)}$ are suppressed in the perturbative limit $g \rightarrow 0$, where we use the identification $t_2 = 4\pi i S = 4\pi i \left(\frac{1}{g^2} - i \frac{\theta}{8\pi^2} \right)$, and for the ST model they have not been determined on the heterotic string side. Above we also see that the BPS degeneracies alone do not suffice to fix the non-perturbative completion. There is an additional data necessary on the heterotic side, which corresponds to picking one of the three (and possibly more) fibrations on the type II side. This discrete data might be a subtle choice in the construction of the gauge bundle before higgsing it, or a flux. It determines the non-perturbative completion of the heterotic string in a decisive way.

6.9 Further 2–parameter K3 fibrations

In this section we give an overview over other 2–parameter K3 fibrations. Using an extension of PALP [30] to include the nef-partitions of complete intersections discussed in Section 2.1 [97] we have searched for K3 fibered complete intersection Calabi–Yau manifolds in codimension 2. The number of five-dimensional reflexive polyhedra with a nef-partition is enormous. Hence, we have restricted ourselves to polyhedra with at most ten points. Nevertheless, we have come up with a large number of examples as Table 1 shows. In the first column, we have indicated the Calabi–Yau threefold X in terms of weight vectors. We give only one of the typically many realizations of X as a complete intersection with the same topological data. From the weight vectors it is also easy to read off the reflexive section yielding the K3 fiber. The possible K3 fibers together with the self intersection number E^2 of the Picard lattice are given by

| | |
|----------------------------------|---|
| $\mathbb{P}_{1,1,1,3}^3[6]$ | 2 |
| $\mathbb{P}_{1,1,1,2,3}^4[2, 6]$ | 2 |
| $\mathbb{P}_{1,1,1,3,3}^4[3, 6]$ | 2 |
| $\mathbb{P}_{1,1,1,1}^3[4]$ | 4 |
| $\mathbb{P}_{1,1,1,1,2}^4[2, 4]$ | 4 |
| $\mathbb{P}_{1,1,1,1,3}^4[3, 4]$ | 4 |
| $\mathbb{P}_{1,1,1,1,1}^4[2, 3]$ | 6 |

In the three cases of weighted projective spaces it is implicitly understood that the singularities coming from the weights with common factor are resolved. The next three columns in Table 1 contain the complete information about the intersection ring and the second Chern class of X . The topological numbers not indicated are fixed by Oguiso’s criterion (3.15). More information

| X | χ | H^3 | E^2 | $c_2 H$ | $n_{0,1}^{(0)}$ | $n_{0,2}^{(0)}$ | $n_{i,k}^{(g)}$ | k |
|---|--------|-------|-------|---------|-----------------|-----------------|--|-----|
| $\mathbb{P} \begin{pmatrix} 3 & 3 & 2 & 2 & 1 & 1 & 0 \\ 3 & 1 & 0 & 0 & 1 & 1 & 2 \end{pmatrix} \begin{bmatrix} 6 & 6 \\ 6 & 2 \end{bmatrix}$ | -84 | 1 | 2 | 22 | 16 | 2 | $n_{i,k}^{(g)} = n_{i,4i-k}^{(g)}, 0 \leq k \leq 2i$ | 1 |
| $\mathbb{P} \begin{pmatrix} 3 & 1 & 1 & 1 & 1 & 1 & 0 \\ 3 & 1 & 1 & 1 & 0 & 0 & 2 \end{pmatrix} \begin{bmatrix} 6 & 2 \\ 6 & 2 \end{bmatrix}$ | -140 | 2 | 2 | 32 | 8 | 0 | $n_{i,k}^{(g)} = n_{i,2i-k}^{(g)}, 0 \leq k \leq i$ | 2 |
| $\mathbb{P} \begin{pmatrix} 3 & 2 & 1 & 1 & 1 & 0 & 0 \\ 1 & 0 & 0 & 0 & 1 & 1 & 1 \end{pmatrix} \begin{bmatrix} 6 & 2 \\ 2 & 2 \end{bmatrix}$ | -140 | 0 | 2 | 24 | 96 | 148 | $n_{0,i} \neq 0, i > 2$ | 2 |
| $\mathbb{P} \begin{pmatrix} 3 & 2 & 1 & 1 & 1 & 1 & 0 \\ 3 & 2 & 0 & 0 & 1 & 1 & 1 \end{pmatrix} \begin{bmatrix} 6 & 3 \\ 6 & 2 \end{bmatrix}$ | -196 | 3 | 2 | 42 | 4 | 0 | $n_{i,2i}^{(g)} = n_i^{(g)}$ (local E_8) | 3 |
| $\mathbb{P} \begin{pmatrix} 5 & 2 & 2 & 1 & 1 & 1 & 0 \\ 3 & 0 & 0 & 1 & 1 & 1 & 2 \end{pmatrix} \begin{bmatrix} 10 & 2 \\ 6 & 2 \end{bmatrix}$ | -196 | 1 | 2 | 34 | 48 | -2 | $n_{i,k}^{(g)} = n_{i,4i-k}^{(g)}, 0 \leq k \leq 2i$ | 3 |
| $\mathbb{P}_{1,1,2,2,6}^4$ | -252 | 4 | 2 | 52 | 2 | 0 | $n_{i,k}^{(g)} = n_{i,i-k}^{(g)}, 0 \leq k \leq [i/2]$ | 4 |
| $\mathbb{P} \begin{pmatrix} 4 & 2 & 1 & 1 & 1 & 1 & 0 \\ 3 & 1 & 0 & 0 & 1 & 1 & 1 \end{pmatrix} \begin{bmatrix} 8 & 2 \\ 6 & 1 \end{bmatrix}$ | -252 | 2 | 2 | 44 | 24 | -2 | | 4 |
| $\mathbb{P} \begin{pmatrix} 3 & 3 & 1 & 1 & 1 & 0 & 0 \\ 0 & 0 & 0 & 2 & 2 & 1 & 1 \end{pmatrix} \begin{bmatrix} 6 & 3 \\ 4 & 2 \end{bmatrix}$ | -252 | 0 | 2 | 36 | 288 | 252 | $n_{0,i} \neq 0, i > 2$ | 4 |
| $\mathbb{P} \begin{pmatrix} 2 & 1 & 1 & 1 & 1 & 0 & 0 \\ 0 & 1 & 1 & 1 & 3 & 2 & 2 \end{pmatrix} \begin{bmatrix} 4 & 2 \\ 4 & 6 \end{bmatrix}$ | -84 | 2 | 4 | 32 | 32 | 4 | $n_{i,k}^{(g)} = n_{i,4i-k}^{(g)}, 0 \leq k \leq 2i$ | 1 |
| $\mathbb{P} \begin{pmatrix} 2 & 1 & 1 & 1 & 1 & 0 & 0 \\ 0 & 0 & 0 & 0 & 0 & 1 & 1 \end{pmatrix} \begin{bmatrix} 4 & 2 \\ 0 & 2 \end{bmatrix}$ | -112 | 4 | 4 | 40 | 16 | 0 | $n_{i,k}^{(g)} = n_{i,2i-k}^{(g)}, 0 \leq k \leq i$ | 2 |
| $\mathbb{P} \begin{pmatrix} 2 & 1 & 1 & 1 & 1 & 0 & 0 \\ 0 & 0 & 0 & 0 & 1 & 1 & 1 \end{pmatrix} \begin{bmatrix} 4 & 2 \\ 1 & 2 \end{bmatrix}$ | -112 | 1 | 4 | 34 | 64 | 24 | $n_{i,k}^{(g)} = n_{i,8i-k}^{(g)}, 0 \leq k \leq 4i$ | 2 |
| $\mathbb{P} \begin{pmatrix} 1 & 1 & 1 & 1 & 1 & 1 & 0 \\ 0 & 0 & 2 & 1 & 1 & 1 & 1 \end{pmatrix} \begin{bmatrix} 4 & 2 \\ 4 & 2 \end{bmatrix}$ | -140 | 6 | 4 | 48 | 8 | 0 | $n_{i,2i}^{(g)} = n_i^{(g)}$ (local E_7) | 3 |
| $\mathbb{P} \begin{pmatrix} 2 & 1 & 1 & 1 & 1 & 0 & 0 \\ 0 & 0 & 0 & 0 & 0 & 1 & 1 \end{pmatrix} \begin{bmatrix} 4 & 2 \\ 1 & 1 \end{bmatrix}$ | -140 | 3 | 4 | 42 | 32 | 0 | $n_{i,4i}^{(g)} = n_i^{(g)}$ (local $\mathbb{P}^1 \times \mathbb{P}^1$) | 3 |
| $\mathbb{P} \begin{pmatrix} 2 & 1 & 1 & 1 & 1 & 0 & 0 \\ 0 & 0 & 0 & 1 & 1 & 1 & 1 \end{pmatrix} \begin{bmatrix} 4 & 2 \\ 2 & 2 \end{bmatrix}$ | -140 | 0 | 4 | 36 | 128 | 144 | $n_{0,i} \neq 0, i > 2$ | 3 |
| $\mathbb{P}_{1,1,2,2,2}^4$ | -168 | 8 | 4 | 56 | 4 | 0 | $n_{i,k}^{(g)} = n_{i,i-k}^{(g)}, 0 \leq k \leq [i/2]$ | 4 |
| $\mathbb{P} \begin{pmatrix} 1 & 1 & 1 & 1 & 1 & 0 & 0 \\ 0 & 0 & 0 & 0 & 0 & 1 & 1 \end{pmatrix} \begin{bmatrix} 4 & 1 \\ 1 & 1 \end{bmatrix}$ | -168 | 5 | 4 | 50 | 16 | 0 | $n_{i,4i}^{(g)} = n_i^{(g)}$ (local \mathbb{P}^2) | 4 |
| $\mathbb{P} \begin{pmatrix} 2 & 1 & 1 & 1 & 1 & 0 & 0 \\ 0 & 0 & 0 & 0 & 0 & 1 & 1 \end{pmatrix} \begin{bmatrix} 4 & 2 \\ 2 & 0 \end{bmatrix}$ | -168 | 2 | 4 | 44 | 64 | 0 | $n_{i,k}^{(g)} = n_{i,4i-k}^{(g)}, 0 \leq k \leq 2i$ | 4 |
| $\mathbb{P} \begin{pmatrix} 3 & 1 & 1 & 1 & 1 & 1 & 0 \\ 2 & 0 & 0 & 1 & 1 & 1 & 1 \end{pmatrix} \begin{bmatrix} 6 & 2 \\ 4 & 2 \end{bmatrix}$ | -196 | 4 | 4 | 52 | 32 | -2 | | 5 |
| $\mathbb{P} \begin{pmatrix} 1 & 1 & 1 & 1 & 1 & 0 & 0 \\ 0 & 0 & 0 & 0 & 0 & 1 & 1 \end{pmatrix} \begin{bmatrix} 3 & 2 \\ 0 & 2 \end{bmatrix}$ | -108 | 6 | 6 | 48 | 24 | 0 | $n_{i,k}^{(g)} = n_{i,2i-k}^{(g)}, 0 \leq k \leq i$ | |
| $\mathbb{P} \begin{pmatrix} 1 & 1 & 1 & 1 & 1 & 0 & 0 \\ 0 & 0 & 0 & 0 & 1 & 1 & 1 \end{pmatrix} \begin{bmatrix} 3 & 2 \\ 1 & 2 \end{bmatrix}$ | -116 | 2 | 6 | 44 | 72 | 18 | $n_{i,k}^{(g)} = n_{i,6i-k}^{(g)}, 0 \leq k \leq 3i$ | |
| $\mathbb{P} \begin{pmatrix} 1 & 1 & 1 & 1 & 1 & 1 & 0 \\ 0 & 0 & 1 & 1 & 1 & 1 & 1 \end{pmatrix} \begin{bmatrix} 3 & 3 \\ 3 & 2 \end{bmatrix}$ | -120 | 9 | 6 | 54 | 12 | 0 | $n_{i,2i}^{(g)} = n_i^{(g)}$ (local E_6) | |
| $\mathbb{P} \begin{pmatrix} 1 & 1 & 1 & 1 & 1 & 0 & 0 \\ 0 & 0 & 0 & 0 & 0 & 1 & 1 \end{pmatrix} \begin{bmatrix} 3 & 2 \\ 1 & 1 \end{bmatrix}$ | -128 | 5 | 6 | 50 | 36 | 0 | $n_{i,3i}^{(g)} = n_i^{(g)}$ (local D_5) | |
| $\mathbb{P}_{1,1,2,2,2,2}^5$ | -132 | 12 | 6 | 60 | 6 | 0 | $n_{i,k}^{(g)} = n_{i,i-k}^{(g)}, 0 \leq k \leq [i/2]$ | |
| $\mathbb{P} \begin{pmatrix} 1 & 1 & 1 & 1 & 1 & 1 & 0 \\ 0 & 0 & 1 & 1 & 1 & 1 & 1 \end{pmatrix} \begin{bmatrix} 4 & 2 \\ 3 & 2 \end{bmatrix}$ | -140 | 8 | 6 | 56 | 18 | 0 | $n_{i,3i}^{(g)} = n_i^{(g)}$ (local $\mathbb{P}^1 \times \mathbb{P}^1$) | |
| $\mathbb{P} \begin{pmatrix} 1 & 1 & 1 & 1 & 1 & 0 & 0 \\ 0 & 0 & 0 & 0 & 0 & 1 & 1 \end{pmatrix} \begin{bmatrix} 3 & 2 \\ 2 & 0 \end{bmatrix}$ | -148 | 4 | 6 | 52 | 54 | 0 | $n_{i,k}^{(g)} = n_{i,3i-k}^{(g)}, 0 \leq k \leq [3i/2]$ | |

65
Table 1: An overview of K3 fibered Calabi–Yau threefolds with $h^{1,1} = 2$

about the spaces X is contained in the Gopakumar-Vafa invariants $n_{i,j}^{(g)}$. For most examples, the $n_{0,i}^{(0)}$ are non-vanishing only for $i = 1, 2$. These values are explicitly given in the table, as well as some special properties of the general $n_{i,j}^{(g)}$ which will be explained below.

We have determined the modular form $\Theta(q)$ in (6.2) for all the examples with $E^2 = 2$ and $E^2 = 4$. The result depends on the value of k in the last column of Table 1. For the examples with $E^2 = 2$, k is related to the Euler number as

$$\chi = -28(1 + 2k) \quad (6.50)$$

and we find for $k = 1, \dots, 4$

$$\Theta^{(k)}(q) = 2^{-8} W E_4 F_6^{(k)} \quad (6.51)$$

with

$$F_6^{(k)}(q) = 4W^{12} - (76 + 7k)W^8X^4 - (180 - 6k)W^4X^8 - (4 - k)X^{12} \quad (6.52)$$

and $W = \theta_3(\frac{\tau}{2})$, $X = \theta_4(\frac{\tau}{2})$, and $E_4(\tau)$ is as in (6.31). Higher genus amplitudes for $k = 4$ have been discussed in Section 6.8 in detail, while some topological aspects of the $k = 1$ example are given in Appendix B. $F_6^{(4)}(q)$ coincides with the expression in (6.39) found in [95].

For the examples with $E^2 = 4$, k is related to the Euler number as

$$\chi = -4(4 + 7k) \quad (6.53)$$

and we find for $k = 1, \dots, 5$

$$\begin{aligned} \Theta^{(k)}(q) = & 2^{-22} (6U^{21} - (4 - k)U^{20}V - (78 + 21k)U^{19}V^2 - (1066 + 47k)U^{18}V^3 \\ & - (28020 + 213k)U^{17}V^4 - (40094 - 20k)U^{16}V^5 - (339960 - 444k)U^{15}V^6 \\ & - (241928 - 164k)U^{14}V^7 - (1244316 - 300k)U^{13}V^8 - (585392 + 50k)U^{12}V^9 \\ & - (2073636 + 774k)U^{11}V^{10} - (691212 + 258k)U^{10}V^{11} - (1756176 + 150k)U^9V^{12} \\ & - (414772 - 100k)U^8V^{13} - (725784 - 492k)U^7V^{14} - (113320 - 148k)U^6V^{15} \\ & - (120282 - 60k)U^5V^{16} - (9340 + 71k)U^4V^{17} - (3198 + 141k)U^3V^{18} \\ & - (26 + 7k)U^2V^{19} - (12 - 3k)UV^{20} + 2V^{21}) \end{aligned} \quad (6.54)$$

with $U = \theta_3(\frac{\tau}{4})$ and $V = \theta_4(\frac{\tau}{4})$ as in (6.15). The cases with $k = 2$ and $k = 4$ have been discussed in detail in Sections 6.4 and 6.3 respectively, cf. (6.24) and (6.16). Again, some topological aspects of the $k = 1$ example are given in Appendix B. We emphasize that unlike the $E^2 = 2$ case (6.51), it is not possible to factor the E_4 Eisenstein series. Since this Eisenstein series is nothing but the theta function $\Theta_{E_8}(q, 0)$ for the E_8 lattice (see also Section 7.1) this hints at the possibility that an E_8 symmetry which was realized in the $E^2 = 2$ case, is broken in the $E^2 = 4$ case.

Observe that in all the examples

$$\text{Coeff}_{q^0} \frac{2\Theta^{(k)}}{\eta^{24}} = \chi \quad (6.55)$$

as was already explained in [65].

It turns out that there is a much simpler basis for the space of modular forms than θ_3 and θ_4 . In this basis more properties of these modular forms can be read off. This will be fully explored in a future publication [98] where we also intend to include the expressions for Θ for the examples with $E^2 = 6$.

The two-parameter K3 fibrations X with the same modular form $\Theta(q)$ and hence the same Euler number can be distinguished by their different topology, i.e. by the numbers H^3 and $c_2 H$. This is also reflected in the instanton numbers as we will discuss now in detail. In the case that the Calabi–Yau threefold X admits a contraction in which the fibers of a ruled surface get blown down, there is a \mathbb{Z}_2 involution on $H_2(X, \mathbb{Z})$ [75]. This implies a relation for the $n_Q^{(g)}$ of the type (5.16). This explains the entries in Table 1 which are of the form $n_{i,k}^{(g)} = n_{i, Mi-k}^{(g)}$, $0 \leq k \leq [Mi/2]$, $i > 0$ and $n_{i,k} = 0$ for $i > 0$ and $k > Mi$. The constant M can be determined from the geometry of X . Alternatively, if X admits a contraction to a local Calabi–Yau whose compact part is a del Pezzo surface S or a \mathbb{P}^2 , there are again restrictions on the $n_Q^{(g)}$, given by (5.15). In this situation, they read $n_{i, M'i}^{(g)} = n_i^{(g)}(S)$ for $i > 0$ and $n_{i,k}^{(g)} = 0$ for $i > 0$ and $k > M'i$. M' is another constant which is also encoded in the geometry of X . The invariants $n_i^{(0)}(S)$ for low degrees and for all S which appear in toric Calabi–Yau complete intersections are listed below [99], [2].

| S | d | 1 | 2 | 3 | 4 | 5 | 6 |
|--|-----|-------|--------|------------|-------------|----------------|----------------|
| local $\mathbb{P}^1 \times \mathbb{P}^1$ | −4 | −4 | −12 | −48 | −240 | −1356 | −1356 |
| local \mathbb{P}^2 | 3 | −6 | 27 | −192 | 1695 | −17064 | −17064 |
| local D_5 | 16 | −20 | 48 | −192 | 960 | −5436 | −5436 |
| local E_6 | 27 | −54 | 243 | −1728 | 15255 | −153576 | −153576 |
| local E_7 | 56 | −272 | 3240 | −58432 | 1303840 | −33255216 | −33255216 |
| local E_8 | 252 | −9252 | 848628 | −114265008 | 18958064400 | −3589587111852 | −3589587111852 |

Finally, there are a few other cases where there seem to be no restrictions on the instanton numbers. This is in particular the case for the examples with $H^3 = 0$. As for the $n_{0,1}^{(0)}$, we observe that they are in general multiples of E^2 . For those X which admit a contraction of a ruled surface or to a del Pezzo surface, $n_{0,1}^{(0)}$ is also a multiple of the constants M and M' , respectively.

We conclude with a remark on the completeness of the table. We have seen that the Euler numbers for the 2-parameter K3-fibrations with $E^2 = 2, 4$ take only particular values, (6.50) and (6.53). Looking at the table, we see that for a fixed Euler number there is a maximal value of H^3 . This value decreases by 2 for $E^2 = 2$ and by 3 for $E^2 = 4$. This is related to the rational homotopy equivalence of these models as follows. If we change H by a rational multiple of the class L of the fiber, $H \rightarrow H' = H - \frac{1}{n}L$, then the requirement that H'^3 and $\int_X c_2 H'$ be integers tells us that $n \mid 24$ and $n \mid 3E^2$. However, not all values of n that are allowed by these conditions actually appear. The lower bound is given by the fact that H^3 must be non-negative. The maximal value of H^3 is k for $E^2 = 2$ and $2k$ for $E^2 = 4$, so it seems to be directly related to the Euler number. All these bounds taken together suggest that it is possible to classify such Calabi–Yau families, at least up to rational homotopy. For example,

these observations suggest the existence of a 2-parameter K3 fibration with $\chi = -196$, $E^2 = 4$, $H^3 = 10$ and $c_2 H = 64$. Moreover, the same argument show that the list of the families with E^6 is far from being complete.

6.10 The STU model and its type II duals

In this section we will study the Gopakumar-Vafa invariants for various type IIA duals X of the STU model. We begin with $X = \mathbb{P} \begin{pmatrix} 6 & 4 & 1 & 0 & 1 & 0 \\ 6 & 4 & 0 & 1 & 0 & 1 \end{pmatrix} \begin{bmatrix} 12 \\ 12 \end{bmatrix}$, which has a K3 fibration structure $\text{K3} \rightarrow X \rightarrow \mathbb{P}^1_{(3)}$. The K3 fiber itself has an elliptic fibration $E \rightarrow \text{K3} \rightarrow \mathbb{P}^1_{(2)}$ compatible with an elliptic fibration structure of X , $E \rightarrow X \rightarrow \mathbb{F}_0$ where the base is the Hirzebruch surface $\mathbb{F}_0 = \mathbb{P}^1_{(2)} \times \mathbb{P}^1_{(3)}$. The fibrations have no reducible fibers and hence the model has 3 Kähler classes: The class of the elliptic fiber E and the classes of $\mathbb{P}^1_{(2)}$, $\mathbb{P}^1_{(3)}$, which we identify in the STU model as follows

$$t_1 = U, \quad t_2 = T - U, \quad \text{and} \quad t_3 = S, \quad (6.56)$$

respectively. With $\chi = -480$ and nonzero classical intersections $\kappa_{111} = 8$, $\kappa_{112} = 2$, $\kappa_{113} = 2$, $\kappa_{123} = 1$ and $\int_X c_2 J_1 = 92$, $\int_X c_2 J_2 = \int_X c_2 J_3 = 24$, the expansion of the prepotential is

$$\mathcal{F}^{(0)} = -\frac{4}{3}t_1^3 - t_1^2 t_2 - t_1^2 t_3 - t_1 t_2 t_3 + \frac{23}{6}t_1 + t_2 + t_3 - \frac{480}{2(2\pi i)^3} \zeta(3) + O(q_i). \quad (6.57)$$

For the STU model we have

$$\Theta(q) = 2E_4 E_6 \quad (6.58)$$

in (6.2) and to restore the T, U dependence the q^l powers in the expansion of the automorphic form multiplying λ^{2g-2} have to be replaced by

$$q^l \rightarrow \frac{1}{(2\pi i)^{3-2g}} \sum_{mn=l} \text{Li}_{3-2g}(e^{2\pi i(mT+nU)}). \quad (6.59)$$

Heterotic/Type II duality predicts that (6.2) counts the invariants $n_Q^{(g)}$ for curves in the classes of a two-dimensional sublattice of $H^2(X, \mathbb{Z})$ generated by $\mathbb{P}^1_{(2)}$ and E , corresponding to the lattice $H^2(\text{K3}, \mathbb{Z})$ of the K3 fiber. This identifies the $t_3 \rightarrow -\infty$ and $q_3 \rightarrow 0$ limit as the weak coupling limit, but otherwise the most useful geometric identification of the heterotic dilaton is an open question.

6.10.1 Propagators and compatibility

In Appendix E.1 we have analyzed in part the complex structure moduli space of the mirror of X , in particular the discriminants and the monodromies. We also computed the Yukawa couplings for this model which are ingredients in the computation of the propagators. From

these results and from (E.3), it is easily checked that $\det[(Y_1)_{ij}] = 0$, while $\det[(Y_2)_{ij}] \neq 0 \neq \det[(Y_3)_{ij}]$. Hence we get less compatibility relations of the type (4.21), (4.22), (4.24). They can be fulfilled by choosing for the non-vanishing A_{jk}^i and A_{ij}

$$\begin{aligned}
A_{12}^1 &= -\frac{1}{4b}, & A_{13}^1 &= -\frac{1}{4c}, & A_{22}^2 &= -\frac{1}{b}, & A_{12} &= -\frac{5}{144b}, \\
A_{13} &= -\frac{5}{144c}, & A_{33}^3 &= -\frac{1}{c}, & A_{23}^2 &= -\frac{1}{4c}, & A_{23}^3 &= -\frac{1}{4b}, \\
A_{22} &= -\frac{5}{72ab}, & A_{33} &= -\frac{5}{72ab}, & A_{23} &= \frac{5}{144a} \left(\frac{1}{b} + \frac{1}{c} \right) & &
\end{aligned} \tag{6.60}$$

Note the $2 \leftrightarrow 3$ symmetry. The propagators then become in leading order

$$\begin{aligned}
S_{11} &= q_2 q_2 + O(q^3), & S_{12} &= -\frac{1}{4} - 60q_1 q_2 - 2q_2 q_3 + O(q^3) \\
S_{22} &= \frac{1}{2} + 240q_1 q_3 + 4q_2 q_3 + O(q^3), & S_{23} &= \frac{1}{2} + 60q_1 + 13320q_1^2 + 60q_1(q_2 + q_3) + 4q_2 q_3 + O(q^3), \\
S_1 &= 90q_1(q_2 + q_3) + O(q^3), & S_2 &= 30q_1 - 150q_1 q_2 - 12690q_1^2 + O(q^3), \\
& & S &= -\frac{5}{2}q_1(1 + (q_2 + q_3) + 1560q_1^2) + O(q^4),
\end{aligned} \tag{6.61}$$

where the remaining propagators follow from the $2 \leftrightarrow 3$ symmetry. We have checked with these propagators that we can satisfy the constraints from the local $\mathbb{P}^1 \times \mathbb{P}^1$ and the predictions from the heterotic string from Mariño and Moore [77] and get integer GV invariants. However, the easiest ansatz (4.28) for the ambiguity f_2 has still to be parameterized by 6 unknown integer GV invariants.

6.10.2 Gopakumar–Vafa versus Donaldson–Thomas invariants

Using the scheme (5.6) we can construct the reduced series whose coefficients of q^r count e.g. $n_{(r,1,0)}^{(g)}$, or more generally curves with $[C]^2 = 2r - 2$. Because of the adjunction formula $[C]^2 + [C][K] = 2g - 2$ and the triviality of the canonical bundle, smooth curves in this class have genus $g = r$.

| g | $r=0$ | 1 | 2 | 3 | 4 | 5 | 6 | 7 | 8 |
|-----|-------|-----|--------|----------|-----------|-------------|--------------|---------------|----------------|
| 0 | -2 | 480 | 282888 | 17058560 | 477516780 | 8606976768 | 115311621680 | 1242058447872 | 11292809553810 |
| 1 | 0 | 4 | -948 | -568640 | -35818260 | -1059654720 | -20219488840 | -286327464192 | -3251739174540 |
| 2 | 0 | 0 | -6 | 1408 | 856254 | 55723296 | 1718262980 | 34256077056 | 506823427338 |
| 3 | 0 | 0 | 0 | 8 | -1860 | -1145712 | -76777780 | -2455936800 | -50899848132 |
| 4 | 0 | 0 | 0 | 0 | -10 | 2304 | 1436990 | 98987232 | 3276127128 |
| 5 | 0 | 0 | 0 | 0 | 0 | 12 | -2740 | -1730064 | -122357100 |
| 6 | 0 | 0 | 0 | 0 | 0 | 0 | -14 | 3168 | 2024910 |
| 7 | 0 | 0 | 0 | 0 | 0 | 0 | 0 | 16 | -3588 |
| 8 | 0 | 0 | 0 | 0 | 0 | 0 | 0 | 0 | -18 |

The genus two predictions appeared already in [77], however with the opposite overall sign. Using the ideas of [63], [2] we can now make a simple quantitative check of string duality to all genus in the type IIA description.

The moduli space of the smooth curve c_g in the class $Q = (g, 1, 0)$ is given by the product the base \mathbb{P}_3^1 with the space parameterizing the locations of the g points, where c_g intersects \mathbb{P}_2^1 ,

the section of the elliptic K3 fibration. The moduli space of such a curve is $\mathcal{M}_0 = \mathbb{P}^1 \times \mathbb{P}^g$ and no curves of genus g exist in the class $(r, 1, 0)$, if $r < g$. Hence we get

$$n_{(g,1,0)}^{(g)} = (-1)^{(g+1)}2(g+1), \quad n_{(r,1,0)}^{(g)} = 0, \quad r < g$$

in agreement with the heterotic string prediction.

Curves with one node in the class $(g+1, 1, 0)$ have genus g . The formula for the Euler number of moduli space with one node is [2] $e(\mathcal{M}_1) = e(\mathcal{C}) + (2g-2)e(\mathcal{M}_0)$, with $e(\mathcal{M}_0) = 2(g+1)$ as calculated above. \mathcal{C} is the universal curve over the moduli space. In our case \mathcal{C} fibres over the Calabi–Yau space X . Every $p \in X$ determines a fiber and the section. The choices of the g remaining points in the section gives a \mathbb{P}^{g-1} and so $e(\mathcal{C}) = -480g$, hence $n_{(g,1,0)}^{(g-1)} = (-1)^{(g+1)}(2(g+1)(2g-2) - 480g)$ or

$$n_{(g+1,1,0)}^{(g)} = (-1)^{(g+1)}(4(g+2)g - 480g - 480),$$

again in perfect agreement with the heterotic prediction. For curves of genus g in the class $(g+2, 1, 0)$, i.e. with two nodes, there are reducible components in $\mathcal{C}^{(2)}$. Unfortunately, this makes the application of [2] more complicated. In particular, the genus g BPS numbers $n_{(g+2,1,0)}^{(g)}$ for curves in the class $(g+2, 1, 0)$ do not lie on a degree 3 polynomial in g . Because of the vanishing of the $n_Q^{(g)}$ for fixed Q and for $g > g_{max}$ we can apply (5.11) and reorganize the partition function in terms of the Donaldson–Thomas invariants $\tilde{n}_{Q=(r,1,0)}^{(m)}$. The first few $\tilde{n}_{(r,1,0)}^{(m)} \in \mathbb{Z}$ are listed below

| m | $r = 0$ | 1 | 2 | 3 |
|-----|----------|------------|-----------------|------------------|
| -3 | | | | -114 |
| -2 | | | 29 | -93120 |
| -1 | | -6 | 21120 | -23125422 |
| 0 | 1 | -3840 | 4959252 | -148113736 |
| 1 | 480 | -861918 | 222239296 | 828968673654 |
| 2 | 114000 | -81368016 | -96779956415 | 135202938212616 |
| 3 | 17857600 | 2384015304 | -21060955624896 | 4245487378821074 |

It is remarkable that the $\tilde{n}_{(r,1,0)}^{(m)}$ actually turn out to be integers, and this result therefore constitutes a non-trivial check of the S–duality in topological strings [72].

6.10.3 Symmetries at large complex structure

Here, we discuss the symmetries of the STU model. Exchanging the two \mathbb{P}^1 's corresponds to an $S \leftrightarrow T - U$ duality on the heterotic side, subject to the question of the best identification of the dilaton S . By construction this symmetry is realized on all amplitudes on X , in particular on $\mathcal{F}^{(g)}$. In the heterotic theory there is a $\mathrm{PSL}(2, \mathbb{Z}) \times \mathrm{PSL}(2, \mathbb{Z})$ action on the complex and Kähler structure moduli U, T of the torus. Furthermore, there is mirror symmetry $U \rightarrow T$,

charge conjugation $(T, U) \rightarrow (-\bar{T}, -\bar{U})$ and parity reversal $T \rightarrow -\bar{T}$. The $U \rightarrow T$ symmetry is realized in the weak coupling limit as

$$\begin{aligned} t_1 &\rightarrow t_1 + t_2 \\ t_2 &\rightarrow -t_2 \end{aligned} \tag{6.62}$$

and is reflected on the BPS numbers as constraints $n_{i,j,0}^{(g)} = n_{i,i-j,0}^{(g)}$ and $n_{i,j,0}^{(g)} = 0$ for $j \geq i$ and $i > 0$. However, the realization among these instanton numbers is not perfect as there is an unpaired number $n_{0,1,0}^{(g=0)} = -2$ corresponding to a $-2\text{Li}_3(q_2)$ contribution to $\mathcal{F}^{(0)}$, which has an interesting interpretation. From the analytic continuation of $\text{Li}_3(x)$ in (6.28) one has

$$\text{Li}_3(q_2) = \text{Li}_3(q_2^{-1}) - \frac{2\pi i}{12} (2t_2^3 + 3t_2^2 + t_2) \tag{6.63}$$

In the conifold flop case a similar change of the classical terms leads to the (weak or birational) topology change. Here we have the prediction of a symmetry in the weak coupling limit and a linear transformation on the t_i should be sufficient to leave $\mathcal{F}^{(0)}$ in the limit invariant. We find that in addition to (6.62) we have to transform the dilaton $t_3 \sim S$ as follows

$$t_3 \rightarrow t_3 - 2t_2. \tag{6.64}$$

Now the changes in the cubic as well as the linear terms in t_i in $\mathcal{F}^{(0)}$ cancel. There is a shift in the quadratic term $\mathcal{F}(t(t')) = \mathcal{F}(t') + \frac{1}{2}(t')^2$, which however is physically irrelevant as the Weyl-Petersson metric $G_{i\bar{j}}$ and the C_{ijk} are unchanged. There are no unpaired instanton numbers at higher genus. However, notice that the bubbling contribution at genus 1 from the genus 0 number $-2\frac{1}{12}\text{Li}_1(q_2)$ together with (6.29) cancels precisely the change in the leading terms $\mathcal{F}^{(1)} \sim \frac{t_i}{24} \int_X c_2 J_i$. The constant map contribution to $\mathcal{F}^{(g)}$, $g > 1$, is just proportional to the Euler number (5.7) and, consistently, the $-2\text{Li}_{3-2g}(q_2)$ bubbling contribution at $\mathcal{F}^{(g)}$ is invariant under $q_2 \rightarrow 1/q_2$.

We could identify $S = t_1 + t_3$, $T = t_1 + t_2$ and $U = t_1$ without changing the heterotic weak coupling limit. In this case the exchange symmetry between the two \mathbb{P}^1 , $t_2 \leftrightarrow t_3$, corresponds to an $S \leftrightarrow T$ exchange symmetry but mirror symmetry $T \leftrightarrow U$ is still accompanied by a shift in the dilaton. It was conjectured in [100] that there is a symmetry acting as an S_3 permutation on STU parameter. However, it is precisely the shift of the dilaton (6.64) that modifies this symmetry for any choice of flat coordinates, as the group Γ generated by the two \mathbb{Z}_2 elements

$$W = \begin{pmatrix} 1 & 0 & 0 \\ 0 & 0 & 1 \\ 0 & 1 & 0 \end{pmatrix} \quad M = \begin{pmatrix} 1 & 1 & 0 \\ 0 & -1 & 0 \\ 0 & -2 & 1 \end{pmatrix} \tag{6.65}$$

contains with

$$T = WM = \begin{pmatrix} 1 & 0 & 1 \\ 0 & 0 & -1 \\ 0 & 1 & -2 \end{pmatrix}$$

an element of infinite order

$$T^n = \begin{pmatrix} 1 & (-)^n \left[\frac{n}{2} \right] & -(-)^n \left[\frac{n+1}{2} \right] \\ 0 & (-)^n (1-n) & (-)^n n \\ 0 & -(-)^n n & (-)^n (n+1) \end{pmatrix}.$$

The existence of a shift symmetry in the non-perturbative heterotic string, which is not related to the usual Peccei-Quinn symmetry on the vector multiplet fields is remarkable and leads to useful restrictions on the symplectic invariants or the BPS spectrum.

6.10.4 Symmetries on the symplectic invariants

The afore-mentioned symmetries preserve the large volume limit. They identify e.g. the symplectic invariants in certain classes. We have already discussed them in the strict weak coupling limit. To analyze the non-perturbative heterotic corrections we have to understand some properties of asymptotic expansions of the GV invariants. We illustrate the point by comparing the GV invariants at genus zero for $d_3 = 0$ and $d_3 = 2$.

| d_1 | $d_2 = 0$ | 1 | 2 | 3 | 4 | 5 |
|-------|-----------|------------|---------------|---------------|------------|-----|
| 0 | | -2 | | | | |
| 1 | 480 | 480 | | | | |
| 2 | 480 | 282888 | 480 | | | |
| 3 | 480 | 17058560 | 17058560 | 480 | | |
| 4 | 480 | 477516780 | 8606976768 | 477516780 | 480 | |
| 5 | 480 | 8606976768 | 1242058447872 | 1242058447872 | 8606976768 | 480 |

For $d_3 = 0$ the Gopakumar-Vafa invariants fulfill $n_{i,j,0}^{(g)} = n_{i,i-j,0}^{(g)}$ and vanish for $j > i$ except for $n_{0,1,0}^{(0)} = -2$ with the discussed change of the classical terms. Note that the numbers depend only on the combination $d_2(d_1 - d_2)$, which is manifest from the formulae (6.56), (6.59).

For $d_3 = 2$ we get the following GV invariants

| d_1 | $d_2 = 0$ | 1 | 2 | 3 | 4 | 5 |
|-------|------------|--------------|---------------|----------------|----------------|----------------|
| 0 | | -6 | -32 | -110 | -288 | -644 |
| 1 | | 2400 | 16800 | 64800 | 184800 | 436800 |
| 2 | 480 | -452160 | -4093920 | -18224640 | -56992800 | -143674560 |
| 3 | 17058560 | 103374720 | 789875200 | 3955306880 | 13696352640 | -37214805760 |
| 4 | 8606976768 | -16013531460 | -115113738240 | -6921322409900 | -2765391112320 | -8288446754100 |

The symmetry M , which should occur for fixed $d_3 = s$, is not manifest in the GV invariants for $d_3 \neq 0$ as it was for $d_3 = 0$. However, this does not mean that it is not present. The symmetry on the indices of the GV invariants $n_{i,j,k}^{(g)} = n_{i,i-j-2k,k}^{(g)}$ with $j = 0 \dots \infty$ requires a resummation of the infinite series to negative powers of q_2 . The key is to choose instead of $\text{Li}_3(\underline{q})$ an expansion scheme of the GV invariants that is manifestly symmetric under M . We therefore expand $\mathcal{F}^{(0)}$ as

$$\mathcal{F}^{(0)} = \sum_{u,s=0}^{\infty} q_1^u q_3^s f_{u,s}(q_2) \quad (6.66)$$

where the mirror symmetry on the heterotic T^2 requires

$$f_{u,s}(1/q) = q^{2s-u} f_{u,s}(q) . \quad (6.67)$$

We make an ansatz for $f_{u,s}(q) = \frac{P_{u,s}(q)}{(1-q)^{4s-2}}$, $s > 0$, so that (6.67) imposes that $P_{u,s}(q) = \sum_{k=n}^d c_{u,r,s} q^r$ is a finite polynomial with symmetric coefficients $c_{u,r,s} = c_{u,d+n-r,s}$ for $k = n \dots d$ in q . The required degree is $d = u + 2s - 2 - n$. Indeed, if we organize the GV invariants according to (6.66) we determine the $c_{u,r,s=d_3=2}$ as

| u | $r = 0$ | 1 | 2 | 3 | 4 | 5 | 6 |
|-----|------------|--------------|--------------|---------------|--------------|--------------|------------|
| 0 | -1 | -18 | -1 | | | | |
| 1 | 0 | 2400 | 2400 | | | | |
| 2 | 540 | -455400 | -13726800 | -455400 | 540 | | |
| 3 | 17058560 | 103360 | 425505280 | 425505280 | 103360 | 17058560 | |
| 4 | 8607012129 | -67655604234 | 110072604195 | -413793025380 | 110072604195 | -67655604234 | 8607012129 |

This establishes M as symmetry in higher order corrections in the heterotic dilaton, i.e. non-perturbative contributions to the heterotic string.

Below we list $c_{1,r,s}$. As in the $c_{u,r,s=fixed}$ table the definition (6.66) resums an infinite number of GV invariants to a finite number of $c_{u,r,s}$

| s | $r = 0$ | 1 | 2 | 3 | 4 | 5 | 6 |
|-----|---------|------|--------|--------|--------|--------|------|
| 0 | 480 | 480 | | | | | |
| 1 | 480 | 480 | | | | | |
| 2 | | 2400 | 2400 | | | | |
| 3 | | 3360 | 31200 | 31200 | 3360 | | |
| 4 | | 4320 | 124320 | 576480 | 576480 | 124320 | 4320 |

Let us give a simple example how the triality symmetry (6.65) can actually be used to fix the Gromov–Witten invariants in some classes completely. We consider a non-compact Calabi–Yau $\mathcal{O}(-2, -2) \rightarrow \mathbb{P}^1 \times \mathbb{P}^1$ which emerges in the limit of large elliptic fiber $t_1 \rightarrow \infty$. This model can be solved by various methods, e.g. local mirror symmetry, localization or the Chern-Simons dual. We can solve the genus zero sector much more efficiently from the STU triality. From (6.67) and the wall crossing behaviour the ansatz for $\mathcal{F}^{(0)}$ has to be

$$\mathcal{F}^{(0)}(q_2; q_3) = C_{clas.} - 2\text{Li}_3(q_3) + \sum_{n=1}^{\infty} \frac{q_2^s}{s^3} \frac{P_{0,s}(q_3)}{(1-q_3)^{4s-2}} .$$

Here $P_{0,s} = \sum_{r=0}^{2s-2} c_{s,r} q_3^r$ is a polynomial whose coefficients fulfill $c_{s,r} = c_{s,d-r}$. Moreover, the symmetry W just states that there must be a symmetric ansatz with the same $c_{s,r}$ but $q_2 \leftrightarrow q_3$ exchanged, i.e. $\mathcal{F}^{(0)}(q_2; q_3) = \mathcal{F}^{(0)}(q_3; q_2)$. It is easy to see that this requirement leads to a

linear system of equations for the $c_{s,r}$, which determines them completely. E.g.

| s | $r = 0$ | 1 | 2 | 3 | 4 | 5 |
|-----|---------|-------|---------|----------|-----------|-----------|
| 0 | | | | | | |
| 1 | -2 | | | | | |
| 2 | -2 | -36 | | | | |
| 3 | -2 | -196 | -900 | | | |
| 4 | -2 | -612 | -9702 | -26376 | | |
| 5 | -2 | -1464 | -53806 | -412868 | -852120 | |
| 6 | -2 | -2980 | -210630 | -3321208 | -16716584 | -29303208 |

It is easy to write recursion relations and sum them up to closed formulas. We find e.g. that $c_{r,1} = 2(1-r)(2-2r-2r^2-r^3)$ and more generally that the degree of $c_{r,m}$ in r is $4m$.

6.10.5 Quasi modular properties in the non-perturbative regime

The $\mathcal{F}^{(g)}$ of the STU model admit not only in strict weak coupling limit but also for finite S an expansion in terms of quasi modular forms. We organize the potentials as $\mathcal{F}^{(g)} = \sum_{m,n} \mathcal{F}_{m,n}^{(g)}(q_U =: q) q_U^m q_S^n$. Then we find that

$$\mathcal{F}_{m,n}^{(g)} = \left(\frac{q}{\eta^{24}} \right)^{n+m} P_{g+6(m+n)-1}(E_2, E_4, E_6) =: Y_{m+n} P_{g+6(m+n)-1}(E_2, E_4, E_6).$$

Here P_d is a weighted homogeneous polynomial of the indicated degree, which can be calculated recursively using the modular transformations on the periods. E_2 appears only in the form $X = E_2 E_4 E_6$ and we have, for the first few $\mathcal{F}_{m,n}^{(g)} = \mathcal{F}_{n,m}^{(g)}$,

$$\begin{aligned} \mathcal{F}_{1,0}^{(0)} &= -2Y_1 E_4 E_6 \\ \mathcal{F}_{1,1}^{(0)} &= -Y_2 E_4 E_6 \left(\frac{67}{36} E_4^3 + \frac{65}{36} E_6^2 + \frac{1}{3} X \right) \\ \mathcal{F}_{1,2}^{(0)} &= -Y_3 E_4 E_6 \left(\frac{7751}{6912} E_4^6 + \frac{3863}{1152} E_4^3 E_6^2 + \frac{5551}{6912} E_6^4 + \frac{319}{864} X E_4^3 + \frac{281}{864} E_6^2 X + \frac{X^2}{36} \right) \\ \mathcal{F}_{1,3}^{(0)} &= -Y_4 E_4 E_6 \left(\frac{1519183}{26873856} E_4^9 + \frac{30434765}{895752} E_4^6 E_6^2 + \frac{23643511}{895752} E_4^3 E_6^4 + \frac{7040645}{26873856} E_6^6 + \right. \\ &\quad \left. \frac{189871}{746496} E_4^6 X + \frac{245249}{373248} E_4^3 E_6^2 X + \frac{117967}{746496} E_6^4 X + \frac{185}{5184} E_4^3 X^2 + \frac{151}{5184} E_6^2 X^2 + \frac{X^3}{648} \right) \\ \mathcal{F}_{2,2}^{(0)} &= -Y_4 E_4 E_6 \left(\frac{2619935}{1327104} E_4^9 + \frac{51044081}{3981312} E_4^6 E_6^2 + \frac{45565703}{3981312} E_4^3 E_6^4 + \frac{5007275}{3981312} E_6^6 + \right. \\ &\quad \left. \frac{260449}{248832} E_4^6 X + \frac{348887}{124416} E_4^3 E_6^2 X + \frac{201265}{248832} E_6^4 X + \frac{151}{864} E_4^3 X^2 + \frac{137}{864} E_6^2 X^2 + \frac{X^3}{108} \right) \end{aligned} \tag{6.68}$$

For the genus one case we obtain

$$\begin{aligned}
\mathcal{F}_{1,0}^{(1)} &= -\frac{1}{6}Y_1X \\
\mathcal{F}_{1,1}^{(1)} &= Y_2 \left(\frac{E_4^3 E_6^2}{72} - \frac{67E_4^3 X}{432} - \frac{65E_6^2 X}{432} - \frac{X^2}{24} \right) \\
\mathcal{F}_{1,2}^{(1)} &= Y_3 \left(\frac{85E_4^6 E_6^2}{3456} + \frac{25E_4^3 E_6^4}{1152} - \frac{3991E_4^6 X}{41472} - \right. \\
&\quad \left. \frac{5963E_4^3 E_6^2 X}{20736} - \frac{2803E_6^4 X}{41472} - \frac{7E_4^3 X^2}{144} - \frac{E_6^2 X^2}{24} - \frac{X^3}{216} \right) \\
\mathcal{F}_{1,3}^{(1)} &= Y_4 \left(\frac{146191E_4^9 E_6^2}{5971968} + \frac{169577E_4^6 E_6^4}{2985984} + \frac{99871E_4^3 E_6^6}{5971968} - \frac{5463727E_4^9 X}{107495424} - \right. \\
&\quad \frac{10819933E_4^6 E_6^2 X}{35831808} - \frac{2775229E_4^3 E_6^4 X}{11943936} - \frac{2424725E_6^6 X}{107495424} - \frac{637631E_4^6 X^2}{17915904} - \\
&\quad \left. \frac{794569E_4^3 E_6^2 X^2}{8957952} - \frac{375599E_6^4 X^2}{17915904} - \frac{791E_4^3 X^3}{124416} - \frac{625E_6^2 X^3}{124416} - \frac{5X^4}{15552} \right) \\
\mathcal{F}_{2,2}^{(1)} &= Y_4 \left(\frac{54847E_4^{12}}{995328} + \frac{1542107E_4^9 E_6^2}{995328} + \frac{10956793E_4^6 E_6^4}{2985984} + \frac{3811975E_4^3 E_6^6}{2985984} + \right. \\
&\quad \frac{38969E_6^8}{1492992} - \frac{1309E_4^9 X}{1327104} + \frac{22031E_4^6 E_6^2 X}{1327104} + \frac{67243E_4^3 E_6^4 X}{3981312} - \\
&\quad \frac{385E_6^6 X}{3981312} - \frac{132911E_4^6 X^2}{1492992} - \frac{176713E_4^3 E_6^2 X^2}{746496} - \frac{101183E_4^6 X^2}{1492992} - \\
&\quad \left. \frac{193E_4^3 X^3}{7776} - \frac{173E_6^2 X^3}{7776} - \frac{X^4}{576} \right)
\end{aligned} \tag{6.69}$$

Another remarkable fact is that in the function $\mathcal{F}_1^{(0)}(U, T)$ in $\mathcal{F}^{(0)} = \text{class.} + \sum_k \mathcal{F}_k^{(0)}(U, T)q_S^k$ has also a product type expansion very similar as in (6.2). Following the approach of [101] the authors of [102] derive an expression for $\mathcal{F}_1(U, T)$ which can be written in the following form

$$\mathcal{F}_1(U, T) = 2 \frac{E_4(U)E_6(U)E_4(T)E_6(T)q_U^2 q_T}{(1 - q_T/q_U)^2 (\prod_{k>0} (1 - q_U^k)^{24} (1 - q_T^k)^{24}) \prod_{m,n>0} (1 - q_U^m q_T^n)^{d(nm)}} , \tag{6.70}$$

where $\sum_{n=-1} d(n)q^n = \frac{E_4^3}{\eta^{24}} - q \frac{d}{dq} \frac{E_4 E_6}{\eta^{24}}$. The methods of [101] are not so closely related to the BPS expansion. One reason is that [101] work with the modular invariant dilaton S_{inv} , which is not a flat coordinate. In this coordinate one does not expect an integer BPS expansion. Secondly they search for a modular expression for $\mathcal{F}_k^{(0)}(U, T)$ and not for the BPS degeneracies. However, for $\mathcal{F}_1^{(0)}(U, T)$ both objections are irrelevant, and this might be the reason that $\mathcal{F}_1^{(0)}(U, T)$ can be written in the form (6.70).

6.11 K3 fibration with Enriques fibers

The intersection form on the middle cohomology of K3 is

$$[E_8(-1) \oplus H] \oplus [E_8(-1) \oplus H] \oplus H,$$

where $E_8(-1)$ is the lattice defined by the negative Cartan matrix of E_8 , and H is the even selfdual lattice of signature $(1, 1)$ defined by $H = \begin{pmatrix} 0 & 1 \\ 1 & 0 \end{pmatrix}$. We describe the bilinear form of this even and selfdual lattice by the matrix M_{K3}^{IJ} , $I, J = 1, \dots, 22$. We denote by Σ^I a basis of 2-cycles of the K3 satisfying $\Sigma^I \cdot \Sigma^J = M_{\text{K3}}^{IJ}$, and by η_I a dual basis of 2-forms satisfying $\int_{\Sigma^I} \eta_J = \delta_J^I$. The Enriques involution I_E exchanges the cohomology elements corresponding to the first two factors and acts by a (-1) on the last factor. The invariant and anti-invariant lattices are $L_+ = (E_8(-2) \oplus H(2))$ and $L_- = (E_8(-2) \oplus H(2) \oplus H)$. The dual type II geometry X of the FHSV model [9] is constructed as a free quotient $X = (\text{K3} \times T^2)/\mathbb{Z}_2$ by simultaneously modding out the Enriques involution I_E on the K3 and a \mathbb{Z}_2 action that inverts the T^2 coordinate z . This model has four singular fibres, which are Enriques surfaces and the Euler number is accordingly $\chi(M) = (0 - 4 \cdot 24)/2 + 4 \cdot 12 = 0$. The $(2, 0)$ -form η of the Enriques fiber, as well as $\bar{\eta}$ and further 2-forms $\tilde{\eta}_i = \eta_i - \eta_{i+10}$, $i = 1, \dots, 10$, are in L_- . The cohomology of X is hence constructed as follows: The $(3, 0)$ form is $\Omega = dz \wedge \eta$. Ten $(2, 1)$ -forms are $\Omega_i = \frac{1}{2} dz \wedge \tilde{\eta}_i$, $i = 1, \dots, 10$ and one $(2, 1)$ -form is $\Omega_{11} = d\bar{z} \wedge \eta$. The 11 $(1, 2)$ -forms and the one $(0, 3)$ -form are constructed analogously. It is likewise straightforward to determine the invariant homology in terms of the one of the covering space. With A and B the standard basis of 1-cycles on T^2 we choose the following invariant cycles

$$\begin{aligned} A^i &= A \times (\Sigma^i - \Sigma^{i+10}), & A^{11} &= B \times \Sigma^{21}, & A^0 &= A \times \Sigma^{21} \\ B_i &= B \times M_{ik}(\Sigma^k - \Sigma^{k+10}), & B_{11} &= A \times \Sigma^{22}, & B_0 &= B \times \Sigma^{22}. \end{aligned} \quad (6.71)$$

This choice is different from the one in [4], because we want to go from the homogeneous coordinates $X^i = \int_{A_i} \Omega$ to the inhomogeneous coordinates $t_i = X^i/X^0$, $i = 1, \dots, 11$ so that $\tau = X^{11}/X^0$ is the modulus of the base and proportional to the heterotic dilation S . The intersection matrix is $A^i \cap B_j = 2\delta_j^i$, $A^{11} \cap B_{11} = A^0 \cap B_0 = 1$. The expansion of the $(3, 0)$ -form in terms of α_I, β^I , the cohomology basis dual to A^I and B_I , is $\Omega = X^I \alpha_I - F_I \beta^I$, where $X^I = \int_{A^I} \Omega$ and $F_I = \int_{B_I} \Omega$ are the period integrals. From Griffith transversality $\Omega_I = \partial_I \Omega = k_I \Omega + \chi_I \in H^{3,0} \oplus H^{2,1}$, i.e. $\int_M \Omega \wedge \partial_I \Omega = 0$ ($\int_M \Omega \wedge \partial_I \partial_J \Omega = 0$) with $\partial_I = \frac{\partial}{\partial X^I}$ it follows that $F_I = \partial_I F$ with $F = \frac{1}{2} X^I F_I$ a homogeneous function of degree 2 in X^I . Other direct consequences are $\int_{B_I} \Omega_J = \partial_I \partial_J F$ and $\Omega = Z^I \Omega_I$. With the invariant bases of homology and cohomology above, and the choice of X^0 , we can write down the prepotential for X in inhomogeneous coordinates

$$\mathcal{F} = -\frac{1}{2} t^s M_{ij} t^i t^j - 2(t^s)^2 + t^s, \quad (6.72)$$

where M_{ij} is the matrix of the lattice $E_8(-2) \oplus H(2)$, t^s is the modulus of the base, identified with the heterotic dilation, and t_i , $i = 1, \dots, 10$ are the moduli of the classes in the fiber. This prepotential is compatible with the heterotic weak coupling limit and is indeed not corrected by genus zero instantons as argued in [9] from the self mirror property of the FHSV model and

the fact that the hypermultiplet moduli space metric is uncorrected by world-sheet instantons and is given by the Kähler potential²⁷

$$K = -\log(t^s - \bar{t}^s) - \log M_{ij}(t^i + \bar{t}^i)(t^j + \bar{t}^j) \quad (6.73)$$

Going through the analysis in section 4.4 reveals that the solution to the holomorphic anomaly equation does not contain any q_s, q_i terms. However, this does not mean that all world-sheet instanton contributions vanish. This situation is analogous to the one for the two torus. In this case the holomorphic anomaly equation states $\partial_\tau \bar{\partial}_{\bar{\tau}} \mathcal{F}^{(1)}(\tau, \bar{\tau}) = -\frac{1}{2(\tau - \bar{\tau})^2}$, where the last term is the Poincaré metric on the upper halfplane. This is easily solved to yield $\mathcal{F}^{(1)}(\tau, \bar{\tau}) = -\log(\tau_2 |f(\tau)|)$. Modular invariance now requires f to be a modular form of weight 1 and its behaviour at $\tau = i\infty$ fixes it to be $f = \eta(\tau)^2$.

In the more complicated case at hand Borchers constructs in [103] a modular form of weight 4 for $O_{L_-}(\mathbb{Z})^+$ on $L \otimes \mathbb{R} + iC$, where $L = E_8(-2) \oplus H \subset L_-$ and C is an open positive cone in $L \otimes \mathbb{R}$. This modular form is given by

$$\Phi(y) = e^{2\pi i(\rho, y)} \prod_{r \in \Pi^+} (1 - e^{2\pi i(r, y)})^{(-1)^{(r, \rho' - \rho)} c((r, r)/2)}, \quad (6.74)$$

where $y \in L \otimes \mathbb{C}$ can be thought of as a parametrization of the period domain of the Enriques surface $D^0 = (O \setminus (\bigcup_d H_d)) / O_{L_-}(\mathbb{Z})$, and $O = \{\omega \in \mathbb{P}(L_- \otimes \mathbb{C}) | (\omega, \omega) = 0, (\omega, \bar{\omega}) > 0\}$ is the period domain of the anti-invariant periods. For all d with $(d, d) = -2$ one excludes orthogonal sets $H_d \in O$ and r runs over the positive roots Π^+ of the fake monster Lie superalgebra which consists of nonzero vectors in L_+ of the form (v, n, m) , where $v \in L$ with norm $(r, r) = v^2 + 2nm \geq -2$ and either $m > 0$ or $m = 0$ and $n > 0$. Finally, $\rho = (0, 0, 1)$ and $\rho' = (0, 1, 0)$. Most remarkably, the $c(n)$ are themselves Fourier coefficients of a modular form for $SL(2, \mathbb{Z})$

$$\sum_n c(n) q^n = \frac{\eta(2\tau)^8}{\eta(\tau)^8 \eta(4\tau)^8} = \frac{1}{q} + 8 + 36q + 128q^2 + 402q^3 + \dots \quad (6.75)$$

The modular transformation properties and the discriminant were sufficient for Harvey and Moore to conclude that the gravitational threshold corrections to the heterotic string are [104]

$$\mathcal{F}^{(1)} = \log \left\| \frac{1}{\eta(2t^s)^{24} \Phi(y)} \right\|^2, \quad (6.76)$$

where t^s is the heterotic dilaton. The double norm in this formula has to be read as the inclusion of the metric and Kähler potential dependent terms as in (4.17). These terms get no q_i, q_s corrections and give the classical contributions to $\mathcal{F}^{(1)}$ in the holomorphic limit. Moreover, due to (5.6), $\mathcal{F}^{(1)}$ has the expansion $\mathcal{F}^{(1)} = \sum_Q n_Q^{(1)} \log(1 - q^Q)$, where q^Q can be identified with $e^{2\pi i(r, y)}$ using the identification of the mirror coordinates on K3 surfaces [106], [107]. Due to the product form of (6.74) and taking the holomorphic limit of (6.76) the GV invariants become the coefficients of the modular form (6.75), which explains their integrality. The physical reason

²⁷This simplifications makes it also much easier to find the attractor points for this model [105].

requiring the product form (6.74) seems to be the same as for the product form of $\eta(\tau)$ in the case of the two torus.

We expect that the calculation of the M2-brane moduli space using the Hilbert scheme of points on the fiber, which lead to (6.2) applies with some modifications to the case at hand. This should be checked by calculating the index on the heterotic side using the methods of [82] [67] [77] and taking the limit [108]. It is tempting to make a prediction taking into account that in the expansion of (6.2) only the even degrees in q contribute to the BPS counting on X . We further use that the genus zero GV invariants are zero and have just argued that the genus one GV invariants are given by the expansion of (6.75). With this information we can calculate Θ and find

$$\Theta = \frac{1}{\eta(8\tau)^8 \eta(4\tau)^4} = q^{-3} + \frac{4}{q} + 14q + 40q^3 + 113q^5 + \dots$$

This expansion has only odd powers and hence does not give rise to genus zero invariants. Note moreover that the absence of the constant term is compatible with $\chi(X) = 0$. The GV invariants at genus one are given by the even powers in (6.2) and reproduce (6.75). In addition, we can read off the GV invariants at all genus.

| g | $\frac{[C]^2}{4} = 0$ | 1 | 2 | 3 | 4 | 5 | 6 | 7 | 8 |
|-----|-----------------------|----|-----|------|-------|--------|---------|----------|-----------|
| 0 | 0 | 0 | 0 | 0 | 0 | 0 | 0 | 0 | 0 |
| 1 | 1 | 8 | 36 | 128 | 402 | 1152 | 3064 | 7680 | 18351 |
| 2 | 0 | -8 | -80 | -448 | -1888 | -6720 | -21344 | -62208 | -169216 |
| 3 | 0 | 2 | 68 | 688 | 4280 | 20176 | 79480 | 275904 | 870464 |
| 4 | 0 | 0 | -24 | -544 | -5488 | -36512 | -187088 | -800896 | -3005312 |
| 5 | 0 | 0 | 3 | 228 | 4206 | 42084 | 293274 | 1602704 | 7349936 |
| 6 | 0 | 0 | 0 | -48 | -1952 | -31736 | -314848 | -2270016 | -13057760 |
| 7 | 0 | 0 | 0 | 4 | 536 | 15786 | 235304 | 2316272 | 17140232 |
| 8 | 0 | 0 | 0 | 0 | -80 | -5120 | -123136 | -1721984 | -16834384 |
| 9 | 0 | 0 | 0 | 0 | 5 | 1040 | 44848 | 936968 | 12475573 |
| 10 | 0 | 0 | 0 | 0 | 0 | -120 | -11120 | -371952 | -7002272 |
| 11 | 0 | 0 | 0 | 0 | 0 | 6 | 1788 | 106316 | 2971880 |
| 12 | 0 | 0 | 0 | 0 | 0 | 0 | -168 | -21280 | -945904 |
| 13 | 0 | 0 | 0 | 0 | 0 | 0 | 7 | 2828 | 221898 |

As we argued above the anomaly equation will only carry information about the holomorphic-antiholomorphic mixing, while the holomorphic information has to be fixed essentially from the modular properties. If the monodromies on t^s and t^i do not mix, the factorisation in (6.76) should hold at higher genus and the model would be solved. This will be investigated further in [108].

7 Other applications to dualities

In this section we give two more applications of the techniques and results presented in the previous sections. First, we count BPS states in a type II compactification on a complete intersection Calabi–Yau manifold which admits an elliptic fibration of D_5 type. Second, we extend heterotic type II duality to free toric \mathbb{Z}_2 quotients, and we show how to construct examples of pairs of Calabi–Yau manifolds with non-trivial fundamental group whose reflexive polyhedra are equal, but the corresponding Calabi–Yau spaces are not self-mirror. In both cases, we illustrate that it is now possible to construct very non-trivial complete intersections satisfying a given set of desired properties.

7.1 Counting BPS states on del Pezzo surfaces

We start with a short review of the work [99] which studied the BPS states of exceptional noncritical strings. These noncritical strings appear in a transition which can be seen in different dual pictures as follows. In the heterotic string we consider E_8 instantons of zero size. If we compactify the theory on a circle, we can turn on Wilson lines so as to break E_8 to E_d . E_d instantons are then believed to be identical to E_8 instantons deformed by these Wilson lines. In the context of M-theory, the configuration dual to an E_8 instanton of finite size is an M5-brane approaching the 9-brane at the end of the world. After the instanton has shrunk to zero size, there is a second phase where the 5-brane moves away from the 9-brane world-volume. An M2-brane stretched between the M5-brane and the 9-brane lives as a string in the common six-dimensional space-time. Since the tension for this string is proportional to the distance between the M5-brane and the 9-brane, we get a tensionless string at the transition point between the two phases.

By the duality to F-theory, the six-dimensional theory is obtained by compactifying on a (elliptically and K3-fibered) Calabi–Yau threefold X . The transition from having an E_d instanton of finite size to the M5-brane departing from the 9-brane is locally the same as the transition in the Kähler moduli space of X obtained by a blow-up of the base of the fibration $\mathbb{P}^2 \rightarrow \mathbb{F}_1$. In type IIB language, the tensionless string can be interpreted as a D3-brane wrapping the exceptional curve e which appears after the blow-up [109]. By compactifying the theory on a circle to five dimensions it turns out, however, that the relevant transition is not where the 2-cycle e has shrunk to zero size but where an entire 4-cycle vanishes. This realizes one of the possibilities for singularities in the Kähler moduli space [110].

A shrinking 4-cycle yields an isolated canonical singularity with a crepant blow-up (for details see e.g. [111]). The 4-cycle in this case is a (generalized) del Pezzo surface $S = S_d$ of degree d . These are either a $\mathbb{P}^1 \times \mathbb{P}^1$ or the blow-up $\text{Bl}_{p_1, \dots, p_d} \mathbb{P}^2$ of \mathbb{P}^2 at $d \leq 8$ general points. The rank of the cohomology lattice is $\text{rk } H^{1,1}(S) = d + 1$. If S is embedded into a Calabi–Yau manifold X , however, then the map $H^{1,1}(X) \rightarrow H^{1,1}(S)$ has rank k , $1 \leq k \leq d + 1$. The sublattice of divisors which are orthogonal to the canonical divisor has the important property

that it is isomorphic to the root lattice of E_d .

$$\Lambda_d = \{x \in H^{1,1}(S, \mathbb{Z}) \mid x \cdot c_1(S) = 0\} \cong R_{E_d} \quad (7.1)$$

This induces a natural action of the Weyl group on $H^{1,1}(S)$. Curves of a given degree therefore fall into representations of the Weyl group of E_d . After the 4-cycle is shrunk, the resulting singularity is still characterized by the degree d . The possible singularity types can be realized as follows [112]: For $6 \leq d \leq 8$ they can be represented as hypersurfaces in \mathbb{C}^4 and for $d = 5$ as a complete intersection in \mathbb{C}^5 . For $d \leq 4$ they cannot be represented as a transverse intersection of hypersurfaces.

Finally, the number of BPS states of the exceptional non-critical string in six-dimensions is given by the number of BPS states coming from a single D3-brane wrapping the curve e , in other words the number of such curves. By a mirror symmetry computation, this number is given by certain world-sheet instanton numbers. Due to the properties of the homology lattice of the vanishing 4-cycle, the generating functional for the number of BPS states in the E_8 case is a modular form associated to the root lattice of E_8 .

$$Z_{E_8} = \frac{\Theta_{E_8}}{\Delta^{\frac{1}{2}}} = \frac{1}{2} \sum_{\alpha=2,3,4} \frac{\theta_\alpha^8(\tau)}{q^{-\frac{1}{2}} \eta(\tau)^{12}} = 1 + 252q + 5130q^2 + 54760q^3 + \dots \quad (7.2)$$

In the E_d case, turning on the Wilson line, the E_8 BPS states split into states which form representations of $E_d \times U(1)^{8-d}$.

As shown for the cases $6 \leq d \leq 8$ in [99], one possibility to realize Calabi–Yau manifolds admitting such singularities is to take an elliptic fibration of E_d type over a Hirzebruch surface \mathbb{F}_1 . The reason for using this choice is that we can take the elliptic fiber of S_d to be that of the Calabi–Yau threefold. Here we are going to complete their analysis by providing the toric description of the D_5 case which, as just mentioned, necessarily requires a complete intersection.

We will first determine the Hodge numbers of this complete intersection. Comparing with the E_6 case in [99] we will need one more Kähler class to account for the complete intersection of the fiber, hence $h^{1,1} = 6$. The requirement that the elliptic fiber be of D_5 type yields for the Euler number $\chi(X) = -2c_{D_5} c_1(\mathbb{F}_1)^2 = -128$ (see [113]), and hence $h^{2,1} = 70$.

The simplest way of constructing an elliptic fibration of D_5 type over an \mathbb{F}_1 is to take the polyhedron $\Delta_{\mathbb{F}_1}^* = \langle (-1, -1), (1, 0), (0, -1), (0, 1) \rangle$ of \mathbb{F}_1 and the polyhedron of $\Delta_{\mathbb{P}^3}^* = \langle (-1, -1, -1), (1, 0, 0), (0, 1, 0), (0, 0, 1) \rangle$ of \mathbb{P}^3 (the ambient space of the D_5 type elliptic curve), and combine them to $\{(\Delta_{\mathbb{F}_1}^*, -1, -1, -1), (0, 0, \Delta_{\mathbb{P}^3}^*)\}$. It can be checked (using PALP [30]) that this polyhedron has the required Hodge numbers. However, since it has eight vertices, five of which correspond to $(\mathbb{C}^*)^5$ rescalings of the ambient toric variety, we see that only three of the six Kähler moduli will be realized torically. In order to get six toric Kähler moduli we need to deform the above polyhedron by adding three more vertices. The deformation which has the desired properties is given in the following table, in which we have collected most of the toric

data in the same way as in (3.12):

$$\begin{array}{cccccccc|cccccc}
D_{0,1} & 1 & 0 & 0 & 0 & 0 & 0 & 0 & f_1 & \sigma_1 & c_1 & c_2 & c_3 & c_4 & & \\
D_{0,2} & 0 & 1 & 0 & 0 & 0 & 0 & 0 & 0 & 0 & 0 & -2 & 0 & 0 & & \\
D_1 & 0 & 1 & -1 & -1 & -1 & -1 & -1 & 0 & 1 & 0 & 0 & 0 & 0 & L_1 & \\
D_2 & 0 & 1 & 1 & 0 & -1 & -1 & -1 & 0 & 1 & 0 & 0 & 0 & 0 & L_1 & \\
D_3 & 0 & 1 & 0 & -1 & -1 & -1 & -1 & 1 & -1 & 0 & 0 & 0 & 0 & S_1 & \\
D_4 & 0 & 1 & 0 & 1 & -1 & -1 & -1 & 1 & 0 & 0 & 0 & 0 & 0 & S_2 & \\
D_5 & 0 & 1 & 0 & 0 & -1 & -1 & -1 & -2 & -1 & 1 & 0 & 0 & 0 & F_1 & \\
D_6 & 0 & 1 & 0 & 0 & -1 & 1 & -1 & 0 & 0 & -1 & 1 & 0 & 0 & F_2 & \\
D_7 & 0 & 1 & 0 & 0 & 1 & 1 & -1 & 0 & 0 & 0 & -1 & 1 & 0 & F_3 & \\
D_8 & 0 & 1 & 0 & 0 & 1 & -1 & 1 & 0 & 0 & 0 & 0 & 1 & -1 & F_4 & \\
D_9 & 0 & 1 & 0 & 0 & 1 & 0 & 0 & 0 & 0 & 0 & 2 & -2 & 1 & D_9 & \\
D_{10} & 1 & 0 & 0 & 0 & 0 & 1 & 0 & 0 & 0 & 2 & 0 & 0 & -1 & D_{10} & \\
D_{11} & 1 & 0 & 0 & 0 & 0 & 0 & 1 & 0 & 0 & 0 & 0 & 0 & 1 & L_2 &
\end{array} \tag{7.3}$$

The Mori generators on the right-hand side of the vertical line correspond to the triangulation that is relevant for the counting of BPS states, in other words to the phase which contains the 4-cycle S_1 (we will comment on other triangulations below). On the top, we have labeled these by generators by f, \dots, c_4 which will become clear below when we discuss the geometry of this Calabi–Yau manifold. In the same discussion we will relabel the divisors according to their geometric interpretation as indicated on the far right of the table. The generators of $\Delta_{\mathbb{F}_1}^*$ are ν_1^*, \dots, ν_4^* , those of \mathbb{P}^3 are $\nu_5^*, \nu_9^*, \dots, \nu_{11}^*$, and the deformation from the simple polyhedron we started with is given by the vertices ν_6^*, ν_7^* and ν_8^* .

Implicitly encoded in the above toric data is also the Stanley–Reisner ideal

$$\mathcal{I}_{SR} = [D_1 D_2, D_3 D_4, D_5 D_{10}, D_6 D_8, D_6 D_9, D_7 D_8, D_7 D_{11}, D_9 D_{11}] \tag{7.4}$$

from which we can determine the intersection numbers of X . For this purpose we need the basis of divisors dual to the basis of Mori generators

$$\begin{aligned}
J_1 &= D_1 + D_3, & J_3 &= 3D_1 + 2D_3 + D_5, & J_5 &= 3D_1 + 2D_3 + D_5 + D_6 + D_7, \\
J_2 &= D_1, & J_4 &= 3D_1 + 2D_3 + D_5 + D_6, & J_6 &= 3D_1 + 2D_3 + D_5 + D_6 + D_7 - D_8,
\end{aligned} \tag{7.5}$$

and the fact that the Calabi–Yau space X is defined by $4J_3 J_4$. The non-zero intersection numbers $\kappa_{i,j,k} = J_i \cdot J_j \cdot J_k$ are

$$\begin{array}{cccccc}
\kappa_{1,1,3} = 1 & \kappa_{1,1,4} = 2 & \kappa_{1,1,5} = 3 & \kappa_{1,1,6} = 2 & \kappa_{1,2,3} = 1 & \kappa_{1,2,4} = 2 \\
\kappa_{1,2,5} = 3 & \kappa_{1,2,6} = 2 & \kappa_{1,3,3} = 3 & \kappa_{1,3,4} = 6 & \kappa_{1,3,5} = 9 & \kappa_{1,3,6} = 6 \\
\kappa_{1,4,4} = 6 & \kappa_{1,4,5} = 9 & \kappa_{1,4,6} = 6 & \kappa_{1,5,5} = 9 & \kappa_{1,5,6} = 6 & \kappa_{2,3,3} = 2 \\
\kappa_{2,3,4} = 4 & \kappa_{2,3,5} = 6 & \kappa_{2,3,6} = 4 & \kappa_{2,4,4} = 4 & \kappa_{2,4,5} = 6 & \kappa_{2,4,6} = 4 \\
\kappa_{2,5,5} = 6 & \kappa_{2,5,6} = 4 & \kappa_{3,3,3} = 8 & \kappa_{3,3,4} = 16 & \kappa_{3,3,5} = 24 & \kappa_{3,3,6} = 16 \\
\kappa_{3,4,4} = 16 & \kappa_{3,4,5} = 24 & \kappa_{3,4,6} = 16 & \kappa_{3,5,5} = 24 & \kappa_{3,5,6} = 16 & \kappa_{4,4,4} = 16 \\
\kappa_{4,4,5} = 24 & \kappa_{4,4,6} = 16 & \kappa_{4,5,5} = 24 & \kappa_{4,5,6} = 16 & \kappa_{5,5,5} = 24 & \kappa_{5,5,6} = 16
\end{array} \tag{7.6}$$

Finally, the linear forms are

$$\begin{aligned} c_2 \cdot J_1 &= 36, & c_2 \cdot J_2 &= 24, & c_2 \cdot J_3 &= 92, & c_2 \cdot J_4 &= 88, & c_2 \cdot J_5 &= 84, \\ c_2 \cdot J_6 &= 24, & & & & & & & & \end{aligned} \quad (7.7)$$

There are two more phases whose Mori generators are:

$$l^{(1)}, l^{(2)}, l^{(3)}, l^{(4)}, -l^{(6)}, l^{(5)} + l^{(6)}, l^{(1)} + l^{(2)} + l^{(5)} + 2l^{(6)} \quad (7.8)$$

and

$$l^{(1)}, l^{(3)}, l^{(4)}, l^{(5)}, -l^{(5)} - l^{(6)}, l^{(2)} - 2l^{(6)}, l^{(1)} + l^{(2)} + l^{(5)} + 2l^{(6)} \quad (7.9)$$

Note that both of these Mori cones are not simplicial. The first phase is obtained by blowing down the curve $D_8 \cap D_{10} = 32c_4$ and resolving the resulting singularity by blowing up the curve $D_9 \cap D_{11}$. If we then blow down the curve $D_9 \cap D_{10}$ and resolve the resulting singularity by blowing up the curve $D_7 \cap D_{11}$, we get the last phase. All of these curves lie in the Calabi–Yau manifold, hence these phases descend to phases of the Calabi–Yau .

With all these data at hand, we can describe the geometrical interpretation of these divisors and curves. The divisors F_i , $i = 1, 2, 3, 4$ are all Hirzebruch surfaces \mathbb{F}_1 . This can be seen as follows: We claim that $f_1 = F_1 \cdot L_1$ is the class of a fiber of $F_1 = \mathbb{F}_1$, and $\sigma_1 = F_1 \cdot S_1$ is the class of the section of F_1 with self-intersection number -1 . This is consistent with the intersection numbers $f_1 \cdot f_1 = L \cdot L|_{F_1} = L^2 F_1 = 0$, $f_1 \cdot \sigma_1 = L_1 \cdot S_1|_{F_1} = L_1 \cdot S_1 \cdot F_1 = 1$, and $\sigma_1 \cdot \sigma_1 = S_1 \cdot S_1|_{F_1} = S_1^2 F_1 = -1$. Furthermore, the canonical class of F_1 is $K_{F_1} = F_1 \cdot F_1 = -2\sigma_1 - 3f_1$ which is precisely the canonical class of a Hirzebruch surface \mathbb{F}_1 .

We then set $\sigma_2 = F_2 \cdot S_1 = \sigma_1 + c_1$, $f_2 = F_2 \cdot L_1 = f_1 + 2c_1$, $\sigma_3 = F_3 \cdot S_1 = \sigma_1 + c_1 + c_2$, $f_3 = F_3 \cdot L_1 = f_1 + 2c_1 + 2c_2$, $\sigma_4 = F_4 \cdot S_1 = \sigma_1 + c_1 + c_2 + c_3 + 2c_4$ and $f_4 = F_4 \cdot L_1 = f_1 + 2c_1 + 2c_2 + 2c_3 + 4c_4$. We can check that $f_i \cdot f_i = 0$, $\sigma_i \cdot f_i = 1$, $\sigma_i \cdot \sigma_i = -1$, and $K_{F_i} = -2\sigma_i - 3f_i$. Finally, from $c_2 \cdot F_i = -4$ we find that $\chi(F_i) = 4$ and $\chi(\mathcal{O}_{F_i}) = 1$, hence showing that the F_i are \mathbb{F}_1 's for $i = 1, 2, 3$. F_4 is slightly different since $c_2 F_4 = 60$ implies that $\chi(\mathcal{O}_{F_4}) = 1$, but $\chi(F_4) = 36$.

The class of the elliptic fiber is $h = c_1 + 2c_2 + 3c_3 + 2c_4$, and since in particular the intersection number $h \cdot F_1 = 1$, we can identify F_1 as the base of the elliptic fibration.

Next, we consider the divisor S_1 . It is a rational elliptic surface, also known as del Pezzo surface dP_9 . First, from $S_1^3 = 0$ and $c_2 \cdot S_1 = 12$ we see that $\chi(S_1) = 12$ and $\chi(\mathcal{O}_{S_1}) = 1$. From the previous paragraph we already know that e.g. $S_1^2 F_1 \neq 0$, so S_1 is an elliptic surface fibered over $\sigma \cong \mathbb{P}^1$. More precisely, since $S_1 \cdot \sigma < 0$, the curve σ must lie inside S_1 . Furthermore, the negative of elliptic fiber h of X intersects σ as $(-h) \cdot \sigma|_{S_1} = 1$. On the other hand, the canonical class of S_1 is $K_{S_1} = S_1 \cdot S_1 = -h$, and satisfies $K_{S_1}^2 = 0$, as it should for a dP_9 . We conclude that the elliptic fiber of S_1 lies in the class $-h$. In addition, we see that the classes $\sigma_i = F_i \cdot S_1$ also belong to the cohomology of S_1 .

The divisor S_2 is a properly elliptic surface. Its canonical class is $K_{S_2} = S_2 \cdot S_2 = h = -K_{S_1}$, and therefore, obviously $K_{S_2}^2 = 0$. In other words, the class of the elliptic fiber of S_2 is h . The

base of the fibration is $f_1 \cong \mathbb{P}^1$ because $S_2 \cdot f_1 < 0$ tells us that f_1 lies inside S_2 , and $h \cdot f_1|_{S_2} = 1$ tells us that h intersects f_1 once.

Finally, since $L_i^2 \cdot D = 0$ for any divisor D , the divisors L_1 and L_2 are the fibers of two different K3 fibrations.

In order to translate to the notation used in [99], we set

$$J_1 = F, \quad J_2 = D, \quad J_3 = E_1, \quad J_4 = E_2, \quad J_5 = W_1, \quad J_6 = W_2. \quad (7.10)$$

where we have two classes E_1, E_2 instead of only E .

Let d_c be the degree of the curve c in X . In the following tables we list all the non-vanishing instanton numbers in (4.11) $n_{d_f, \dots, d_{c_4}}$ with $d_f = 0$ and $d_{\sigma_1} = 1$ up to order $d = \sum d_i = 21$. In table 2 we have listed the invariants for $(d_f, d_{\sigma_1}, d_{c_1}) = (0, 1, 1)$. The three tables correspond to $d_{c_2} = 1, 2, 3$, respectively. In addition, we also find that $n_{0,1,1,0,0,0} = 1$ and $n_{0,1,1,4,6,4} = 1$. We see that these two invariants together with the three sums of the last columns of table 2 precisely agree with the invariants in table 4 of [99].

| | 0 | 1 | 2 | Σ | | 0 | 1 | 2 | 3 | 4 | Σ | | 2 | 3 | 4 | Σ | |
|---|----|----|----|----------|----|---|----|----|----|----|----------|----|----|----|----|----------|----|
| 0 | 1 | | | 1 | 1 | 1 | | | | | | 3 | 1 | | | 1 | |
| 1 | 10 | 16 | 1 | 27 | 2 | 1 | 16 | 10 | | | 27 | 4 | 10 | 16 | 1 | 27 | |
| 2 | | 1 | 16 | 10 | 27 | 3 | | 16 | 52 | 16 | 84 | 5 | | 1 | 16 | 10 | 27 |
| 3 | | | | 1 | 1 | 4 | | | 10 | 16 | 1 | 27 | 6 | | | 1 | 1 |

Table 2: Decomposition of E_6 reps into the D_5 reps forming the degree (d_{c_3}, d_{c_4}) invariants for $d_{c_2} = 1, 2, 3$, respectively.

Increasing d_{c_1} by one we obtain table 3 containing the invariants for $(d_f, d_{\sigma_1}, d_{c_1}) = (0, 1, 2)$. Again, the sums in the last columns provide a complete agreement with the invariants of the E_6 case in table 5 of [99].

| | 0 | 1 | 2 | 3 | 4 | Σ | | 1 | 2 | 3 | 4 | 5 | Σ | | 2 | 3 | 4 | 5 | 6 | Σ |
|---|---|----|----|----|---|----------|---|----|-----|-----|-----|----|----------|---|----|-----|-----|-----|----|----------|
| 1 | | | | | | | 2 | | | | | | | 4 | 10 | 16 | 1 | | | 27 |
| 2 | 1 | 16 | 10 | | | 27 | 3 | 16 | 52 | 16 | | | 84 | 5 | 52 | 272 | 200 | 16 | | 540 |
| 3 | | 16 | 52 | 16 | | 84 | 4 | 16 | 200 | 272 | 52 | | 540 | 6 | 10 | 272 | 660 | 272 | 10 | 1224 |
| 4 | | | 10 | 16 | 1 | 27 | 5 | | 52 | 272 | 200 | 16 | 540 | 7 | | 16 | 200 | 272 | 52 | 540 |
| 5 | | | | | | | 6 | | | 16 | 52 | 16 | 84 | 8 | | | 1 | 16 | 10 | 27 |

Table 3: Decomposition of E_6 reps into the D_5 reps forming the degree (d_{c_3}, d_{c_4}) invariants for $d_{c_2} = 2, 3, 4$, respectively.

We can also look at doubly wound states, *i.e.* states with $d_{\sigma_1} = 2$. Table 3 contains the invariants for $(d_f, d_{\sigma_1}, d_{c_1}) = (0, 2, 2)$. The vertical sums in the last columns fully agree with the first three invariants of the E_7 case in table 3 of [99].

Similar to the E_8 case in (7.2), we can use the theta function for the D_5 lattice, $\Theta_{D_5}(q) = \frac{1}{2}(\theta_3(q)^5 + \theta_4(q)^5)$, to write down a generating function for some of the numbers of BPS states

| | 0 | 1 | 2 | 3 | 4 | Σ |
|---|----|-----|------|-----|----|----------|
| 1 | | | | | | |
| 2 | -2 | -32 | -20 | | | -54 |
| 3 | | -32 | -100 | -32 | | -164 |
| 4 | | | -20 | -32 | -2 | -54 |
| 5 | | | | | | |

| | 1 | 2 | 3 | 4 | 5 | Σ |
|---|-----|------|------|------|-----|----------|
| 2 | | | | | | |
| 3 | -32 | -100 | -32 | | | -164 |
| 4 | -32 | -360 | -480 | -100 | | -972 |
| 5 | | -100 | -480 | -360 | -32 | -972 |
| 6 | | | -32 | -100 | -32 | -164 |

| | 2 | 3 | 4 | 5 | 6 | Σ |
|---|-----|------|-------|------|------|----------|
| 4 | -20 | -32 | -2 | | | -54 |
| 5 | -32 | -360 | -480 | -100 | | -972 |
| 6 | -20 | -480 | -1112 | -480 | -20 | -2112 |
| 7 | | -32 | -360 | -480 | -100 | -972 |
| 8 | | | -2 | -32 | -20 | -54 |

Table 4: Decomposition of E_6 reps into the D_5 reps forming the degree (d_{c_3}, d_{c_4}) invariants for $d_{c_2} = 2, 3, 4$, respectively.

in the D_5 case

$$Z_{D_5} = \frac{1}{2} \sum_{\alpha=3,4} \frac{\theta_\alpha(q)^5}{q^{-\frac{1}{2}}\eta(q)^{12}} = 1 + 52q + 660q^2 + 5440q^3 + \dots \quad (7.11)$$

If we compare with the instanton expansion, we find $n_{0,1,0,0,0,0} = 1$, $n_{0,1,1,2,3,2} = 52$ (see Table 2), and $n_{0,1,2,4,6,4} = 660$ (see Table 3). In general, one would therefore expect that $Z_{D_5} = \sum_k n_{0,1,k,2k,3k,2k} q^k$. We are unable to check the coefficient of the q^3 term since it appears at total degree 25 but we only computed up to the total degree 21. However, going back to the discussion of curves and divisors of X , we see that the curve $(0, 0, 1, 2, 3, 2) = c_1 + 2c_2 + 3c_3 + 2c_4$ has a direct geometric interpretation: It is the anticanonical divisor $-K_{S_1}$ of the del Pezzo surface S_1 . This is the same curve as $(0, 0, 1)$ in the E_8 case in [99]. The curves contributing to Z_{E_8} , or Z_{D_5} , are always of the form $\sigma - kK_{S_1}$, $k = 0, 1, 2, \dots$, where σ is the exceptional section of the Hirzebruch surface $F_1 = \mathbb{F}_1$. Therefore, we have in general

$$Z_G = \frac{\Theta_G(q)}{q^{-\frac{1}{2}}\eta(q)^{12}} = \sum_k n(\sigma - kK_{S_1}) q^k \quad (7.12)$$

For the instanton numbers with other degrees a similar relation should hold, but with $\Theta_G(q)$ replaced by the full theta function of the root lattice of G , $\Theta_G(q, z)$, cf. e.g. [114].

7.2 Type II/heterotic duality of free quotients

In this section we first present free quotients that are both elliptically and K3 fibered. We also show that there are also hypersurfaces with that property. In Appendix D we give a list of the Hodge numbers of such free quotients, both in codimension one and two.

We computed $\mathcal{F}^{(1)}$ in Appendix A.2 for the $(2,30)$ model. This model was shown to be a free \mathbb{Z}_2 quotient in Section 2.5. The result for $\mathcal{F}^{(1)}$ is that

$$\mathcal{F}^{(1)} \sim \frac{t_2}{2} + \dots \quad (7.13)$$

has a different normalization than (4.17). This holds for any free \mathbb{Z}_2 quotient of a K3 fibration, and is confirmed by the integrality of the instanton expansion. With the identification of the complexified volume of the base $t_2 = 4\pi i S$ with the dilaton S of the dual heterotic string the prepotential of the Type II string on the above fibration is immediately compatible with the one of a perturbative $N = 2$ heterotic string [48]. However, the comparison of $\mathcal{F}^{(1)}$ is not consistent with the analysis of [7] of type II and heterotic string duality in 4d, because the argument in [7] leads to the requirement that $\int_X c_2 J_2 = 24$.

Heterotic–type II duality requires K3 fibered Calabi–Yau threefolds on the type II side. The base of such fibrations is a \mathbb{P}^1 , with homogeneous coordinates $(z_1 : z_2)$. The algebraic \mathbb{Z}_n action on the base can be chosen to be of the form $(z_1, z_2) \mapsto (e^{\frac{2\pi i}{n}} z_1, z_2)$. Over the fixed points the \mathbb{Z}_n action on the K3 must be free otherwise the action on the full Calabi–Yau will not be free. The only free actions on K3 surfaces are \mathbb{Z}_2 involutions which restricts the possible freely acting groups to \mathbb{Z}_2 . Hence, the action on the base is $(z_1, z_2) \mapsto (-z_1, z_2)$. A rather general method to find the heterotic dual is the adiabatic argument of [115]. The double covers of our toric free quotients are very similar to a dual of the STU model, $\mathbb{P}_{1,1,2,8,12}^4$ [24], and everything goes through with the exception that at the end of the argument we get a lattice which is different from $\Gamma^{2,18}$. When we apply the fiberwise duality, then the monodromy-invariant part of the lattice should be the same, up to the \mathbb{Z}_2 quotient. We would expect a splitting of the heterotic fiber T^4 into an invariant T^2 and a variable T^2 , although the splitting is more complicated than in the case of the STU model. The variable T^2 fibered over the \mathbb{P}^1 will give the K3 factor on the heterotic side. Now, note that for the quotient \mathbb{Z}_2 acts on the base \mathbb{P}^1 by -1 on the affine coordinate $\frac{z_1}{z_2}$. Therefore, the K3 factor gets replaced by a fibration of a T^2 over “half” a \mathbb{P}^1 .

Finally, we need to know the effect of this quotient on $\mathcal{F}^{(1),\text{het}}$. It is well-known that there is a term in the 10d low energy effective action of the heterotic string of the form

$$\int d^{10}x \sqrt{-g} e^{-\phi_{10}} (A(R^2 + \text{tr}F^2)^2 + B\zeta(3)t_8 t_8 R^4) \quad (7.14)$$

which comes from string tree-level scattering amplitudes [116]. One term in this expression is of the form $(R^2)^2$. Dimensional reduction on the K3 factor of $\text{K3} \times T^2$ down to six dimensions yields a $N = (1, 0)$ theory with a term in the action of the form

$$\chi_{\text{K3}} \text{Vol}(\text{K3}) \int d^6x \sqrt{-g} e^{-\phi_{10}} R^2 \quad (7.15)$$

Further reduction on the T^2 with radii R_1, R_2 down to four dimensions yields a term of the form

$$24 \text{Vol}(\text{K3}) R_1 R_2 \int d^4x \sqrt{-g} e^{-\phi_{10}} R^2 \quad (7.16)$$

Defining the dilaton as $\text{Re}S = \text{Vol}(\text{K3}) R_1 R_2 e^{-\phi_{10}}$ this term becomes

$$24 \int d^4x S R^2 \quad (7.17)$$

Since this describes a coupling to R^2 it contributes to $\mathcal{F}^{(1),\text{het}}$. In the case of the free \mathbb{Z}_2 quotient, we argued above that the K3 factor gets replaced by “half” a K3. Therefore, we would expect

that the contribution from the R^2 term in the reduction to six dimensions is reduced by a factor of 2. This would then yield a term

$$12 \int d^4x SR^2 \quad (7.18)$$

in four dimensions. This is in agreement with the computation from the type II side (7.13).

Next, we give an example for each of the two types of elliptic fibers which occur for the free \mathbb{Z}_2 quotients that we discussed in Section 2.2. Both of these examples belong to the class of free quotients that are both elliptically and K3 fibered. The fiber of the first example is of E_7 type, i.e. a hypersurface $\mathbb{P}^2(1, 1, 2)[4]$. The simplest model has Hodge numbers (3, 43) and is realized by the polyhedron

$$\begin{array}{cccccc|ccc}
 & & & & & & c^{(1)} & c^{(2)} & c^{(3)} \\
 D_0 & 1 & 0 & 0 & 0 & 0 & -4 & 0 & 0 \\
 D_1 & 1 & 1 & 0 & 0 & 0 & 2 & 0 & 0 \\
 D_2 & 1 & 0 & 1 & 0 & 0 & 1 & -2 & 0 \\
 D_3 & 1 & -1 & 0 & 0 & 0 & 0 & 0 & 0 \\
 D_4 & 1 & -2 & -1 & 0 & 0 & 1 & 0 & -2 \\
 D_5 & 1 & 0 & 0 & 1 & 0 & 0 & 1 & 0 \\
 D_6 & 1 & 0 & 2 & -1 & 0 & 0 & 1 & 0 \\
 D_7 & 1 & 1 & 1 & 1 & 2 & 0 & 0 & 1 \\
 D_8 & 1 & -5 & -3 & -1 & -2 & 0 & 0 & 1
 \end{array} \quad (7.19)$$

where the divisor corresponding to the third point does not intersect the hypersurface. The non-zero intersections numbers are

$$\begin{array}{cccc}
 \kappa_{111} = 4, & \kappa_{112} = 2, & \kappa_{113} = 2, & \kappa_{123} = 1 \\
 c_2 \cdot J_1 = 28, & c_2 \cdot J_2 = 12, & c_2 \cdot J_3 = 12 &
 \end{array} \quad (7.20)$$

The second type of elliptic fiber is a degree (2,2) hypersurface in $\mathbb{P}^1 \times \mathbb{P}^1$. The simplest model has Hodge numbers (4, 36) and is realized by the polyhedron

$$\begin{array}{cccccc|cccc}
 & & & & & & c^{(1)} & c^{(2)} & c^{(3)} & c^{(4)} \\
 D_0 & 1 & 0 & 0 & 0 & 0 & -2 & -2 & 0 & 0 \\
 D_1 & 1 & 1 & 0 & 0 & 0 & 1 & 0 & 0 & 0 \\
 D_2 & 1 & 0 & 1 & 0 & 0 & 0 & 0 & 1 & 0 \\
 D_3 & 1 & -1 & 0 & 0 & 0 & 1 & 0 & 1 & 0 \\
 D_4 & 1 & -2 & -1 & 0 & 0 & 0 & 0 & -2 & 0 \\
 D_5 & 1 & 0 & 0 & 1 & 0 & 0 & 1 & 0 & 0 \\
 D_6 & 1 & 0 & 0 & -1 & 0 & 0 & 1 & 0 & -2 \\
 D_7 & 1 & 1 & 1 & 1 & 2 & 0 & 0 & 0 & 1 \\
 D_8 & 1 & -1 & -1 & -3 & -2 & 0 & 0 & 0 & 1
 \end{array} \quad (7.21)$$

This is a fibration of D_5 type over a Hirzebruch surface \mathbb{F}_1 . The non-zero intersections numbers are

$$\begin{array}{cccc}
 \kappa_{112} = 4, & \kappa_{113} = 2, & \kappa_{122} = 4, & \kappa_{123} = 2 \\
 \kappa_{124} = 2, & \kappa_{134} = 1, & \kappa_{224} = 2, & \kappa_{234} = 1 \\
 c_2 \cdot J_1 = 24, & c_2 \cdot J_2 = 14, & c_2 \cdot J_3 = 12 & c_2 \cdot J_4 = 12
 \end{array} \quad (7.22)$$

A further example stems from a close cousin of the STU models discussed in Section 6.10. It is obtained by replacing the E_8 type fiber by a E_7 type fiber, which can be realized by the hypersurface $\mathbb{P}_{1,1,2,4,8}^4$ [16]. This space has several candidates for a heterotic dual, given e.g. in [52], [117]. In principle, one could use them to explicitly carry out the \mathbb{Z}_2 quotient as indicated above, and study the heterotic dual. There are also many realizations of such free \mathbb{Z}_2 quotients as complete intersections, see Appendix D. There are also free quotients of K3 fibrations which are not elliptically fibered e.g. the (2,30) model and the space X_4 in Appendix B.

In the remainder of this section we want to compare our toric construction of free quotients with another construction which does not refer to a toric ambient space. As we reviewed in Section 6.11 Ferrara, Harvey, Strominger, and Vafa constructed in [9] a Calabi–Yau manifold as follows:

$$X = \frac{\text{K3} \times T^2}{(I_E, -1)} \quad (7.23)$$

where I_E is the Enriques involution. X has $(h^{1,1}, h^{1,2}) = (11, 11)$ and fundamental group $\pi_1(X) = \mathbb{Z}_2$. Its double cover \tilde{X} has $(h^{1,1}, h^{1,2}) = (21, 21)$. X is mirror to itself up to discrete torsion. Due to peculiar properties of the vector and hyper multiplet moduli spaces at tree level, this model has no instanton corrections. This is a local statement and seems not to be affected by the discrete torsion which is a global property.

With the techniques developed in the previous sections and with the package for analyzing lattice polytopes [30], it is possible to construct complete intersection Calabi–Yau spaces in toric varieties with very similar properties. One can find polyhedra Δ_{K3} and Δ_{T^2} and build from them a polyhedron Δ_Y such that

$$Y = \frac{\text{K3} \times T^2}{\sigma} \quad (7.24)$$

where σ is a free involution. Y has $(h^{1,1}, h^{1,2}) = (11, 11)$ and fundamental group $\pi_1(Y) = \mathbb{Z}_2$. Its double cover \tilde{Y} , however, has $(h^{1,1}, h^{1,2}) = (19, 19)$. We find two pairs of polyhedra (Δ_Y, ∇_Y) in five dimensions such that Y and Y^* are both quotients by such free involutions. However, as can be seen from their double covers, or from their intersection rings below, or from the fact that they admit instanton corrections, that they are not self-mirror in the sense that the mirror map is non-trivial. The reason for our failure to construct a toric realization of the FHSV model X is that all nef-partitions of the free quotient models do not respect the factorization $\text{K3} \times T^2$ of the polytopes for the toric ambient spaces.

On the other hand, we do find free quotients of $\text{K3} \times T^2$ polytopes whose nef-partitions respect the factorization, but all of these manifolds have $h^{0,1}(X) = 1$, hence lead to extended supersymmetry in 4d. Their fundamental groups and their Hodge data were already discussed in Section 2.2.

In the following we will give a detailed discussion of some realizations of the Calabi–Yau spaces Y mentioned above. In codimension 2 there are 58 free quotient polyhedra admitting nef-partitions with Hodge numbers $(h^{1,1}, h^{1,2}) = (11, 11)$. For only 4 of those their mirror is also a free quotient and thus contained in this list. We show that two of them are self-mirror

in the sense that the mirror construction by Batyrev and Borisov reviewed in Section 2.1 yields the same nef partition for both Y and Y^* in the same polyhedron, i.e. in terms of (2.5) we have $\Delta = \nabla$ and $\Delta_l = \nabla_l$, $l = 1, 2$. We explicitly present these two polyhedra and some of their properties in the following subsections. The remaining two are ordinary mirror pairs with the additional property that both Y and Y^* are free \mathbb{Z}_2 quotients. All the other spaces have mirrors which are not free quotients. This is the generic situation. As a final remark we want to point out that in contrast to the FHSV model, our two models are self-mirror without turning on discrete torsion. It would be interesting to understand whether it is possible to turn on discrete torsion, and how this affects our picture. Unfortunately, the role of discrete torsion in the mirror symmetry of complete intersections in toric varieties is barely understood, see e.g. [118].

7.2.1 Model E_7

We consider the product of an elliptic curve of E_7 type, i.e. a degree 4 hypersurface E_1 in \mathbb{P}_{112}^2 , with a K3 surface given as a hypersurface Y in $\mathbb{P}_{\Delta_Y^*}$ where the polyhedron Δ_Y^* is

$$\begin{pmatrix} -1 & 0 & 0 & 1 & 1 & -1 & 2 & 1 & 1 & 0 & 0 \\ 1 & 1 & 0 & 0 & -1 & 0 & -1 & 0 & 0 & 0 & 0 \\ -1 & 0 & 1 & 2 & -1 & -1 & 0 & 0 & 1 & -1 & 0 \end{pmatrix} \quad (7.25)$$

The first seven columns denote the vertices of Δ_Y^* . The Picard number of Y is $\rho(Y) = 6$. This K3 surface admits two different elliptic fibrations. The one we are interested in is as follows. The first, third and fifth vertex span the polyhedron for $\mathbb{P}_{1,1,2}^2$ in which we take a degree 4 hypersurface E_2 . Finally, we take a free quotient by a \mathbb{Z}_2 action on the product which yields the following Gorenstein cone

$$\begin{pmatrix} 1 & 0 & 0 & 0 & 1 & 0 & 1 & 1 & 0 & 0 & 1 & 0 & 1 & 0 & 0 & 0 \\ 0 & 1 & 1 & 1 & 0 & 1 & 0 & 0 & 1 & 1 & 0 & 1 & 0 & 1 & 1 & 1 \\ 0 & 0 & 0 & 0 & -2 & 0 & 0 & 2 & 0 & 0 & 0 & 0 & 0 & 0 & 0 & 0 \\ 0 & 0 & -1 & -1 & -2 & -2 & 1 & 0 & 0 & 0 & 1 & 1 & -1 & -1 & 0 & -1 \\ 0 & 0 & -2 & -1 & 0 & -3 & 0 & 0 & 0 & 1 & 1 & 2 & 0 & -1 & 0 & -1 \\ 0 & 0 & -1 & -1 & -1 & -2 & 0 & 1 & 0 & 0 & 1 & 1 & 0 & -1 & 0 & -1 \\ 0 & 0 & -1 & 2 & 0 & 0 & 0 & 0 & 1 & 0 & -1 & -1 & 0 & 0 & -1 & 1 \end{pmatrix} \quad (7.26)$$

The Calabi–Yau space we are interested in is given as a complete intersection in this ambient space. The first two lines determine the partition for the two defining equations of the complete intersection. The resulting Calabi–Yau manifold has Hodge numbers $h^{1,1} = h^{2,1} = 11$. We denote the points of Δ^* by ν_{01}^* , ν_{02}^* , ν_1^* , ν_2^* , \dots , ν_{14}^* and correspondingly the coordinates $x_{01}, x_{02}, x_1, x_2, \dots, x_{14}$ and the divisors $D_i = \{x_i = 0\}$. In these terms, the \mathbb{Z}_2 acts by -1 on the coordinates x_1, x_3, x_5 and x_7 . x_3, x_6 and x_5 form the coordinates of the \mathbb{P}_{112}^2 in which the torus E_1 lives. x_1, x_{10} and x_7 are the coordinates of the \mathbb{P}_{112}^2 in which the elliptic fiber E_2 of the K3 surface lives. Note that the \mathbb{Z}_2 has the same action on both of the $\mathbb{P}_{1,1,2}^2$.

The mirror polyhedron ∇^* is by (2.5)

$$\begin{pmatrix} 1 & 0 & 1 & 1 & 0 & 0 & 1 & 0 & 0 & 1 & 0 & 0 & 1 & 0 & 0 & 0 \\ 0 & 1 & 0 & 0 & 1 & 1 & 0 & 1 & 1 & 0 & 1 & 1 & 0 & 1 & 1 & 1 \\ 0 & 0 & -1 & 2 & 1 & 0 & 0 & -1 & 2 & -1 & 0 & 1 & 1 & 1 & 1 & 0 \\ 0 & 0 & 0 & 0 & -1 & 1 & 0 & -1 & -1 & 0 & -1 & 1 & 0 & -1 & 0 & -1 \\ 0 & 0 & 1 & 3 & 0 & 0 & -1 & 0 & 1 & -1 & 1 & 1 & 1 & 1 & 1 & 0 \\ 0 & 0 & 2 & -4 & 1 & -1 & 0 & 1 & -1 & 2 & -1 & -3 & -2 & -1 & -2 & 1 \\ 0 & 0 & 1 & -1 & 0 & 0 & -1 & 0 & 0 & 0 & 0 & 0 & -1 & 0 & 0 & 0 \end{pmatrix} \quad (7.27)$$

If we denote the points by $\nu_{01}, \nu_{02}, \nu_1, \nu_2, \dots, \nu_{14}$, one can check that this polyhedron is the same as Δ^* , and has the same partition as in (7.26) if we make the following identifications on the vertices ν_1, \dots, ν_{10} and $\nu_1^*, \dots, \nu_{10}^*$

$$\begin{array}{ccccc} \nu_5^* \leftrightarrow \nu_1 & \nu_9^* \leftrightarrow \nu_8 & \nu_7^* \leftrightarrow \nu_4 & \nu_2^* \leftrightarrow \nu_{10} & \nu_1^* \leftrightarrow \nu_6 \\ \nu_{10}^* \leftrightarrow \nu_3 & \nu_6^* \leftrightarrow \nu_5 & \nu_3^* \leftrightarrow \nu_2 & \nu_4^* \leftrightarrow \nu_9 & \nu_8^* \leftrightarrow \nu_7 \end{array} \quad (7.28)$$

The polyhedron Δ^* in (7.26) admits 24 star-triangulations which yield twelve simplicial and twelve non-simplicial Mori cones. The twelve triangulations corresponding to the simplicial Mori cones each have nine generators, seven of which descend to the complete intersection. These triangulations form seven phases. If we combine the linear forms for the Mori basis J_i in to a vector $(c_2 \cdot J_1, \dots, c_2 \cdot J_7)$ then we find

$$\begin{array}{ll} (0, 12, 24, 24, 24, 36, 48) & \text{three times} \\ (0, 12, 12, 24, 24, 24, 24) & \text{twice} \\ (0, 12, 12, 24, 24, 24, 24) & \text{once} \\ (0, 12, 12, 12, 24, 24, 36) & \text{twice} \\ (0, 12, 12, 24, 24, 24, 48) & \text{once} \\ (0, 12, 12, 24, 24, 24, 48) & \text{twice} \\ (0, 12, 12, 12, 24, 24, 24) & \text{once} \end{array} \quad (7.29)$$

If such a vector appears in more than one line, then the corresponding intersection numbers are different.

7.2.2 Model D₅

We consider the product of an elliptic curve of D₅ type, *i.e.* a degree (2, 2) hypersurface E_1 in $\mathbb{P}^1 \times \mathbb{P}^1$, with with a K3 surface given as a hypersurface Y in $\mathbb{P}_{\Delta_Y^*}$ where the polyhedron $\overline{\Delta}_Y^*$ is

$$\begin{pmatrix} 0 & 0 & 1 & 1 & -1 & 0 & 0 & 1 & 1 & 1 & 0 \\ 1 & 0 & 2 & 1 & -1 & 0 & -1 & 1 & 0 & 1 & 0 \\ 0 & 1 & 0 & 1 & 0 & -1 & 0 & -1 & 0 & 0 & 0 \end{pmatrix} \quad (7.30)$$

The first nine columns denote the vertices of $\overline{\Delta}_Y^*$. The Picard number of Y is $\rho(Y) = 6$. This K3 surface admits two different elliptic fibrations. The fiber of the first fibration is given by a hypersurface in the del Pezzo surface dP_2 spanned the vertices 1, 3, 5, 7, and 9. The fiber of the second fibration is given by a hypersurface in another del Pezzo surface dP_2 spanned by

the vertices 2, 4, 5, 6, and 8. We choose the first fibration and call the fiber E_2 . Finally, we take a free quotient by a \mathbb{Z}_2 action on the product which yields the following Gorenstein cone

$$\begin{pmatrix} 1 & 0 & 1 & 0 & 0 & 1 & 1 & 0 & 0 & 1 & 1 & 0 & 0 & 0 & 0 \\ 0 & 1 & 0 & 1 & 1 & 0 & 0 & 1 & 1 & 0 & 0 & 1 & 1 & 1 & 1 \\ 0 & 0 & 0 & 2 & 2 & 0 & 0 & 0 & 0 & 0 & 0 & 0 & -2 & -2 & 0 \\ 0 & 0 & -1 & 1 & 0 & 1 & 0 & 2 & 0 & 0 & -1 & 1 & -1 & 1 & 0 \\ 0 & 0 & 0 & 0 & 0 & 1 & -1 & 0 & 0 & 1 & -1 & 0 & 0 & 0 & 0 \\ 0 & 0 & 0 & 1 & 1 & 1 & 0 & 0 & 0 & 0 & -1 & 0 & 0 & -1 & -1 \\ 0 & 0 & -1 & 1 & 0 & 0 & 0 & 1 & 1 & 0 & 0 & 0 & 0 & 1 & 0 \end{pmatrix} \quad (7.31)$$

The Calabi–Yau space we are interested in is given as a complete intersection in this ambient space. The first two lines determine the partition for the two defining equations of the complete intersection. The resulting Calabi–Yau manifold has Hodge numbers $h^{1,1} = h^{2,1} = 11$. We denote the points of Δ^* by ν_{01}^* , ν_{02}^* , ν_1^* , ν_2^* , \dots , ν_{14}^* and correspondingly the coordinates $x_{01}, x_{02}, x_1, x_2, \dots, x_{14}$ and the divisors $D_i = \{x_i = 0\}$. In these terms, the \mathbb{Z}_2 acts by -1 on the coordinates x_3, x_4, x_5 , and x_{11} . x_4, x_5, x_8 , and x_9 form the coordinates of the $\mathbb{P}^1 \times \mathbb{P}^1$ in which the torus E_1 lives. x_2, x_6, x_7, x_{10} , and x_{12} are the coordinates of the $d\mathbb{P}_2$ in which the elliptic fiber E_2 of the K3 surface lives.

The mirror polyhedron ∇^* is by (2.5)

$$\begin{pmatrix} 1 & 0 & 0 & 1 & 0 & 1 & 0 & 1 & 1 & 1 & 0 & 1 & 1 & 1 & 0 & 1 \\ 0 & 1 & 1 & 0 & 1 & 0 & 1 & 0 & 0 & 0 & 1 & 0 & 0 & 0 & 1 & 0 \\ 0 & 0 & 0 & -1 & -1 & 1 & 0 & 0 & -1 & 0 & 1 & 0 & 0 & 1 & 0 & 0 \\ 0 & 0 & 1 & 0 & -1 & 0 & -1 & 0 & 0 & 0 & 1 & 0 & 0 & 0 & 0 & 0 \\ 0 & 0 & 0 & -1 & 0 & 1 & 0 & 1 & -1 & -1 & 0 & 1 & -1 & 1 & 0 & 0 \\ 0 & 0 & -1 & 2 & 1 & -2 & 1 & 0 & 2 & 0 & -1 & 0 & 0 & -2 & 0 & 0 \\ 0 & 0 & -1 & 1 & 1 & 1 & 1 & 1 & 0 & 1 & -1 & 0 & 0 & 0 & -1 & 1 \end{pmatrix} \quad (7.32)$$

If we denote the points by $\nu_{01}, \nu_{02}, \nu_1, \nu_2, \dots, \nu_{14}$, one can check that this polyhedron is the same as Δ^* , and has the same partition as in (7.31) if we make the following identifications on the vertices ν_1, \dots, ν_{13} and $\nu_1^*, \dots, \nu_{13}^*$

$$\begin{array}{llll} \nu_1^* \leftrightarrow \nu_{13} & \nu_{11}^* \leftrightarrow \nu_7 & \nu_{13}^* \leftrightarrow \nu_{10} & \nu_9^* \leftrightarrow \nu_9 \\ \nu_5^* \leftrightarrow \nu_5 & \nu_8^* \leftrightarrow \nu_1 & \nu_4^* \leftrightarrow \nu_3 & \nu_3^* \leftrightarrow \nu_{11} \\ \nu_{10}^* \leftrightarrow \nu_{12} & \nu_2^* \leftrightarrow \nu_8 & \nu_6^* \leftrightarrow \nu_4 & \nu_7^* \leftrightarrow \nu_2 \\ \nu_{12}^* \leftrightarrow \nu_6 & & & \end{array} \quad (7.33)$$

The polyhedron $\overline{\Delta}^*$ in (7.31) admits 16 star-triangulations which yield eight simplicial and eight non-simplicial Mori cones. The eight triangulations corresponding to the simplicial Mori cones each have nine generators, eight of which descend to the complete intersection. There they form a unique phase. If we combine the linear forms for the Mori basis J_i into a vector $(c_2 \cdot J_1, \dots, c_2 \cdot J_8)$ then we find

$$(0, 12, 12, 12, 12, 12, 24, 36) \quad (7.34)$$

8 Conclusions and Outlook

We have analyzed a number of aspects of string dualities for Calabi–Yau complete intersections in toric varieties. Toric geometry, in spite of its limitations, makes it easy to construct and analyze large numbers of examples and we found, compared to the hypersurface case, surprisingly rich geometries, like new types of K3 fibrations and free quotients with small Hodge numbers, as well as interesting new physical phenomena. We discussed the large redundancy of the construction due to degeneracies in polytopes and nef partitions and it turned out, for example, that the geometry only depends on the degrees of the partitions.

We developed efficient computational tools that combine and extend existing software and demonstrated the feasibility of a systematic analysis of a large number of examples, including the computation of the mirror map and of symplectic invariants for multi-parameter models. Our examples were found either by scanning our list of some $2 \cdot 10^8$ reflexive polyhedra in 5d for manifolds with special properties, like in the discussion of 2-parameter K3 fibrations in section 6, or by targeted engineering of polytopes with certain characteristics, like elliptic fibrations of D_5 type or self-mirror free quotients that were constructed in section 7.

It turned out, however, that given the large number of polyhedra, together with the large number of nef partitions, our methods still are not very efficient. Improvements in efficiency can be achieved if the redundancy in the combinatorial information can be reduced, i.e. if the following problems can be solved. We need a better formula for the generating function of the Hodge numbers, both for computational and conceptual reasons. We found e.g. empirical evidence that the non-intersecting divisors are independent of the triangulation, hence this information should be already contained in the combinatorics of the Gorenstein cones. As we mentioned above one should also find an argument that the geometry only depends on the degrees of the nef partition.

An obvious question is about the completeness of the list of Calabi–Yau families that we present here. An interesting estimate is given by the one parameter models. One can classify them to some extent by classifying fourth order linear differential operators with given number of regular singular points, a monodromy group in $\mathrm{Sp}(4, \mathbb{Z})$ and integral instanton expansion. For three regular singular points the result is that there are 14 such differential equations [119]. Thirteen can be identified directly with the Picard–Fuchs equations of mirrors of smooth hypersurfaces or complete intersections in toric varieties with Picard number one, that appear in our list. The last case can be obtained as one parameter restriction of the mirror of the *STU* model²⁸. If the restriction to three singular points is dropped, one gets more one parameter models, though no classification has been completed. For some of them it is clear by construction that they come from restrictions of multi moduli hypersurfaces or complete intersections in toric varieties [120], but it is an interesting question whether all of them can be reached in this way.

²⁸The first restriction leads to the two parameter deformation space of the mirror of a $(2, 12)$ complete intersection in a blow-up of $\mathbb{P}_{1,1,1,1,1,4,6}^4$ as discussed in appendix E.2. We like to thank C. Doran for an e-mail correspondence regarding this.

The approach via the classification of the monodromy problem is particularly general because it makes no assumptions on the geometrical realization of the deformation space. Since the generalized complex structure families are also special Kähler²⁹, as expected from the $N = 2$ supergravity point of view, one might wonder whether those deformation spaces are also realized by or closely related to the models we represent. Unfortunately, there is no non-trivial example of those generalized deformation spaces known that one could check.

The table 1 of 2-parameter K3 fibrations in section 6.9 gives a hint on the completeness of our list of Calabi–Yau families. Even though this list is far from being complete, a classification of 2-parameter K3 fibrations in toric ambient spaces seems feasible due to the observations made from that table. The K3 fibers must necessarily have 1 parameter. Apart from those mentioned in Section 6.9 there seem to be only a few more in higher codimension, e.g. $\mathbb{P}^5[2, 2, 2]$. Furthermore, it is experimentally observed that there seems to be an upper bound on the Euler number of toric Calabi–Yau threefolds and for elliptic fibrations this is even proven [121] in general. The tools developed for analyzing lattice polytopes [30] can be used to construct further polytopes with the desired properties, although their efficiency has to be improved for this purpose. At any rate, more entries in the list are expected to give more clues for tackling a classification.

By providing the propagators of Kodaira–Spencer gravity we are now able to compute the higher genus Gopakumar–Vafa invariants in all classes and study the truly non-perturbative BPS states of the heterotic string. Beyond genus two this was possible in practice only up the knowledge of a rational function of the mirror maps. These mirror maps $z_i(\underline{t})$ are the natural invariants of the full non-perturbative duality group G in $\mathrm{Sp}(2h^{1,1} + 2, \mathbb{Z})$, like the J -invariant is for $\mathrm{SL}(2, \mathbb{Z})$, and like the J -invariant they have an integral expansion. We found very non-trivial relations between the multi-parameter mirror maps, but in order to fix the rational function one needs additional physical information about the leading order behaviour of the $\mathcal{F}^{(g)}$ at the boundaries in the non-perturbative regime of the heterotic moduli space, which goes beyond the knowledge of the non-perturbative duality symmetries. In some non-compact limits this information is available using large N transitions and the resulting Chern-Simons or matrix model descriptions of the topological string [51, 59, 74]. This information was used, but has in general not fixed the rational functions completely. In the perturbative limit the modular properties and simple models for the D-brane moduli spaces allowed us to fix the all genus information at this boundary component of the moduli space completely. This information is known to be intimately tied to root multiplicities of generalized Kac-Moody superalgebras and the corresponding vertex algebras [82]. The staggering integrality properties of the non-perturbative BPS expansions, confirmed here to higher genus, nourishes the speculations that generalized structures of this type will enable us to understand the non-perturbative heterotic string. However we also saw that these extensions are not uniquely fixed by the perturbative BPS expansion and the quest how to fix the algebraic structure of the non-perturbative completion is open. In this context it was intriguing to see in the STU model that quasi-modular forms appear in the higher $F^{(g)}$, i.e. in higher orders in the type II string coupling, as well as in higher orders of non-perturbative heterotic effects, i.e. in $\exp(2\pi i S)$.

²⁹We are grateful to N. Hitchin for pointing that out to us.

Acknowledgement

It is a pleasure to thank V. Batyrev, J. Bryan, R. Dijkgraaf, G. Moore, Y. Ruan, S. Stieberger, S. Theisen, D. van Straten, E. Verlinde, D. Zagier, E. Zaslow for discussions and in particular S. Katz for verifying various higher genus invariants. A. K. thanks the AEI in Golm, the ESI in Vienna and the Aspen Center for physics for hospitality. This work is supported in part by the FWF projects P15553 and P15584.

A Periods, Picard–Fuchs equations, and instanton numbers of the (2,30) model

A.1 The fundamental period for a toric complete intersection Calabi–Yau space

We start our discussion with the construction of the fundamental period ϖ of a toric complete intersection Calabi–Yau manifold. This is a straightforward generalization of the construction for hypersurfaces as is explained in detail e.g. in [19]. Given the cycle $\gamma \subset \mathbb{T}$ defined by $|t_1| = \dots = |t_d| = 1$ and the Laurent polynomials $f_l(t)$ in (2.6), this period integral is

$$\varpi = \int_{\gamma'} \Omega = \frac{1}{(2\pi i)^d} \int_{\gamma} \left(\prod_{l=1}^r \frac{a_{0,l}}{f_l} \right) \frac{dt_1}{t_1} \wedge \dots \wedge \frac{dt_d}{t_d}, \quad (\text{A.1})$$

where γ' is the restriction of γ to X^* . The set A_l of lattice points of ∇_l can be reduced to those points which actually correspond to the complete intersection. Recall that in the hypersurface case one can exclude all interior points of facets of Δ . In the present situation, we have seen that there are even divisors corresponding to vertices that do not intersect X^* , so we can exclude those vertices as well. They can be found after performing a careful analysis of the intersection ring. Using the expansions

$$\frac{a_{0,l}}{f_l} = \frac{1}{1 - \sum_{m \in A_l} a_m (-a_{0,l})^{-1} t^m} = \sum_{K_l=0}^{\infty} \left(\sum_{m \in A_l} a_m (-a_{0,l})^{-1} t^m \right)^{K_l} \quad (\text{A.2})$$

and further expand the expressions $(\dots)^{K_l}$ as

$$-l_{0,l} := K_l = \sum_{m \in A_l} l_m. \quad (\text{A.3})$$

where the powers l_m of the monomials t^m are partitions of K_l . It is clear that the integral in (A.1) gets a non-zero contribution if and only if the vectors

$$l = (l_{0,1}, \dots, l_{0,r}; l_1, \dots, l_s) \quad \text{with} \quad s + r = \sum_{l=1}^r \#A_l \quad \text{and} \quad l_i \in \mathbb{Z}_{\geq 0} \quad (\text{A.4})$$

are relations of $\Gamma(\nabla_l) \cap \overline{N}$, where $\Gamma(\nabla_l) \subset \overline{N}_{\mathbb{R}}$ is the Gorenstein cone of the nef partition $\Pi(\nabla) = \{\nabla_1, \dots, \nabla_r\}$ ($\Gamma(\nabla_l) \cap \overline{N}$ is constructed by the lattice points of $e_l \times A_l \in \overline{N} = \mathbb{Z}^r \oplus N$ ($l = 1, \dots, r$), cf. also Section 2.1). Here is another instance of the fact mentioned in Section 2.1 that we actually need a triangulation $T = T(\Gamma(\Delta^*))$ of the Gorenstein cone to determine a basis for the relations l . Thus we get

$$\varpi_0 = \sum_{l_1, \dots, l_s} \frac{(-l_{0,1})! \dots (-l_{0,r})!}{l_1! \dots l_s!} (-a_{0,1})^{l_{0,1}} \dots (-a_{0,r})^{l_{0,r}} a_1^{l_1} \dots a_s^{l_s}, \quad (\text{A.5})$$

We choose the basis (3.6) for the Mori generators and introduce torus invariant coordinates:

$$z_b = \prod_{l=1}^r a_{0,l} l_{0,l}^{(b)} \prod_{i=1}^s a_i l_i^{(b)}. \quad (\text{A.6})$$

Writing each relation l as $\sum_{a=1}^h n_a l^{(a)}$, we end up with

$$\varpi = \sum_{n_1, \dots, n_h} \left[\frac{\prod_{l=1}^r \left(-\sum_{a=1}^h n_a l_{0,l}^{(a)} \right)!}{\prod_{j=1}^s \left(\sum_{a=1}^h n_a l_j^{(a)} \right)!} \prod_{a=1}^h \left((-1)^{\sum_{l=1}^r l_{0,l}^{(a)}} z_a \right)^{n_a} \right]. \quad (\text{A.7})$$

Note that we have to restrict the sum over the integers n_a to those linear combinations of the relations that are of the form (A.4). With the abbreviation $z_i \frac{d}{dz_i} =: \theta_i$ the set of Picard–Fuchs differential operators is generally given by

$$\mathcal{L}_a = \prod_{l_i^{(a)} > 0} \prod_{j=0}^{l_i^{(a)} - 1} \left(\sum_{b=1}^h l_i^{(b)} \theta_b - j \right) - \prod_{l_i^{(a)} < 0} \prod_{j=0}^{-l_i^{(a)} - 1} \left(\sum_{b=1}^h l_i^{(b)} \theta_b - j \right) z_a \quad (\text{A.8})$$

Once we have determined the fundamental period (A.7) and the Picard–Fuchs operators (A.8), we can determine the Yukawa couplings (4.4) and the mirror map (4.6) in the same way as for toric hypersurfaces. In the next subsection, we explicitly demonstrate this considering as example the (2,30) model introduced and discussed in Sections 2.5 and 3.2.

A.2 Periods, Picard–Fuchs equations, and instanton numbers of the (2,30) model

Let us first calculate explicitly the fundamental period $\varpi(z_1, z_2)$ of the mirror of $X_{(A)}$, the first realization (2.14) of the (2,30) model with nef partition $E_1 = \{\nu_1^*, \nu_3^*, \nu_4^*, \nu_8^*\}$, $E_2 = \{\nu_2^*, \nu_5^*, \nu_6^*, \nu_7^*\}$. The polytopes $\nabla_1 = \langle \{0\}, E_1 \rangle$ and $\nabla_2 = \langle \{0\}, E_2 \rangle$ defined before (2.5) determine the mirror as a complete intersection in terms of the Newton polynomials as in (2.6)

$$\begin{aligned} f_1(t) &= 1 - \sum_{i: \nu_i^* \in E_1} a_i t^{\nu_i^*} = 1 - a_1 t_1 - a_2 t_3 - a_3 t_4 - \frac{a_4}{t_1} = 1 - p_1(t) \\ f_2(t) &= 1 - \sum_{i: \nu_i^* \in E_2} b_i t^{\nu_i^*} = 1 - b_1 t_2 - \frac{b_2}{t_1^2 t_2 t_3 t_4} - b_3 t_1 t_2 t_3 t_5^2 - \frac{b_4}{t_1 t_2 t_3 t_5^2} = 1 - p_2(t). \end{aligned}$$

The relevant points of the ∇_l are $E_l \cup \{0\}$ ($l = 1, 2$). The origin $\{0\}$ contributes as monomial $a_0 t^0 = a_0$ ($b_0 t^0 = b_0$) which gives 1 after rescaling the Newton polynomials. Plugging the basis of relations (3.11) in (A.7) yields for the fundamental period

$$\varpi(z_1, z_2) = \sum_{n_1, n_2 \geq 0} \frac{(4n_1)! (2(n_1 + n_2))!}{(n_1!)^4 (2n_1)! (n_2!)^2} z_1^{n_1} z_2^{n_2}. \quad (\text{A.9})$$

with

$$z_1 = \frac{a_1^2 a_2 a_3 a_4 a_5}{a_{0,1}^4 a_{0,2}^2}, \quad z_2 = \frac{a_6 a_7}{a_{0,2}^2}. \quad (\text{A.10})$$

In this example, the Picard–Fuchs operators (A.8) factorize into $-2\theta_1(2\theta_1 - 1)(\theta_1 + \theta_2)\mathcal{D}_1 = \mathcal{L}_1 - 2\theta_1(2\theta_1 - 1)\theta_1^2\mathcal{L}_2$ and $\mathcal{D}_2 = \mathcal{L}_2$ so that we end up with the two reduced differential operators

$$\begin{aligned} \mathcal{D}_1 &= \theta_1^2(\theta_2 - \theta_1) + (2\theta_1 + 2\theta_2 - 1)(8(4\theta_1 - 1)(4\theta_1 - 3)z_1 - 2\theta_1^2 z_2) \\ \mathcal{D}_2 &= \theta_2^2 - 2(\theta_1 + \theta_2)(2\theta_1 + 2\theta_2 - 1)z_2 \end{aligned} \quad (\text{A.11})$$

annihilating $\varpi(z_1, z_2)$. The solutions can be easily characterized by the topological triple couplings (3.14) and the Mori generators (3.11) of $X_{(A)}$ as discussed in Section 4.3. The first solution is of course $X^0 = \varpi$ given in (A.9). The next two solutions are

$$\begin{aligned} X^1 &= \varpi_1(z_1, z_2) = \frac{\varpi}{2\pi i}(\log(z_1) + \sigma_1) \\ X^2 &= \varpi_2(z_1, z_2) = \frac{\varpi}{2\pi i}(\log(z_2) + \sigma_2) \end{aligned}$$

For the present example, the integral expansion of the instanton contribution (4.11) with respect to (d_1, d_2) yields:

| d_1 | $d_2 = 0$ | 1 | 2 | 3 | 4 | 5 | 6 |
|-------|-----------|------------|-------------|-------------|--------------|-------------|-------------|
| 0 | | 8 | | | | | |
| 1 | 384 | 1088 | 384 | | | | |
| 2 | 4688 | 117088 | 247680 | 117088 | 4688 | | |
| 3 | 146816 | 12092928 | 84309504 | 148640576 | 84309504 | 12092928 | 146816 |
| 4 | 5462064 | 1205851824 | 20072874752 | 86051357872 | 135328662848 | 86051357872 | 20072874752 |

The discriminant of the Picard–Fuchs system has two components

$$\Delta_1 = (1 - a)^2 - b(2 + 2a - b), \quad \Delta_2 = 1 - b, \quad (\text{A.12})$$

where we rescaled $a = 256z_1$ and $b = 4z_2$. We have also calculated the triple intersection couplings and found

$$\begin{aligned} Y_{111} &= 2 \frac{1 + a - b}{a^3 \Delta_1} & Y_{112} &= 2 \frac{1 - a + b}{a^2 b \Delta_1} \\ Y_{122} &= 2 \frac{3 - a + b}{ab \Delta_1 \Delta_2} & Y_{222} &= 2 \frac{1 - a + b(6 + b - a)}{b^2 \Delta_1 \Delta_2^2} \end{aligned} \quad (\text{A.13})$$

We calculate $\mathcal{F}^{(1)}$ [58], [46] with the boundary conditions at infinity $\mathcal{F}^{(1)} \sim \frac{20}{24}t_1 + \frac{12}{24}t_2 + O(q)$ and $\mathcal{F}^{(1)} \sim \frac{1}{12} \log(\Delta_1)$, $\mathcal{F}^{(1)} \sim -\frac{21}{12} \log(\Delta_2)$ at the corresponding discriminants. The integrality of the Gromov–Witten invariants for this choice confirms the different normalization of the classical terms, found in subsection 3.2.2, in $\mathcal{F}^{(1)}$ with respect to the K3 fibration case.

| d_1 | $d_2 = 0$ | 1 | 2 | 3 | 4 | 5 | 6 |
|-------|-----------|-------------|---------------|---------------|----------------|---------------|---------------|
| 0 | | | | | | | |
| 1 | -132 | -704 | -132 | | | | |
| 2 | -1714 | -186112 | -459736 | -186112 | -1714 | | |
| 3 | -166656 | -36828672 | -335463120 | -634764672 | -335463120 | -36828672 | -166656 |
| 4 | -9733904 | -5892361760 | -132167284928 | -647978879168 | -1060524299520 | -647978879168 | -132167284928 |

As we mentioned before the large complex structure variables defined by the polyhedron can differ even for topologically equivalent families. In particular, the Picard–Fuchs equations for the variables $(\tilde{z}_1, \tilde{z}_2)$ defined by (3.40) are formally different from (A.11), namely

$$\begin{aligned}\tilde{\mathcal{D}}_1 &= \tilde{\theta}_1^2(\tilde{\theta}_1 - \tilde{\theta}_2) - 8(4\tilde{\theta}_1 - 3)(4\tilde{\theta}_1 - 1)(2\tilde{\theta}_1 + 2\tilde{\theta}_2 - 1)\tilde{z}_1 \\ \tilde{\mathcal{D}}_2 &= \tilde{\theta}_2^2 - 2(\tilde{\theta}_1 - \tilde{\theta}_2 + 1)(2\tilde{\theta}_1 + 2\tilde{\theta}_2 - 1)\tilde{z}_2.\end{aligned}\tag{A.14}$$

The triple intersections are

$$\begin{aligned}Y_{111} &= 2\frac{1 + \tilde{a}}{\tilde{a}^3\tilde{\Delta}_1}, & Y_{112} &= 2\frac{1 - \tilde{a}}{\tilde{a}^2\tilde{b}\tilde{\Delta}_1} \\ Y_{122} &= 2\frac{1 + \tilde{a}}{\tilde{a}\tilde{b}\tilde{\Delta}_1\tilde{\Delta}_2}, & Y_{222} &= 2\frac{1 - \tilde{a}}{\tilde{b}^2\tilde{\Delta}_1\tilde{\Delta}_2}\end{aligned}\tag{A.15}$$

with

$$\tilde{\Delta}_1 = (1 - \tilde{a})^2 - 4\tilde{a}\tilde{b}, \quad \tilde{\Delta}_2 = 1 + \tilde{b}$$

As the A-models are topologically equivalent we should find a rational transformation of variables preserving the large complex structure limit $(z_1 = 0, z_2 = 0) \mapsto (\tilde{z}_1 = 0, \tilde{z}_2 = 0)$ and identifying (A.11) with (A.14). To find this transformation we make the following ansatz:

$$\frac{\Delta_1(a, b)}{P(a, b)} = \tilde{\Delta}_1(\tilde{a}, \tilde{b}) \quad \text{and} \quad \frac{\Delta_2(a, b)}{P(a, b)} = \tilde{\Delta}_2(\tilde{a}, \tilde{b}),\tag{A.16}$$

where $P(a, b)$ is some rational function and $\tilde{a} = 256\tilde{z}_1$, $\tilde{b} = 4\tilde{z}_2$. Solving for \tilde{a} and \tilde{b} gives:

$$\begin{aligned}\tilde{b} &= \frac{-1 - P + b}{P}, \\ \tilde{a} &= \frac{-4 - 2P + 4b \pm 2\sqrt{4(-1 + b)^2 - P(-3 + a^2 + 2b + b^2 - 2a(1 + b))}}{2P}.\end{aligned}$$

This transformation is rational if and only if we can get rid of the square root. Setting

$$P = -(b - 1)^2\tag{A.17}$$

completes the square in the expression under the square root and we find (for the plus sign in (A.17)):

$$\tilde{a} = \frac{a}{1 - b}, \quad \tilde{b} = \frac{b}{1 - b},\tag{A.18}$$

It is straightforward to check that (A.15) transform by (A.18) into (A.13). Here we used the transformation property that Y_{x_i, x_j, x_k} transforms in $\text{Sym}[(T^*M)^3] \otimes \mathcal{L}^2$, i.e. $Y_{x_i, x_j, x_k} =$

$\frac{l_x}{l_z} \sum_{a,b,c} \frac{\partial z_a}{\partial x_i} \frac{\partial z_b}{\partial x_j} \frac{\partial z_c}{\partial x_k} Y_{z_a, z_b, z_c}$, where l_x, l_z correspond to choices of sections in \mathcal{L}^2 . In our case we have $\frac{\tilde{l}}{l} = \frac{1}{1-b}$.

This phenomenon is not special to complete intersections, it can also occur for hypersurfaces. We list here a few examples of topologically equivalent realizations of well-known hypersurfaces, some of which have made their appearance in Section 6.

$$\begin{aligned} \mathbb{P}^4_{1,2,2,3,4}[12] &\cong \mathbb{P} \begin{pmatrix} 2 & 1 & 1 & 1 & 1 & 0 \\ 1 & 2 & 1 & 1 & 0 & 1 \end{pmatrix} \begin{bmatrix} 6 \\ 6 \end{bmatrix} & (h^{1,1}, h^{2,1}) = (2, 74) \\ \mathbb{P}^4_{1,1,2,2,2}[8] &\cong \mathbb{P} \begin{pmatrix} 1 & 1 & 1 & 0 & 1 & 0 \\ 1 & 1 & 0 & 1 & 0 & 1 \end{pmatrix} \begin{bmatrix} 4 \\ 4 \end{bmatrix} & (h^{1,1}, h^{2,1}) = (2, 86) \\ \mathbb{P}^4_{1,1,2,2,2,6}[12] &\cong \mathbb{P} \begin{pmatrix} 3 & 1 & 1 & 0 & 1 & 0 \\ 3 & 1 & 0 & 1 & 0 & 1 \end{pmatrix} \begin{bmatrix} 6 \\ 6 \end{bmatrix} & (h^{1,1}, h^{2,1}) = (2, 128) \\ \mathbb{P}^4_{1,1,2,8,12}[24] &\cong \mathbb{P} \begin{pmatrix} 6 & 4 & 1 & 0 & 1 & 0 \\ 6 & 4 & 0 & 1 & 0 & 1 \end{pmatrix} \begin{bmatrix} 12 \\ 12 \end{bmatrix} & (h^{1,1}, h^{2,1}) = (3, 243) \end{aligned}$$

In each example, the Mori cones of the two Calabi–Yau threefolds are different. In the first example, the corresponding polyhedra arise from different blowups of the same simplex associated to $\mathbb{P}^4_{1,1,1,1,2}$. In the other examples, the reflexive section \mathbb{P}^3_w of the K3 fiber is extended in two different ways by two additional points yielding the \mathbb{P}^1 base of the K3 fibration. The Picard–Fuchs equations as well as the triple intersections can be mapped onto each other in a similar way as above. For the last example this is shown in detail in Appendix E.1. We observe that in all these examples the number of vertices and points of Δ is the same, while a single vertex is added to the simplex Δ^* .

B A selection of other models

In this section we will present a few more codimension two complete intersection Calabi–Yau manifolds, but without going into so much detail as in the last section. The selection contains manifolds with the next smallest Hodge numbers after (2,30): These are (2,36) and (2,44). The latter is particularly interesting since it has realizations as both a simply connected space and a free \mathbb{Z}_2 quotient.

In Section 3.1 we mentioned that there are nine polyhedra admitting nef-partitions giving

Hodge numbers (2,44). The CICYs obtained from first five polyhedra are

$$X_1(272_{12}, 8_7) \sim \mathbb{P} \left(\begin{array}{cccccc} 2 & 1 & 1 & \mathbf{1} & 1 & 0 & 0 \\ 0 & 1 & 1 & \mathbf{3} & 3 & 2 & 2 \end{array} \right) \left[\begin{array}{c} 4 \\ 6 \end{array} \middle| \begin{array}{c} 2 \\ 6 \end{array} \right] \quad (\text{B.1})$$

$$X_2(294_{13}, 9_8) \sim \mathbb{P} \left(\begin{array}{cccccc} 2 & 1 & 1 & 1 & 1 & 0 & 0 & 0 \\ 0 & 1 & 1 & 1 & \mathbf{3} & 2 & 2 & 0 \\ 0 & 0 & 0 & 0 & 1 & 0 & 0 & 1 \end{array} \right) \left[\begin{array}{c} 4 \\ 4 \\ 0 \end{array} \middle| \begin{array}{c} 2 \\ 6 \\ 2 \end{array} \right] \quad (\text{B.2})$$

$$X_3(298_{16}, 9_8) \sim \mathbb{P} \left(\begin{array}{cccccc} 2 & 1 & 1 & \mathbf{3} & \mathbf{1} & 0 & 0 & 0 \\ 0 & 1 & 1 & \mathbf{3} & \mathbf{3} & 2 & 2 & 0 \\ 0 & 0 & 0 & 1 & \mathbf{0} & 0 & 0 & 1 \end{array} \right) \left[\begin{array}{c} 6 \\ 6 \\ 2 \end{array} \middle| \begin{array}{c} 2 \\ 6 \\ 0 \end{array} \right] \quad (\text{B.3})$$

$$X_4(232_{10}, 9_7) \sim \mathbb{P} \left(\begin{array}{cccccc} 2 & \mathbf{1} & 1 & 1 & 1 & 0 & 0 & 0 \\ 4 & \mathbf{2} & 2 & 2 & 0 & 1 & 1 & 0 \\ 1 & \mathbf{0} & 0 & 0 & 0 & 0 & 0 & 1 \end{array} \right) \left[\begin{array}{c} 4 \\ 8 \\ 2 \end{array} \middle| \begin{array}{c} 2 \\ 4 \\ 0 \end{array} \right] / \mathbb{Z}_2 : 11010100 \quad (\text{B.4})$$

$$X_5(232_{12}, 9_8) \sim \mathbb{P} \left(\begin{array}{cccccc} 2 & 1 & \mathbf{1} & 1 & 1 & 0 & 0 & 0 \\ 2 & 1 & \mathbf{1} & 0 & 0 & 1 & 1 & 0 \\ 1 & 0 & \mathbf{0} & 0 & 0 & 0 & 0 & 1 \end{array} \right) \left[\begin{array}{c} 4 \\ 4 \\ 2 \end{array} \middle| \begin{array}{c} 2 \\ 2 \\ 0 \end{array} \right] / \mathbb{Z}_2 : 11010100 \quad (\text{B.5})$$

The remaining four polytopes yield blow-ups of the ambient spaces of X_1 , X_3 , X_4 and X_5 , respectively. These blow-ups are obtained by adding a vertex $\nu_{bt}^* = -\nu_i^*$, where ν_i^* is the vertex whose weights are in bold face. Only the blow-up of the ambient space of X_3 descends to the complete intersection.

Some of the nine polytopes admit several nef partitions and/or several triangulations. Similar to the (2, 30) example, it turns out that for a given polytope there is only one topologically inequivalent manifold. This justifies the notation in (B.2) to (B.5). A representative will be given below.

X_2 , X_4 , X_5 , as well as the blow-up of X_3 , have reflexive hyperplane sections of codimension one, and hence admit K3 fibrations (or a \mathbb{Z}_2 quotient thereof in the cases of X_4 or X_5). In addition X_3 itself also admits a K3 fibration, which however does not come from a toric morphism in the ambient space. In fact, X_3 and its blow-up are related in the same manner as $X_{(B)}$ and $X_{(C)}$ discussed in Section 2.5.

Two out of the nine polytopes have lattice points which are not vertices. These are related to the ambient spaces of X_4 and its blowup. In fact, there is only one such lattice point, namely $\nu_5^* = \frac{1}{2}(\nu_6^* + \nu_7^*)$. This can be seen by subtracting twice the (redundant) first weight vector from the second one. We included that point to make the K3 fiber of X_4 visible, although it is redundant for the characterization of the polytope. X_4 is thus the same variety as the one given in (3.1). Finally, it turns out that X_4 and X_5 are topologically equivalent, for the same reason as $X_{(A)}$ and $X_{(B)}$ in Section 3.2 were equivalent, cf. also the discussion below (2.19). Note that X_4 and X_5 are free \mathbb{Z}_2 quotients.

We summarize the reduced data for X_1 to X_4 in the same way as we did for $X_{(A)}$ in (3.12),

$$\begin{array}{cccc} \kappa_{111} = 4 & \kappa_{112} = 2 & \kappa_{122} = 0 & \kappa_{222} = 0 \\ c_2 J_1 = 28 & & c_2 J_2 = 12 & \end{array}$$

There are three polyhedra yielding nef-partitions with Hodge numbers $(2,36)$. They all admit two non-unimodular star triangulations. After going through the procedure explained in detail in Section 3.2.3 we can describe the (reduced) data for the first polyhedron as follows

$$\begin{array}{cccccccc|cc} & & & & & & & & c^{(1)} & c^{(2)} \\ D_{0,1} & 1 & 0 & 0 & 0 & 0 & 0 & 0 & -2 & -2 \\ D_{0,2} & 0 & 1 & 0 & 0 & 0 & 0 & 0 & -2 & -2 \\ D_1 & 0 & 1 & 1 & 0 & 0 & 0 & 0 & 0 & 1 \\ D_2 & 0 & 1 & 0 & 1 & 0 & 0 & 0 & -1 & 2 \\ D_3 & 1 & 0 & 0 & 0 & 1 & 0 & 0 & 1 & 0 \\ D_4 & 0 & 1 & 0 & 0 & 0 & 1 & 0 & 1 & 1 \\ D_5 & 1 & 0 & 0 & 1 & 1 & 1 & 2 & 1 & 1 \\ D_6 & 1 & 0 & -1 & -3 & -3 & -4 & -4 & 0 & 1 \\ D_7 & 0 & 1 & 0 & 0 & -1 & -1 & -1 & 2 & -2 \end{array}$$

$$\begin{array}{cccc} \kappa_{111} = 2 & \kappa_{112} = 2 & \kappa_{122} = 2 & \kappa_{222} = 1 \\ c_2 \cdot J_1 = 20 & & c_2 \cdot J_2 = 22 & \end{array}$$

It turns out that all nef-partitions and triangulations yield topologically equivalent complete intersections with identical Mori cones.

C Toric Calabi–Yau spaces with small Picard numbers

In this appendix we compile the Hodge data with $h^{1,1} \leq 3$ that have been obtained for weighted projective spaces and more general toric ambient spaces. The results are complete for hypersurfaces and they are probably (at least almost) complete for codimension 2:

| H:(1, $h^{1,2}$) | weighted projective | toric |
|-------------------|---------------------|-------|
| hypersurfaces: | 101 103 145 149 | 21 |
| codimension 2: | 61 73 79 89 129 | 25 37 |

| H:(2, $h^{1,2}$) | weighted projective | toric |
|-------------------|------------------------------|--|
| hypersurfaces: | 74 86 95 106 122 128 132 272 | 29 38 83 84 90 92 102 116 120 144 |
| codimension 2: | 62 68 (83 84 90) | 30 36 44 50 54 56 58 59 60 64 66 70 72 76 77 78 80 82 100 112 |

| H:(3, $h^{1,2}$) | weighted projective | toric |
|-------------------|---|---|
| hypersurfaces: | 66 69 75 87 99 103 105 123 131 165 195 231 243 | 43 45 51 57 59 63 65 67 71 72 73 76 77 78 79 81 83 84 85 89 91 93 95 107 111 115 119 127 141 |
| codimension 2: | 47 55 61 87 (45 51 57 67 71 77 81 83 89 91 93 111) | 23 24 27 29 31 33 35 37 39 41 42 44 48 49 50 52 53 54 56 58 60 62 64 68 70 80 101 113 |

Complete intersections in products of projective spaces were enumerated completely for arbitrary codimension many years ago [122]. The relevant Hodge data from [123] are

$$\begin{array}{ll}
 \mathbf{65} & 73 \ 89 \ 101 & \text{for } h^{11} = 1, \\
 \mathbf{46} & \mathbf{47} \ 50 \ \mathbf{55} \ 56 \ 58 \ 59 \ 62 \ 64 \ 66 \ 68 \ 72 \ 76 \ 77 \ 83 \ 86 & \text{for } h^{11} = 2, \\
 27 \ 31 \ 33 \ 35 & \mathbf{36} \ 37 \ \mathbf{38} \ 39 \ \mathbf{40} \ 41 \ 43\text{-}45 \ \mathbf{46} \ 47\text{-}61 \ 63 \ 66 \ 69 \ 72 \ 75 & \text{for } h^{11} = 3.
 \end{array}$$

Bold-face numbers are those values of h^{12} that do not occur in the above tables. As a check for the completeness of our results we used the lists that are available at [124] to verify that the missing values indeed require codimension 3 or more. Possible representations of minimal codimension are

$$\mathbb{P}^7[2 \ 2 \ 2 \ 2] \equiv \mathbb{P}(1 \ 1 \ 1 \ 1 \ 1 \ 1 \ 1 \ 1) [2 \ 2 \ 2 \ 2]_{-128}^{1,65}$$

i.e. 4 quartics in \mathbb{P}^7 for the example with Picard number 1, and

$$\begin{array}{lll}
 \mathbb{P}^2 \begin{bmatrix} 2 & 1 & 0 & 0 \\ 1 & 1 & 2 & 2 \end{bmatrix}_{-88}^{2,46}, & \mathbb{P}^2 \begin{bmatrix} 2 & 1 & 0 \\ 1 & 1 & 3 \end{bmatrix}_{-90}^{2,47}, & \mathbb{P}^3 \begin{bmatrix} 2 & 1 & 1 \\ 1 & 2 & 1 \end{bmatrix}_{-106}^{2,55},
 \end{array}$$

$$\begin{array}{llll}
 \mathbb{P}^2 \begin{bmatrix} 2 & 1 & 0 \\ 1 & 1 & 1 \\ 0 & 1 & 2 \end{bmatrix}_{-66}^{3,36}, & \mathbb{P}^2 \begin{bmatrix} 2 & 1 & 0 & 0 \\ 1 & 0 & 1 & 1 \\ 0 & 1 & 2 & 1 \end{bmatrix}_{-70}^{3,38}, & \mathbb{P}^1 \begin{bmatrix} 1 & 1 & 0 \\ 1 & 0 & 2 \\ 1 & 2 & 1 \end{bmatrix}_{-74}^{3,40}, & \mathbb{P}^1 \begin{bmatrix} 1 & 1 & 0 \\ 2 & 0 & 1 \\ 1 & 2 & 1 \end{bmatrix}_{-86}^{3,46}
 \end{array}$$

for $h^{11} = 2$ and $h^{11} = 3$, respectively. The data for codimension 2 weight systems and polytopes can be found at [11].

D Free quotients of elliptic K3 fibrations

In this appendix we present the Hodge data and some polytopes that we found for free \mathbb{Z}_2 quotients of elliptic K3 fibrations. More complete data are collected in [11].

Among all Calabi–Yau hypersurfaces in toric varieties there are 16 polytopes that correspond to free quotients. This can be compatible with a K3 fibration only for \mathbb{Z}_2 quotients because the action on the base \mathbb{P}^1 always has fixed points and the K3 fibers only admit a free \mathbb{Z}_2 action. The well-known example of the free \mathbb{Z}_5 quotient of the quintic has no fibration. The two \mathbb{Z}_3 examples are elliptic. The remaining 13 polytopes have fundamental group \mathbb{Z}_2 and are elliptic and K3 fibrations. The Hodge numbers of these manifolds and of their double covers are

| $h^{11} \ h^{12} \ [\chi]$ | double cover | $h^{11} \ h^{12} \ [\chi]$ | double cover | $h^{11} \ h^{12} \ [\chi]$ | double cover |
|----------------------------|--------------|----------------------------|--------------|----------------------------|--------------|
| 3 43 [-80] | 3 83 [-160] | 4 28 [-48] | 4 52 [-96] | 5 29 [-48] | 7 55 [-96] |
| 3 59 [-112] | 3 115 [-224] | 4 36 [-64] | 4 68 [-128] | | |
| 3 75 [-144] | 4 148 [-288] | 4 44 [-80] | 5 85 [-160] | | |

At codimension 2 we found 72 polytopes with nef partitions and elliptic K3 structure that correspond to a free quotient. In 3 cases the lattice quotient actually corresponds to a \mathbb{Z}_4 quotient, but only the \mathbb{Z}_2 refinement of the lattice is compatible with the nef partition.

| $h^{11} h^{12} [\chi]$ | double cover | $h^{11} h^{12} [\chi]$ | double cover | $h^{11} h^{12} [\chi]$ | double cover |
|------------------------|--------------|------------------------|--------------|------------------------|--------------|
| 3 23 [-40] | 3 43 [-80] | 4 22 [-36] | 5 41 [-72] | 5 25 [-40] | 7 47 [-80] |
| 3 27 [-48] | 3 51 [-96] | 4 24 [-40] | 5 45 [-80] | 5 27 [-44] | 8 52 [-88] |
| 3 29 [-52] | 3 55 [-104] | 4 26 [-44] | 6 50 [-88] | 5 29 [-48] | 6 54 [-96] |
| 3 31 [-56] | 3 59 [-112] | 4 36 [-64] | 6 70 [-128] | 5 33 [-56] | 7 63 [-112] |
| 3 33 [-60] | 4 64 [-120] | 4 42 [-76] | 5 41 [-152] | 5 35 [-60] | 7 67 [-120] |
| 3 39 [-72] | 4 76 [-144] | 4 58 [-108] | 6 114 [-216] | 5 41 [-72] | 8 80 [-144] |
| 6 24 [-36] | 10 46 [-72] | 7 19 [-24] | 11,35 [-48] | 8 14 [-12] | 13 25 [-24] |
| 6 26 [-40] | 9 49 [-80] | | | | |

The hypersurface with Hodge data (3,43) and the complete intersection (4,36) are discussed in Section 7.2.

A surprise in view of the Heterotic-Type II anomaly conditions [125], [117] is the small number of hypermultiplets even for small numbers (like $h^{11} = 3$) of vectors. Some of the corresponding polytopes are

$$\begin{aligned}
& \mathbb{P}_{-40}^{3,23} \left(\begin{array}{cccccccc} 1 & 1 & 1 & 1 & 0 & 0 & 0 & 0 \\ 0 & 0 & 0 & 0 & 1 & 1 & 0 & 0 \\ 0 & 0 & 0 & 0 & 0 & 0 & 1 & 1 \end{array} \right) \left[\begin{array}{c|c} 2 & 2 \\ 2 & 0 \\ 0 & 2 \end{array} \right] / \mathbb{Z}_2 : 11101010 \\
& \mathbb{P}_{-48}^{3,27} (2 \ 2 \ 1 \ 1 \ 1 \ 1) [4|4] / \mathbb{Z}_4 : 022130 \\
& \mathbb{P}_{-52}^{3,29} \left(\begin{array}{cccccc} 2 & 2 & 1 & 0 & 2 & 1 & 0 \\ 0 & 0 & 0 & 1 & 0 & 0 & 1 \end{array} \right) \left[\begin{array}{c|c} 4 & 4 \\ 2 & 0 \end{array} \right] / \mathbb{Z}_2 : 10111000 \\
& \mathbb{P}_{-56}^{3,31} \left(\begin{array}{cccccc} 0 & 2 & 1 & 1 & 0 & 2 & 2 \\ 1 & 1 & 0 & 0 & 1 & 1 & 0 \end{array} \right) \left[\begin{array}{c|c} 4 & 4 \\ 2 & 2 \end{array} \right] / \mathbb{Z}_2 : 1110001 \\
& \mathbb{P}_{-60}^{3,33} \left(\begin{array}{cccccc} 2 & 2 & 1 & 2 & 0 & 1 & 0 & 0 \\ 1 & 1 & 0 & 2 & 1 & 0 & 1 & 0 \\ 0 & 0 & 0 & 1 & 0 & 0 & 0 & 1 \end{array} \right) \left[\begin{array}{c|c} 4 & 4 \\ 4 & 2 \\ 2 & 0 \end{array} \right] / \mathbb{Z}_2 : 10111000 \\
& \mathbb{P}_{-72}^{3,39} \left(\begin{array}{cccccc} 0 & 2 & 1 & 4 & 2 & 2 & 1 & 0 \\ 1 & 1 & 0 & 1 & 0 & 1 & 0 & 0 \\ 0 & 0 & 0 & 1 & 0 & 0 & 0 & 1 \end{array} \right) \left[\begin{array}{c|c} 8 & 4 \\ 2 & 2 \\ 2 & 0 \end{array} \right] / \mathbb{Z}_2 : 11101000 \\
& \mathbb{P}_{-36}^{4,22} \left(\begin{array}{cccccc} 2 & 2 & 1 & 0 & 1 & 2 & 0 & 0 \\ 0 & 0 & 1 & 2 & 1 & 2 & 2 & 0 \\ 0 & 0 & 0 & 1 & 0 & 0 & 0 & 1 \end{array} \right) \left[\begin{array}{c|c} 4 & 4 \\ 4 & 4 \\ 2 & 0 \end{array} \right] / \mathbb{Z}_2 : 01110100 \\
& \mathbb{P}_{-40}^{4,24} \left(\begin{array}{cccccc} 2 & 2 & 1 & 0 & 0 & 2 & 1 & 0 \\ 1 & 1 & 0 & 1 & 1 & 0 & 0 & 0 \\ 0 & 0 & 0 & 1 & 0 & 0 & 0 & 1 \end{array} \right) \left[\begin{array}{c|c} 4 & 4 \\ 2 & 2 \\ 2 & 0 \end{array} \right] / \mathbb{Z}_2 : 10110100 \\
& \mathbb{P}_{-44}^{4,26} \left(\begin{array}{cccccc} 2 & 2 & 1 & 1 & 0 & 0 & 0 & 2 \\ 1 & 1 & 0 & 0 & 0 & 1 & 1 & 0 \\ 0 & 0 & 0 & 0 & 1 & 0 & 0 & 1 \end{array} \right) \left[\begin{array}{c|c} 4 & 4 \\ 2 & 2 \\ 2 & 0 \end{array} \right] / \mathbb{Z}_2 : 01101100
\end{aligned}$$

Note that the second example also has fundamental group \mathbb{Z}_2 since $\mathbb{P}_{221111} [4|4]/\mathbb{Z}_2 : 000110$ is simply connected. Further examples can be found at [11].

E More details on the STU models

E.1 Discriminants and monodromy

We first give the precise relation between the STU models with (12, 12) and (10, 14) instanton embedding. This facilitates the use of the literature, where certain aspects are discussed in one or the other case. The 24 instantons in the gauge bundle on the heterotic K3 are embedded in both cases into the $E_8 \times E_8$ so that this group breaks completely and leads to 3 vector multiplets, apart from the graviphoton, and 243 hypermultiplets, apart from the type II dilaton [52]. On the type II side the symmetric embedding (12, 12) is identified with the elliptic fibration over the Hirzebruch surface \mathbb{F}_0 , while the (10, 14) embedding corresponds to the elliptic fibration over the Hirzebruch surface \mathbb{F}_2 . The latter is realizable as a degree 24 hypersurface in the weighted projective space $\mathbb{P}_{1,1,2,8,12}^4$. The models describe the same complex and symplectic families, but one complex structure deformation (hypermultiplet) is fixed in the second realization [126]. In this case there is a unique K3 fibration, whose base is also the base of the rational fibration \mathbb{F}_2 . Decomposing the Kähler class as $J = \sum_{i=1}^3 \tilde{t}_i J_i$ with J_1 , J_2 , and J_3 the classes of the elliptic fiber, the fiber of \mathbb{F}_2 and the base, respectively, we have

$$\tilde{t}_1 = U, \quad \tilde{t}_2 = T - U, \quad \text{and} \quad \tilde{t}_3 = \tilde{S}. \quad (\text{E.1})$$

The identification of \tilde{t}_1 and \tilde{t}_2 is uniquely defined by the identical perturbative heterotic limit. However $S = \tilde{S} - (T - U)$, which reflects that we have no canonical geometric way of identifying the heterotic dilaton. All topological data including the topological string amplitudes $n_{i,j,k}^{(g)} = \tilde{n}_{i,j+k,k}^{(g)}$ are identified by the coordinate change in the vector multiplet moduli space.

For the (12, 12) and (10, 14) models one gets two conifold discriminants

$$\begin{aligned} \Delta_1 &= [(1-a)^2 - a^2(b+c)]^2 - 4a^4bc, & \tilde{\Delta}_1 &= [(1-\tilde{a})^2 - \tilde{a}^2\tilde{b}]^2 - \tilde{a}^4\tilde{b}^2\tilde{c}, \\ \Delta_2 &= (1-(b+c))^2 - 4bc, & \tilde{\Delta}_2 &= (1-\tilde{b})^2 - \tilde{c}\tilde{b}^2, \\ & & \tilde{\Delta}_s &= 1 - \tilde{c}, \end{aligned} \quad (\text{E.2})$$

but the (10, 14) has in addition an explicit strong coupling discriminant $\tilde{\Delta}_s$. However, it is easily seen that the Yukawa couplings

$$\begin{aligned} Y_{111} &= \frac{8(1-a)}{a^3\Delta_1}, & Y_{112} &= \frac{2((1-a)^2+a^2(b-c))}{a^2b\Delta_1}, & Y_{222} &= \frac{(2a-1)((1-a)^2+(b-c)((1-a)^2+a^2(1-c-3b)))}{2b^2\Delta_1\Delta_2} \\ Y_{122} &= \frac{2(1-a)a}{b\Delta_1}, & Y_{123} &= \frac{(1-a)((1-a)^2-a^2(b+c))}{abc\Delta_1}, & Y_{223} &= \frac{(2a-1)((1-a)^2+(b-c)(b-c)((1-a)^2+a^2(1-c-3b)))}{2bc\Delta_1\Delta_2} \end{aligned} \quad (\text{E.3})$$

transform into each other by

$$\begin{aligned} \tilde{a} &= a \\ \tilde{b} &= b+c \\ \tilde{c} &= \frac{4bc}{(b+c)^2}, \end{aligned} \quad (\text{E.4})$$

without change of the gauge of Ω (vacuum line bundle [57]). This is of course reflected by the transformation of the Picard–Fuchs operators. Here we display the ones for (12, 12)

$$\begin{aligned}\mathcal{L}_1 &= 5 - 36(1 - 2(a - b\partial_b - c\partial_c) + a(1 - a)\partial_a)\partial_a \\ \mathcal{L}_2 &= (1 + c\partial_c)\partial_c - (1 + b\partial_b)\partial_b \\ \mathcal{L}_3 &= a(a\partial_a - 4c\partial_c)\partial_a + 2b(3 + 4c\partial_c + 2b\partial_b - 2a\partial_a)\partial_b + 2(3c + 2(c(c - 1)\partial_c - 1))\partial_c,\end{aligned}\tag{E.5}$$

which under (E.4) transform³⁰ into the ones listed in [5] for $\mathbb{P}_{1,1,2,8,12}^4$ [24]. This situation is the same as the one discussed in Appendix A with the only difference that here we do not need to change the choice of the section of \mathcal{L}^2 .

The transformations (E.4) are useful, because now information that appeared in the literature about the moduli space of either of these models can be connected. One example is that the $\mathbb{P}_{1,1,2,8,12}^4$ [24] realization has an obvious \mathbb{Z}_{24} symmetric point in the moduli space corresponding to the Fermat form of the constraint. This symmetry identifies this point with the Gepner point where an orbifold of an $N = (2, 2)$ minimal tensor product with levels $\vec{k} = (22, 22, 10, 1)$ is conjectured to be the exact σ -model description. By (E.4) it is easily identified in the moduli space of the $E \rightarrow X \rightarrow \mathbb{F}_0$ description, where a \mathbb{Z}_2 subgroup of the \mathbb{Z}_{24} acts as permutation of the \mathbb{P}^1 's. It is known that certain complete intersections with one modulus have no Gepner point. On the other hand, some complete intersections do have Gepner points related to DE nondiagonal invariants [127]. The above analysis shows that hypersurfaces in toric varieties can have Gepner points even if the polynomial cannot be written in weighted projective space. The same argument also applies to the other examples listed at the end of Appendix A. Extending (E.1) we note from instanton numbers and intersection numbers that $\mathcal{F}(t(\tilde{t})) = \mathcal{F}(\tilde{t})$ and from this it follows that $\Pi_{\mathbb{F}_0} = B\Pi_{\mathbb{F}_2}$, where B is a symplectic matrix ($F_0 = X^0(2\mathcal{F} - t^i\partial_i\mathcal{F})$)

$$\begin{aligned}X^0 &= \tilde{X}^0, & F_0 &= \tilde{F}_0, \\ X^1 &= \tilde{X}^1, & F_1 &= \tilde{F}_1, \\ X^2 &= \tilde{X}^2, & F_2 &= \tilde{F}_2 - \tilde{F}_3, \\ X^3 &= \tilde{X}^3 + \tilde{X}^2, & F_3 &= \tilde{F}_3.\end{aligned}\tag{E.6}$$

We will now discuss the monodromies in the large volume base (X, F) of the \mathbb{F}_0 or (12, 12) model. At the principal conifold discriminants Δ_1 and Δ_2 one has

$$C_1 = \begin{pmatrix} 1 & 0 & 0 & 0 & -1 & 0 & 0 & 0 \\ 0 & 1 & 0 & 0 & 0 & 0 & 0 & 0 \\ 0 & 0 & 1 & 0 & 0 & 0 & 0 & 0 \\ 0 & 0 & 0 & 1 & 0 & 0 & 0 & 0 \\ 0 & 0 & 0 & 0 & 1 & 0 & 0 & 0 \\ 0 & 0 & 0 & 0 & 0 & 1 & 0 & 0 \\ 0 & 0 & 0 & 0 & 0 & 0 & 1 & 0 \\ 0 & 0 & 0 & 0 & 0 & 0 & 0 & 1 \end{pmatrix}, \quad C_2 = \begin{pmatrix} 1 & 0 & 0 & 0 & 0 & 0 & 0 & 0 \\ 0 & 1 & 0 & 0 & 0 & -1 & 2 & 2 \\ 0 & 0 & 1 & 0 & 0 & 2 & -4 & -4 \\ 0 & 0 & 0 & 1 & 0 & 2 & -4 & -4 \\ 0 & 0 & 0 & 0 & 1 & 0 & 0 & 0 \\ 0 & 0 & 0 & 0 & 0 & 1 & 0 & 0 \\ 0 & 0 & 0 & 0 & 0 & 0 & 1 & 0 \\ 0 & 0 & 0 & 0 & 0 & 0 & 0 & 1 \end{pmatrix}.\tag{E.7}$$

This follows from the Picard–Lefschetz formula. For the single vanishing cycle ν the monodromy transformation of the cycle γ is given by

$$\gamma \rightarrow \gamma + \langle \gamma, \nu \rangle \nu.$$

³⁰Keeping in mind that the essential information in \mathcal{L}_i is the differential left ideal they span at a generic point in the moduli space.

One establishes e.g. by numerical analytic continuation that $\nu_1 = F_0$ vanishes at Δ_1 and $\nu_2 = F_1 - 2F_2 - 2F_3$ vanishes at Δ_2 .

The transformations (E.4) show that the strong coupling singularity $\tilde{\Delta}_s$ is identified with the \mathbb{Z}_2 singularity $(b - c)^2$ corresponding to the exchange of the two \mathbb{P}^1 classes. This divisor appears in the \mathbb{F}_0 moduli space by blowing up the contact order two point between Δ_2 and $\frac{1}{b+c}$ at $a = 0$. Physically the local expansion of the topological string was identified as the large N dual of Chern-Simons theory on a lens space S^3/\mathbb{Z}_2 . One parameter was identified with the 't Hooft coupling, and the other as the non-trivial Wilson line in $H^1(S^3/\mathbb{Z}_2)$. This theory can be solved exactly by a matrix model [59]. On the other hand, from the space time point of view it is a strong coupling point with an $SU(2)$ $N = 4$ spectrum. Due to conformal invariance, the Weyl reflection is not augmented by shifts and in the large volume basis the monodromy around $(b - c)^2$ generates the $t_2 \leftrightarrow t_3$ exchange

$$W = \begin{pmatrix} 1 & 0 & 0 & 0 & 0 & 0 & 0 & 0 \\ 0 & 1 & 0 & 0 & 0 & 0 & 0 & 0 \\ 0 & 0 & 0 & 1 & 0 & 0 & 0 & 0 \\ 0 & 0 & 1 & 0 & 0 & 0 & 0 & 0 \\ 0 & 0 & 0 & 0 & 1 & 0 & 0 & 0 \\ 0 & 0 & 0 & 0 & 0 & 1 & 0 & 0 \\ 0 & 0 & 0 & 0 & 0 & 0 & 0 & 1 \\ 0 & 0 & 0 & 0 & 0 & 0 & 1 & 0 \end{pmatrix}. \quad (\text{E.8})$$

Other monodromies are given by the $t_i \rightarrow t_i + 1$ shifts from moves around $a, b, c = 0$ and can be read off from the classical intersection data

$$T_1 = \begin{pmatrix} 1 & 0 & 0 & 0 & 0 & 0 & 0 & 0 \\ 1 & 1 & 0 & 0 & 0 & 0 & 0 & 0 \\ 0 & 0 & 1 & 0 & 0 & 0 & 0 & 0 \\ 0 & 0 & 0 & 1 & 0 & 0 & 0 & 0 \\ 9 & 4 & 1 & 1 & 1 & -1 & 0 & 0 \\ -4 & -8 & -2 & -2 & 0 & 1 & 0 & 0 \\ -1 & -2 & 0 & -1 & 0 & 0 & 1 & 0 \\ -1 & -2 & -1 & 0 & 0 & 0 & 0 & 1 \end{pmatrix} \quad T_2 = \begin{pmatrix} 1 & 0 & 0 & 0 & 0 & 0 & 0 & 0 \\ 0 & 1 & 0 & 0 & 0 & 0 & 0 & 0 \\ 1 & 0 & 1 & 0 & 0 & 0 & 0 & 0 \\ 0 & 0 & 0 & 1 & 0 & 0 & 0 & 0 \\ 2 & 0 & 0 & 0 & 1 & 0 & -1 & 0 \\ 0 & -2 & 0 & -1 & 0 & 1 & 0 & 0 \\ 0 & 0 & 0 & 0 & 0 & 0 & 1 & 0 \\ 0 & -1 & 0 & 0 & 0 & 0 & 0 & 1 \end{pmatrix}. \quad (\text{E.9})$$

and $T_3 = WT_2W$.

Around the Gepner point in the \mathbb{F}_2 realization one has a \mathbb{Z}_{24} symmetry. This is reflected by 24 rational solutions of the indicial equations of the Picard–Fuchs equation corresponding to a branching of order 24 in the solutions. One can choose $b_3 = 8$ linearly independent solutions, on which \mathbb{Z}_{24} acts by cyclic exchanges of the branches. Analytic continuation to the large complex structure points is possible due to Barnes integral representation. In contrast to the connecting matrix from the conifolds to infinity, where the non-trivial numbers $\zeta(2) \int_X c_2 J/24$ and $\zeta(3)\chi$ containing the topological data arise from the analogue of the Gauss resummation for the hypergeometric function ${}_2F_1$, the connection matrix from the \mathbb{Z}_{24} point to infinity is integer [75], [128]. A nice open string interpretation of the connection matrix was given in [129], [130]. In particular [130] calculates the matrix for the \mathbb{F}_2 case. Conjugated to the \mathbb{F}_0

basis it is

$$A = \begin{pmatrix} 1 & 0 & 0 & 0 & 1 & 0 & 0 & 0 \\ -1 & 1 & 1 & 1 & -1 & 1 & -2 & -2 \\ 1 & 0 & -2 & -1 & 1 & -2 & 4 & 4 \\ 2 & 0 & -1 & -2 & 2 & -2 & 4 & 4 \\ -2 & 0 & 0 & 0 & -1 & 0 & 0 & 1 \\ 0 & 2 & 1 & 0 & 0 & 1 & 0 & 0 \\ 1 & 0 & -1 & -1 & 1 & -1 & 2 & 3 \\ 0 & 1 & 0 & 0 & 0 & 0 & 1 & 0 \end{pmatrix}. \quad (\text{E.10})$$

The combination $M = T_3 A C A C T_2$

$$M = \begin{pmatrix} 1 & 0 & 0 & 0 & 0 & 0 & 0 & 0 \\ 0 & 1 & 1 & 0 & 0 & 0 & 0 & 0 \\ 0 & 0 & -1 & 0 & 0 & 0 & 0 & 0 \\ 0 & 0 & -2 & 1 & 0 & 0 & 0 & 0 \\ 0 & 0 & 0 & 0 & 1 & 0 & 0 & 0 \\ 0 & 0 & 0 & 0 & 0 & 1 & 0 & 0 \\ 0 & 0 & 1 & 0 & 0 & 1 & -1 & -2 \\ 0 & 0 & 0 & 0 & 0 & 0 & 0 & 1 \end{pmatrix}. \quad (\text{E.11})$$

is identified precisely with the mirror symmetry transformation $T \leftrightarrow U$ of the two torus T^2 of the heterotic string including the shift in the quadratic term, which cancels in $\mathcal{F}_0 = 2\mathcal{F} - t_i \partial_i \mathcal{F}$ and shows up only in $\partial_2 F$ ³¹.

E.2 Restriction to Calabi–Yau families with less moduli

We can consider the restriction $b = c$ in the complex structure moduli space of the mirror of $X = \mathbb{P} \begin{pmatrix} 6 & 4 & 1 & 0 & 1 & 0 \\ 6 & 4 & 0 & 1 & 0 & 1 \end{pmatrix} \begin{bmatrix} 12 \\ 12 \end{bmatrix}$, in other words we identify the classes t_2 and t_3 of the two \mathbb{P}^1 's in (6.56). There is a toric realization of this restriction given by the complete intersection

$$X' = \mathbb{P} \begin{pmatrix} 6 & 4 & 0 & 1 & 1 & 1 & 1 \\ 3 & 2 & 1 & 0 & 0 & 0 & 0 \end{pmatrix} \begin{bmatrix} 2 & 12 \\ 0 & 6 \end{bmatrix} \quad (\text{E.12})$$

This model has the same Hodge numbers as X , $(h^{1,1}, h^{2,1}) = (3, 243)$, but only two of the three Kähler moduli are realized torically, namely the elliptic fiber and the combination of the two \mathbb{P}^1 's. One way to see this is to compare the Mori generators $l^{(a)}$ of X with those of X'

$$\begin{aligned} l'^{(1)} &= l^{(1)} &= (0, -6, 3, 2, 1, 0, 0, 0, 0) \\ l'^{(2)} &= l^{(2)} + l^{(3)} &= (-2, 0, 0, 0, -2, 1, 1, 1, 1). \end{aligned} \quad (\text{E.13})$$

and to compute the intersection ring

$$\begin{aligned} \kappa_{111} &= 8, & \kappa_{112} &= 4, & \kappa_{122} &= 2, & \kappa_{222} &= 0, \\ c_2 J_1 &= 92, & c_2 J_2 &= 48. \end{aligned} \quad (\text{E.14})$$

³¹The fact that the $ACAC$ element leaves the large complex structure limit invariant was already noted in [130].

Another way is to look at the Picard–Fuchs operators in (E.5) and set $b = c$ which yields the same operators as those obtained from (E.13) and (A.8) with $a = 432z_1$ and $b = 4z_2$

$$\begin{aligned}\mathcal{L}_1 &= \theta_1(\theta_1 - 2\theta_2) - 12(6\theta_1 - 1)(6\theta_1 - 5)z_1, \\ \mathcal{L}_2 &= \theta_2^3 - 2(2\theta_2 - 1)(2\theta_2 - \theta_1 - 2)(2\theta_2 - \theta_1 - 1)z_2.\end{aligned}\tag{E.15}$$

and the discriminants in (E.2) reduce to

$$\Delta_1 = (1 - 432z_1)^2 - 2985984z_1^2z_2, \quad \Delta_2 = 1 - 16z_2, \quad \Delta_3 = 1 - 432z_1.\tag{E.16}$$

For the GV invariants we then get a relation of the form (5.14)

$$n_{i,j}^{(g)}(X') = \sum_k n_{i,k,j-k}^{(g)}(X).\tag{E.17}$$

Next, we can consider the sublocus of the complex structure moduli space of the mirror of X' defined by the limit $z_1 \rightarrow 0$, $z_2 \rightarrow \infty$ such that $z_1^2z_2$ remains fixed. We will now argue that there is a toric realization of a singular one-parameter family X'' parameterized by this sublocus. For this purpose, we set $x = z_1^2z_2$ and $y = z_1$, and get $\theta_x = \theta_2$ and $\theta_y = \theta_1 - 2\theta_2$. In these variables, the operators in (E.15) become

$$\begin{aligned}\mathcal{L}_1 &= \theta_y(2\theta_x + \theta_y) - 12y(12\theta_x + 6\theta_y + 5)(12\theta_x + 6\theta_y + 1), \\ \mathcal{L}_2 &= \theta_x^3 - \frac{2x}{y^2}(2\theta_x + 1)\theta_y(\theta_y - 1).\end{aligned}\tag{E.18}$$

With the ansatz $\varpi(z_1, z_2) = \sum_{n=0}^{\infty} a_n(x)y^n$ for the fundamental period of X' , $\varpi(z_1, z_2) = \sum_{n_1, n_2} \frac{(6n_1)!(2n_2)!}{(n_2!)^4(n_1-2n_2)!(2n_1)!(3n_1)!} z_1^{n_1} z_2^{n_2}$ we find

$$\begin{aligned}\theta_x^3 a_0 - 4x(2\theta_x + 1)a_2 + O(y) &= 0 \\ ((2\theta_x + 1)a_1 - 12(12\theta_x + 1)(12\theta_x + 5)a_0)y + \\ + (2(2\theta_x + 2)a_2 - 12(12\theta_x + 7)(12\theta_x + 11)a_1)y^2 + O(y^3) &= 0\end{aligned}\tag{E.19}$$

Multiplying the first of these equations with θ_x , multiplying the order y^2 term with $x(2\theta_x + 1)$ and the order y term with $-12x(12\theta_x + 7)(12\theta_x + 11)$ in the second equation, we can eliminate a_1 and a_2 , and in the limit $y \rightarrow 0$ we find that

$$\mathcal{L} = \theta^4 - 144x(12\theta_x + 1)(12\theta_x + 5)(12\theta_x + 7)(12\theta_x + 11)\tag{E.20}$$

annihilates $a_0(x)$. This is precisely the Picard–Fuchs operator corresponding to the Mori generator

$$l'''^{(1)} = 2l'^{(1)} + l''^{(2)} = (-2, -12, 6, 4, 0, 1, 1, 1, 1),\tag{E.21}$$

which is the Mori generator for the complete intersection $X'' = \mathbb{P}_{1,1,1,1,4,6}^5[2, 12]$. Note that due the two weights having a common factor, $Z'' = \mathbb{P}_{1,1,1,1,4,6}^5$ is singular, and since we do not blow-up the singularity, X'' is a singular Calabi–Yau family. Another way to see this is to look for toric blow-ups $Z' \rightarrow Z''$ such that the polyhedron $\Delta_{Z'}^*$ is reflexive and admits a nef partition. There are two minimal such blow-ups, Z'_1 and Z'_2 , where we added the vertices

$\nu_{7,1}^* = (0, 0, 0, 2, 3)$ and $\nu_{7,2}^* = (0, 0, 0, 1, 2)$, respectively. Z'_1 is exactly the ambient space of the two-parameter family X' in (E.12). (Z'_2 is the ambient space for the complete intersection $\mathbb{P} \left(\begin{smallmatrix} 6 & 4 & 1 & 1 & 1 & 1 & 0 \\ 2 & 1 & 0 & 0 & 0 & 0 & 1 \end{smallmatrix} \right) \left[\begin{smallmatrix} 6 & 8 \\ 2 & 2 \end{smallmatrix} \right]$ with $(h^{1,1}, h^{2,1}) = (1, 149)$.) Since X' intersects $D_{7,1}$, blowing down $D_{7,1}$ will yield a singular manifold X'' .

The fundamental period $a_0(x)$ of X'' is the solution ${}_4F_3(\frac{1}{12}, \frac{5}{12}, \frac{7}{12}, \frac{11}{12}; 1, 1, 1; x)$ of a generalized hypergeometric system, and is the 14th one-parameter system with three regular points and integral monodromy [119]. The discriminant $\Delta = 1 - 2985984x$ follows from (E.20) and agrees with the limit of (E.16). The Gopakumar–Vafa invariants $n_d^{(g)}$ are

| g | $d = 1$ | 2 | 3 | 4 | 5 |
|-----|---------|--------------|-------------------|-------------------------|-------------------------------|
| 0 | 678816 | 137685060720 | 69080128815414048 | 51172489466251340674608 | 46928387692914781844159094240 |
| 1 | 480 | -1191139920 | 1399124442888000 | 8310445299962958677280 | 22083962595341011092128873088 |

The ambiguity f_2 for the genus two invariants can only be fixed up to two integer invariants. Furthermore, due to the complicated nature of the map $X' \rightarrow X''$ there is no simple relation between the $n_d^{(g)}(X'')$ and $n_{i,j}^{(g)}(X')$. If we were able to solve these two problems, we could further constrain the six unknown GV invariants of the STU model in Section 6.10.1.

References

- [1] J. M. Maldacena, G. W. Moore and A. Strominger, *Counting BPS black holes in toroidal type II string theory*, arXiv:hep-th/9903163.
- [2] S. Katz, A. Klemm and C. Vafa, *M-theory, topological strings and spinning black holes*, Adv. Theor. Math. Phys. **3** (1999) 1445 [arXiv:hep-th/9910181].
- [3] H. Ooguri, A. Strominger and C. Vafa, *Black hole attractors and the topological string*, arXiv:hep-th/0405146.
- [4] R. Dijkgraaf, E. Verlinde and M. Vonk, *On the partition sum of the NS five-brane*, arXiv:hep-th/0205281.
- [5] S. Hosono, A. Klemm, S. Theisen and S. T. Yau, *Mirror symmetry, mirror map and applications to Calabi–Yau hypersurfaces*, Commun. Math. Phys. **167** (1995) 301 [arXiv:hep-th/9308122].
- [6] S. Hosono, A. Klemm, S. Theisen and S. T. Yau, *Mirror symmetry, mirror map and applications to complete intersection Calabi–Yau spaces*, Nucl. Phys. B **433** (1995) 501 [arXiv:hep-th/9406055].
- [7] P. S. Aspinwall and J. Louis, *On the Ubiquity of K3 Fibrations in String Duality*, Phys. Lett. **B369** (1996) 233, [arXiv:hep-th/9510234].
- [8] K. Oguiso, *On algebraic Fiber space structures on a Calabi–Yau 3-fold*, Int. J. of Math. **4** (1993) 439.
- [9] S. Ferrara, J. A. Harvey, A. Strominger and C. Vafa, *Second quantized mirror symmetry*, Phys. Lett. **B361** (1995) 59 [arXiv:hep-th/9505162].
- [10] M. Kreuzer, H. Skarke, *All abelian symmetries of Landau–Ginzburg potentials*, Nucl. Phys. **B405** (1993) 305 [arXiv:hep-th/9211047].
- [11] <http://hep.itp.tuwien.ac.at/~kreuzer/CY/hep-th/0410018.html>
- [12] W. Fulton, *Introduction to toric varieties*, Princeton Univ. Press, Princeton (1993).
- [13] T. Oda, *Convex bodies and algebraic geometry*, Springer, Berlin Heidelberg (1988).
- [14] V. I. Danilov, *The geometry of toric varieties*, Russian Math. Survey **33**, n.2 (1978) 97.
- [15] D. Cox, *Recent developments in toric geometry*, AMS Proc. Symp. Pure Math. **62** (1997) 389 [arXiv:alg-geom/9606016].
- [16] D. Cox, *The homogeneous coordinate ring of a toric variety*, J. Alg. Geom. **4** (1995) 17 [arXiv:alg-geom/9210008].
- [17] V. V. Batyrev, *Dual polyhedra and mirror symmetry for Calabi–Yau hypersurfaces in toric varieties*, J. Alg. Geom. **3** (1994) 493 [arXiv:alg-geom/9310003].
- [18] V. V. Batyrev, L. A. Borisov, *On Calabi–Yau complete intersections in toric varieties*, in *Higher-dimensional complex varieties*, (Trento, 1994), 39–65, de Gruyter, Berlin, (1996) [arXiv:alg-geom/9412017].
- [19] D. A. Cox and S. Katz, *Mirror Symmetry And Algebraic Geometry*, Mathematical Surveys and Monographs, **68** (1999), American Mathematical Society, Providence, RI

- [20] V. V. Batyrev, L. A. Borisov, *Mirror duality and string theoretic Hodge numbers*, Invent. Math. **126** (1996) 183 [arXiv:alg-geom/9509009].
- [21] V. I. Danilov, A. G. Khovanskii, *Newton polyhedra and an algorithm for computing Hodge-Deligne numbers*, Math. USSR Izvestiya **29** (1987) 279.
- [22] I. M. Gelfand, M. M. Kapranov, A. V. Zelevinsky, *Discriminants, Resultants, and Multidimensional Determinants*, Birkhäuser, Boston (1994).
- [23] R. P. Stanley, *Enumerative Combinatorics*, Vol. 1, Cambridge Studies in Advanced Mathematics **49**, Cambridge Univ. Press (1997).
- [24] J. Stienstra, *Resonant hypergeometric systems and mirror symmetry*, in *Integrable systems and algebraic geometry*, Proceedings of the 41st Taniguchi symposium, World Scientific, (1998) 412–452 [arXiv:alg-geom/9711002].
- [25] A. R. Mavlyutov, *Semiample hypersurfaces in toric varieties*, Duke Math. J. **101** (2000) 85–116 [arXiv:math.AG/9812163].
- [26] M. Kreuzer, E. Riegler, D. Sahakyan, *Toric complete intersections and weighted projective space*, J. Geom. Phys. **46** (2003) 159–173 [arXiv:math.AG/0103214].
- [27] M. Kreuzer, H. Skarke, *Complete classification of reflexive polyhedra in four dimensions*, Adv. Theor. Math. Phys. **4** (2000) 6 [arXiv:hep-th/0002240].
- [28] M. Kreuzer, H. Skarke, *Reflexive polyhedra, weights and toric Calabi–Yau fibrations*, Rev. Math. Phys. **14** (2002), no. 4, 343–374 [arXiv:math.AG/0001106].
- [29] <http://hep.itp.tuwien.ac.at/~kreuzer/CY.html>
- [30] M. Kreuzer, H. Skarke, *PALP: A package for analyzing lattice polytopes*, Comput. Phys. Comm. **157** (2004), no. 1, 87–106 [arXiv:math.SC/0204356].
- [31] B. A. Ovrut, T. Pantev and R. Reinbacher, *Torus-fibered Calabi–Yau threefolds with non-trivial fundamental group*, JHEP **0305** (2003) 040 [arXiv:hep-th/0212221].
- [32] R. Donagi, B. A. Ovrut, T. Pantev and R. Reinbacher, *$SU(4)$ instantons on Calabi–Yau threefolds with $\mathbb{Z}_2 \times \mathbb{Z}_2$ fundamental group*, JHEP **0401** (2004) 022 [arXiv:hep-th/0307273].
- [33] P. Candelas, E. Derrick and L. Parkes, *Generalized Calabi–Yau manifolds and the mirror of a rigid manifold*, Nucl. Phys. B **407** (1993) 115 [arXiv:hep-th/9304045].
- [34] V. V. Batyrev, L. A. Borisov, *Dual cones and mirror symmetry for generalized Calabi–Yau manifolds*, in *Mirror Symmetry II*, eds. B. Greene, S. T. Yau, Adv. Math. **1** (1997) 71–86 [arXiv:alg-geom/9402002].
- [35] P. Berglund, T. Hübsch, *A generalized construction of mirror manifolds*, Nucl. Phys. **B393** (1993) 377 [arXiv:hep-th/9201014].
- [36] M. Kreuzer, H. Skarke, *Orbifolds with discrete torsion and mirror symmetry*, Phys. Lett. **B357** (1995) 81 [arXiv:hep-th/9505120].
- [37] S. Hosono, B. H. Lian and S. T. Yau, *GKZ generalized hypergeometric systems in mirror symmetry of Calabi–Yau hypersurfaces*, Commun. Math. Phys. **182** (1996) 535 [arXiv:alg-geom/9511001].
- [38] C. Haase and G. M. Ziegler, *On the maximal width of empty lattice simplices*, Europ. J. Combinatorics **21** (2000) 111.

- [39] A. Avram, M. Kreuzer, M. Mandelberg, H. Skarke, *Searching for K3 fibrations*, Nucl. Phys. **B494** (1997) 567 [arXiv:hep-th/9610154].
- [40] M. Kreuzer, H. Skarke, *Calabi–Yau fourfolds and toric fibrations*, J. Geom. Phys. **466** (1997) 1 [arXiv:hep-th/9701175].
- [41] Y. Hu, C. H. Liu and S. T. Yau, *Toric morphisms and fibrations of toric Calabi–Yau hypersurfaces*, Adv. Theor. Math. Phys. **6** (2003) 457 [arXiv:math.ag/0010082].
- [42] G. Ewald, *Combinatorial convexity and algebraic geometry*, GTM 168, Springer (1996).
- [43] A. Klemm, S. Theisen, *Mirror maps and instanton sums for complete intersections in weighted projective space*, Mod. Phys. Lett. **A9** (1994) 1807 [arXiv:hep-th/9304034].
- [44] E. Witten, *Phases of $N=2$ theories in two dimensions*, Nucl. Phys. **B403** (1993) 159 [arXiv:hep-th/9301042].
- [45] C. T. C. Wall, *Classification Problems in Differential Topology. V: On Certain 6-manifolds*, Invent. Math. **1** (1966) 355 – 374, Corrigendum. Ibid. **2** (1967) 306.
- [46] P. Berglund, S. Katz and A. Klemm, *Mirror symmetry and the moduli space for generic hypersurfaces in toric varieties*, Nucl. Phys. B **456** (1995) 153 [arXiv:hep-th/9506091].
- [47] V. V. Batyrev, *On the classification of smooth projective toric varieties*, Tohoku Math. J., II. Ser. **43** (1991) 569 – 585.
- [48] A. Klemm, W. Lerche, P. Mayr, *K3-fibrations and heterotic-type II string duality*, Phys. Lett. **B357** (1995) 313 [arXiv:hep-th/9506112].
- [49] L. J. Billera, P. Filliman, B. Sturmfels, *Constructions and complexity of secondary polytopes*, Adv. in Math. **83** (1990) 155.
- [50] P. S. Aspinwall, B. R. Greene and D. R. Morrison, *The Monomial divisor mirror map*, Internat. Math. Res. Notices **12** (1993), 319–337 [arXiv:alg-geom/9309007].
- [51] M. Aganagic, A. Klemm, M. Marino and C. Vafa, *The topological vertex*, arXiv:hep-th/0305132.
- [52] S. Kachru and C. Vafa, *Exact results for $N=2$ compactifications of heterotic strings*, Nucl. Phys. B **450** (1995) 69 [arXiv:hep-th/9505105].
- [53] S. Katz, *Gromov–Witten, Gopakumar–Vafa, and Donaldson–Thomas invariants of Calabi–Yau threefolds*, arXiv:math.ag/0408266.
- [54] K. Hori, S. Katz, A. Klemm, R. Pandharipande, R. Thomas, C. Vafa, R. Vakil, and E. Zaslow, *Mirror symmetry*, Clay Mathematics Monographs, **1** (2003), American Mathematical Society, Providence, RI.
- [55] E. Witten, *Mirror manifolds and topological field theory*, in *Essays on mirror manifolds*, 120–158, Internat. Press, Hong Kong, (1992) [arXiv:hep-th/9112056].
- [56] S. Barannikov and M. Kontsevich, *Frobenius Manifolds and Formality of Lie Algebras of Polyvector Fields*, Internat. Math. Res. Notices **4** (1998) 201 – 215 [arXiv:alg-geom/9710032].
- [57] M. Bershadsky, S. Cecotti, H. Ooguri and C. Vafa, *Kodaira–Spencer theory of gravity and exact results for quantum string amplitudes*, Commun. Math. Phys. **165** (1994) 311 [arXiv:hep-th/9309140].

- [58] M. Bershadsky, S. Cecotti, H. Ooguri and C. Vafa, *Holomorphic anomalies in topological field theories*, Nucl. Phys. B **405** (1993) 279 [arXiv:hep-th/9302103].
- [59] M. Aganagic, A. Klemm, M. Marino and C. Vafa, *Matrix model as a mirror of Chern-Simons theory*, JHEP **0402** (2004) 010 [arXiv:hep-th/0211098].
- [60] A. Klemm and E. Zaslow, *Local mirror symmetry at higher genus*, in *Winter School on Mirror Symmetry, Vector Bundles and Lagrangian Submanifolds (Cambridge, MA, 1999)*, AMS/IP Stud. Adv. Math. **23** (2001) 183 – 207 [arXiv:hep-th/9906046].
- [61] E. Witten, *Quantum background independence in string theory*, arXiv:hep-th/9306122.
- [62] R. Gopakumar and C. Vafa, *M-theory and topological strings. I*, [arXiv:hep-th/9809187].
- [63] R. Gopakumar and C. Vafa, *M-theory and topological strings. II*, [arXiv:hep-th/9812127].
- [64] V. Kaplunovsky and J. Louis, *On Gauge couplings in string theory*, Nucl. Phys. B **444**, 191 (1995) [arXiv:hep-th/9502077].
- [65] I. Antoniadis, E. Gava, K. S. Narain and T. R. Taylor, *$N=2$ type II heterotic duality and higher derivative F terms*, Nucl. Phys. B **455** (1995) 109 [arXiv:hep-th/9507115].
- [66] C. Faber, R. Pandharipande, *Hodge integrals and Gromov–Witten theory*, Invent. Math. **139** (2000) 173–199 [arXiv:math.AG/9810173].
- [67] R. E. Borcherds, *Automorphic forms with singularities on Grassmannians*, Invent. Math. **132** (1998) 491–562 [arXiv:alg-geom/9609022].
- [68] M. Kontsevich, *Product formulas for modular forms on $O(2,n)$ (after R. Borcherds)* Astérisque **245** (1997), Exp. No. 821, 41–56. [arXiv:alg-geom/9709006].
- [69] T. Kawai and K. Yoshioka, *String Partition function and Infinite Products* [arXiv:hep-th/0002169].
- [70] S. K. Donaldson, R. P. Thomas, *Gauge theory in higher dimensions*, in *The geometric universe*, 31–47, (1998) Oxford Univ. Press.
- [71] R. P. Thomas, *A holomorphic Casson invariant for Calabi–Yau 3-folds, and bundles on $K3$ fibrations*, J. Differ. Geom. **54** (2000) 367–438, [arXiv:math.ag/9806111].
- [72] N. Nekrasov, H. Ooguri and C. Vafa, *S -duality and topological strings*, arXiv:hep-th/0403167.
- [73] D. Maulik, N. Nekrasov, A. Okounkov and R. Pandharipande, *Gromov–Witten theory and Donaldson–Thomas theory I*, [arXiv:math.AG/0312059].
- [74] D. Ghoshal and C. Vafa, *$c = 1$ string as the topological theory of the conifold*, Nucl. Phys. B **453** (1995) 121 [arXiv:hep-th/9506122].
- [75] P. Candelas, X. De La Ossa, A. Font, S. Katz and D. R. Morrison, *Mirror symmetry for two parameter models. I*, Nucl. Phys. B **416** (1994) 481 [arXiv:hep-th/9308083].
- [76] M. Aganagic, M. Marino and C. Vafa, *All loop topological string amplitudes from Chern-Simons theory*, Commun. Math. Phys. **247** (2004) 467 [arXiv:hep-th/0206164].
- [77] M. Marino and G. W. Moore, *Counting higher genus curves in a Calabi–Yau manifold*, Nucl. Phys. B **543** (1999) 592 [arXiv:hep-th/9808131].
- [78] A. Klemm and P. Mayr, *Strong Coupling Singularities and Non-abelian Gauge Symmetries in $N = 2$ String Theory*, Nucl. Phys. B **469** (1996) 37 [arXiv:hep-th/9601014].

- [79] S. Katz, D. R. Morrison and M. Ronen Plesser, *Enhanced Gauge Symmetry in Type II String Theory*, Nucl. Phys. B **477** (1996) 105 [arXiv:hep-th/9601108].
- [80] S. T. Yau and E. Zaslow, *BPS States, String Duality, and Nodal Curves on K3*, Nucl. Phys. B **471** (1996) 503 [arXiv:hep-th/9512121].
- [81] S. Hosono, M. H. Saito, and A. Takahashi, *Holomorphic anomaly equation and BPS state counting of rational elliptic surface*, Adv. Theor. Math. Phys. **3** (1999) 177 – 208 [arXiv:hep-th/9901151].
- [82] J. A. Harvey and G. W. Moore, *Algebras, BPS States, and Strings*, Nucl. Phys. B **463** (1996) 315 [arXiv:hep-th/9510182].
- [83] A. Beauville, *Counting rational curves on K3 surfaces*, Duke Math. J. **97** (1999) 99–108, [arXiv:alg-geom/9701019]
- [84] R. Dijkgraaf, *Fields, strings, matrices and symmetric products*, in *Moduli of curves and abelian varieties*, Aspects Math., **E33**, (1999) 151–199, Vieweg, Braunschweig, [arXiv:hep-th/9912104].
- [85] L. Göttsche and W. Soergel, *Perverse sheaves and the cohomology of Hilbert schemes of smooth algebraic surfaces*, Math. Ann. **296** (1993) 235–245.
- [86] Y. Ruan, *Topological sigma model and Donaldson–type invariants in Gromov–Witten theory*, Duke Math. Jour. **83** (1996) 491.
- [87] A. Strominger, *Massless black holes and conifolds in string theory*, Nucl. Phys. B **451** (1995) 96 [arXiv:hep-th/9504090].
- [88] C. Vafa, *A Stringy test of the fate of the conifold*, Nucl. Phys. B **447** (1995) 252 [arXiv:hep-th/9505023].
- [89] P. Candelas and X. C. de la Ossa, *Comments on Conifolds*, Nucl. Phys. B **342** (1990) 246.
- [90] S. Kachru, A. Klemm, W. Lerche, P. Mayr and C. Vafa, *Nonperturbative results on the point particle limit of $N=2$ heterotic string compactifications*, Nucl. Phys. B **459** (1996) 537 [arXiv:hep-th/9508155].
- [91] M. Gross, *The deformation space of Calabi–Yau n -folds can be obstructed*, in *Mirror Symmetry II* AMS/IP Stud. Adv. Math. **1** (1997) 101 [arXiv:alg-geom/9402014].
- [92] K. Förger and S. Stieberger, *String amplitudes and $N = 2$, $d = 4$ prepotential in heterotic $K3 \times T^{**2}$ compactifications*, Nucl. Phys. B **514** (1998) 135 [arXiv:hep-th/9709004].
- [93] L. J. Dixon, V. Kaplunovsky and J. Louis, *Moduli dependence of string loop corrections to gauge coupling constants*, Nucl. Phys. B **355**, 649 (1991).
- [94] M. Serone, *$N = 2$ type I heterotic duality and higher derivative F -terms*, Phys. Lett. B **395**, 42 (1997) [Erratum-ibid. B **401**, 363 (1997)] [arXiv:hep-th/9611017].
- [95] T. Kawai, *String duality and modular forms*, Phys. Lett. B **397** (1997) 51 [arXiv:hep-th/9607078].
- [96] V. Kaplunovsky, J. Louis and S. Theisen, *Aspects of duality in $N=2$ string vacua*, Phys. Lett. B **357**, 71 (1995) [arXiv:hep-th/9506110].
- [97] E. Riegler, *Toric Geometry and Mirror Symmetry in String Theory*, Ph.D. thesis, TU Vienna, (2004).

- [98] Work in progress.
- [99] A. Klemm, P. Mayr and C. Vafa, *BPS states of exceptional non-critical strings*, Nuclear Phys. B Proc. Suppl. **58** (1997), 177–194 [arXiv:hep-th/9607139].
- [100] M. J. Duff, R. Minasian and E. Witten, *Evidence for Heterotic/Heterotic Duality*, Nucl. Phys. B **465** (1996) 413 [arXiv:hep-th/9601036].
- [101] M. Henningson and G. W. Moore, *Counting Curves with Modular Forms*, Nucl. Phys. B **472** (1996) 518 [arXiv:hep-th/9602154].
- [102] P. Berglund, M. Henningson and N. Wyllard, *Special geometry and automorphic forms*, Nucl. Phys. B **503** (1997) 256 [arXiv:hep-th/9703195].
- [103] R. E. Borcherds, *The moduli space of Enriques surfaces and the fake Monster Lie superalgebra*, Topology **35** (1996) 699–710.
- [104] J. A. Harvey and G. W. Moore, *Exact gravitational threshold correction in the FHSV model*, Phys. Rev. D **57** (1998) 2329 [arXiv:hep-th/9611176].
- [105] G. W. Moore, *Arithmetic and attractors*, [arXiv:hep-th/9807087].
- [106] I. V. Dolgachev, *Mirror symmetry for lattice polarized K3 surfaces*, J. Math. Sci. **81** (1996) 2599 [alg-geom/9502005].
- [107] P. S. Aspinwall, *K3 surfaces and string duality*, in *Fields, strings and duality* (1997) 421–540, World Sci. Publishing, River Edge, NJ. [arXiv:hep-th/9611137].
- [108] Work in progress.
- [109] N. Seiberg and E. Witten, *Comments on String Dynamics in Six Dimensions*, Nucl. Phys. B **471** (1996) 121 [arXiv:hep-th/9603003].
- [110] P. M. H. Wilson, *The Kähler cone on Calabi–Yau threefolds*, Invent. Math. **107** (1992) 561–583, Erratum: Invent. Math. **114** (1993) 231–233.
- [111] D. R. Morrison and C. Vafa, *Compactifications of F-Theory on Calabi–Yau Threefolds – II*, Nucl. Phys. B **476** (1996) 437 [arXiv:hep-th/9603161].
- [112] Kyoji Saito, *Einfach-elliptische Singularitäten*, Invent. Math. **23** (1974) 289 – 325.
- [113] A. Klemm, B. Lian, S. S. Roan and S. T. Yau, *Calabi–Yau fourfolds for M- and F-theory compactifications*, Nucl. Phys. B **518** (1998) 515 [arXiv:hep-th/9701023].
- [114] S. Hosono, *Counting BPS states via holomorphic anomaly equations*, in *Calabi–Yau varieties and mirror symmetry*, (Toronto, 2001), Fields Inst. Commun. **38** (2003) 57–86 [arXiv:hep-th/0206206].
- [115] C. Vafa and E. Witten, *Dual string pairs with $N = 1$ and $N = 2$ supersymmetry in four dimensions*, Nucl. Phys. Proc. Suppl. **46** (1996) 225 [arXiv:hep-th/9507050].
- [116] D. J. Gross and J. H. Sloan, *The Quartic Effective Action For The Heterotic String*, Nucl. Phys. B **291** (1987) 41.
- [117] G. Aldazabal, A. Font, L. E. Ibanez and A. M. Uranga, *New branches of string compactifications and their F-theory duals*, Nucl. Phys. B **492** (1997) 119 [arXiv:hep-th/9607121].
- [118] P. S. Aspinwall and D. R. Morrison, *Chiral rings do not suffice: $N=(2,2)$ theories with nonzero fundamental group*, Phys. Lett. B **334** (1994) 79 [arXiv:hep-th/9406032].

- [119] C. F. Doran, J. Morgan, *Integral Monodromy and Calabi–Yau Moduli*, in preparation.
- [120] V. V. Batyrev, I. Ciocan-Fontanine, B. Kim, D. van Straten, *Conifold Transitions and Mirror Symmetry for Calabi–Yau Complete Intersections in Grassmannians*, Nucl. Phys. B **514** (1998) 640, [alg-geom/9710022].
- [121] M. Gross, *A finiteness theorem for elliptic Calabi–Yau threefolds*, Duke Math. J. **74** (1994), 271–299. [arXiv:alg-geom/9305002]
- [122] P. Candelas, A. M. Dale, C. A. Lutken and R. Schimmrigk, *Complete Intersection Calabi–Yau Manifolds*, Nucl. Phys. B **298** (1988) 493.
- [123] P. S. Green, T. Hübsch, C. A. Lütken, *All the Hodge numbers for all Calab–Yau complete intersections*, Class. Quant. Grav. **6** (1989) 105
- [124] <http://thew02.physik.uni-bonn.de/~netah/cy.html>
- [125] P. Candelas and A. Font, *Duality between the webs of heterotic and type II vacua*, Nucl. Phys. B **511** (1998) 295 [arXiv:hep-th/9603170].
- [126] D. R. Morrison and C. Vafa, *Compactifications of F-Theory on Calabi–Yau Threefolds – I*, Nucl. Phys. B **473** (1996) 74 [arXiv:hep-th/9602114].
- [127] J. Fuchs, A. Klemm, C. Scheich and M. G. Schmidt, *Spectra And Symmetries Of Gepner Models Compared To Calabi–Yau Compactifications*, Annals Phys. **204** (1990) 1.
- [128] P. Candelas, A. Font, S. Katz and D. R. Morrison, *Mirror symmetry for two parameter models. II*, Nucl. Phys. B **429** (1994) 626 [arXiv:hep-th/9403187].
- [129] I. Brunner, M. R. Douglas, A. E. Lawrence and C. Romelsberger, *D-branes on the quintic*, JHEP **0008** (2000) 015 [arXiv:hep-th/9906200].
- [130] P. Mayr, *Phases of supersymmetric D-branes on Kaehler manifolds and the McKay correspondence*, JHEP **0101** (2001) 018 [arXiv:hep-th/0010223].